

UNCLASSIFIED

AD 408 716

DEFENSE DOCUMENTATION CENTER

FOR

SCIENTIFIC AND TECHNICAL INFORMATION

CAMERON STATION, ALEXANDRIA, VIRGINIA



UNCLASSIFIED

NOTICE: When government or other drawings, specifications or other data are used for any purpose other than in connection with a definitely related government procurement operation, the U. S. Government thereby incurs no responsibility, nor any obligation whatsoever; and the fact that the Government may have formulated, furnished, or in any way supplied the said drawings, specifications, or other data is not to be regarded by implication or otherwise as in any manner licensing the holder or any other person or corporation, or conveying any rights or permission to manufacture, use or sell any patented invention that may in any way be related thereto.

USARV Proc 961 Ver. 1
AD No. 08716

DDC PRE COPY

5 82 300

63-4-2

PROCEEDINGS VOL. I
August 1961

1

408 716

PROCEEDINGS

of the

Seal - 4

SYMPOSIUM ON ATMOSPHERIC ACOUSTIC PROPAGATION

Sponsored By

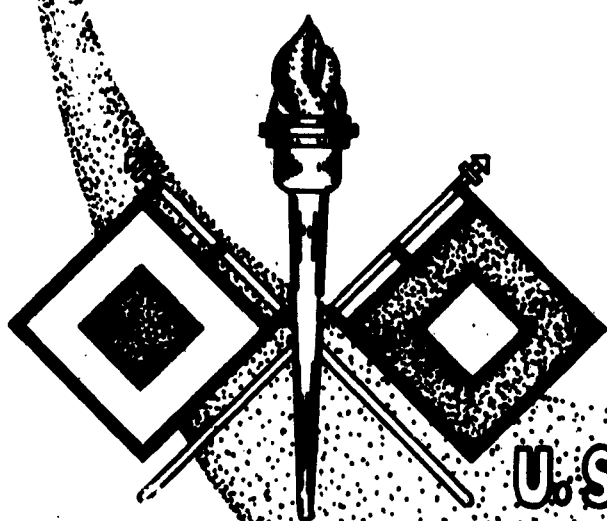
U. S. ARMY SIGNAL MISSILE SUPPORT AGENCY

and

TEXAS WESTERN COLLEGE

EL PASO, TEXAS

PROPERTY OF
TECHNICAL LIBRARY



DDC
RECEIVED
JUN 20 1963
TISA D

U.S. ARMY
SIGNAL MISSILE SUPPORT AGENCY
WHITE SANDS MISSILE RANGE
NEW MEXICO


7376
\$17.00

HEADQUARTERS
U. S. ARMY SIGNAL MISSILE SUPPORT AGENCY
WHITE SANDS MISSILE RANGE
NEW MEXICO

August 1961

1. "Proceedings of the Symposium on Atmospheric Acoustic Propagation" has been prepared under the supervision of the Missile Meteorology Division and is published for the information of all concerned.
2. Approval for the symposium documented in this publication was granted by SIGMD-7a letter dated 25 April 1961.

FOR THE COMMANDER:


ALBERT CUNNINGHAM
Captain, Signal Corps
Adjutant

(4) \$17.00

(5) 82 300

(6) PROCEEDINGS

of the

SYMPOSIUM ON ATMOSPHERIC ACOUSTIC PROPAGATION

Vol. 2 =

AD-328554

14 - 16 June, 1961

TEXAS WESTERN COLLEGE

And

FORT BLISS

El Paso, Texas. VOLUME I.

(7)-(10) A

(11) Aug 61. (12) 68p. (13) - (19) A (20) U

(21) NA

SYMPOSIUM COMMITTEE

Marvin Diamond, USA SMSA, Chairman

Willis L. Webb, USA SMSA

Robert L. Schumaker, TWC

Thomas G. Barnes, TWC

Lyman

PREFACE

The complete Proceedings of the Symposium on Atmospheric Acoustic Propagation will be published in two volumes. Volume I is composed of papers presented during the unclassified sessions. Classified papers will be issued separately as Volume II which may be obtained by appropriately cleared organizations that have a "need to know." Requests for Volume II should be directed to:

Commanding Officer
U. S. Army Signal Missile Support Agency
Attn: SIGWS-RD-M4-1D
White Sands Missile Range
New Mexico

Material in the two volumes was prepared by the authors and received only minor editing before publication. Although in proof-reading the mats from which volumes were reproduced every possible effort was made to correct typographical errors, there can be no guarantee that we were completely successful, particularly in those papers having mathematical equations. Since checking with the authors would have delayed publication to a great extent, the Symposium Committee asks the authors' indulgence and trusts that the papers as published meet with their approval.

The Symposium Committee

August 1961

TABLE OF CONTENTS

	Page
Preface-----	iii
Welcoming Addresses	
Dr. Joseph M. Ray, President, Texas Western College-----	1
Lt. Col. Glenn A. Welde, Deputy Commander, U. S. Army Signal Missile Support Agency-----	2
SESSION I: Willis L. Webb, USA SMSA, Chairman.	
I - 1 Shock Propagation at Large Distances by Jack Reed-----	3
I - 2 The Wavelength Limits of Atmospheric Ray Acoustics by E. Alan Dean-----	7
I - 3 Progress in the Calculation of the Sound Field in the Atmospheric Duct by James B. Calvert-----	13
I - 4 Some Effects of Flight Path Upon the Distribution of Sonic Booms by Donald L. Lansing-----	24
I - 5 A Nomogram for Calculating the Resulting Overpressure From the Detonation of Small-Yield High Explosives by Jack D. Fletcher-----	44
SESSION II: Major Clarence E. Morrison, USA SMSA, Chairman.	
II - 1 Absorption of Sound in the Atmosphere by E. Alan Dean-----	50
II - 2 The Influence of Atmospheric Parameters on Sound Absorption by Robert C. Amme-----	57
II - 3 Ballistic Versus Spherical Fronts Originating from Supersonic Missiles by Robert L. Schumaker and Aurora Bustos-----	69
II - 4 Acoustical Determination of Winds by Means of a Circular Microphone Array by Robert O. Olsen-----	76
II - 5 An Acoustical Technique for Calibrating High Altitude Temperature Sensors by Harold Ballard-----	83
II - 6 Detailed Acoustic Structure Above the Tropopause by Willis L. Webb-----	100

SESSION III: Henry Rachele, USA SMSA, Chairman.

III - 1	Infrasonic Capacitor Microphone Systems by Carlos McDonald--	119
III - 2	Problems in the Construction of Infrasonic Microphones by Mike Izquierdo-----	131
III - 3	Pulsonde Telemetry System by George Q. Clark-----	135
III - 4	Theory for Meteorological Correction to Artillery Sound Ranging Data by Donald M. Swingle-----	141
III - 5	Evaluation of Meteorological Corrections for Sound Ranging by Abraham Golden-----	149
III - 6	Atmospheric and Geometric Considerations in Sound Location Data Processing by Donald M. Swingle-----	162
III - 7	Blast Prediction for Small-Scale High-Explosive Experiments by Jack E. Chinn-----	168
III - 8	Theory of Acoustic Background at High Altitude by William C. Meecham-----	177
III - 9	Acoustic Background at High Altitudes by John W. Wescott---	182
III - 10	Ambient Acoustic Noise at High Altitudes by James C. Hart--	195

SESSION IV: Marvin Diamond, USA SMSA, Chairman.

IV - 1	*Preliminary Analysis of Acoustic Disturbances Generated by the Scout ST-1 by James F. Bettle-----	213
IV - 2	Sound Transmission Loss for Near-Vertical Atmospheric Propagation by E. Alan Dean-----	224
IV - 3	Acoustic Phenomena Observed on Rocket-Borne High Altitude Explosions by William Nordberg (Presented by Wendell Smith)-	233
IV - 4	Transcript of Panel Discussion of Atmospheric Acoustics----	245
	List of Attendees-----	263

*Presented during Classified Session but included in this volume because
the paper was unclassified.

WELCOMING ADDRESS

Dr. Joseph M. Ray
President
Texas Western College

Ladies and Gentlemen, you are welcome.

It is incumbent on college presidents, apparently it is a constitutional requirement by virtue of their make up, to know everything; and I, of course, do know precisely that. I am a social scientist so I don't quite know, although I do know in general, what you people are up to.

I am acquainted with the words in the name of your conference. I became associated with, indeed addicted to the consumption of, atmosphere some 53 years ago. Acoustics we are playing with right now, and I understand this. And of course I am, I say modestly, acquainted with the concept of propagation. The point again is that I do understand the words, but I do not quite understand the association of the words.

We are pleased to have you here at Texas Western College, not because of the fact that the president of the college knows everything and understands precisely what it is you are to engage yourselves with, but by virtue of the quality of the group and by virtue of the importance of the work you do, we are honored by your presence. We want to contribute what we can. We are pleased to know that you have come from far places. I would ask that you not be too smug in your assumption of superiority over the ordinary run of man because this is the age of specialization, and some people will give you full credit for keeping track of the sound of rockets as they go through the air. But when it comes to other things, it could be as the kids say, "you don't know from nothing."

Again, we are happy to have you here. It is a privilege to us and we hope you profit much from your conference here.

WELCOMING ADDRESS
Lt. Col. Glenn A. Welde, Deputy Commander
U. S. Army Signal Missile Support Agency
White Sands Missile Range

Acoustics and Sound - - - taking my cue from them, I will "sound-off" WELCOME and signal to you our appreciation for your attendance and participation in this symposium.

The need for scientific "sounding-off"-- the communication of ideas--- was the motivation and guiding thought in planning this series of discussions. For we all are aware that scientific knowledge loses some of its value if there is no timely transmission of that knowledge throughout the scientific community.

In a recent syndicated column, the urgency of an "idea clearing house" was emphasized. The article said in part, and I quote,

"If competent, highly-trained brainpower is the nation's most valuable, and rarest, resource, it is surely a waste if it spends its time in thumbing through indexes in libraries. With the ever-increasing flood of literature, a scientist can spend more time doing paper research than the Lab research he's paid for."

The misuse of brainpower is in itself bad enough, but the waste is compounded by the inadequacy of the professional journals to print all the newest ideas and latest concepts. Quoting again from the column:

"With tens of thousands of laboratories cranking out endless rivers of data, the trade papers can't possibly do their job. Some of the better ones are publishing material submitted as far back as three years with the backlog growing each month. Even more appalling, important contributions are being published in little-known periodicals, which no one reads, simply because the line is too long at the bigger journals. These important works often pass completely without notice only to be rediscovered much later by duplicated effort which could have been avoided. -----The worst problem is the politics of getting works published. This perverts many periodicals from their proper purposes, making them even less efficient means of transmitting scientific advancements."

Thus, even in the event that the scientist did spend more time in the library than in the laboratory, he would still be uninformed of recent developments in his field.

That summarizes the problem for which we hope symposiums, such as the one we are conducting, will be at least a partial solution. We have in this gathering some of the greatest minds- - the foremost authorities - - in the field of acoustics. Through the papers presented here, as well as in the panel and group discussions, the most modern techniques, the newest concepts, and most advanced theories currently under consideration in the United States will be transmitted from scientific mind to scientific mind. In this communication lies the path of our mutual technical advancement.

SHOCK PROPAGATION AT LARGE DISTANCES*

Jack W. Reed
Sandia Corporation
Albuquerque, New Mexico

Shock Propagation at Large Distances

A common approach to problems of long distance shock propagation is to assume ideal acoustic transmission. This means small amplitude waves are propagated without loss of energy and without change of pressure-time form. Each part of the wave travels at sound speed. Pressure amplitudes may be calculated from the geometric divergence of energy. As a wave passes a point, total sound energy flux density, ξ , is proportional to the integral over time of the squared overpressure, $(\Delta p)^2$, or

$$\xi = \int_0^T \frac{(\Delta p)^2}{\rho c} dt, \quad (1)$$

from $t = 0$ at wave arrival to $t = T$, the wave period or duration, where c is sound speed and ρ is air density. Net or source energy, W , is the total flux integrated over the wave front area, A ,

$$W = \int_A \xi dA. \quad (2)$$

Combining these two integrals shows that

$$\Delta p = (W \rho c)^{1/2} (KAT)^{-1/2} \quad (3)$$

where the integration constant K depends on the shape of the pressure-time wave trace.¹ Thus for three common wave geometries

Plane Wave: $A = \text{constant}, \quad \longrightarrow \Delta p = \text{constant},$

Conical Wave: $A \sim \text{radius}, r, \quad \longrightarrow \Delta p \sim r^{-1/2}$

Spherical Wave: $A \sim \text{radius squared}, \quad \longrightarrow \Delta p \sim r^{-1}$

In passing, we note the following on yield scaling for explosive (spherical) blasts: times, including pulse duration, T , are proportional to the cube root of yield, $W^{1/3}$, in close-in high-pressure regions.² If this carries into acoustic range,

$$\Delta p \sim W^{1/3}$$

A more sophisticated treatment of weak shocks, which recognizes that amplitudes so small as to travel in true acoustic manner are really of no concern was described by DuMond et al in 1946.³ Based on an equilibrium N-wave shape, which should eventually be reached by any perturbation, two derivations are made for the pressure-distance functions which are in agreement. One is based on thermal considerations for energy absorption in lead and tail pressure rises while the other is based on a hydrodynamical model for the linear intermediate part

*Work performed under the auspices of U. S. Atomic Energy Commission

of the N-wave form. In summary DuMond predicted, and verified experimentally to 2-millibar conical wave overpressures from 40-mm projectiles, that for the

$$\text{Conical wave: } \Delta p \sim r^{-3/4}.$$

The same theory applied to explosion geometry results in

$$\text{Spherical Wave: } \Delta p \sim r^{-1}(\ln r/a_1)^{-1/2}$$

where a_1 is an integration constant.

This later form is somewhat dependent on yield at even large but fixed range. Propagation becomes more nearly acoustic with increasing yield and thus with scaled initial range. This may be intuitively noted from the fact that with smaller yields, a larger fraction of total wave energy is concentrated near the frontal discontinuity where diabatic or dissipative processes operate.

DuMond's derivation suffers from some now apparent errors in assumption. Most important, shock pressure rise times are not nearly so short as his theory indicates, i.e., at 10-millibars overpressure rise time is 10^{-7} second; at 1-microbar rise time is 10^{-3} second. In millibar overpressure regions rise times are more like several milliseconds to give more nearly adiabatic compressions. Furthermore, waves do not necessarily become N-shaped at great distances; many recordings from atomic blast waves which were refracted back to ground from ozonosphere (100,000-150,000 feet MSL) or ionosphere (300,000-500,000 feet MSL, levels to 135 mile horizontal ranges have maintained the typical explosion shock front form of an N-shaped positive phase but a round, smaller-amplitude negative phase. Of course DuMond is not responsible for the N-shape generation assumption which was much earlier suggested by Lord Rayleigh,⁴ and still has considerable logical attraction.

Finally, verification at short ranges of a few yards has limitations imposed by the poor definition of absorptivity. This is an extremely small quantity that only becomes important when compounded exponentially over large distance. Yet verification at very long range presents many other very practical difficulties.

Empirical data on explosives blasts led Perkins et al⁵ to accept

$$\Delta p \sim r^{-1.4}.$$

Their data source is not clear however, and may be measurements from Pacific Proving Ground nuclear tests, in which case the fast decay at ground level may have been caused by atmospheric refraction of waves away from ground in the unstable tropical air mass.

On the other hand, a purely acoustic propagation assumption also has many questionable facets. It is first doubtful whether any man-made model perfectly duplicates nature; then it is further unlikely that

of the N-wave form. In summary DuMond predicted, and verified experimentally to 2-millibar conical wave overpressures from 40-mm projectiles, that for the

$$\text{Conical wave: } \Delta p \sim r^{-3/4}.$$

The same theory applied to explosion geometry results in

$$\text{Spherical Wave: } \Delta p \sim r^{-1}(\ln r/a_1)^{-1/2}$$

where a_1 is an integration constant.

This later form is somewhat dependent on yield at even large but fixed range. Propagation becomes more nearly acoustic with increasing yield and thus with scaled initial range. This may be intuitively noted from the fact that with smaller yields, a larger fraction of total wave energy is concentrated near the frontal discontinuity where adiabatic or dissipative processes operate.

DuMond's derivation suffers from some now apparent errors in assumption. Most important, shock pressure rise times are not nearly so short as his theory indicates, i.e., at 10-millibars overpressure rise time is 10^{-7} second; at 1-microbar rise time is 10^{-3} second. In millibar overpressure regions rise times are more like several milliseconds to give more nearly adiabatic compressions. Furthermore, waves do not necessarily become N-shaped at great distances; many recordings from atomic blast waves which were refracted back to ground from ozonosphere (100,000-150,000 feet MSL) or ionosphere (300,000-500,000 feet MSL, levels to 135 mile horizontal ranges have maintained the typical explosion shock front form of an N-shaped positive phase but a round, smaller-amplitude negative phase. Of course DuMond is not responsible for the N-shape generation assumption which was much earlier suggested by Lord Rayleigh,⁴ and still has considerable logical attraction.

Finally, verification at short ranges of a few yards has limitations imposed by the poor definition of absorptivity. This is an extremely small quantity that only becomes important when compounded exponentially over large distance. Yet verification at very long range presents many other very practical difficulties.

Empirical data on explosives blasts led Perkins et al⁵ to accept

$$\Delta p \sim r^{-1.4}.$$

Their data source is not clear however, and may be measurements from Pacific Proving Ground nuclear tests, in which case the fast decay at ground level may have been caused by atmospheric refraction of waves away from ground in the unstable tropical air mass.

On the other hand, a purely acoustic propagation assumption also has many questionable facets. It is first doubtful whether any man-made model perfectly duplicates nature; then it is further unlikely that

completely loss-free energy propagation is possible. In this case it only appears that losses are so small as to be nearly indistinguishable with laboratory scales. Further reference to atomic blast records shows that at 135 miles (Nevada Test Site circular recording array range) pressure wave periods are much longer than at on-site ranges (less than 20 miles). Positive phase duration extensions are in general, but not very exact, agreement with expectations from finite-amplitude, sharp-front wave propagation speeds and an assumption that the zero-overpressure point following the positive phase travels at sound speed.

As previously mentioned, high frequency components in a sharp front wave are slightly attenuated in atmospheric transmission. Applying the appropriate Schrodinger's (classical-theory) intensity absorption coefficient⁶ to Fourier components of the positive phase blast N-wave, (i.e., with attenuation proportional to frequency squared and inversely proportional to air density), shows that even for one-ton high explosives waves very little peak amplitude reduction results from sea level propagation even to 135 miles. However, along more common ray paths to this range, through low air density ozonosphere regions, classical attenuation causes amplitude reduction to about one-half. For kilotons or larger yields only a few percent reduction is calculated for ozonosphere signals. However, these calculations were based on close-in wave periods which are known to increase with great range and thus should reduce the overall attenuating effect as lower frequency Fourier components are added. Furthermore, as high frequency components are absorbed to round off the wave front, re-shocking likely reforms them to some degree. Sound attenuation by atmospheric turbulence, as described by Jorand,⁷ depends on frequency, f , as $f^{2/3}$ and not on air density. A treatment by Lighthill⁸ may also be interpreted to remove density dependence and give dependence on $f^{1/3}$. Obviously the situation has become too confusing for treatment with naive models.

Empirical analysis at very long range is fraught with inaccuracy. Amplitudes measured are mainly determined by atmospheric refraction effects which may combine convergent focusing with interference among ray paths, etc. These may be roughly calculated if rare bits of high altitude wind and temperature data happen to be available. Still, atmospheric variability is such as to allow only approximate accuracy instead of order-of-magnitude estimate otherwise possible. To avoid refraction effects, the obvious solution, other than maintaining uniform conditions over a hundred-mile tube, is to record waves along vertical ray paths, parallel to the sound velocity gradients of our stratified atmosphere which bend low elevation angle rays and turn fronts. This experiment has not been carried out to small millibar or microbar blast pressure levels necessary to accurately set the exponent for distance in the pressure-distance decay law. If we assume that r^{-1} and $r^{-3/2}$ bound the true decay, high altitude nuclear tests have only been made where the ground-zero pressure difference between r^{-1} and $r^{-3/2}$ predictions is less than a factor of two. Instrument inaccuracies ($\pm 20\%$) obscure resolution from these tests.

Project Banshee tests at WSMR, beginning about July 1, 1961, will allow measurements where predictions differ by as much as a factor of twenty. Instruments twenty percent accurate will here give resolution of the distance exponent to a few percent.

At Sandia Corporation we have just finished some measurements from one-pound charges at heights to 500 feet above ground. In these tests factor-of-five differences separate forecasts by the two laws. Preliminary analysis of our records shows that the exponent average is about 1.25, and Banshee recorder set ranges will be made on the basis of this figure.

REFERENCES

1. Cox, E. F., Sound Propagation in Air, Handbuch der Physik, Chapter 22, Vol. 48, Springer-Verlag, Berlin, 1958.
2. Sachs, R. G., The Dependence of Blast on Ambient Pressure and Temperature, Ballistic Research Laboratories Report 466, U. S. Army, Aberdeen Proving Ground, Maryland, 1944.
3. DuMond, J. W. M., Cohen, E. R., Panofsky, D. K. H., and Deeds, E., A Determination of the Wave Forms and Laws of Propagation and Dissipation of Ballistic Shock Waves, Journal of the Acoustical Society of America, Vol. 18, No. 1, pp 97-118, July, 1946.
4. Lord Rayleigh, Theory of Sound, Dover Publications, New York, 1945.
5. Perkins, B., Lorrain, P. H., and Townsend, W. H., Forecasting the Focus of Air Blasts due to Meteorological Conditions in the Lower Atmosphere, Ballistic Research Laboratories Report No. 1118, U. S. Army, Aberdeen Proving Ground, Maryland, Oct., 1960.
6. Schrödinger, E., Zur Akustik der Atmosphäre, Physikalische Zeitschrift, Vol. 18, pp 445-53, 1917.
7. Jorand, M., Contribution a l'etude de l'amortissement des sons dans l'atmosphère libre, Jour. de Mécanique et de Physique de l'Atmosphère, Vol. 1, No. 1, pp 43-47, Jan-Mar 1959.
8. Lighthill, M. J., On the Energy Scattered from the Interaction of Turbulence with Sound or Shock Waves, Proc. Cambridge Philosophical Society, Vol. 49, p. 531, 1953.

THE WAVELENGTH LIMITS OF ATMOSPHERIC
RAY ACOUSTICS*

E. Alan Dean

Schellenger Research Laboratories
Texas Western College

In the investigation of various types of long range atmospheric acoustic propagation, much use has been made of ray acoustics to describe the sound field. Ray acoustics represents a limiting case of the plane wave solution, and as such, it is evident that the direction of propagation and amplitude should vary only slightly for distances of the order of a wavelength. However, both theory and experiment indicate that the energy spectra for long range propagation is predominantly infrasonic, casting doubt as to the validity of the ray acoustic solution. This paper is a preliminary investigation of the wavelength limits of ray acoustics imposed by the atmosphere.

~~It is evident that for very long wavelengths, the ray solution~~ will be inaccurate and that the more complicated normal-mode solution ought to be used. The dividing line between these two types of problems is nebulous and depends to a great extent on the knowledge of the atmospheric variables, speed of sound c , velocity y , and density ρ . Since these are rarely known accurately as functions of position, a complicated method of solution for the sound field would be of no more value than a somewhat less accurate method. If, however, the second method's accuracy is a function of the over-all variation of the atmospheric variables, which is generally known, then the more accurate method should be used.

Thus, in comparing methods of solution, there is some justification for the use of a more or less standard atmosphere, neglecting any horizontal and time variations and, to a large extent, wind, since they are rarely known in practical cases. The inaccuracies introduced by this simplification form a separate problem, and are important to either the ray acoustic or normal-mode solution.

The justification of ray acoustics is dependent on the ray's description of the wavefront, which in turn, is described by the eikonal equation. The assumptions upon which ray acoustics rest can therefore be obtained from an investigation of the eikonal equation, which is derived from the wave equation,

$$\ddot{\phi} = [c(z)]^2 \nabla^2 \phi,$$

where it has been assumed that the atmosphere is a layered-inhomogeneous medium, or that the sound speed and density are only functions of height, z . The eikonal equation is obtained by considering a velocity potential

*Supported by U. S. Signal Missile Support Agency, Contract DA 29-040-ORD-2410

solution of the form

$$\phi = A(\mathbf{r}) \exp \{ j[\omega t - k_0 \psi(\mathbf{r})] \},$$

where A is an amplitude function, ψ is a length function, and j , ω , and k_0 have their usual meanings of: imaginary unit, angular frequency, and wave number.

Substitution of this value into the wave equation and equating real and imaginary parts results in the pair of equations which determine A and ψ :

$$k_0^2 |\nabla \psi|^2 - \frac{\nabla^2 A}{A} = \left(\frac{\omega}{c} \right)^2 \quad (1)$$

$$\frac{2}{A} \nabla A \cdot \nabla \psi + \nabla^2 \psi = 0 \quad (2)$$

These are complicated equations and do not materially decrease the complexity of the problem, however, the simple assumption

$$\frac{\nabla^2 A}{A} \ll \left(\frac{\omega}{c} \right)^2$$

reduces equation (1) to

$$|\nabla \psi|^2 = \left(\frac{\omega}{k_0 c} \right)^2,$$

which is known as the eikonal equation.

With the substitution of $k_0 = \frac{\omega}{c_0}$, the eikonal equation takes on the familiar form:

$$\left(\frac{\partial \psi}{\partial x} \right)^2 + \left(\frac{\partial \psi}{\partial y} \right)^2 + \left(\frac{\partial \psi}{\partial z} \right)^2 = \frac{c_0^2}{[c(\mathbf{r})]^2}, \quad (3)$$

the solution of which yields the eikonal $\psi(x, y, z)$. The physical significance of the eikonal becomes apparent by setting the phase of ϕ equal to a constant ωt_0 . This yields

$$\psi(x, y, z) = c_0 (t - t_0),$$

the equation of a surface which varies its position with time. This surface of constant phase is, of course, the wavefront, and the vector $\nabla \psi$ is parallel to the rays and has a magnitude equal to the index of refraction.

Equation (2), which would allow a solution for A, reduces to an identity in the order of terms retained in the eikonal equation, since the assumption $\frac{\nabla^2 A}{A} \ll \left(\frac{\omega}{c}\right)^2$ implies that both terms in the second equation are much less than $k_0 |\nabla \psi|^2$. Because of this, the eikonal solution of the wave equation is not a solution for A, which must be obtained by other means. Suppose an intensity function is chosen so that

$$I = \frac{W}{4\pi r^2} [B(r)]^2 e^{-2\int \alpha ds},$$

where W is the source acoustic power, r is the distance from the source, B is a correction factor due to refractive focusing, and α is the pressure absorption coefficient. Using the relation $I = \frac{p^2}{\rho c}$ (which is true for both plane and spherical waves), and the relation between the rms sound pressure and the velocity potential, $p = |\rho \omega \phi|$, the resultant amplitude for ϕ is

$$A = \frac{A_0}{r} \sqrt{\frac{c}{\rho}} B e^{-\int \alpha ds}.$$

Supposing that the absorption coefficient is constant in a particular region, this becomes:

$$A = \frac{A_0}{r} \eta e^{-\alpha r},$$

where $\eta = \sqrt{\frac{c}{\rho}} B$. Since the sound ray can only be translated, not rotated by a wind, a rotation of the coordinate system reduces the problem to two dimensions. After some simplification $\nabla^2 A/A$ becomes

$$\left(\frac{1}{r} + \alpha\right)^2 - \frac{1}{r} \left(\frac{1}{r} + \alpha\right) + \frac{1}{r^2} + \frac{2}{\eta^2} \left(\frac{\partial \eta}{\partial z}\right)^2 - \frac{2z}{\eta r} \left(\frac{1}{r} + \alpha\right) - \frac{1}{\eta} \frac{\partial^2 \eta}{\partial z^2}$$

which, because of the assumed inequality, must be less than $\left(\frac{\omega}{c}\right)^2$. This will be assured if the following inequalities exist:

$$r \gg 2\pi\lambda \quad (4)$$

$$\alpha\lambda \ll 2\pi \quad (5)$$

$$\frac{\partial \eta}{\partial z} \ll \frac{\pi\eta}{\lambda} \quad (6)$$

$$\frac{\partial^2 \eta}{\partial z^2} \ll \frac{4\pi^2 \eta}{\lambda^2} \quad (7)$$

It can now be shown that these inequalities indeed cause

$$\frac{2k_0}{A} \nabla A \cdot \nabla \psi \ll \frac{\omega^2}{c^2}$$

and

$$k_0 \nabla \cdot \nabla \psi \ll \frac{\omega^2}{c^2}$$

which reduce equation (2) to an identity. These inequalities, upon substitution of the eikonal value for $\nabla \psi$, simplification, and the use of \underline{n} as a unit vector in the direction of the ray become: (See Lindsay, Mechanical Radiation, Sect 1.12)*

$$\frac{\nabla A}{A} \cdot \underline{n} \ll \frac{\pi}{\lambda}$$

$$\nabla \cdot \underline{n} \ll \frac{2\pi}{\lambda}$$

and

$$\frac{\nabla c}{c} \cdot \underline{n} \ll \frac{2\pi}{\lambda}$$

These three inequalities express the normally stated requirements that (1), the change in amplitude per wavelength must be much less than the amplitude itself, (2) the change in direction cosines per wavelength is much less than unity and, (3) the change in velocity per wavelength is much less than the velocity itself. Calculation of ∇A from the assumed amplitude function shows that inequalities (4) through (6) insure the first requirement. Also since $\eta = \eta(c)$, inequality (6) demands that the third requirement is met. Finally, assuming no wind, Snell's law provides the information that requirement (3) includes requirement(2).

To investigate the requirements η places on the wavelength limits, first consider that B is caused by a change in the divergence of the rays, and that if requirement (2) is satisfied, changes in B may be neglected. Thus:

$$\eta = c^{1/2} \rho^{-1/2} = \eta_0 \left(\frac{T}{T_0} \right)^{3/4} \left(\frac{P_0}{P} \right)^{1/2}$$

after use of the ideal gas law and the relation $c^2 = \frac{\gamma RT}{M}$. This yields

$$\frac{\partial \eta}{\partial z} = \eta \left(\frac{3}{4T} \frac{\partial T}{\partial z} - \frac{1}{2P} \frac{\partial P}{\partial z} \right)$$

However, by the hydrostatic equation,

$$\frac{\partial P}{\partial z} = -\rho g$$

*R. B. Lindsay, 1960. Mechanical Radiation. New York: McGraw Hill.

where g is the acceleration due to gravity. This yields the following expression for inequality (6):

$$\lambda \left(\frac{3}{4} \frac{\partial T}{\partial z} + \frac{gM}{2R} \right) \ll 2 \pi T,$$

which will be satisfied if both terms on the left are $\ll 2 \pi T$, choosing the second,

$$\lambda \ll \frac{4 \pi RT}{3gM}, \quad (8)$$

where a factor of three has been included to yield an even power of ten for the frequency limit, which becomes:

$$f \gg \frac{37 g}{4 \pi c} \approx 10^{-2} \text{ cps.}$$

Letting inequality (8) be the wavelength restriction, it is also necessary for

$$\frac{\partial T}{\partial z} < \frac{2gM}{R}.$$

This may be expressed in terms of the specific heat at constant pressure,

$c_p = \frac{5}{2} \frac{R}{M}$ for a diatomic gas. Thus

$$\frac{\partial T}{\partial z} < 5 \frac{g}{c_p} \quad (9)$$

or that the temperature gradient should be less than five times the dry adiabatic lapse rate. A gradient as large as this is not likely to be found in the atmosphere.

Finally, the right side of inequality (7) may be expanded to

$$\frac{\partial^2 \eta}{\partial z^2} = \frac{n}{T^2} \left(\frac{3}{4} \frac{\partial T}{\partial z} + \frac{gM}{2R} \right)^2 - \frac{\eta}{T^2} \left(\frac{3}{4} \frac{\partial T}{\partial z} + \frac{gM}{2R} \right) \frac{\partial T}{\partial z} + \frac{n}{T} \left(\frac{3}{4} \frac{\partial^2 T}{\partial z^2} \right)$$

The first two terms are much less than $4 \pi^2 \eta / \lambda^2$ because of inequalities (8) and (9), leaving the fact that

$$\frac{\partial^2 T}{\partial z^2} < \frac{g^2 M^2}{R^2 T} \approx 2 \times 10^{-5} \text{ } ^\circ\text{K}/\text{m}^2$$

This requirement is of importance at the tropopause where the temperature gradient changes rapidly. According to charts from Webb and Jenkins, "Speed of Sound in the Stratosphere",* the greatest change in

*W. L. Webb and K. R. Jenkins. 1960. "Speed of Sound in the Stratosphere". U. S. Army Signal Missile Support Agency Special Report 37.

the temperature gradient is just below the tropopause, where the gradient changes from its normal tropospheric value to zero in about a kilometer. Since the normal tropospheric gradient is about $6 \times 10^{-3} \text{ }^{\circ}\text{K/m}$, this yields $\frac{\partial^2 \eta}{\partial z^2} \approx 6 \times 10^{-6}$, about the maximum value that will not require adjustment of the previously set wavelength limit which depends on the density gradient.

Although it is not likely that the density gradient will vary appreciably, or that the temperature gradient will be as large as 5 times the dry adiabatic lapse rate, it is quite possible that the change in temperature gradient at the tropopause will be larger than 6×10^{-6} at times. Therefore care should be used in applying inequality (8) to the atmosphere. It must also be noticed that inequality (4), not mentioned yet, requires that ray acoustics be applied only at distances from the source which are very large compared to a wavelength. For instance, about 3 km for a one cps signal. Whereas, inequality (5) is independent of wavelength since the maximum absorption per wavelength is independent of frequency. ~~This maximum value for molecular absorption, the most important for low frequency signals, is much less than 2π .~~

For simplicity, wind has been excluded. Wind not only affects the velocity gradient (the component in the direction of the ray is added to the local sound speed to obtain the velocity of the wavefront), but also changes the wave equation itself. Both effects need investigation. However, the wind velocity seems to vary quite a lot, and it is doubtful if the investigation is justified since the inaccuracies of the ray solution ought not be much more serious than the inaccuracies in our knowledge of the wind field in space and time.

In conclusion, the limiting wavelength for atmospheric ray acoustics, neglecting wind, is normally given by inequality (8), where consideration of the change in temperature gradient must also be made.

PROGRESS IN THE CALCULATION OF THE SOUND FIELD
IN THE ATMOSPHERIC ACOUSTIC DUCT

by

James B. Calvert
Denver Research Institute

INTRODUCTION:

In this paper I wish to present in a simple way the basic ideas which are now guiding our work at Denver on the subject expressed in the title. One of our objectives is the systematic construction of the applied physical theory. We have found that there is a wealth of information in some areas, and a dearth in others. And, above all, there is much that is as yet unassimilated or uncorrelated. Here I will present an indication of the answers to two of the questions we have asked ourselves. To develop these answers fully requires only the expenditure of a little more time; other questions remain to be answered.

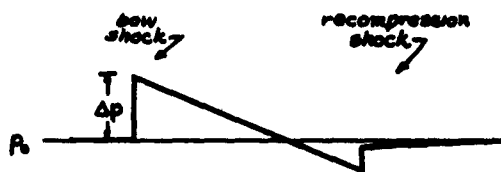
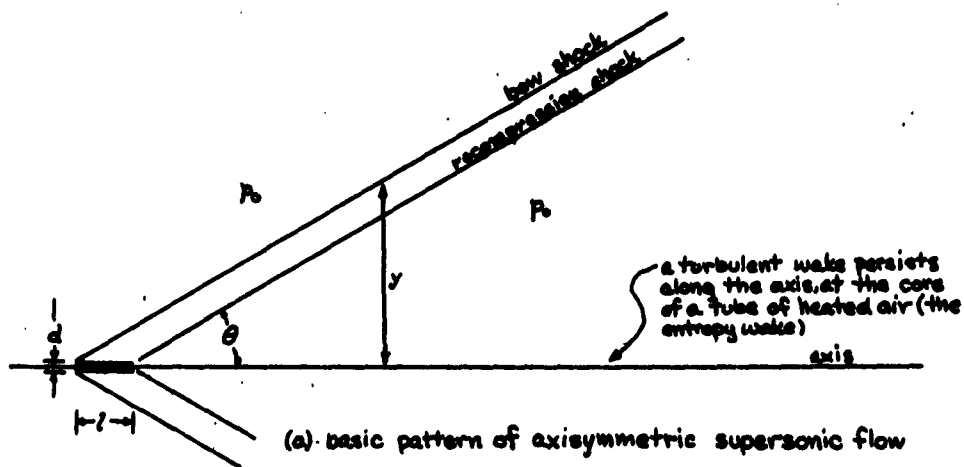
The first section discusses the nature of the signal generated by a supersonic projectile, a source relatively neglected compared with the more common explosion and supersonic-aircraft sources, in which the literature is extensive.

In the last section the propagation of sound in a natural waveguide is discussed. The wave approach seems to offer the most satisfying and fruitful analysis of long-range propagation, in which infrasonic frequencies are important.

THE ACOUSTIC SIGNAL OF A SUPERSONIC PROJECTILE:

Consider an axially symmetric body moving at constant supersonic speed through uniform air. Imagine two Mach cones, the first with its apex near the nose of the body and the second with its apex near the rear. So long as the medium is homogeneous, the strongest part of the acoustic signal generated will lie between these cones. The principal components of this signal are the bow shock (which lies slightly ahead of the forward Mach cone) and the recompression shock (which lies near the rear Mach cone). Between these two shocks lie a number of weaker shocks arising from less violent behavior of the flow about the projectile.

The general pattern of the flow is shown in Fig. 1(a). θ , the Mach angle, is given by $\sin \theta = M^{-1}$, where M is the free-stream Mach number. In Fig. 1(b) we see the general form of the pressure



(b) pressure variation far from the axis (after Lighthill).

I-3 Figure 1

variation in passing from ahead of the bow shock to behind the recompression shock, far from the axis ($y/l \gg 1$). The overpressure in the bow shock may be estimated from the formula

$$\frac{\Delta p}{p_0} = \frac{(M^2 - 1)^{1/2}}{2} \left(\frac{d}{l} \right) \left(\frac{y}{l} \right)^{-3/4} \quad (1)$$

where p_0 is the free-stream pressure and the significance of Δp , d , y , and l is shown in Fig. 1. For a discussion of axisymmetric supersonic flow, see Lighthill (7).

From $M = 1.4$ to $M = 10$ the factor $(M^2 - 1)^{1/2}$ varies only from 1.0 to 1.8. We see then that Δp depends chiefly on the fineness ratio (d/l) and only weakly on M . Substituting $R = y \cos \theta$ in (1) and expressing θ in terms of M , we find for large M :

$$\frac{\Delta p}{p_0} \approx \frac{(d/l)}{M^{5/4}} \left(\frac{R}{l} \right)^{-3/4} \quad (2)$$

For $R/l \gg 1$, R is the radius of curvature of a locally cylindrical shock wave. Let us compare Eq. (2) for Δp with the Brinkley-Kirkwood theory of shock wave propagation (Brinkley (3)). For small $\Delta p/p_0$ we have for a cylindrical shock wave:

$$R^{1/2} \Delta p = A [2(R^{1/2} - B^{1/2})]^{-1/2}, \quad D = \frac{\gamma + 1}{6\gamma p_0} A^2 R^{1/2} \Delta p, \quad (3)$$

where A and B are constants, $\gamma = c_p/c_v$, and p_0 is the free-stream pressure. Here D is, approximately, the energy content of the shock wave and is given by

$$D = R \Delta p \mu v \quad (4)$$

where R = radius of curvature of the wave

p = peak overpressure

u = particle velocity just behind the shock

$\frac{1}{\mu} = - \left(\frac{\partial \log \Delta p u R}{\partial t} \right)$, evaluated at the shock

v = a factor depending on the shape of the pressure-time curve of the shock.

Equations (3) hold for weak shocks. In our case they describe the propagation of the bow shock, which is considered to extend backward as far as the point at which the overpressure becomes zero.

From (3) we see that for $R \gg B$, Δp falls off as R^{-1} ; compare $\Delta p \sim R^{-1}$ in Eq. (2). Taking the approximate values

$$\mu \sim \frac{1}{4Mc}, \quad \nu \sim \frac{2}{3},$$

where l is the length of the projectile, M its Mach number, and c the local sound speed, we may evaluate the constants A and B in (3) at a certain value of $R=R_0$, where $R_0 \gg 1$, $\Delta p \ll p_0$. We find:

$$A = \Delta p_0 \left(\frac{17^3 R_0^{\frac{1}{2}}}{M(\gamma+1) \Delta p_0 / p_0} \right)^{\frac{1}{2}}, \quad B = R_0 \left(1 - \frac{17^3}{2M(\gamma+1) R_0 \Delta p_0 / p_0} \right)^2,$$

where Δp_0 is the peak overpressure at $R=R_0$.

We note that $D \sim R^{-\frac{1}{2}}$; hence the energy content per unit area (intensity) falls off as $R^{-3/2}$, which may be compared to $I \sim R^{-1}$ for a non-discontinuous wave without absorption. The difference is, of course, due to energy dissipation in the shock front. This effect persists even for infinitesimal $\Delta p/p_0$. If we should take $\Delta p \sim R^{-3/4}$ from Eq. (2) instead of $\Delta p \sim R^{-1}$ from Eq. (3), we find that $I \sim R^{-5/4}$, which still gives an excess of dissipation.

Considering that the above analysis gives at least a qualitative account of the shock wave acoustic signal, it is evident that the acoustic superposition principle is invalid so long as a surface of discontinuity is present in the field. In particular, the study of the refraction of this kind of signal must take into account the discontinuity. We also note that a shock wave propagating upward in the atmosphere tends to develop a more pronounced shock front. The increase in Δp may be roughly estimated from the relation:

$$\frac{(\Delta p)^2}{p_0 c} = \text{constant}. \quad (5)$$

This increase in Δp leads to a greater rate of energy dissipation.

Elementary ray-tracing may describe the path of the shock quite well so long as the ray does not pass through any "critical" regions. One of these critical regions is that in which the signal is totally reflected; others are regions of caustic foci (of which the preceding is a particular case) and shadow zones. It is quite possible that energy dissipation is excessive near caustic foci, and that the discontinuity may even be destroyed on passing through a caustic focus. A phenomenon certainly occurring on reflection is the trans-

fer of energy to a wave train following the initial pulse, with an accompanying decrease in the amplitude of the initial pulse. This is seen on examination of microbarograph records of explosion pulses returned from high altitudes (see, for example, Cox (4)).

Thus the conditions of propagation must strongly affect the character of the signal observed at great distances. The situation may be described qualitatively as follows. The shocks emanating from the projectile are deflected and modified by the structure of the surrounding medium, dissipating a great deal of energy and generating a train of non-discontinuous waves. One frequency that may be favored is that corresponding to a wavelength of approximately $1/M$. In general, the resultant frequency distribution may, to a greater or lesser degree, resemble the Fourier transform of the initial signal. It may be useful to note that reflection of a finite-amplitude signal of angular frequency ω is accompanied by the production of signals of frequency 2ω (Feng (6)). The higher-frequency components will be filtered out at high altitudes by gas-kinetic absorption. At length we will be concerned with the propagation of a rather complex signal, its frequency spectrum determined jointly by the conditions of propagation and the initial signal form.

We have not yet mentioned the turbulent wake as an acoustic source. It will radiate a random signal, corresponding to the randomness of the turbulence, with an intensity well below that due to the shock waves. It is probable that at large distances the only remnant of the signal will lie in frequency between $\nu = 0.1 \text{ sec}^{-1}$ and $\nu = 1.0 \text{ sec}^{-1}$. The region around $\nu = 1 \text{ sec}^{-1}$ is characterized by molecular absorption due to Oxygen (Amme (1)). In summary, the turbulent wake acts as a random-phase, cylindrically-symmetric source, its frequency spectrum determined by that of the turbulence.

SOUND CHANNEL PROPAGATION:

It is well-known that the sound speed minimum in the terrestrial atmosphere which usually occurs between the troposphere and about 15 km. above gives rise to waveguide propagation of sound. In the ARDC model atmosphere the minimum speed is about 300 m/sec and at the boundaries of the channel the speed is 340 m/sec. These limits correspond to the trapping of rays with grazing angles of less than

$$\alpha_{\max} = \cos^{-1} \frac{c_{\min}}{c_{\max}} \sim 20^\circ.$$

Where it is important to know where signals from a given source may arrive, as in prediction of blast damage from nuclear explosions, ray-tracing may be directly applied with adequate results. When detailed information of signal intensity and character is needed, very little information can be obtained from ray pictures in many cases. To obtain a suitable description of the propagation it is necessary to base the analysis directly on the fundamental wave properties of the acoustic field. A first step is the derivation of corrections to ray analysis that allow, for example, the calculation of intensities near caustic foci. Such calculations have been made by several authors (e.g., Marsh (8); Haskell(9)).

Two of the more important characteristics of propagation, attenuation and signal character, may depend sensitively on wavelike aspects of the field. For example, the "lateral waves" affect the attenuation, and dispersion affects the signal character (these terms will be explained below). Wave properties seem particularly important at large ranges.

The emphasis in the study of "waves in layered media" has been on the propagation of sound in the sea, and the propagation of electromagnetic waves in the atmosphere. The general theory, however, (as presented in Waves in Layered Media by Brekhovskikh (2)) is equally applicable to atmospheric sound propagation.

To illustrate the basic properties of waveguide propagation, it is convenient to consider a very simple waveguide mode: a uniform medium bounded above and below by perfectly reflecting surfaces. To make the reflection correspond to total internal reflection, let the reflection coefficient $V = -1$ at each surface. Assuming the superposition principle, we may Fourier-analyze the signal and henceforth work with harmonic waves. The wave-equation system is

$$\nabla^2 \psi + k^2 \psi = 0, \quad \psi = 0 \text{ at } Z = 0, \quad Z = h$$

where ψ is the acoustic potential (p , \bar{v} , and ψ vary as $e^{-i\omega t}$, taking the real part, and $\bar{v} = -\nabla \psi$, $p = i\omega \rho \psi$). The wave number $k = \frac{\omega}{c} = \frac{2\pi}{\lambda}$ where c is the sound speed. The z -axis is vertical; the origin is on the lower surface.

Separation in rectangular coordinates yields the usual plane waves, standing in the z -direction and travelling horizontally; separation in cylindrical coordinates (convenient for treating localized sources) gives

$$\psi = \sin \frac{1\pi z}{h} H_c^{(1)}(n_1 r); \quad i = 1, 2, \dots, \infty; \quad n_1^2 = k^2 - \frac{1^2 \pi^2}{h^2}$$

where $H_0^{(1)}$ is the zero-order Hankel function of the first kind, which describes an outgoing cylindrical wave. For $l > kh/\pi$, the waves are not travelling, but are exponentially damped. These "inhomogeneous" waves are necessary for satisfying boundary conditions at the source; for large l their attenuation coefficient is about $l\pi/h$, and so they may be neglected when the radial distance is a few duct widths.

Each value of l gives a "normal mode" of wave propagation in the duct. The number of travelling modes is about equal to the width of the duct in half-wavelengths:

$$N = h/(\lambda/2)$$

For higher frequencies N is large. For example, at $\nu = 1$ cps, $N \approx 200$ in the atmospheric duct (i.e., assuming that all rays are trapped; see below). As an illustrative exercise, let us estimate the accuracy with which the "path" of a signal is described by a ray. For large r , the normal modes are asymptotically

$$\psi \sim \frac{1}{\sqrt{r}} \left\{ e^{i(n_1 r + \frac{1}{h} \pi z - \frac{3}{4} \pi)} - e^{i(n_1 r - \frac{1}{h} \pi z - \frac{3}{4} \pi)} \right\}$$

which is a superposition of waves corresponding to a symmetrical pair of rays drawn at grazing angles of

$$\alpha = \pm \sin^{-1} \frac{1}{kh} \approx \pm \sin^{-1} \left(\frac{1}{2} \frac{\lambda}{h} \right)$$

The complete mode spectrum allows rays at only a finite number of angles. This signifies that the path cannot be localized except with an uncertainty of

$$\Delta \alpha \approx \left(\frac{\lambda}{2h} \right) \cos \alpha$$

in angle. This is a characteristic feature of wave motion. Compare the analogous concept of trajectory in quantum mechanics with the above. From the correspondence between the ray and wave pictures, we see at once that in an atmospheric duct we will not have as many normal modes as in a perfect channel. Indeed, for $\alpha < 20^\circ$, the number of normal modes will be approximately $N/3$; for $\nu = 1$ cps, then, the number of trapped modes will be about 70.

From the angular uncertainty in ray direction, we may calculate the distance R at which the linear uncertainty is equal to the width of the duct. We have

$$R \Delta \alpha = h, \quad \Delta \alpha \approx \frac{\lambda}{2h}$$

whence $R = hN$. For $h = 15$ km., the following tabulation gives $R/10$ for several frequencies:

ν , cps	$R/10$, km.
3	1000
1	300
0.3	100
0.1	30
0.03	10
0.01	3

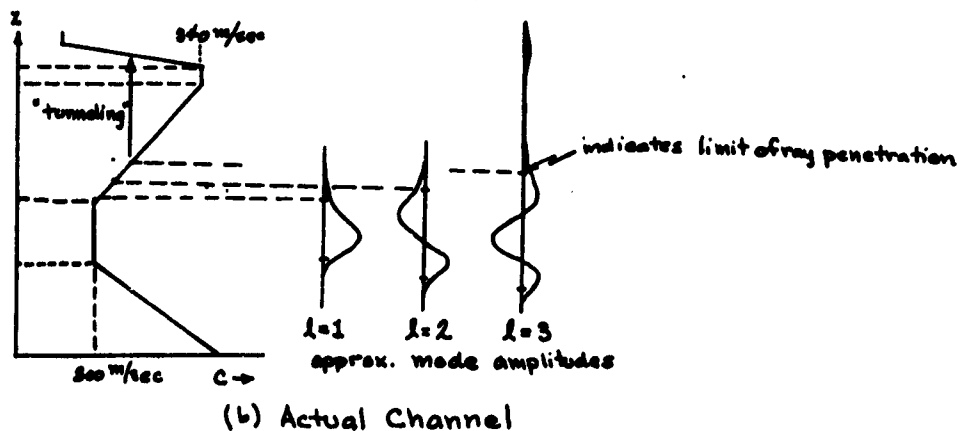
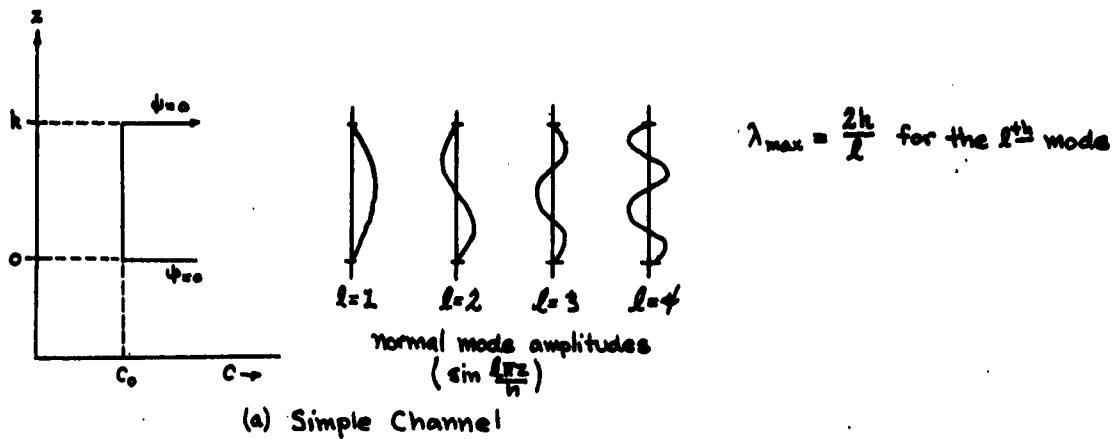
At ranges of about 3000 km (~ 2000 mi) we might expect the ray picture to be of dubious utility at 1 cps, even assuming that the form of the duct is perfectly known. The accuracies listed above are, of course, maximum possible accuracies.

More realistic sound channels may be investigated by the general theory, although with a good deal of mathematical complexity. Analytic methods are definitely preferable to numerical methods, since the analytic insight allows flexibility of application to actual conditions. Numerical methods may, however, guide the choice of an appropriate analytic model, and may be employed for routine calculation. At the University of Denver we will use numeric methods in applying the general theory to its atmospheric applications to these ends.

In a realistic model, the mode amplitudes are similar to those in a simple model, but behave somewhat as shown in Fig. 2. As long as the channel is horizontally uniform the radial factors are unchanged. In addition to the normal modes, the lateral waves play an important role. Lateral waves are associated with the channeling of energy, and are analogous to the standing waves established on total internal reflection at a plane interface. Lateral waves are fed by the normal modes and extend past the geometric edges of the channel.

The attenuation of the signal as measured will be anomalously high compared to that calculated from the normal modes alone; the difference is the energy absorbed from the lateral waves. Since the region above the duct is characterized by high gas-kinetic absorption (which is due to the finite mean free path) attenuation in the lateral waves will be important for the higher frequencies and for the higher normal modes.

Without attenuation, the intensity of the normal modes decays as r^{-1} (and intensity in the lateral waves as r^{-2}). At moderate ranges, absorption in the lateral waves leads to a $r^{-3/2}$ decay of the normal modes. At greater ranges, the attenuation becomes exponential.



I-3 Figure 2

An interesting effect related to the penetration of the acoustic field beyond the geometric channel is an effect analogous to quantum-mechanical tunneling. Above the speed maximum forming the top of the channel the speed drops rapidly to the relatively low value of about 260 m/sec. Channeled waves could also propagate here, but they are separated from the upper minimum by a forbidden band of high velocity. In the wave picture, each normal mode has a finite amplitude in the upper channel--the energy "tunnels" beneath the high-velocity barrier into this region. At these high altitudes (on the order of 90 km) the attenuation is high even for frequencies as low as 1 cps. The tunneling, therefore, represents a constant drain on the energy in the lower channel. If a mode should resonate with the upper channel, i.e., have a reasonable amplitude there, it will be rapidly attenuated. The higher modes are particularly susceptible to tunneling.

Dispersion is another evidence of the wave character of the field; in general the phase velocity depends on the frequency for each normal mode. The group velocity, which differs from the phase velocity by a term depending on this variation, is important in the study of the signal form. In dispersive propagation the relative phase of the frequency components of the signal is continually changing, resulting in radical alterations of form. In addition, the different modes are characterized by different velocities. The appearance of signals that have propagated over a great distance is as characteristic of the dispersion as it is of the initial signal.

We conclude that the study of acoustic sources and their signals must be concerned with the conditions of propagation as well as with the source itself, and that the basis of the propagation study should be the explicit wave character of the field, especially for great distances.

REFERENCES:

- (1) Amme, R. C., The Absorption of Sound at High Altitudes, DRI Technical Note (Feb 1961)
- (2) Brekhovskikh, L. M., Waves in Layered Media (Trans) (Academic Press, New York, 1960)
- (3) Brinkley, S. R. and J. G. Kirkwood, "Theory of Propagation of Shock Waves" Phys. Rev. 71, 606 (May 1947)
- (4) Cox, E. F., "Far Transmission of Air Blast Waves" Physics of Fluids, 1, 95 (March 1958)
- (5) DRI, Status Report, Cont. No. Da-23-072-ORD-1486 (Nov. 1960)
- (6) Feng Shao-Sung, "Reflection of Finite-Amplitude Waves" Akust. Zhur. 6, 491 (Oct 1960)
- (7) Lighthill, M. J., Higher Approximations in Aerodynamic Theory (Princeton Univ. Press, Princeton, 1960) (Chapter 6)
- (8) Marsh, H. W., "The Use of Ray Methods and First Order Diffraction Corrections", USL Tech Memo No. 1100-61-54, New London Connecticut, 1954.
- (9) Haskell, N. A., "Asymptotic Approximation for the Normal Modes in Sound Channel Wave Propagation" J. Appl. Phys. 22, 157 (1951)

SOME EFFECTS OF FLIGHT PATH UPON THE DISTRIBUTION OF SONIC BOOMS

Donald L. Lansing

National Aeronautics and Space Administration
Langley Research Center, Virginia

INTRODUCTION

The sonic boom has become one of the important operating problems associated with flight at supersonic speeds. At present, the sonic boom is associated only with the operation of high speed military aircraft, but the problem will certainly carry over to the future operation of supersonic transports. In fact, the sonic boom is considered to be one of the most serious problems connected with the transport development program. Accordingly, the sonic boom has continued to be the subject of intensive theoretical and experimental investigation.

There are two quantities associated with the boom which are of particular interest in aircraft operations: The strength and the location, ~~on the ground, of the shock waves emanating from the aircraft.~~ These two quantities depend upon a wide variety of variables, some of which are shown in Figure 1. The various factors listed there under Aircraft Design and Atmospheric Conditions have been treated theoretically in a considerable number of papers, references 1-16. Many wind-tunnel tests and flight tests have been performed in an attempt to assess the validity of these theories for aircraft operating at constant altitudes and constant Mach numbers, references 17-24.

The present paper will be concerned mainly with the factor listed under Aircraft Operations called "Flight Maneuvers". Any rapid deviations of the aircraft from constant altitude and constant speed flight can produce considerable modifications in the location and the strength of the ground shock-wave pattern. Military aircraft performing simple maneuvers in the course of routine flights have, on several past occasions, produced some rather unusual sonic boom patterns; at least this is strongly implied by the distribution of complaints received after the flights. Since maneuvers such as turns, climbs, and dives are a normal part of routine aircraft operations, some means for estimating the effects of maneuvers on the sonic boom is necessary.

The Nature of the Sonic Boom for Uniform Flight-

Before introducing the complications of the sonic boom which can result from maneuvers consider briefly the nature of the sonic boom for level, constant-speed flight, see Figure 2. This figure shows several shock fronts and ray paths as they would appear in an atmosphere in which the speed of sound decreases linearly with altitude. The shock fronts are, of course, responsible for the boom; whereas the rays are the paths along which the shock travels from its origin on the flight path to the ground are shown. Both the shock fronts and the rays are arcs of circles. These two families of curves intersect one another at right angles.

The curvature of the shock fronts and ray paths is a direct result of the refracting effect of the inhomogeneous atmosphere. In a homogeneous atmosphere the shocks and the rays would each be straight lines; in three

FACTORS AFFECTING THE SONIC BOOM

AIRCRAFT DESIGN

**CONFIGURATION (FINENESS RATIO)
LIFT (WEIGHT)
DRAG**

AIRCRAFT OPERATIONS

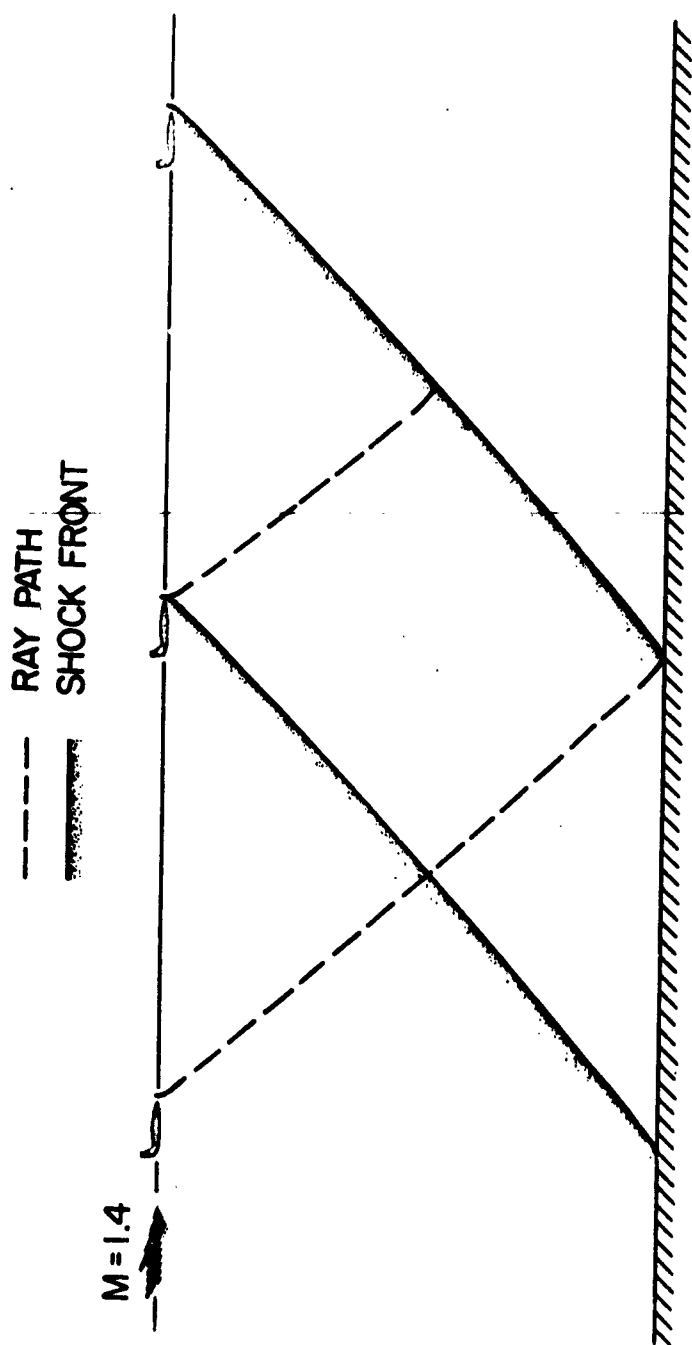
**ALTITUDE
MACH NUMBER
* FLIGHT MANEUVERS**

ATMOSPHERIC CONDITIONS

**WIND DIRECTION
WIND VELOCITY GRADIENT
SPEED OF SOUND GRADIENT
PROPAGATION LOSSES**

NASA

I-4 Figure 1.- Factors affecting the sonic boom.



NASA

I-4 Figure 2.- Ray paths and shock fronts for level flight.

dimensions the complete shock front would be the familiar Mach cone. The exact size and shape of the circular ray paths is determined by the aircraft altitude and velocity and the gradient in the speed of sound. Under the appropriate conditions the rays can be refracted to the extent they do not reach the ground.

Note that the two shock fronts are not the same shock traveling parallel to the ground; only that portion of the shock between the two rays is common to both fronts. The N-shaped pressure pulse characteristic of the sonic boom requires a second "tail" shock immediately behind the aircraft in addition to the single "bow" shock shown in the figure. For the sake of simplicity, however, in what follows any single shock front should always be interpreted as a complete sonic boom.

The Effects of Maneuvers-

Theoretical studies of the effect of maneuvers on the location and strength of sonic booms have been carried out from the standpoint of geometrical acoustics in a homogeneous atmosphere by a number of investigators. The problem of determining the shape and extent of the shock wave originating from a sound source traveling at supersonic speeds in non-uniform motion has been treated for example, by Prandtl, and Lilley and Struble and their collaborators, references 25-28. The problem of predicting the variations in the strength of the shock which are induced by maneuvers has been treated by Rao, reference 29, Randall, reference 14, and Struble, et al, reference 28.

Only a meager amount of experimental evidence relating to the effect of maneuvers on the shock pressures is available. Some rocket sled tests carried out in this country by the Armour Research Foundation and several flights of a fighter aircraft in England afford some qualitative support to the existing theories, but the results are insufficient for drawing any general conclusions, references 30 and 31.

In order to help fulfill this need for experimental data a flight test program is being planned for the purpose of measuring the ground shock wave pressures of aircraft executing predetermined flight maneuvers similar to those encountered in actual military and civilian aircraft operations.

Purpose of this paper-

The present paper is a summary of one aspect of the theoretical studies being carried out in connection with this program. The objective of these studies is to determine, for the purpose of locating pressure measuring devices, the ground areas over which intensified shock pressures are likely to occur. The analytical work is based upon the acoustic theory of the propagation of sound in an inhomogeneous atmosphere. For the purpose of the calculations presented in this paper the speed of sound is assumed to decrease linearly with altitude at a rate of .0040 ft/sec per foot. This type of variation agrees substantially with measured data and is a useful assumption up to altitudes between 35,000 or 40,000 feet.

In the course of the investigation it was found that the classical equations which govern the acoustic approximation of the shock-wave shape could be put into a form which does not seem to be available in the literature and which is very convenient for machine computation. Using this form of the equations it has been possible to obtain the ground shock-wave patterns for a much wider variety of flight maneuvers than can be readily handled by graphical procedures. It is hoped that these equations might prove useful to others concerned with the sonic boom problem.

Analysis

The basic equations which theoretically govern the shape and extent of the shock wave of a supersonic aircraft in arbitrary motion are the following:

$$(x - x_0)^2 + (y - y_0)^2 + (z - z_0 + A)^2 = R^2 \quad (1)$$

$$(x - x_0)\dot{x}_0 + (y - y_0)\dot{y}_0 + (z - z_0 + A)(\dot{z}_0 - \dot{A}) = -R\dot{R} \quad (2)$$

in which x_0 , y_0 , z_0 and \dot{x}_0 , \dot{y}_0 , \dot{z}_0 denote the position and velocity of the aircraft along the flight path, and A and R are functions depending upon the inhomogeneous atmosphere assumed. If the speed of sound a decreases linearly with altitude according to the relation $a = a_g - mz$ it can be shown that:

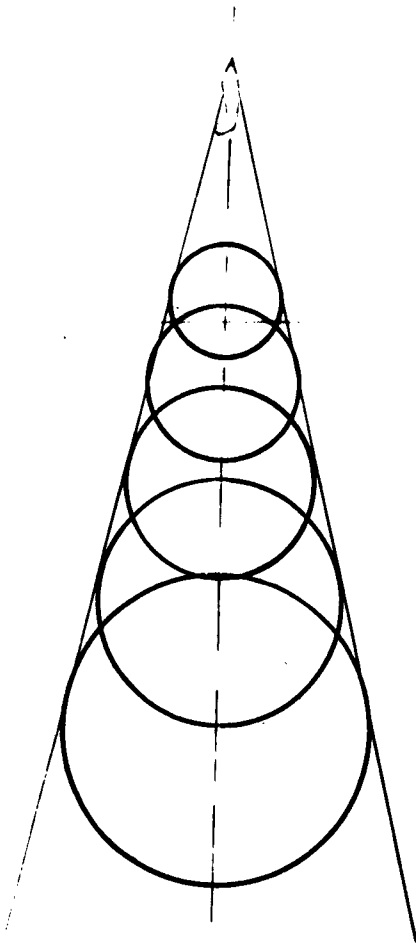
$$A = \frac{a_0}{m} \left[\cosh m(t - \tau) - 1 \right] \quad \dot{A} = -a_0 \sinh m(t - \tau)$$

$$R = \frac{a_0}{m} \sinh m(t - \tau) \quad \dot{R} = -a_0 \cosh m(t - \tau)$$

where $a_0 = a_g - mz_0$, a_g is the speed of sound at the ground, and t is the time at which the shape of the shock-wave is to be obtained. The parameter τ , which represents an arbitrary previous time at which the aircraft position and velocity were $x_0(\tau)$, $y_0(\tau)$, $z_0(\tau)$ and $\dot{x}_0(\tau)$, $\dot{y}_0(\tau)$, $\dot{z}_0(\tau)$ respectively, accounts for the past history of the aircraft along the flight path, see reference 14.

The first equation describes the shape of a single wave front expanding about an arbitrary point (x_0, y_0, z_0) of the flight path. The second equation, considered simultaneously with the first, constitutes the condition that these wave fronts form an envelope. Within the approximations of acoustic theory this envelope represents the shock wave of the aircraft. Figure 3 illustrates an aircraft in level constant speed flight in a homogeneous atmosphere, $m = 0$. In this case, the wave fronts are circles with centers on the flight path and the envelope is the familiar Mach cone.

These two equations can be solved so as to obtain the three dimensional shape of the shock wave, the ground shock wave pattern, and a vertical cross section of the wave explicitly in terms of the aircraft position and velocity along the flight path. The manner in



$$1. (x-x_0)^2 + (y-y_0)^2 + (z-z_0+A)^2 = R^2$$

$$2. (x-x_0) \dot{x}_0 + (y-y_0) \dot{y}_0 + (z-z_0+A) (\dot{z}_0 - \dot{A}) = -R\dot{R}$$

I-4 Figure 3.- The Mach cone for level flight.

NASA

which this is accomplished for the ground pattern is briefly as follows:

Introduce a "spherical" coordinate system R, θ, ψ defined by

$$\begin{aligned}x - x_0 &= R \cos \psi \cos \theta \\y - y_0 &= R \cos \psi \sin \theta \\z - A &= R \sin \psi\end{aligned}\tag{3}$$

Substituting equations (3) into equations (1) and (2) it is seen that equation (1) is identically satisfied and equation (2) becomes

$$\dot{x}_0 \cos \psi \cos \theta + y_0 \cos \psi \sin \theta + (\dot{z}_0 - \dot{A}) \sin \psi = -\dot{R}\tag{4}$$

Since $z = 0$ on the ground we have

$$\sin \psi = -\frac{A}{R}, \quad \cos \psi = \frac{\sqrt{R^2 - A^2}}{R}$$

Substituting these relations into equation (4) and solving for θ we obtain

$$\begin{aligned}\cos \theta &= \frac{1}{V_1^2 \sqrt{R^2 - A^2}} \left[\dot{x}_0 D \pm \dot{y}_0 \sqrt{V_1^2 (R^2 - A^2) - D^2} \right] \\ \sin \theta &= \frac{1}{V_1^2 \sqrt{R^2 - A^2}} \left[\dot{y}_0 D \pm \dot{x}_0 \sqrt{V_1^2 (R^2 - A^2) - D^2} \right]\end{aligned}$$

which, with equation (3) gives the desired equations for the ground pattern,

$$\begin{aligned}x &= x_0 + \frac{1}{V_1^2} \left[\dot{x}_0 D \pm \dot{y}_0 \sqrt{V_1^2 (R^2 - A^2) - D^2} \right] \\ y &= y_0 + \frac{1}{V_1^2} \left[\dot{y}_0 D \pm \dot{x}_0 \sqrt{V_1^2 (R^2 - A^2) - D^2} \right]\end{aligned}$$

where

$$V_1^2 = \dot{x}_0^2 + \dot{y}_0^2$$

and

$$D = \dot{z}_0 A + a_g R$$

This form of the solution is very convenient for machine computation. One obtains, from each point of the flight path, two points on the ground shock wave pattern. The ground pattern can be traced out if the position and velocity of the aircraft are known at a sufficient number of time intervals. From these equations the ground patterns for various typical flight maneuvers have been obtained. Some of these results are shown in Figures 4-9.

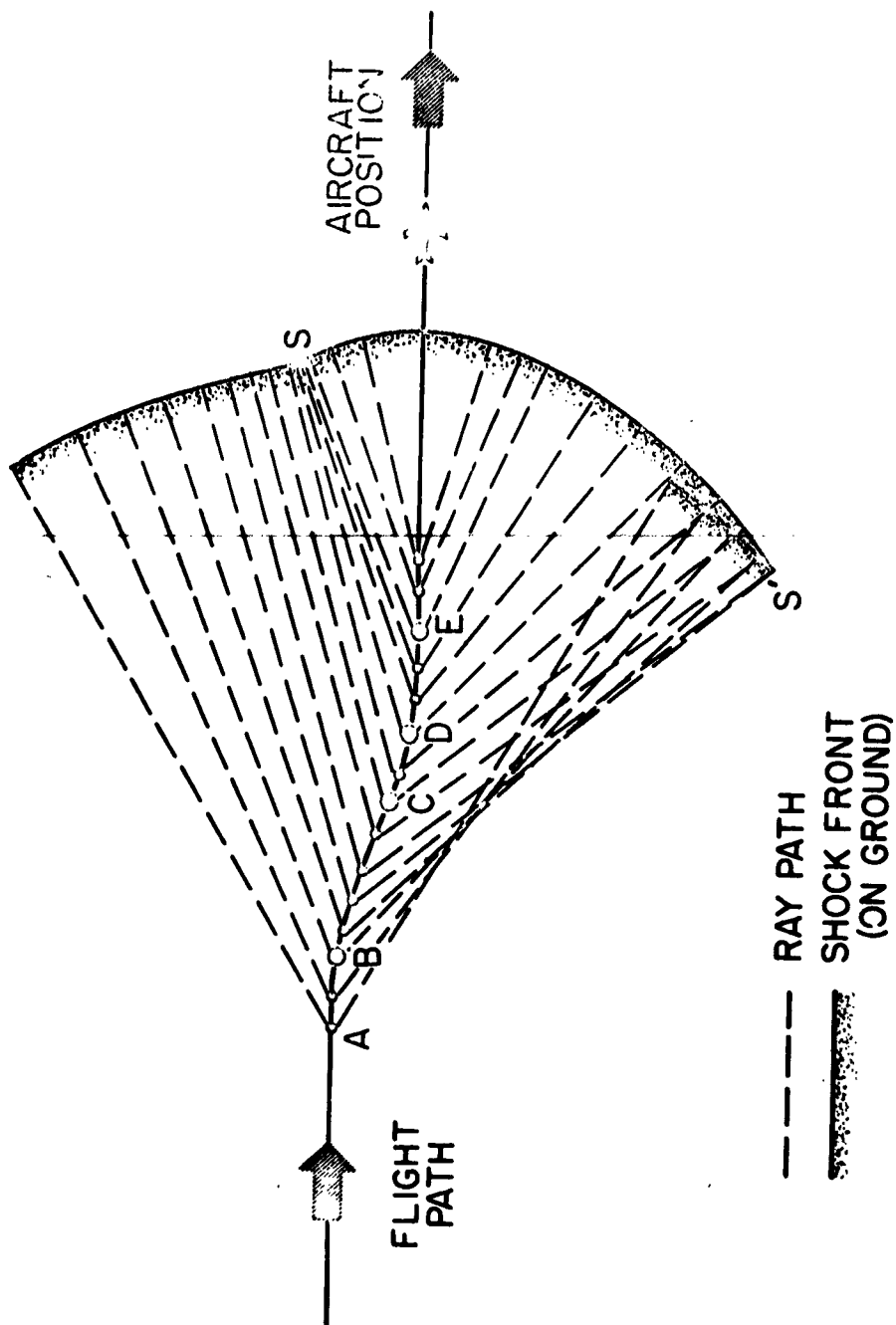
Applications and Discussion

Some Details of a Typical Ground Pattern; Focal Points and Cusps

First of all, it is helpful to consider in detail the sort of effects which maneuvers may have upon a typical ground pattern. Figure 4 shows, in plan view, the shock front on the ground produced by a side-slip type of maneuver at constant altitude. The flight path, being viewed from above, lies in a plane at 30,000 feet altitude. The velocity component parallel to the two straight portions of the path is held constant, and corresponds to a Mach number of 1.3. The maneuver between A and E displaces the aircraft laterally a distance of 3 miles as the aircraft travels forward a distance of 14 miles. As a result of the lateral velocity the Mach number at the middle of the maneuver has increased slightly to 1.35.

The lines connecting the flight path to the shock front indicate the vertical planes of the rays along which the shock waves from various points of the flight path travel in order to reach the ground. The aircraft is in the indicated position at the time the shock front is formed. The points along the flight path from which the rays emerge are taken at equal intervals of time. Since the Mach number of the aircraft changes only slightly along the flight path the distance between consecutive points is nearly the same and about the same amount of energy travels between any pair of consecutive rays. Any focusing of the rays implies a focusing of the energy being transmitted along them.

This figure clearly illustrates two different effects which flight path curvature may have upon the distribution of sonic booms. First, point S is a focal point of the shock wave. The shock waves originating between points D and E and traveling downward to the left of the flight path converge in the neighborhood of S. The shocks originating near D are weaker than those originating near E since they have traveled a greater distance. However, the effect of focusing the shocks and energy originating over a considerable portion of the flight path in such a concentrated area will lead to increased pressures. Second, note the cusp in the shock at S' which is formed as the shock is folded back upon itself. Two shocks of approximately equal intensity follow one another very closely in the neighborhood of such a cusp and coalesce at the cusp. The shorter branch of the cusp shown here is about 5 miles long, the distance between the two branches is at most 1 mile. The energy originating between points B and C of the flight path which would be spread over a considerable area for level uniform flight is now concentrated in two shocks near the tip of the cusp. At the present time it is not certain whether the two shock waves in such a long and narrow cusp will remain

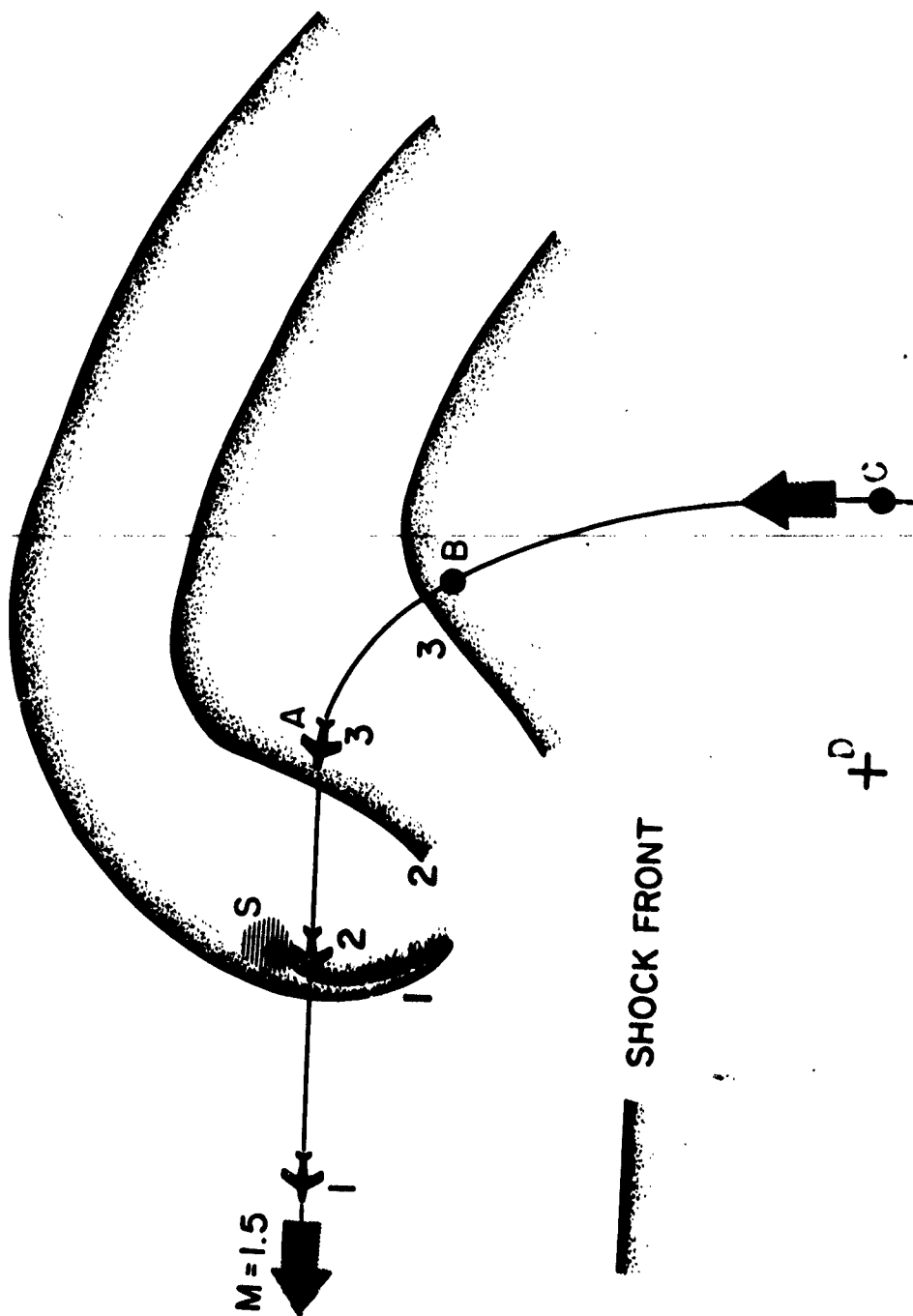


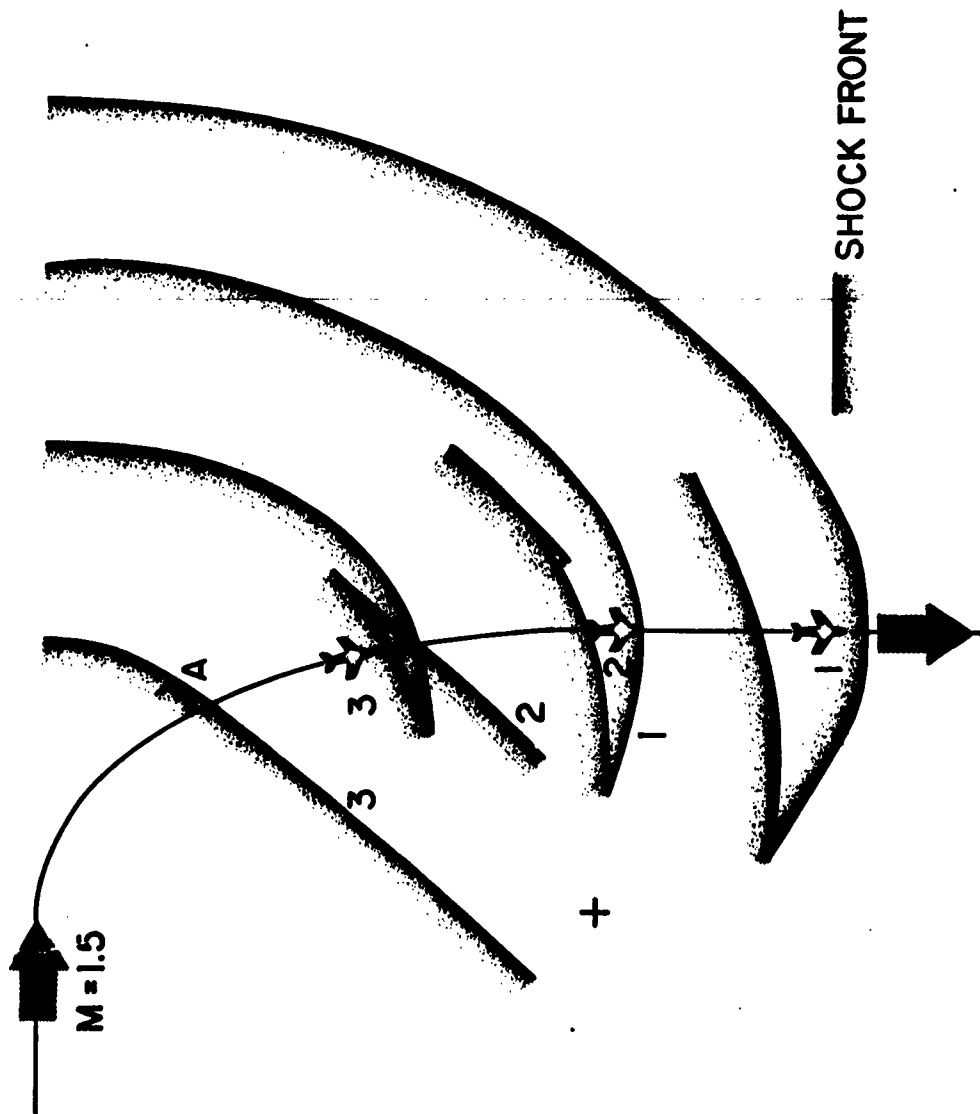
I-4 Figure 4.- Ground shock wave showing formation of cusps and foci.

115A

Horizontal left turn

I-4 Figure 6.- Ground shock wave for an elliptical turn.

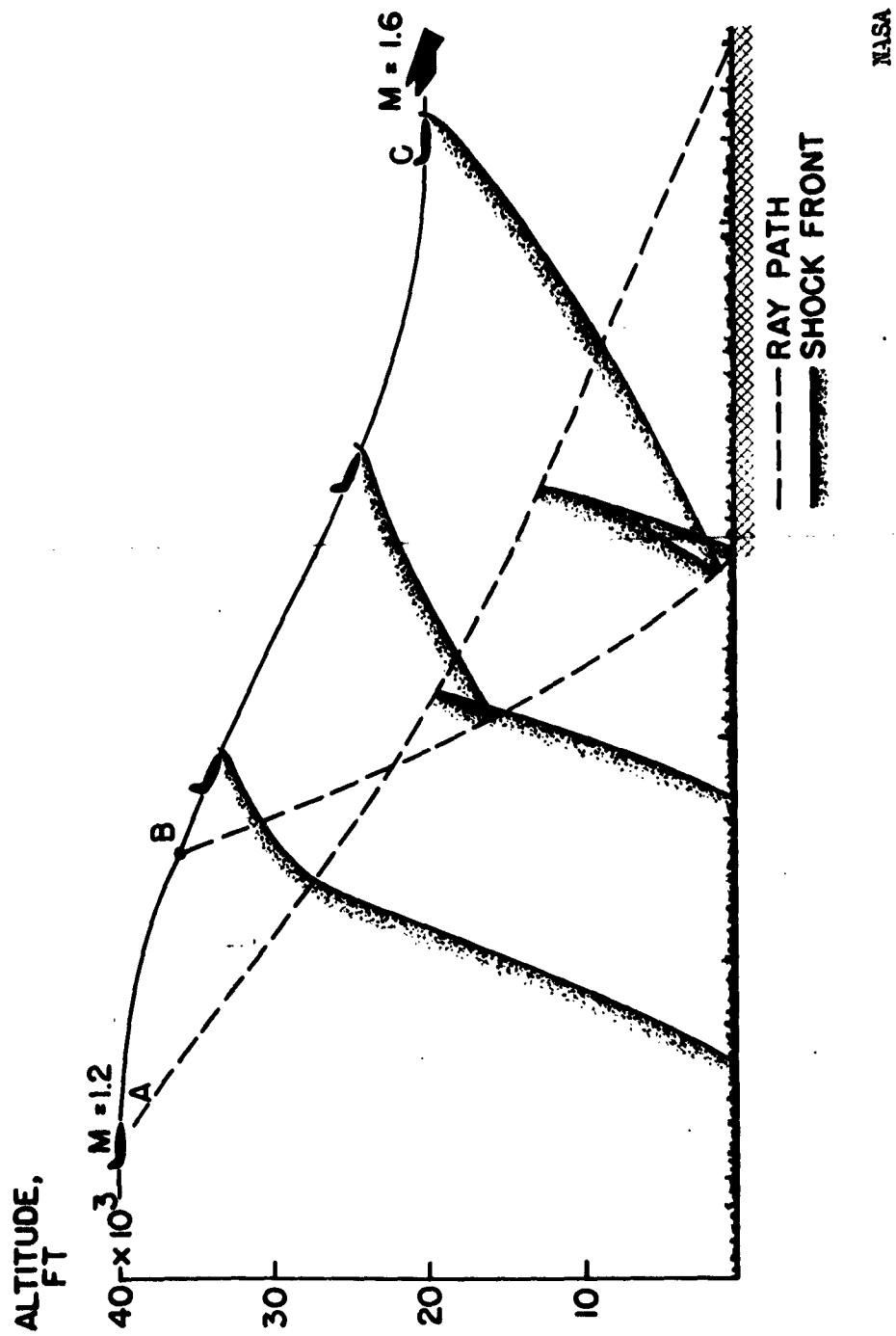




Horizontal right turn

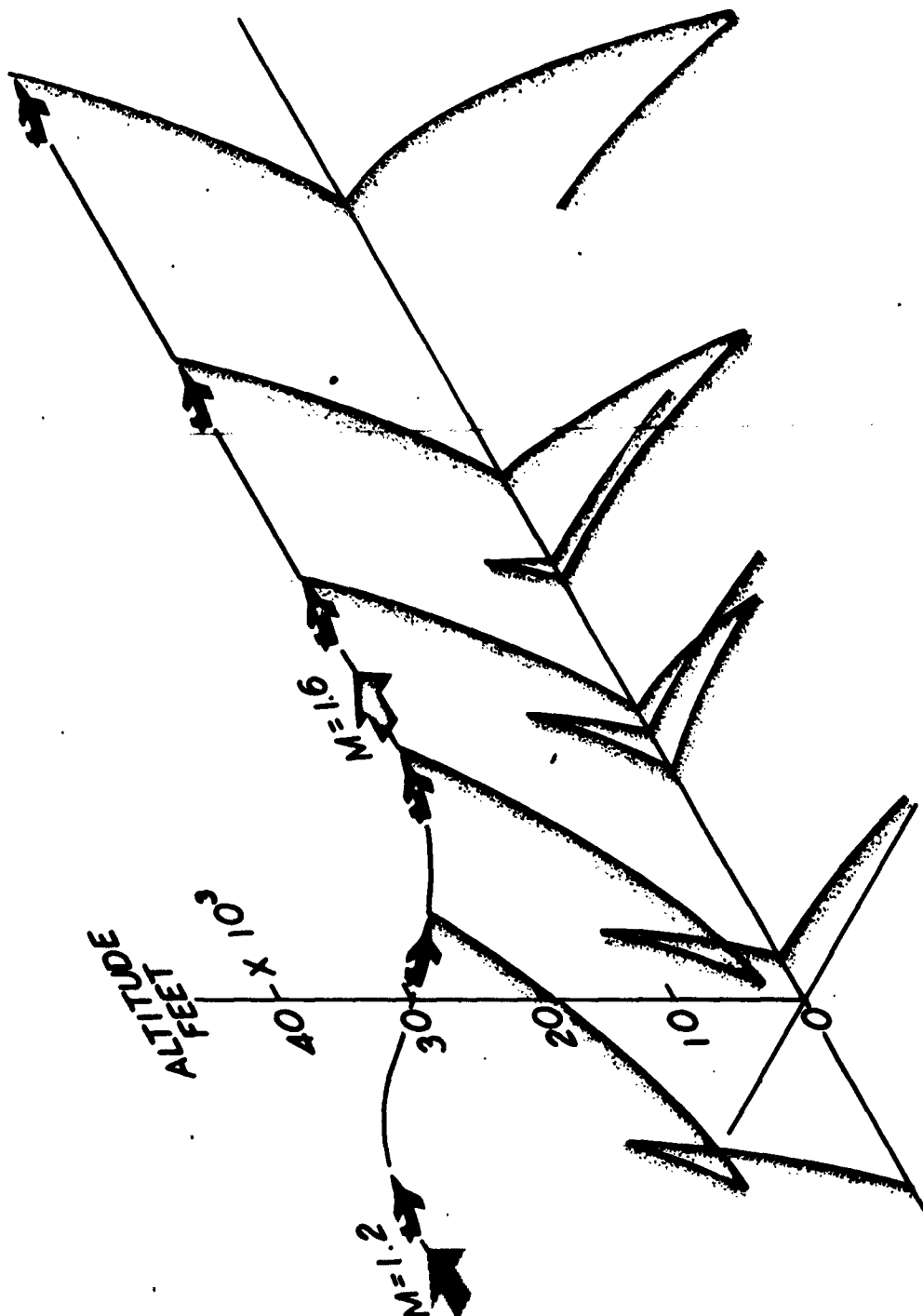
I-4 Figure 7.- Ground shock wave for an elliptical turn.

315A



Vertical cross section

I-4 Figure 8.- Ray paths and shock fronts for a dive.



NASA

Vertical cross section and ground pattern

Figure 9.- Shock wave pattern for a dive.

I-4

distinct so as to give rise to multiple sonic booms or whether they will coalesce near the cusp so as to form a single intensified shock.

Thus the convergence of the rays in the neighborhood of focal points and the overlapping of the rays which leads to cusps gives a qualitative indication of the relative energy concentration and shock pressures along the ground pattern, but is insufficient in itself for predicting the magnitudes of the pressures. In fact, linear theory estimates of the pressures based upon the convergence of the rays predicts infinite pressures at cusps and focal points. Indeed, both the location and the strength of the shock waves in the vicinity of cusps and focal points will be determined in a large degree by the complicated nonlinear mechanisms of shock propagation. Since the operation of these mechanisms on a large scale in the presence of a nonuniform medium is not well understood no attempt has been made here to include these effects in the results.

Horizontal Maneuvers-

Figure 5 shows several ground shock wave patterns for the same maneuver shown in Figure 4. The numbers in the figure relate the aircraft position to the corresponding ground pattern. It will be recalled that the rays and, therefore, the shock waves, originating between points B and C of the flight path overlap. This leads to two cusps on the right side of the flight path. The waves originating between D and E of the flight path are focused in the neighborhood of point S on the left side of the flight track. The shaded area around S indicates a region in which the shock waves are highly concentrated and will produce a more intense boom.

Figures 6 and 7 show several ground patterns for a horizontal elliptical turn. Again the view is from above the flight path, which also lies at an altitude of 30,000 feet. The Mach number along the path is held constant at 1.5. In Figure 6 the segment AC of the flight path is a quadrant of an ellipse whose center lies at D. The distance CD is about 8.8 miles, and AD is about 17.6 miles. The shock waves originating between points B and C and travelling toward the inside of the flight path are focused in the neighborhood of point S. The cusp which is formed spreads over the ground toward the lower left. Figure 7 shows several ground patterns for the same path as in Figure 6 but with the aircraft flying in the reverse direction. This path does not create a focal point as in the previous case. However, the shock begins to fold over itself in the vicinity of A. This "knot" in the shock develops into a pair of cusps which spread along the ground directly beneath the flight track. These two figures indicate how a change in the direction of motion of the aircraft along a given path can alter the ground shock wave. The differences are associated with the different rates of change of the normal acceleration along the two paths.

Vertical Maneuver-

If the aircraft moves in a fixed vertical plane, as in a climb or dive, the ground pattern will be symmetric with respect to the flight

track. In this case a vertical cross section of the shock wave in the plane of the flight path also shows some interesting features and is helpful in interpreting the ground pattern.

Figure 8 shows a vertical cross section of the shock wave produced by an aircraft in a dive. The dive which can be described by one-half of a sine wave begins at point A at 40,000 feet and $M = 1.2$, and terminates at point C at 20,000 feet and $M = 1.6$. Prior to and subsequent to the dive the aircraft is assumed to be in level constant speed flight. The distance from A to C along the ground is about 15 miles so that the maximum dive angle, greatly exaggerated in the figure, is about 21 degrees. The rays emanating from points of the flight path between A and B intersect that the shock is folded back upon itself as it propagates toward the ground. Below the intersection of these two rays the shock consists of three branches which join together to form two cusps. The lowest shock of this group, having originated along the level portion of the flight path preceeding the dive, is much weaker than the other two shocks since it has traveled a greater distance. However, two shocks of nearly equal intensity coalesce at each cusp. Intensified shock pressures are expected where these cusps hit the ground. Three separate rays meet at every point within the hatched area at the right of the figure: one originating from the level flight path preceeding the dive, one originating from the path between A and B, and another from the flight path beyond point B. Hence, three separate shock waves strike each point of the ground along this area. Multiple sonic booms would be expected in this region which is about 8 miles long.

Figure 9 shows a three dimensional view of both the vertical cross section and the ground pattern for the dive of Figure 8. The ground pattern is symmetric with respect to the flight path so that only the part on the right side of the flight track is shown. The three shocks which are developed in the vertical plane spread laterally about 6 miles and result in multiple booms over an appreciable ground area. As the aircraft proceeds along the low-altitude level portion of the flight path the complicated shock pattern produced by dive hits the ground and vanishes. The ground shock is left with a fold which gradually unravels as the aircraft continues so that the end result is the familiar hyperbolic shaped ground shock.

Acceleration along a straight and level flight path, as well as flight path curvature, can cause the rays to overlap. An aircraft in level flight which accelerates through Mach number one creates a single cusp in the vertical plane. The two booms which result from this type of shock front have been observed by British investigators in the flight tests mentioned previously.

Concluding Remarks

In conclusion, an analytical technique has been presented for obtaining some indication of the ground areas likely to experience intensified pressures or multiple booms as a result of flight maneuvers and the results of some applications have been discussed. It has been shown that intensified

shock pressures may occur over limited areas at some distance from the flight path. The method for locating these regions has been programmed for the IBM 650 electronic computer and is available for application to any specific maneuver. It is hoped that flight test measurements will provide a means for establishing correlation between experiment and theory and will present some indication of the ground pressures.

REFERENCES

1. Whitham, G. B.: The Flow Pattern of a Supersonic Projectile. Communications on Pure and Appl. Math., vol. V, no. 3, August 1952, pp. 301-348.
2. Lansing, Donald L.: Calculated Effects of Body Shape on the Bow-Shock Overpressures in the Far Field of Bodies in Supersonic Flow. NASA TR R-76.
3. Warren, C. H. E.: An Estimation of the Occurrence and Intensity of Sonic Bangs. R. A. E. Tech. Note Aero. 2334, September 1954.
4. DuMond, J. W. M., et al: A Determination of the Wave Forms and Laws of Propagation and Dissipation of Ballistic Shock Waves. Jour. Acou. Soc. America, vol. 18, no. 1, July 1946, pp. 97-118.
5. Walkden, F.: The Shock Pattern of a Wing-Body Combination, Far From the Flight Path. Aero. Quarterly, vol. IX, pt. 2, May 1958, pp. 164-194.
6. Rhyning, I. L., Yoler, Y. A.: Supersonic Boom of Wing-Body Configurations. Jour. of the Aero-Space Sci., vol. 28, no. 4, April 1961.
7. Morris, J.: An Investigation of Lifting Effects on the Intensity of Sonic Booms. Jour. of Royal Aeronautical Soc., vol. 64, October 1960.
8. Goebel, T. P.: A Correlation of Sonic Boom Measurements. North American Aviation Report No. NA-61-136, March 1961.
9. Rhyning, I. L.: The Supersonic Boom of a Projectile Related to Drag and Volume. Jour. Aero-Space Sci., vol. 28, no. 2, February 1961.
10. Buseman, A.: The Relation Between Minimizing Drag and Noise at Supersonic Speeds. Proceedings of the Conference on High-Speed Aeronautics, Poly. Inst. of Brooklyn, January 1955.
11. Goebel, T. P.: Development of a Method for Estimation of Supersonic Boom Intensities Based on Wave Drag, North American Aviation Report NA-61-136, Appendix B, March 1961.
12. Kornhauser, E. T.: Ray Theory for Moving Fluids. Jour. Acou. Soc. of America, vol. 25, no. 5, September 1953, pp. 945-949.
13. Theilheimer, F. and Rudlin, L.: The Influence of Atmospheric Pressure and Temperature Variations on Shock-Wave Propagation. NAVORD Report 2707, October 1953.
14. Randall, D. G.: Methods for Estimating Distributions and Intensities of Sonic Bangs. A. R. C. Tech. Report, R&M No. 3113, August 1957.

15. Meyer, R. E. and Ho, D. V.: Note on Shock Propagation in a Stratified Atmosphere. Brown University Tech. Report 35, August 1960.
16. Goebel, T. P.: Approximate Effect of Flight Path Angle and of Wind and Temperature Gradients on Cut-Off Mach Number. North American Aviation Report NA-61-136, Appendix D, March 1961.
17. Carlson, H. W.: An Investigation of Some Aspects of the Sonic Boom by Means of Wind Tunnel Measurements of Pressures about Several Bodies at a Mach number of 2.01. NASA TN D-161, December 1959.
18. Carlson, H. W.: An Investigation of the Influence of Lift on Sonic Boom Intensity by Means of Wind Tunnel Measurements of the Pressure Fields of Several Wing-Body Combinations. NASA TN D-881.
19. Hubbard, H. H. and Maglieri, D. J.: Ground Measurements of the Shock Wave Noise from Bomber-Type Aircraft in the Altitude Range from 30,000 to 50,000 Feet. NASA TN D-880.
20. Hubbard, H. H., Maglieri, D. J. and Lansing, D. L.: Ground Measurements of the Shock Wave Noise from Airplanes in Level Flight at Mach Numbers to 1.4 and Altitudes to 45,000 Feet. NASA TN D-48, September 1959.
21. Lina, L. J., and Maglieri, D. J.: Ground Measurements of Airplane Shock Wave Noise at Mach Numbers to 2.0 and at Altitudes to 60,000 Feet. NASA TN D-235, March 1960.
22. Mullens, M. E.: A Flight Test Investigation of the Sonic Boom. AFFTC-TN-56-20, U. S. Air Force, May 1956.
23. Daum, F. L. and Smith, N.: Experimental Investigation of the Shock-Wave Pressure Characteristics Related to the Sonic Boom. WADC-TN-55-203, U. S. Air Force, August 1955.
24. Smith, H. J.: Experimental and Calculated Flow Fields Produced by Airplanes Flying at Supersonic Speeds. NASA TN D-621, November 1960.
25. Lilley, G. M., et al: On Some Aspects of the Noise Propagation From Supersonic Aircraft. College of Aeronautics, Cranfield. Report No. 71, February 1953.
26. Prandtl, L.: Propagation of Sound By Bodies Moving at High Speeds. Heft 7, Schriften der Deutschen Akademie der Luftfahrtforschung, February 1938.
27. Fisher, D.: Weather Aspects of the Sonic Boom. Bureau of Naval Weapons Report RRS4-60-24, May 1960.
28. Struble, R. A. et al: Theoretical Investigations of Sonic Boom Phenomena. WADC Tech. Report 57-412, August 1957.

29. Rao, P. S.: Supersonic Bangs. Aero. Quarterly, vol. 7, pt. I, February 1956, pt. II, March 1956.
30. Main Rocket Sled Tests for Sonic Boom Program. Armour Research Foundation Project No. D094, Quarterly Report V, January-March, 1957.
31. Keir, T. H.: Experience of Supersonic Flying Over Land in the United Kingdom. NATO Report 250, September 1959.

**A NOMOGRAM FOR CALCULATING THE OVERPRESSURE
FROM THE DETONATION OF SMALL-YIELD HIGH EXPLOSIVES ***

Jack D. Fletcher

University of California Lawrence Radiation Laboratory
Livermore, California

For the past six years the University of California Lawrence Radiation Laboratory has been engaged in experimental work which results in sound propagation. It is not concerned, primarily, with the long-range propagation of sound although some of the explosions have probably been heard at very long ranges. The Laboratory is, instead, concerned with what might be called micro-range sound propagation.

At a site about twenty miles from the Livermore Laboratory and about seven miles from a small agricultural community, high explosives are shot daily. The yields of these shots range from a few grams to several hundred pounds. Our problem in the weather group is to predict the yield in equivalent pounds of TNT that might be detonated without disturbing residents of the surrounding communities. This very briefly outlines our basic concern in the field of sound propagation at LRL.

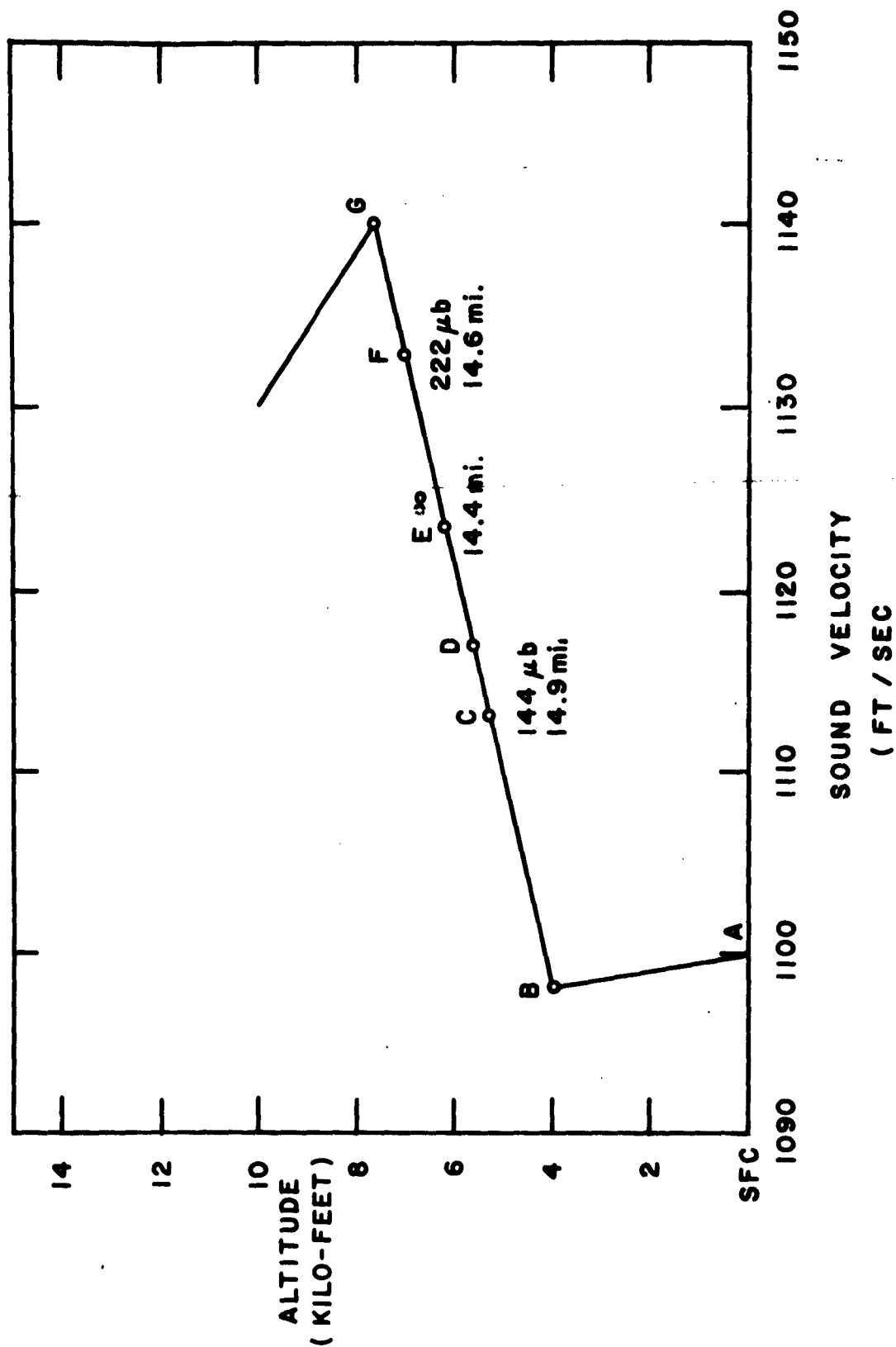
Our other problem is to continue to develop a more-or-less objective technique with which any one of several people working in the group might come up with essentially the same yield that might be detonated on any given day under the prevailing micrometeorological conditions.

The nomogram that is described is one of the objective techniques that allows us to issue prescribed weight limits.

The nomogram was developed to facilitate the analysis of the sound propagation properties of a given atmosphere. It produces answers that might also be attained by a hand calculation or by electronic computer if one is available. If the micrometeorologic situation is one in which the sound velocity in the direction of interest decreases linearly with height from the surface to any given altitude between 1000 feet to 10,000 feet and then increases with height to another altitude, the nomogram may be used. The nomogram, based on classical theory by Cox et al.,¹ predicts the distance of the inner boundary of the first noise zone. This is important since starting rays with equal amounts of energy will tend to concentrate or converge near the inner boundary of this first noise zone at a theoretical point of infinite intensity.² But since infinite pressure from a shot is unrealistic, we have arbitrarily taken the calculated pressure at .2 of a mile from the theoretical infinity for use in the prediction of overpressure from the nomogram. It should also be stated that the predicted overpressures are those that would be expected from a 10-pound yield of TNT high explosive.

Figure 1 shows a V-H profile presented by points ABG. If this were an actual V-H profile drawn from the latest micrometeorological data, the nomogram would predict 225 ~~lb~~ at a distance 14.4 miles. If the end point on the V-H profile was at point D, the proper analysis of the V-H profile

*Work was performed under auspices of the U. S. Atomic Energy Commission.



I - 5 FIGURE 1

should also predict 225 μ b at a distance of 14.4 mi. The calculated pressure for any end point between points D&F will produce pressures higher than 225 μ b. If, however, the end point on an actual V-H profile in which the sound velocity started to increase at 4000 feet was at point C, the pressure would be less and distance somewhat beyond that calculated for the infinite intensity distance. The calculated pressure for point C is 144 μ b at a distance of 14.9 mi. The dotted lines on the nomogram, in Figure 2, show the change in velocity that the end point on a V-H profile must have in excess of the surface velocity to predict maximum realistic overpressure.

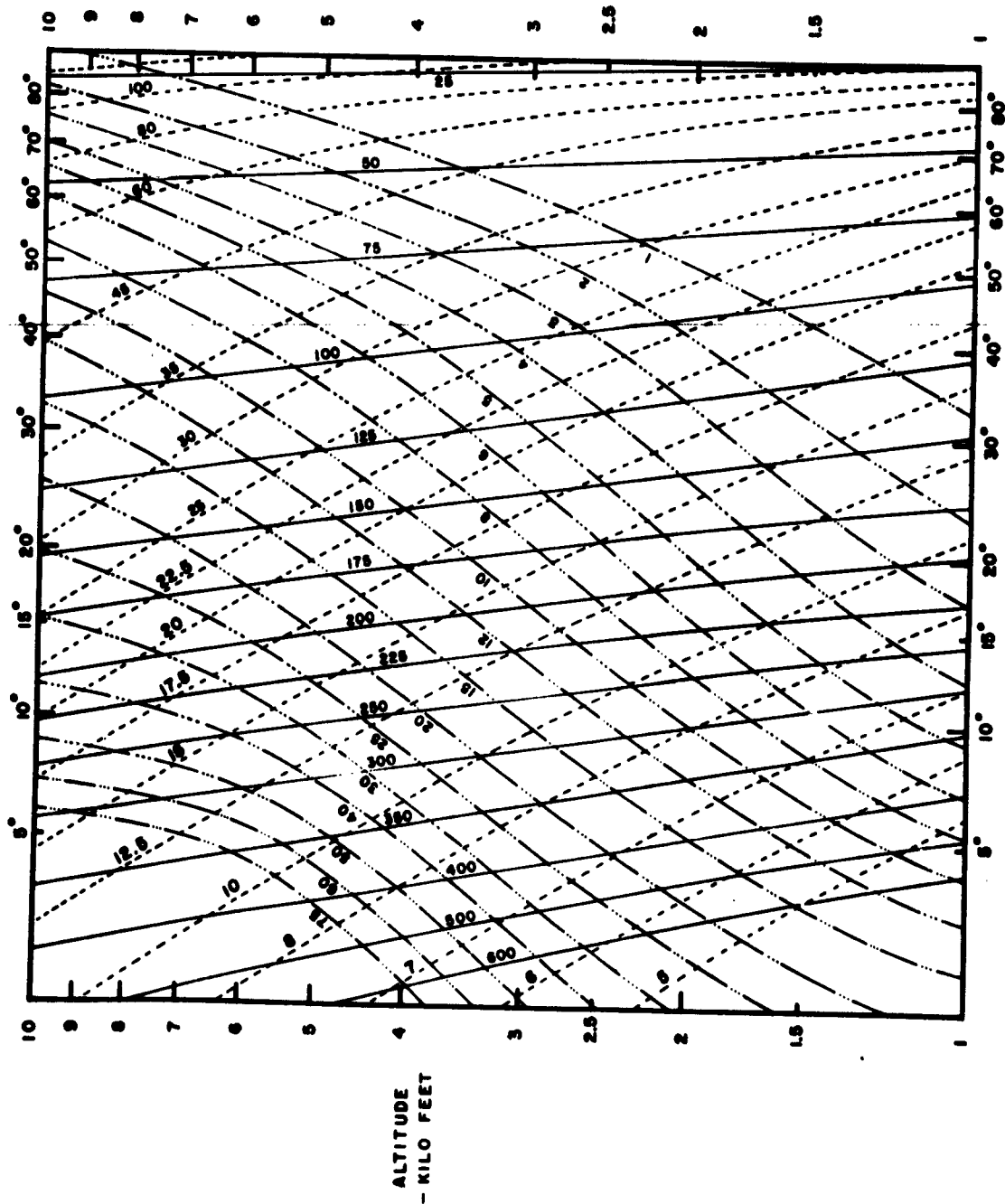
The most critical parameter in the analysis of V-H profile is the slope, or the rate of increase of sound velocity, from B to G in Figure (1). The other important parameter is the altitude at which the sound velocity starts its increase. These two parameters taken from a V-H profile will allow the prediction of overpressure and the distance of the inner boundary of the first noise zone from the nomogram.

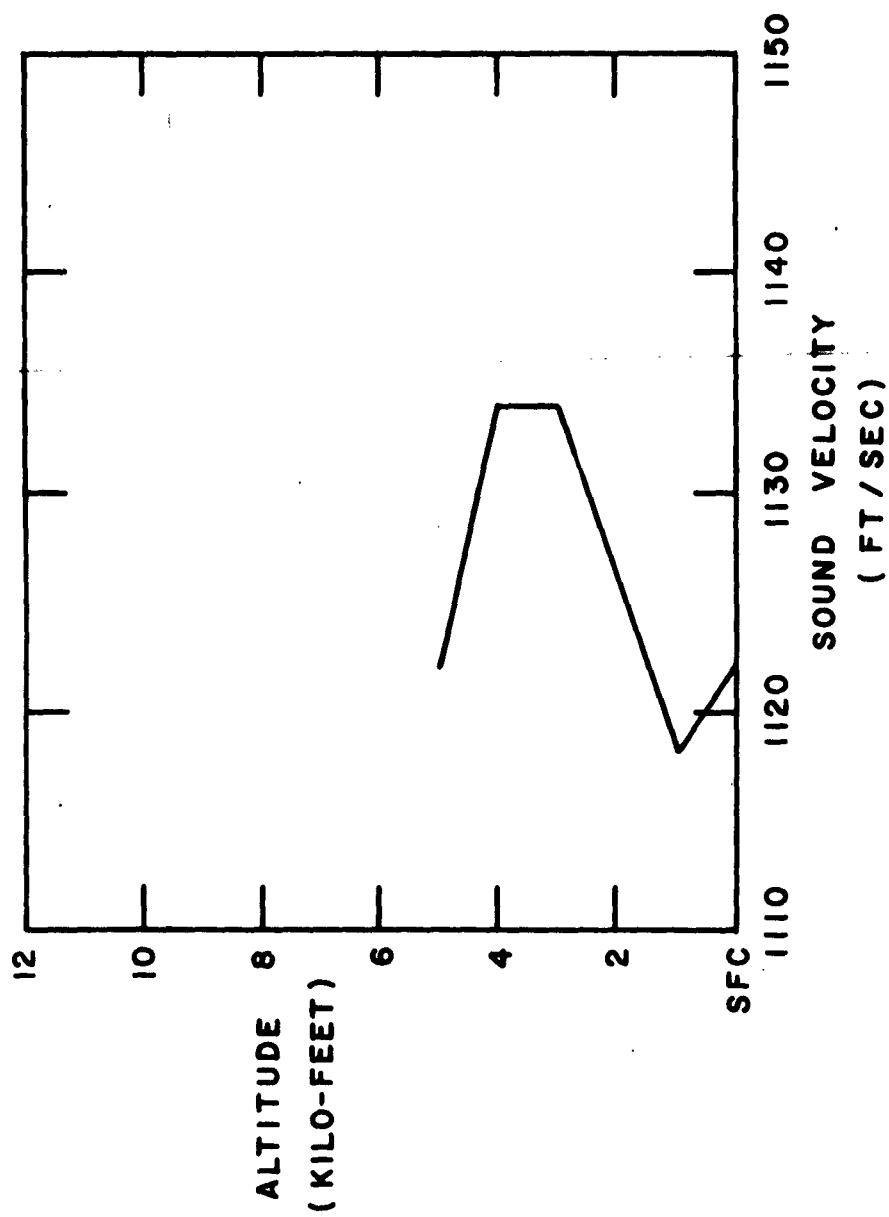
Figure 2 shows the nomogram. The abscissa is the slope of the positive phase of the V-H profile, and the ordinate is the altitude at which the slope becomes positive. The solid, more-or-less vertical lines show the overpressure predicted in microbars, the dashed lines curving upward to the left show the distance of infinite intensity, and the dotted lines curving upward to the right show the change in sound velocity that the end point on the V-H curve must have in excess of the surface velocity to reach the maximum overpressure shown by the pressure lines. If the actual change in velocity exceeds the ΔV shown by the dotted lines, the pressure lines will be representative.

Figure 3 shows an actual V-H profile for the atmosphere over our test site on February 9, 1961. The analysis of this profile shows a positive slope of 20° with the increase starting at 1000 feet. From the nomogram we obtain a predicted overpressure of 200 μ b at a distance of 9 miles, based on a 10-pound shot. The direction of interest for this particular profile is on a bearing of 50° from the test site. Seven to nine miles from the test site on this bearing we have 4 permanent microbarograph stations. A 30-pound shot fired 35 minutes prior to this meteorological run produced overpressure of from 75 μ b to 120 μ b among the array of microbarographs.

On February 9, 1961 a cold front occlusion was orientated east-west across Northern California and was moving south. A velocity shear, which dominated the V-H profile, was at about 3500 feet at 1200Z. The shear level lowered throughout the morning and was evident at 2000 feet over the test site at shortly after shot time.

We have found that in situations in which frontal movement is 15 to 20 knots the height of the positive slope will gradually lower until frontal passage and not lift appreciably until several hours after the front has passed. On the other hand slowly moving fronts may not even produce a positive slope to the V-H profile until they are within a few miles of the test site. Allowable shot yields usually rise quite rapidly after the passage of a slow moving front.





I - 5 FIGURE 3

Three hundred microbars have been arbitrarily chosen at LRL as the overpressure that we do not wish to exceed. So by establishing the 300 μ b limit and by having the predicted overpressure for 10 pounds from the nomogram we can attain a maximum shot yield by assuming that the relationship between pressure and yield is

$$\left(\frac{P_1}{P_2} \right)^{2.3} = \frac{W_1}{W_2}$$

and where P_2 is the predicted pressure taken from the nomogram, W_2 is 10 pounds, and P_1 is the limit we do not wish to exceed (300 μ b). W_1 will then be the shot yield that is allowable. In Figure 3 the predicted overpressure is 200 μ b. According to the above relationship, the allowable shot yield is 25 pounds.

We realize, as anyone associated with meteorology must realize, that trying to predict overpressure to the nearest microbar, the nearest 10 microbars, or even the nearest 100 microbars is difficult because of the variability of the meteorological parameters. Then even if we had a satisfactory weather data gathering system we probably wouldn't have the proper microbarograph network to adequately check on the results of the good weather data. By realizing all of the things, the staff at LRL is attempting to improve on both problems in micro-range sound propagation. First our microbarograph system is being enlarged and being made more flexible. Secondly a technique is being developed with which the micro-meteorological variables important to the propagation of sound, namely winds and temperature, would be acquired continuously. Data from instruments attached to a captive balloon, tethered at 2000 feet, would be telemetered to an electronic computer for analysis.

We have now developed a low cost transistorized transmitter for temperature measurement that is capable of flying from a 30-gram pilot balloon. It is still in the developmental stage but our first runs show very encouraging possibilities.

Good data acquisition, such as either of these two techniques may prove to be, cannot help but make nomograms or any other device used in the study of micro-range sound propagation much more meaningful.

REFERENCES

1. Cox, Phagge & Reed, Meteorology directs where the blast will strike, AMSB, March 1954.
2. Cox, Handbuch der Physik, Ch. 22, Vol. 48.

ABSORPTION OF SOUND IN THE ATMOSPHERE*

E. Alan Dean

Schellenger Research Laboratories
Texas Western College

The propagation of sound is essentially adiabatic. As in all macroscopic phenomena, however, there is a small increase in entropy associated with sound propagation. This increase in entropy decreases the ordered motion which a sound wave describes. The change from order to disorder results in a transfer of energy from the wave in the form of heat. This energy transfer is known as absorption and effects an exponential decrease in such variables as sound pressure so that

$$p = p_0 e^{-\alpha x}$$

describes the pressure of a plane wave traveling in the x direction.

The absorption coefficient α has been the subject of much theoretical and experimental effort, and the amount of literature on the subject is large. These remarks will be confined to that portion related to atmospheric absorption of frequencies less than 1000 cps. For a complete treatment, refer to the book by Herzfeld and Litovitz** or the review article by Markham, Beyer, and Lindsay.***

Because of historical reasons, the absorption of sound has been divided into "classical" and "anomalous" absorption. The classical absorption, first investigated by Stokes and Kirchhoff, includes the absorption due to viscosity, heat conduction, diffusion, and heat radiation, while the anomalous absorption is generally interpreted to be due to the relaxation of excited molecular energy levels. The classification is purely arbitrary, since the classical processes can be shown to exhibit relaxation, and the anomalous absorption has been considered to be the effect of the so called "second" viscosity coefficient. Atmospheric absorption is more conveniently classified into (1) viscothermal-rotation absorption, (2) vibrational absorption, and (3) radiative absorption.

The viscous absorption may be expressed as

$$\alpha_\eta = \frac{2}{3} \frac{\omega^2 \eta}{\rho c^3},$$

where η is the dynamic viscosity, ρ is the density and c is sound speed. Likewise the thermal conductive absorption is

$$\alpha_K = \frac{K}{2} \left(\frac{1}{c_v} - \frac{1}{c_p} \right) \frac{\omega^2}{\rho c^3}$$

* Supported by U. S. Army Signal Missile Support Agency, Contract 29-040-ORD-1237.

** K. F. Herzfeld and T. A. Litovitz. 1959. Absorption and Dispersion of Ultrasonic Waves. New York: Academic Press.

*** J. J. Jarkham, R. T. Beyer, and R. B. Lindsay. 1951. Absorption of sound in fluids. Rev. Mod. Phys. 23:353.

where K is the thermal conductivity, c_v is the specific heat at constant volume, and c_p is the specific heat at constant pressure. The absorption due to diffusion in a gas mixture has been expressed by Kohler*, but Herzfeld and Litovitz report that it amounts to less than 1% of the viscous and thermal absorptions, so that this absorption will be neglected.

Therefore, the first approximation to the classical absorption (neglecting radiation) is the sum of the viscous and thermal absorptions, which, after clearing fractions and substituting for ρc^2 the term γP , where γ is the ratio of specific heats, becomes

$$\alpha_c = \frac{\omega^2}{\gamma P c} \left[\frac{2}{3} \eta + \frac{(\gamma-1)K}{2c_p} \right]$$

The use of Prandtl number $\Pi = \frac{\eta c_p}{K}$ reduces the expression to

$$\alpha_c = \frac{\omega^2 \eta}{\gamma P c} \left[\frac{2}{3} + \frac{\gamma-1}{2\Pi} \right]$$

Experimental measurement in monoatomic gases support the above closely; however, the measured absorption in polyatomic gases is consistently greater than calculated results. The absorption in air is particularly distressing, as the measured values are sometimes 300 times as large as the classical value. To explain anomalous absorption, Herzfeld and Rice proposed a theory of molecular relaxation, in which, because of the rapid variation in density, the specific heats become complex functions of frequency. The complex specific heats cause a complex propagation constant which leads to absorption.

The energy of a gas resides not only as translational energy, but also in the form of rotational and vibrational energy. The number of molecules in an excited state (rotational or vibrational) depends upon the temperature, but there is a finite time which is necessary to establish equilibrium between the temperature and internal energy. This process may be described in terms of a frequency dependent molar heat. Consider a mole of gas which is compressed adiabatically, the compressional period being much greater than any relaxation time involved. The equilibrium lag is negligible and the heat capacity is the sum of the unexcited and excited capacities: this is termed the low frequency molar heat, C_0 . However, if the compressional period is much shorter than the relaxation time, the gas would never reach equilibrium and the heat capacity would be that of the unexcited capacity alone. This is denoted C_∞ , the high frequency molar heat. This leads to an internal molar heat of

$$C_i = C_0 - C_\infty$$

* M. Kohler. 1949. Schallabsorption in binaren Gasmischungen. Zeit. Physik 127:41.

The derivation of the anomalous absorption resulting from this process may be found in the literature. One expression is

$$\alpha = \frac{\omega}{2c} \left[\frac{\omega^2 R c_0}{(R + c_0) c_0 + \omega^2 \tau (R + c_0) c_0} \right]$$

where τ is the relaxation time and R is the gas constant. For rotational relaxation, τ is extremely small and the second term of the denominator may be neglected. With the substitution of

$$c_0 = \frac{5R}{2} \text{ and } c = \frac{3}{2} R,$$

the expression is simplified to

$$\alpha_R = \frac{2\tau R \omega^2}{35 c^2}$$

Assuming that the excitation is the result of molecular collisions, the relaxation time may be expressed as $\tau_R = Z_R \tau_c$, where τ_c is the time between molecular collisions and Z_R is the collision number for rotation. After use of the kinetic theory relation $\tau_c = 0.787 \frac{\eta}{p}$, the absorption becomes

$$\alpha_R = 0.045 Z_R \frac{\omega^2 \eta}{P_c}$$

Therefore, the viscothermal-rotational absorption is

$$\alpha_1 = \frac{\omega^2 \eta}{P_c} \left[\frac{10}{21} + \frac{1}{7\eta} + 0.045 Z_R \right]$$

where the value $\gamma = \frac{7}{5}$ has been used.

Using Greenspan's* value of $Z_R = 4.82$ and obtaining the other values from the Tables of Thermal Properties of Gases**, this absorption becomes

$$1.8 \times 10^{-11} f^2 \text{ m}^{-1}$$

at 0°C and 760 mm Hg. Considering the mean deviations of η , η , and Z_R ,

* M. Greenspan. 1959. Rotational Relaxation in nitrogen, oxygen, and air. Acoust Soc. A., Jour. 31:55.

** J. Hilsenrath, et al: 1955. Tables of Thermal Properties of Gases. National Bureau of Standards Circular 564.

this value should have a precision of about 3%.

The variation with frequency is apparent, also it can be seen that this type of absorption varies inversely with pressure. In fact, most measurements of absorption use pressure rather than frequency as the independent variable. The variation with temperature is more complicated, the significant variation being that of $\frac{\eta}{c}$, with smaller variations due to \bar{M} and possibly Z_R . Using the Sutherland formula for the viscosity of air,

$$\frac{\eta}{c} = \frac{\eta_0}{c_0} \left(\frac{T}{T_0} \right) \left(\frac{T_0 + S}{T + S} \right)$$

By using the value of $S = 110$ and neglecting the smaller change due to \bar{M} and Z_R ,

$$\alpha_1(T) = (\alpha_1)_0 \left[\frac{1.40T}{T + 110} \right]$$

expresses the temperature variation for this type of absorption. The standard deviation at temperatures other than 0°C should not be greater than 5%.

Although vibrational absorption is governed by the same relation as rotational absorption, the details are quite different. The rotational molar heats for the diatomic constituents of air have their full classical value of R , and equilibrium is obtained quickly. To the contrary, the vibrational molar heats are extremely small, requiring quantum considerations, and many collisions are required for equilibrium. Since $C_1 \approx 0$, the absorption becomes

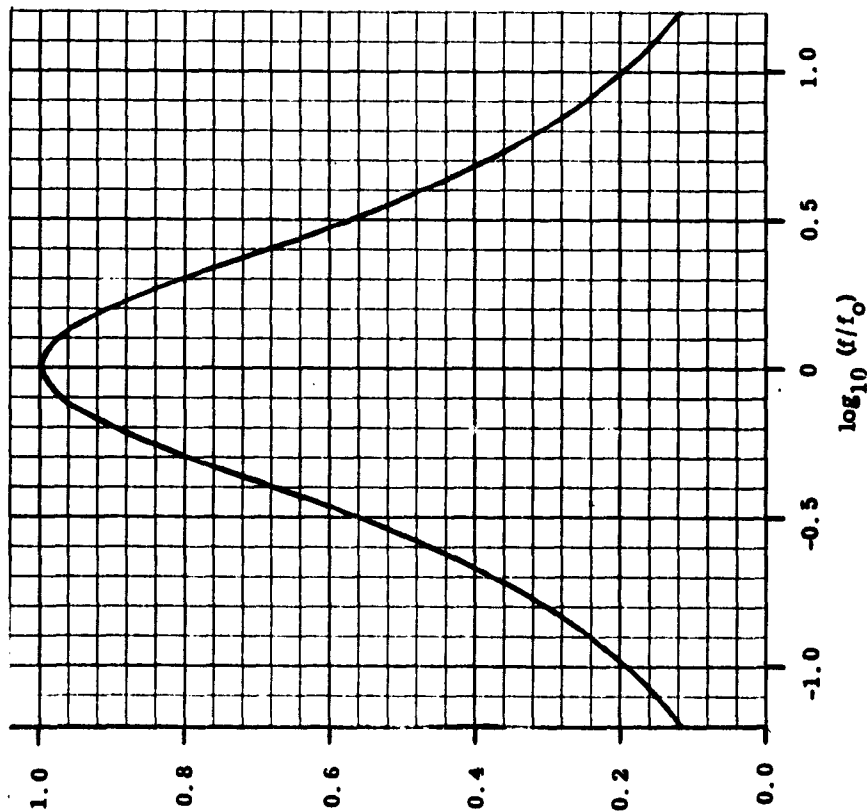
$$\alpha_2 = \frac{\omega}{2c} \left[\frac{\omega \tau_v R C_1}{(R + C_0) C_0} \right] \frac{1}{1 + \omega^2 \tau_v^2}$$

Setting $C_0 = \frac{5}{2}R$ and $2\pi f_0 = \frac{1}{\tau_v}$, this becomes

$$\alpha_2 = \frac{\omega C_1}{35Rc} \cdot \frac{2\pi f_0}{f^2 + f_0^2}$$

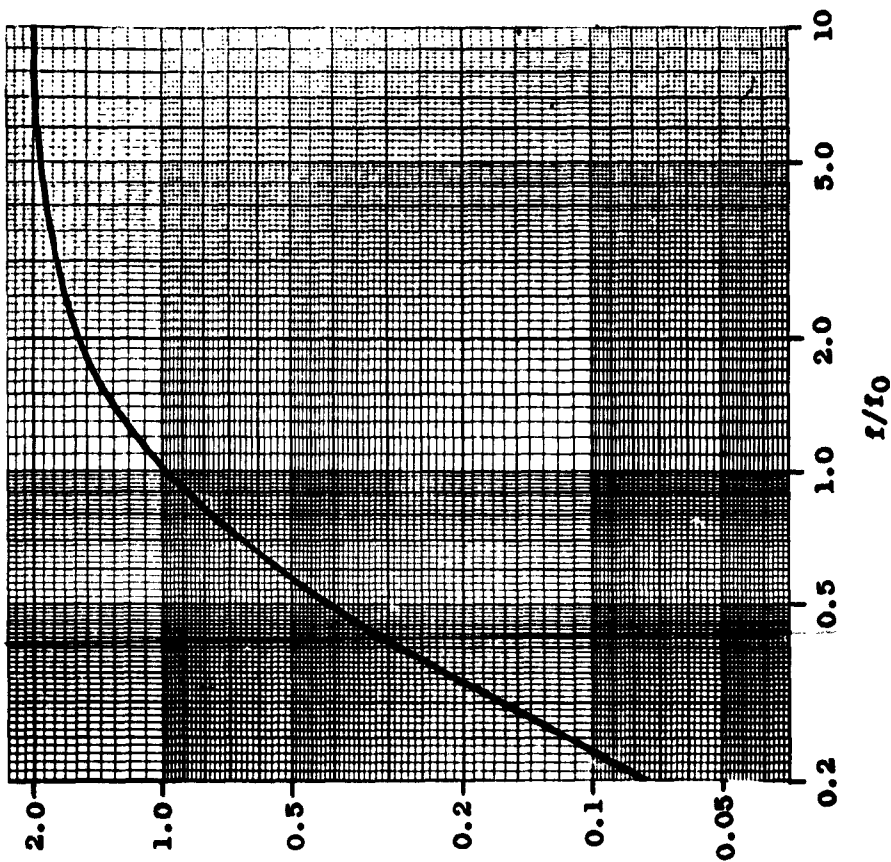
The right-hand factor has a maximum value of unity when $f = f_0$ and decreases for $f > f_0$, or $f < f_0$, as seen in figure 1. Because of this consideration, the left hand factor, when divided by λ , is called the maximum absorption per wavelength. If the absorption per unit length, rather than the absorption per wavelength is displayed, Figure 2 results. Below the relaxation frequency f_0 , the absorption varies as the square of the frequency, and above this frequency, it levels off at a value twice that at f_0 .

The maximum absorption per wavelength varies with temperature and composition. By using the Einstein specific heat equation and after consideration of the mole fraction of the relaxing gas one obtains a



II-1 Figure 1. Relaxation absorption per wave length vs frequency.

A plot of $2W/(W^2 + 1)$ vs $\log W$.



II-1 Figure 2. Relaxation absorption vs frequency.

A plot of $2W^2/(W^2 + 1)$ vs W .

theoretical expression for this maximum which has been verified by experiment. The difficulty in obtaining an expression for α_s is in determining a value for f_0 . This problem is to be considered in the following paper by Dr. Ames, and we will merely list the salient points obtained from absorption measurements.

Neglecting the small vibration energy of H_2 , α_s is dependent on the vibration of oxygen whose relaxation time depends strongly on water vapor concentration. Several investigators have used reverberation techniques to measure the absorption. The results are:

1) The maximum absorption per wavelength closely follows the theory. Measurements from 0°C to 55°C support the expected temperature variation.

2) The relation between f_0 and humidity may still be considered unknown. There is a large spread in data concerning this, with the general trend seeming to be of the form

$$f_0 = a + bh + ch^2$$

where h is the humidity. Although there is some agreement as to the quadratic nature, the coefficients derived by various authors do not agree. This is particularly true for a and b since for small h there is trouble in measuring both absorption and humidity.

3) Data for pure O_2 , when compared with air data, shows that the O_2 - N_2 collision has an effectiveness of the same order as an O_2 - O_2 collision.

4) In the temperature range from 20 to 55°C, little change is noted in f_0 . For this range at least, f_0 seems to be independent of temperature.

5) Measurements are inconclusive as to the pressure dependence of f_0 .

6) Extrapolation of the absorption in O_2 due to H_2O and NH_3 point to an O_2 - O_2 collision effectiveness yielding an f_0 of 50 cps. Likewise, the corresponding f_0 for dry air is certainly not greater than 100 cps, and is, probably about 50 cps.

The absorption due to radiative heat transfer can be shown to be*

$$\alpha_s = \frac{qc}{2C_p \gamma T}$$

where q is a radiation constant (the constant in Newton's law of cooling). It is readily apparent that this type absorption is independent of frequency;

* E. A. Dean. 1959. Absorption of low frequency sound in a homogeneous atmosphere. Schellenger Research Laboratory Contract DA 29-040-ORD-1237.

however, values of the constant are based upon gross estimations, necessitating a new means of evaluation of q if the absorption at low frequencies is to be known with any degree of accuracy.

Markham, Beyer and Lindsay have suggested that q be related to the Stefan-Boltzmann law. P. W. Smith Jr.** has attacked the problem by a more general method. Recognizing the fact that the problem is more one of radiation of heat from a gas than one of radiation from a solid body Smith has derived a complicated expression for q . Knowledge of the infrared absorption spectrum is required to evaluate the constant, and Smith does not pursue the question further, but does note that there is a maximum value for q :

$$q_{\max} = 0.23 \frac{16\sigma T^3 \omega}{c_p \rho c}$$

which at least indicates the frequency dependence of α_3 . Substitution of this value yields

$$\alpha_3 = 0.53 \frac{\sigma T^3 \omega}{c_p} \left[F(P, T, h) \right]$$

where σ is the Stefan-Boltzmann constant, and F is a function of pressure (slightly because of pressure broadening), temperature (because of Plank's radiation law), and humidity. (H_2O is the major absorber), and is equal to or less than one. Since $\alpha_3 \propto \omega$ and $\alpha_1 \propto \omega^2$, there is a cross-over point, beyond which, $\alpha_1 > \alpha_3$. This is about 100 cps, so that α_3 is only important at low frequencies. Consider the following table as an example of the importance of this type of absorption:

Absorption of Sound (db/100 miles)

Type

P = 0.1 Atm., T = 200°K (≈50,000 ft) P = 0.01 Atm., T = 250°K (≈100,000 ft)

	1 cps	10 cps	100 cps	1 cps	10 cps	100 cps
α_1	.00025	.025	2.5	.0025	.25	25
α_2 (max)	.33	3.3	33	2.0	20	200
α_3 (max)	.02	0.2	2.0	.4	4	40

Thus at high altitude and low frequency, α_3 is of possible importance. It is also apparent from the above table that low frequency sound may be propagated long distances without significant absorption, that α_2 is the most important type of absorption, and that temperature effects are considerable for both α_2 and α_3 .

**P. W. Smith Jr. 1957. Effect of heat radiation on sound propagation in gases. Acoust. Soc. Am. Jour, 29:693.

THE INFLUENCE OF ATMOSPHERIC PARAMETERS ON RELAXATION ABSORPTION

R. C. Anne
University of Denver
Denver Research Institute

Relaxation Absorption is defined as that absorption which arises because of the failure of the various molecular degrees of freedom to keep pace with the acoustic cycle. Hence, relaxation absorption is frequency sensitive, and goes to zero as the frequency decreases.

We recall that the energy of a gas may be expressed as the sum:

$$E = E(\text{translational}) + E(\text{rotational}) + E(\text{vibrational})$$

and that at equilibrium, energy is distributed among these degrees of freedom in accordance with the quantum mechanical partition theorem. If we say that the temperature of the gas is suddenly increased, we mean that the average translational energy becomes suddenly higher. Then through the process of collisions, the energy rises also for each of the internal degrees of freedom. The gas, when cooled again, will return to its initial equilibrium, with each degree of freedom exhibiting its own characteristic relaxation time. We call τ_r the relaxation time associated with rotation and τ_v , that associated with a single vibrational mode. Then, if R is the collision rate,

$$\tau_r R = Z_r,$$

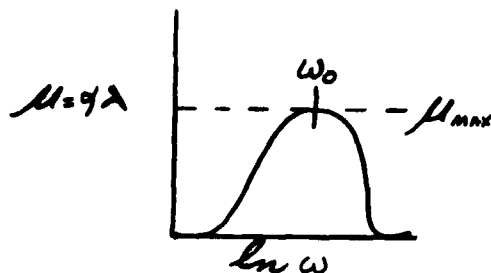
the average number of collisions required to remove a quantum of rotational energy, and

$$\tau_v R = Z_v$$

the average number of collisions required to deactivate the excited vibrational state. The latter equation assumes the energy of vibration, $h\nu$, is $\gg kT$.

Rotational quanta are small, and Z_r is usually on the order of 10, making τ_r at STP extremely short ($\sim 10^{-9}$ second). On the other hand, thermal collisions are much less effective at de-exciting vibrations, and Z_v may be very large. For O_2 at room temperature, Z_v is uncertain but around 10^8 , placing τ_v at about 1/20 second.

As the acoustic frequency increases from zero, we find that at some point the internal energy exchange with translation is not sufficiently rapid, and the specific heat associated with that particular mode of oscillation, C_{int} , is said to "lag" the acoustic cycle. C_{int} starts failing to participate in the oscillations. This gives rise to a new γ , altering the velocity of sound, and creating a sometimes large, "anomalous" absorption.



In the above figure, α is the intensity absorption per unit length and μ is the intensity absorption per wavelength; $\mu = \alpha \lambda$. ω is the acoustic angular frequency: $\omega = 2\pi f$. ω_0 is the frequency at which the maximum absorption, μ_{\max} , occurs.

At low frequencies, it may be shown that α , the absorption due to rotation, is proportional to ω^2 as is the classical absorption. Thus:

$$\frac{\alpha}{\alpha_{cl}} = 1 + 0.067 Z_r,$$

for linear molecules. This equation is due to Herzfeld and Zmuda (1951). $0.067 Z_r$ is usually < 1 . In air, Z_r might vary from one constituent to another and one would have to take this fact into account to be rigorous.

Z_r is temperature dependent and also probably impurity-dependent, but little is known at present along this line.

If the temperature is low (i.e., if $C_{vib}/R \ll 1$) the maximum absorption for vibrational relaxation gives (R is the gas constant):

$$\alpha_m = \mu_m / \lambda = \frac{\pi^2 R C_{vib} f_0}{2 C_p C_v V},$$

where V is the sonic velocity. For air at $210^\circ K$,

$$\alpha_m = 6.7 \times 10^{-4} / \tau_v \quad (\text{db/mile}).$$

How does one obtain τ_v ? Experimentally, its measurement is difficult at low temperature and frequencies, because the absorption under these conditions is quite small. Measurements at room temperature and higher may be carried out by use of shock tubes, resonance tubes, reverberation chambers and interferometers. The results vary widely with temperature and composition.

Knötzel and Knötzel (1948), using the reverberation technique, measured ω_0 for oxygen at room temperature with water vapor present. They reported:

$$f_0 = \omega_0^{(x)} / 2\pi = 50 + K_1 x + K_2 x^2,$$

where K_1 and K_2 are parameters which dependent on temperature, and x is the mole fraction of H_2O . For pure oxygen, $f_0 = 50$ cps, or

$$\tau_v = R / z_v = 3.2 \text{ milliseconds.}$$

The collision rate R depends both on temperature and pressure. Z_v depends on temperature and has long been the study of numerous investigators. Landau and Teller were the first to derive an expression for $Z_v(T)$ and Schwartz, Slawsky, and Herzfeld have studied the effect in recent years, along with T. A. Litovitz and others.

Figure 1. This graph shows how small the vibrational heat capacity for O_2 becomes at low temperatures, thus validating some of our prior assumptions.

Figure 2. This is an abbreviated form of the Schwartz-Slawsky-Herzfeld (SSH) equation. A is actually slightly temperature dependent and so is s , the range of the repulsive forces between the two colliding molecules. B is a constant, μ is the reduced mass for the collision, and ν is the vibrational frequency (for O_2 , $\nu = 1580 \text{ cm}^{-1}$). s may be related to r_0 , the Lennard-Jones collision diameter. ϵ is the well depth appearing in the Lennard-Jones potential, $\phi(r)$.

Figure 3. Application of SSH equation gives the dashed, straight line shown here, where $Z_v f(T)$ is plotted vs $T^{-1/3}$ on semi-log. The dots represent several measurements, the 288°K . point being the result of Knötzel and Knötzel. Let us consider the propagation of sound at room temperature of about 288°K . There appears to be a noticeable deviation between theory and experiment at this temperature, giving

$$Z_v (\text{exper.}) = 50 \text{ cps},$$

$$Z_v (\text{theor.}) = 17 \text{ cps}.$$

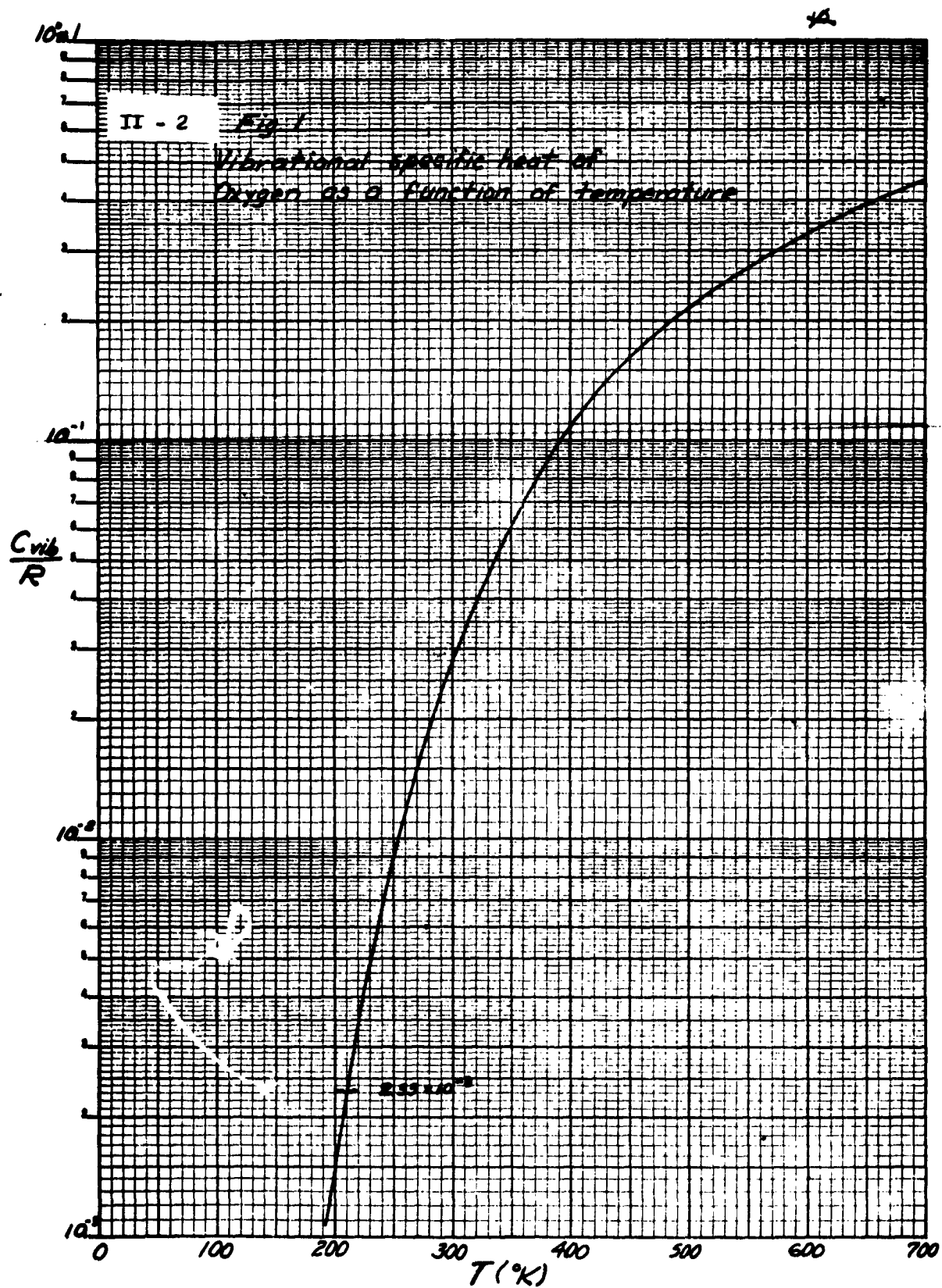
Figure 4. These are the very recent results (5/1961) of J. G. Parker using the resonance tube. He studied the influence of H_2 on oxygen deactivation at room temperature. Extrapolating to 0 pct. H_2 gives about 9 cps for pure O_2 . The discrepancy with Knötzel's work cannot be explained at this time, but the theoretical value is now bracketed by the two results.

Figure 5 shows the difference between Parker's work for Z_v and the results of other investigators.

Figure 6. In the atmosphere at 60,000 feet, only oxygen exhibits any significant vibrational relaxation absorption. The actual relaxation time is a result of the combined influence of molecular collisions of O_2 with all the other gases of the atmosphere. In the equation

$$\frac{1}{\tau_v} = \frac{1}{\tau_{O_2}} + \sum_i \frac{1}{\tau_i} = \frac{R_{O_2}}{Z_{O_2}} + \sum_i \frac{R_i}{Z_i}$$

τ_i represents the relaxation time of an O_2 molecule colliding with the i th constituent of the atmosphere. The R_i can be calculated simply if the temperature, pressure and composition are known. The Z_i we may calculate from SSH theory.



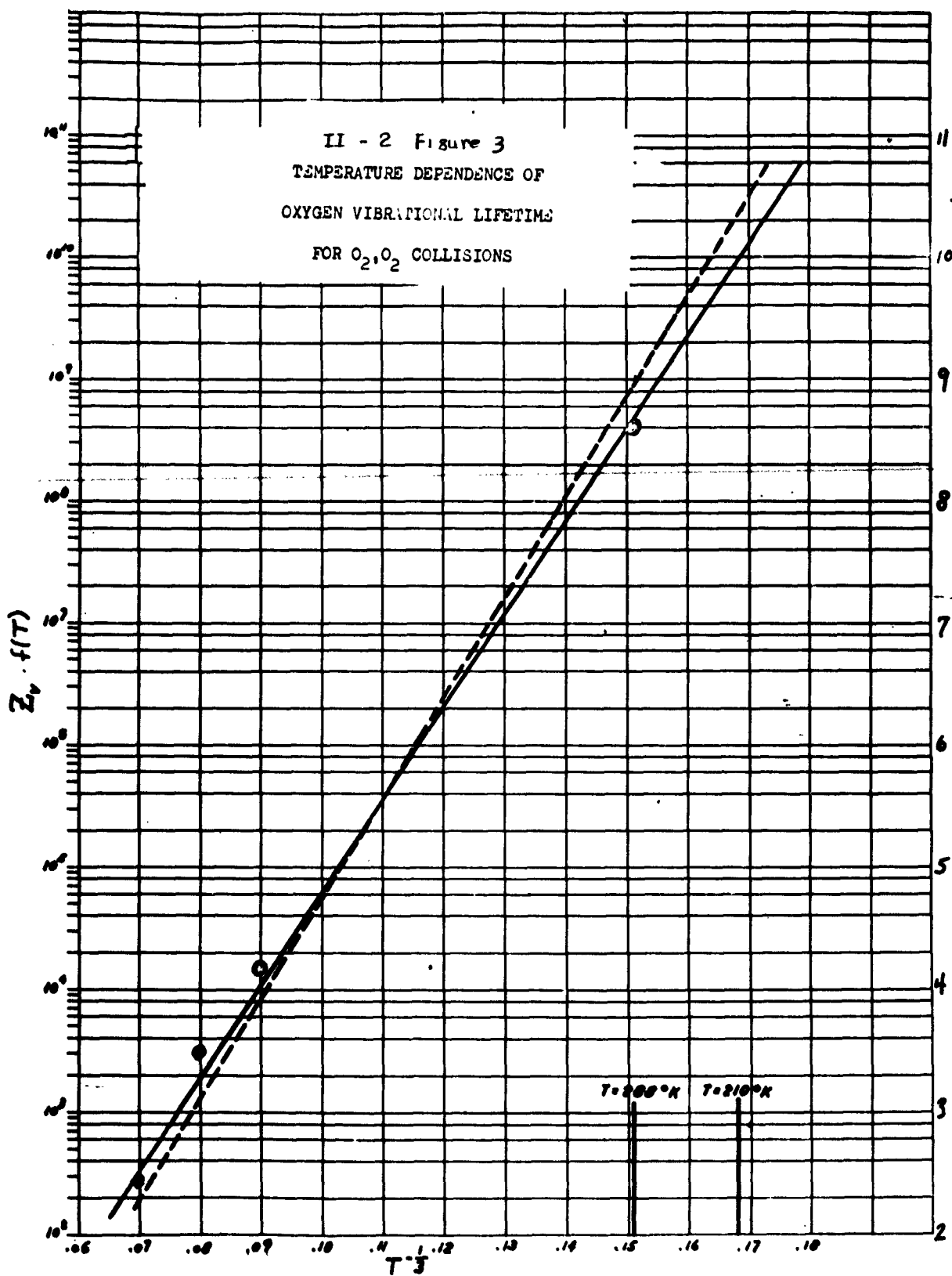
$$Z_v = A \exp \left[\frac{3}{2} \left(\frac{\theta'}{T} \right)^{1/3} \right] [f(T)]^{-1} ,$$

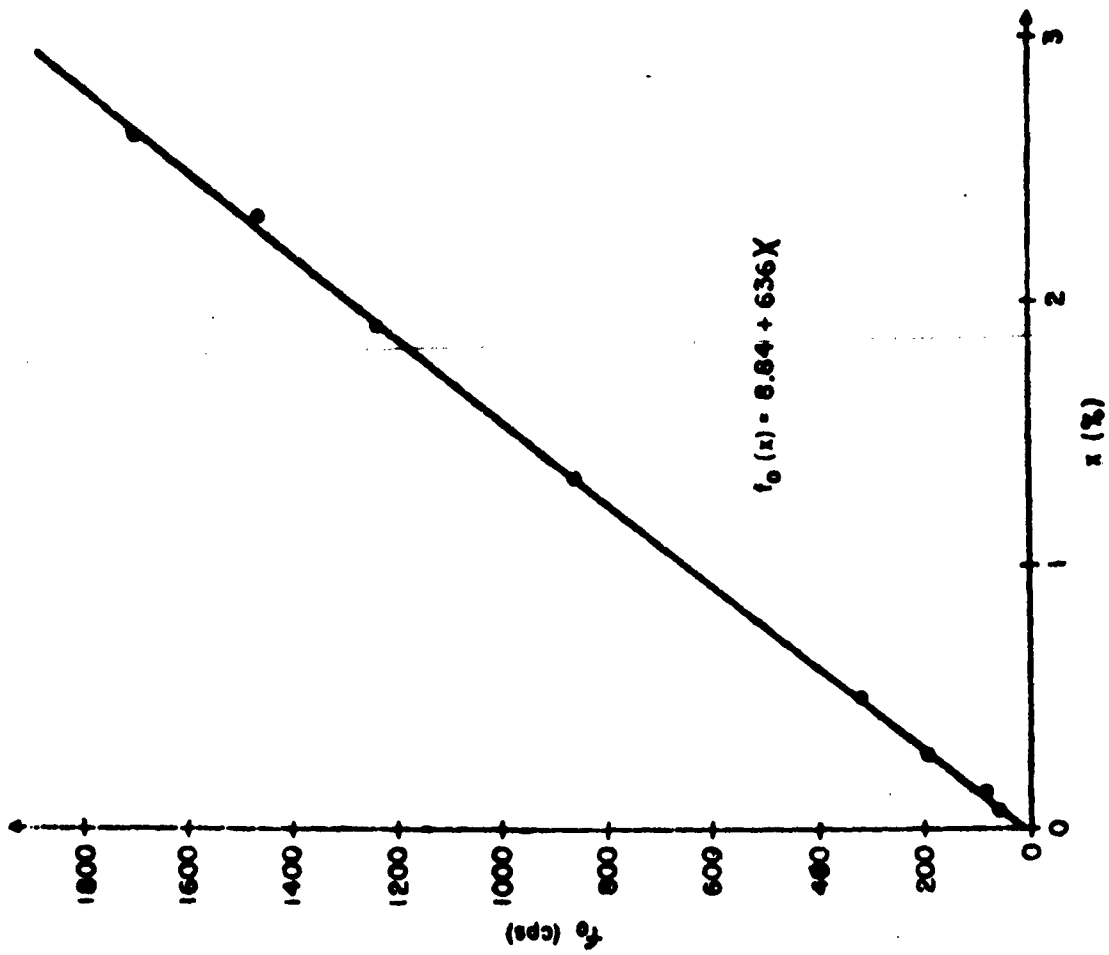
$$f(T) = T^{-1/6} \exp \left[\frac{h\nu + 2\epsilon}{2\pi T} \right] ,$$

$$\theta' = B \mu s^2 v^2 .$$

$$\varphi(r) = 4\epsilon \left[\left(\frac{r_0}{r} \right)^{12} - \left(\frac{r_0}{r} \right)^6 \right]$$

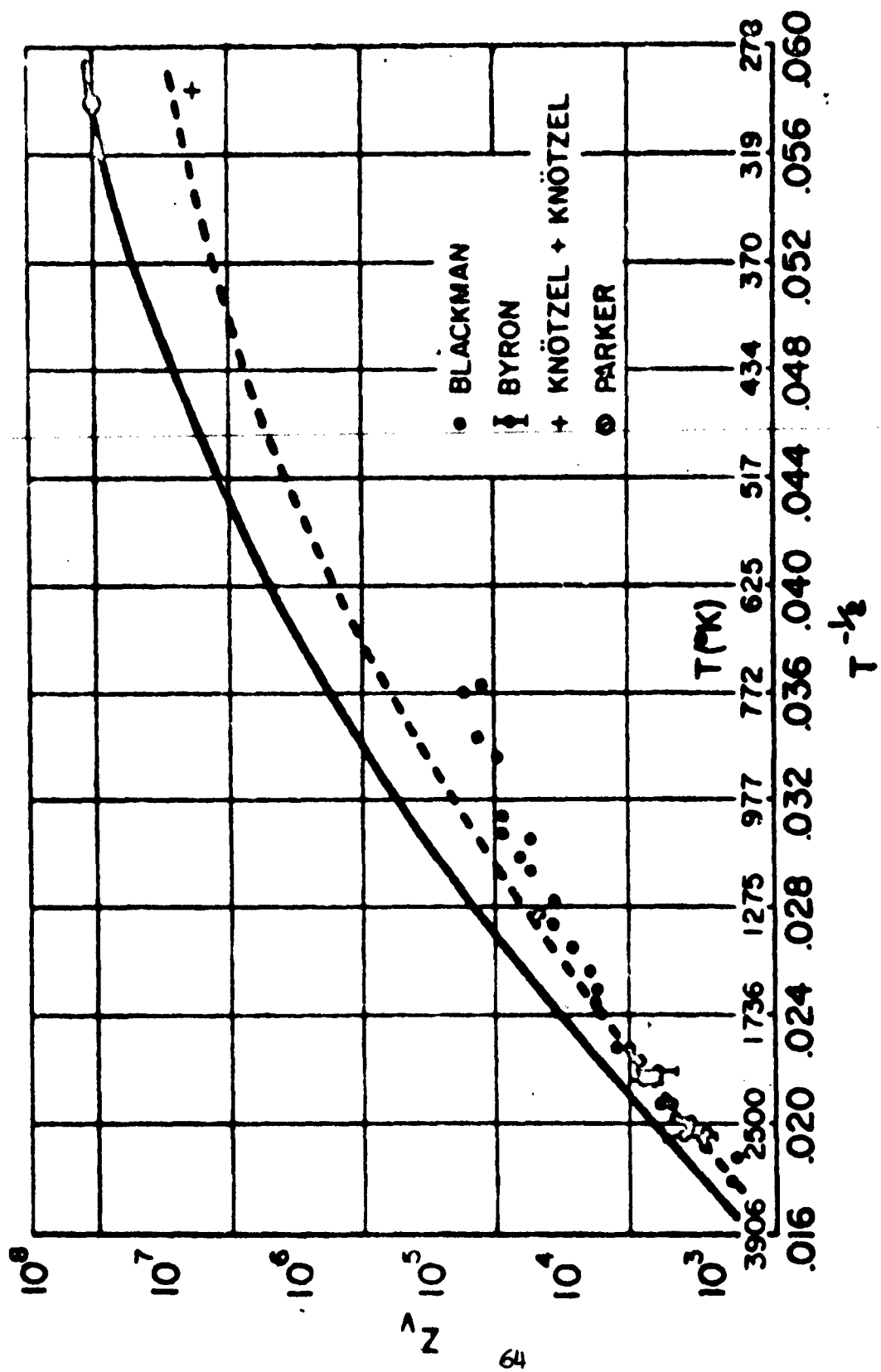
II-2 Fig. 2. Vibrational Collision Lifetime
According to Litovitz, Herzfeld, Schwartz,
& Slawsky, with the L-J potential.





Variation of the relaxation frequency with hydrogen concentration.

II - 2 Figure 4



II - 2 Figure 5

$$\frac{1}{\tau_v} = \frac{1}{\tau_a} + \sum_{i=1}^n \frac{1}{\tau_i}$$

$$= \frac{R_a}{Z_v(a)} + \sum_{i=1}^n \frac{R_i}{Z_{vi}}$$

II-2 Fig. 6. Relaxation time for Q_2 in a mixture of n non-vibrating constituents.

Figure 7. Since the composition of the air is known except for water vapor, recent work on the variation of humidity with altitude is useful. This graph represents the efforts of various investigators. Murcray's work at the University of Denver is the most recent. We have taken an overall average for the mixing ratio at 60,000 feet, which corresponds to $x = 10^{-7}$. For comparison, the mole fraction of helium is about half that.

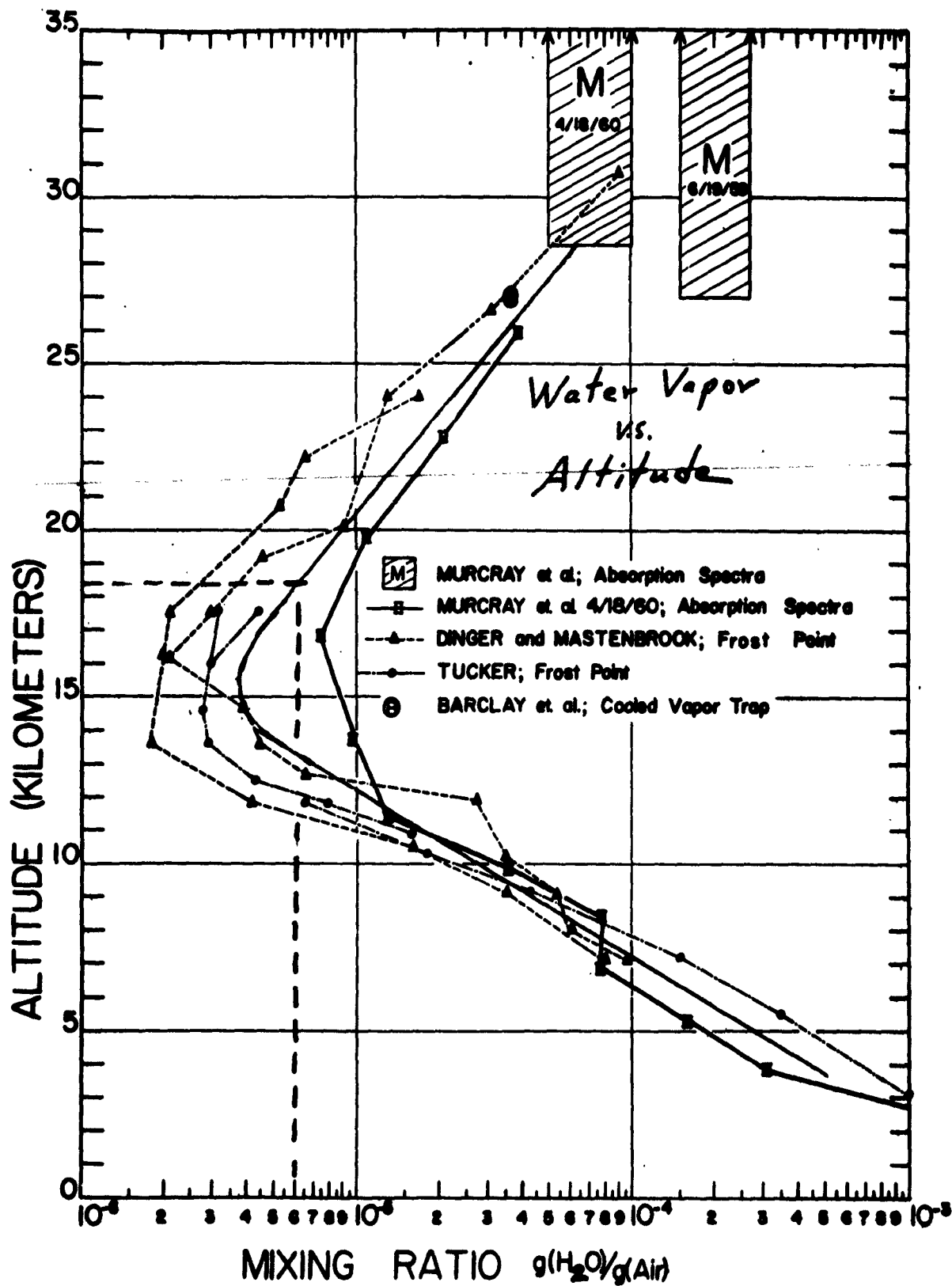
Figure 8. (table) Recalling that Z_v varies exponentially as $1/s^2$, we collect here the values for this quantity for O_2 colliding with several of the atmospheric constituents. r_0^A is a measure of the change in s , the repulsive range. The relaxation time for O_2 , N_2 collisions will be larger than for O_2 , O_2 , but the abundance of N_2 is sufficient to offset this. O_2 , Ar collisions and O_2 , CO_2 collisions may be neglected. The resulting $1/s^2$ for O_2 , H_2O collisions by no means suggests that water vapor would have the importance that it does in de-exciting O_2 vibrations. This is because the mechanism of energy exchange is entirely different from the assumptions made in deriving the SSH equation, so that this result is not applicable in the case of H_2O . Instead, we must use a modified K_1 from Knötzel's equation. The mole fraction x is so small that the second order term may be neglected. Finally, helium collisions appear to be immensely efficient in the deactivation process. The difficulty really comes in knowing whether this number for $1/s^2$ is correct, since the O_2 , He interaction is not well understood. At best, we can suppose 0.0991 to be a probable lower limit.

Finally, when one calculates all the R's and Z's in the equation for $1/\tau_v$, one finds

$$f_0 = 1/2\pi\tau_v = \begin{array}{l} 0.09 \text{ (for } O_2, O_2) \\ + .10 \text{ (for } O_2, N_2) \\ + .11 \text{ (for } O_2, He) \\ + .06 \text{ (for } O_2, H_2O) \text{ estimated;} \end{array}$$

$$f_0 = 0.36 \text{ cps.}$$

which is a probable upper limit to f_0 . We can be reasonably certain that f_0 does in fact lie below 1 cps at 60,000 feet. A calculation for f_0 at any other temperature and pressure would proceed in similar manner.



<u>B, A</u> <u>Collision</u>	<u>r_0^A (Å)</u>	<u>μs^2</u>
O_2, O_2	3.433	0.5819
O_2, N_2	3.681	0.5858
O_2, H_2O	2.725	0.3367
O_2, He	2.576	0.0991

II-2 Fig. 8. Variation of μs^2 for collisions of O_2 with certain atmospheric constituents.

BALLISTIC VS. SPHERICAL FRONTS ORIGINATING FROM SUPERSONIC MISSILES

Robert L. Schumaker

Aurora Bustos

Schellenger Research Laboratories

INTRODUCTION

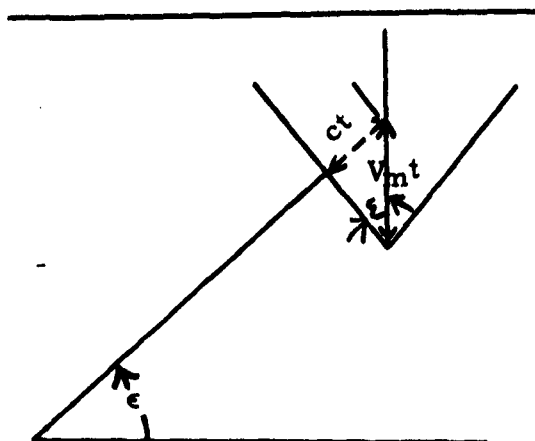
The SOTIM process is one in which acoustical data is used to determine the speed and position of a missile in space and the time of origin of the shock fronts which it originates. Thus a portion of the trajectory of the missile can be determined with respect to both position and time. From the order of arrival of the shock front at a geometric array of microphones on the ground, the azimuth of the sound source is established as well as the angle of elevation. This angle of elevation is then related to the angle between the shock front and the trajectory to establish the speed of the missile.* On the basis of this method every ~~acoustical wave is related~~ to the speed of the missile (and the Mach cone) as a positive part of SOTIM analysis. Incidentally SOTIM stands for Sonic Observations of Trajectories and Impacts of Missiles. However, not all waves are necessarily ballistic waves, and a technique is herein outlined so that such waves can be distinguished from ballistic waves. Furthermore they can be identified as having originated from a more or less spherical front, for example, as an explosion.

SOTIM data analyses disclosed eight missiles for which an occurrence of the nature described was verified, and these were chosen from about 100 unclassified Aerobee firings from which we at Schellenger Research Laboratories were provided field data by White Sands Missile Range. Such cases (non-ballistic cases) will hereafter be referred to as "events". These eight missiles are listed in Table 1, giving the date of firing and approximate altitude and origin time of the event.

The factors which determine that a group of waves were spherical in their origin, as opposed to being conical as are the ballistic waves from a missile, can be extracted from discussions of (1) the speed** and time curves associated with event waves and (2) the wave shape of disturbances recorded on the tape from the event in comparison to the usual ballistic disturbances. Of course, magnetic tape recordings would have permitted an electronic harmonic analysis, as we now conduct in our data analysis laboratory, but this was not used for these field recordings, hence was not applicable here.

*Webb, W. L., McPike, A. A., Thompson, H. F., Sound Ranging Technique for Determining the Trajectory of Supersonic Missiles, Progress Reports #1 and 2, White Sands Missile Range, 11 March 1955 and 25 July 1955.

**It will become evident that the term speed when used in reference to an event refers to a ratio and does not represent the rate of descent.



II-3 Figure 1. Relating the speed of the missile to the angle of elevation of the sound source

II-3 TABLE 1

<u>Missile</u>	<u>Firing Date</u>	<u>Altitude of Origin</u> (ft MSL)	<u>Time of Origin</u> (sec)
AF 104	5 May 1959	124,000	$x + 340$
AF 109	24 June 1959	96,000	$x + 441$
IGY NN 3.23 F	21 July 1959	96,000	$x + 432$
AF 37	28 August 1959	109,000	$x + 480$
AA 3.124 C	19 January 1960	122,000	$x + 453$
AA 2.143 C	12 February 1960	124,000	$x + 351$
NRL 60	19 April 1960	104,000	$x + 454$
AA 1.126	15 September 1960	124,000	$x + 296$

x = firing time

SPEED AND TIME CURVE

The speed of a missile (V_m) is determined by

$$V_m = \frac{c}{\sin \epsilon}$$

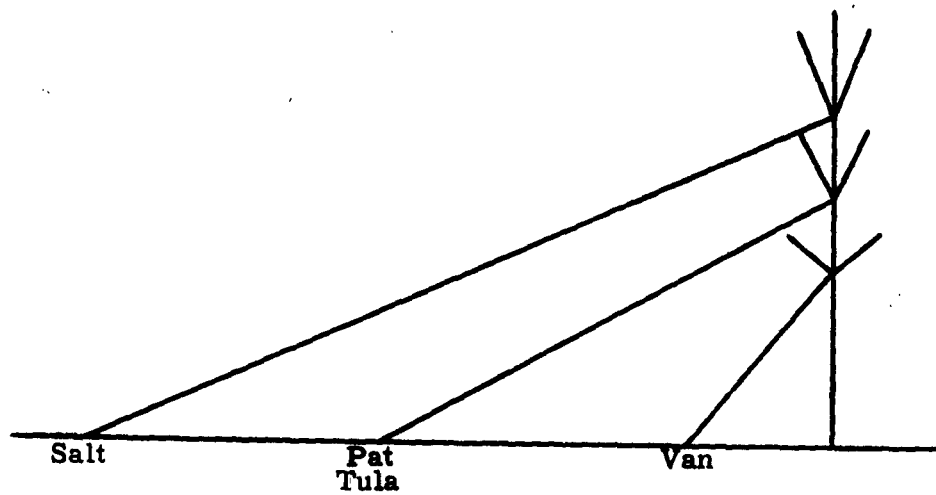
where c is the local speed of sound and ϵ is the Mach angle (see Figure 1). The wave front which travels to the array on the ground is represented by a ray drawn perpendicular to the wave front. Assuming no refraction and a vertical trajectory during descent, ϵ is also the angle of elevation measured at the array. However, in practice, the ray is refracted in traveling through the atmosphere both by the wind and the temperature gradient. Therefore, the ϵ and azimuth angle received at the array must be corrected by applying Snell's law at each boundary of the atmospheric layers as chosen from RAOB weather data. On the average about 70 layers are chosen and more than 1000 calculations are required to trace the ray back to its source. RAOB weather data is available for each firing to altitudes of approximately 100,000 ft MSL.

In the cases considered the missile was undergoing a near-vertical descent. It is most likely that in the region from which SOTIM data is received, approximately 40,000 ft to 130,000 ft altitude, the missile would be decelerating. Thus the arrays situated at various distances from the vertical trajectory would indicate various speeds at different altitudes and times along the trajectory (See Figure 2). An altitude versus speed curve constructed for such a situation would be similar to the curve shown in Figure 3, which is, as are all of the examples, selected from the data of specific missiles. If two arrays happen to be equidistant from the line of descent, the speed of the missile, altitude and time of origin calculated from data received at the two arrays should agree. This agreement is illustrated by the Pat and Tula arrays in Figure 3.

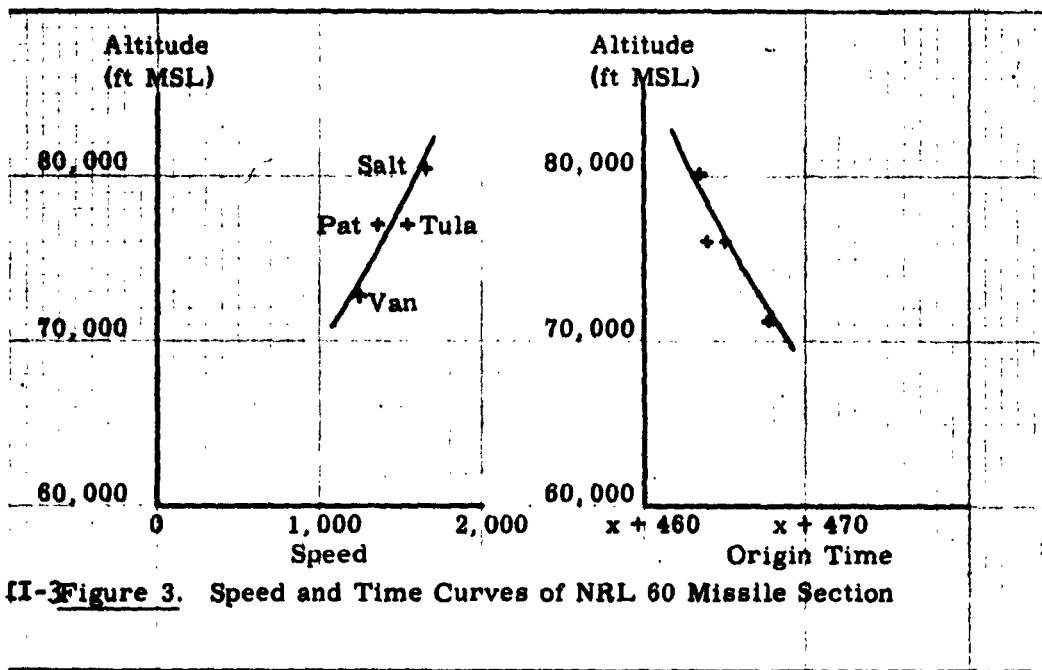
In an event, several arrays which are not equidistant from the line of descent record the sound source at a single altitude at the same time; but each array indicates a different speed for the missile. A typical graph of speed vs. altitude for an event is shown next (Figure 4). Such a case is assumed to be caused by something other than ballistic waves from a missile section for the following reasons.

(1) Ballistic waves from a missile section at one altitude should not give such a discrepancy in speed.

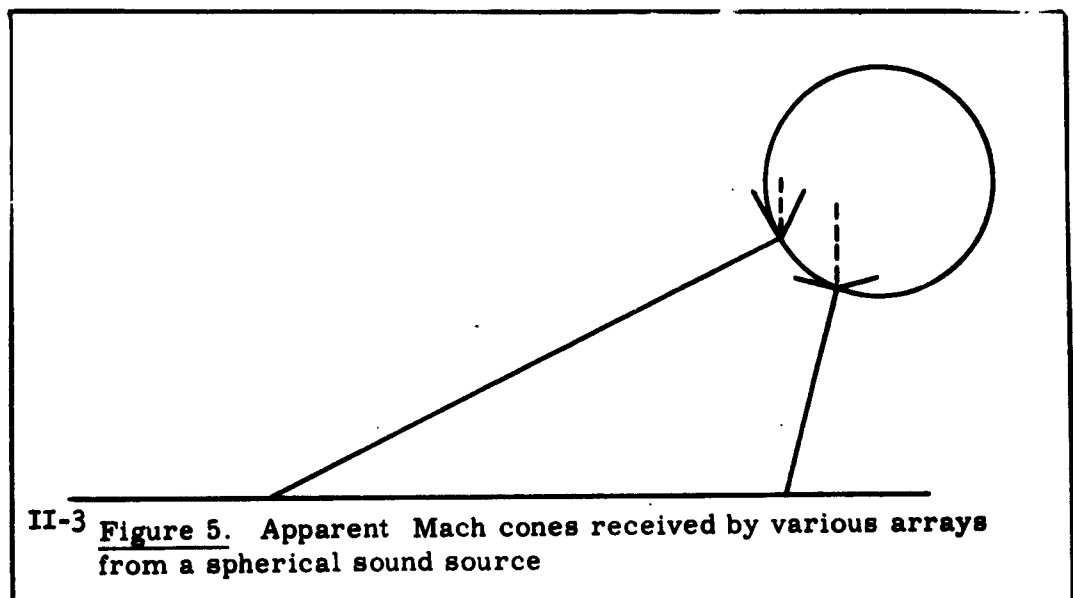
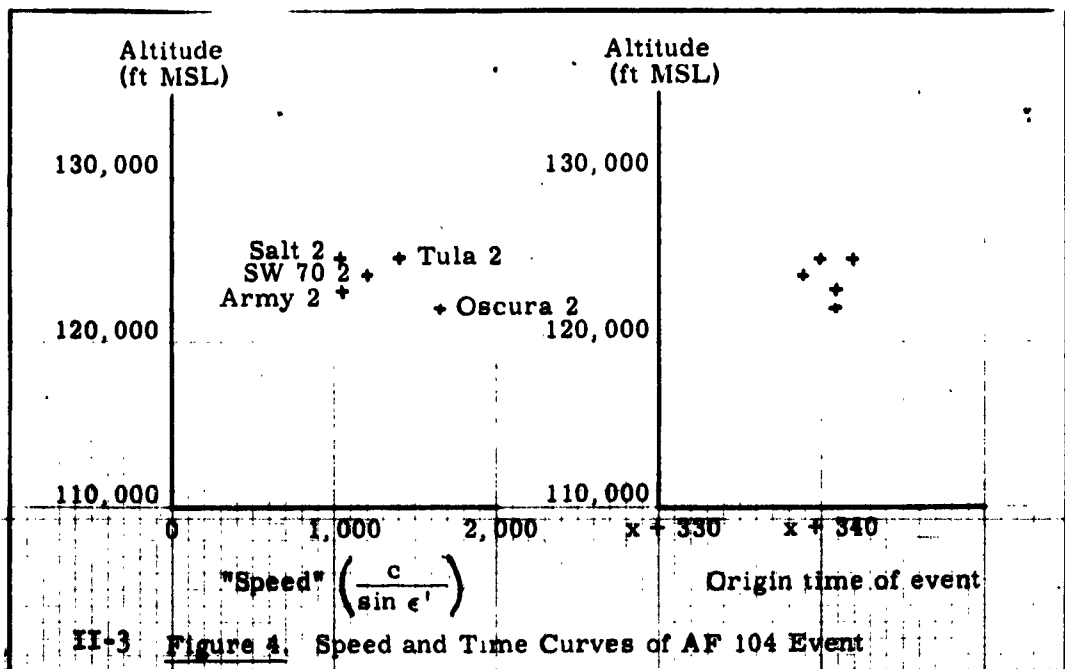
(2) It is improbable that so many arrays on the ground would receive waves from a ballistic wave front all originating from a common altitude. This is because the arrays are scattered over a large portion of the missile range, and their position would not likely be at points where they could receive the sound in question. It has been assumed that the speed of sound and wind profiles do not have pronounced horizontal variation over the area encompassing the various arrays of microphones.



II-3 **Figure 2.** Sound fronts generated by a missile section decelerating through space are shown by rays traveling to four arrays.



II-3 **Figure 3.** Speed and Time Curves of NRL 60 Missile Section



One of the distinguishing factors noted for a group of event waves was that the "speed" indicated for the missile increased as the range increased. Assuming straight line propagation, in order for a group of arrays to establish a missile at a given altitude and time, they must be equidistant from the line of descent, as noted previously. This variation of "speed" with range serves as a criterion for distinguishing between a ballistic and spherical sound source. As shown in Figure 5, the sound front received at the array would have originated from a section of the spherical front whose tangent at that point would make an angle of ϵ with the vertical. From Figure 5, it can be seen that the array situated at the greatest distance from the source would necessarily indicate the fastest speed. A table listing all the waves received from the eight events is included in the appendix at the end of this report. In this table it will be shown that speed increases with range in every case.

Another interesting factor distinguishing the spherical front from the ballistic front is that all arrays in operation should hear the former but not necessarily the latter or ballistic type. When a graph is plotted with range vs. travel time for the waves already correlated with the event, the predicted arrival times at other arrays can be obtained by interpolation. An example of such a graph is shown in Figure 6. Since these waves may have been overlooked in the original analysis due to relative weakness, for example, they can be located and correlated with the event. The waves which were found using this method are listed in Table 2.

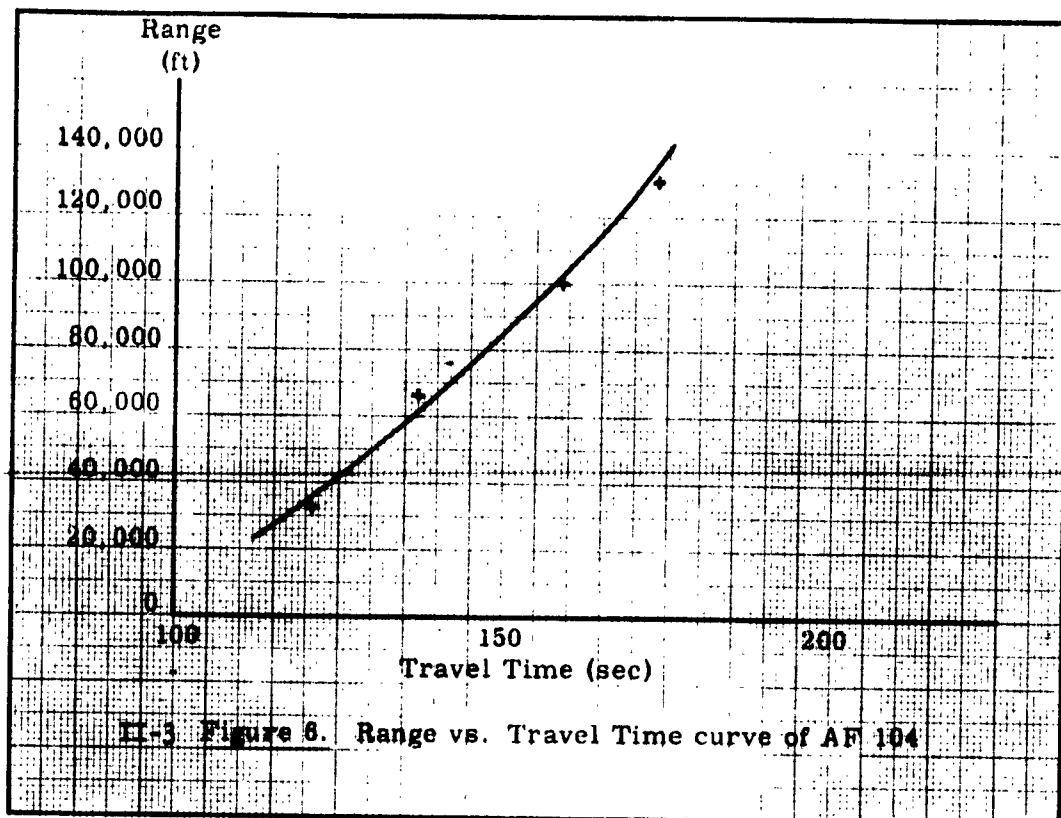
EXTENSION TO NON-VERTICAL

It is to be noted that this method for distinguishing between ballistic and spherical waves can be extended to a missile undergoing non-vertical descent, that is, still moving with a horizontal component of velocity after re-entry into the atmosphere.*

CONCLUSIONS

To the extent of available information, no events which would initiate spherical fronts were programmed for the missiles during the portions of the trajectories where they were observed; therefore, the nature of the event cannot be explained and warrants, perhaps, an investigation, as to the source. Furthermore, the data indicates what can be accomplished from acoustical data analyses. Unannounced and not even programmed events have been identified as having originated at a certain altitude (within a thousand feet or so) at a time (within a second or so) at a range of 50 miles or so.

*Robert L. Schumaker, "Extension of SOTIM Analysis to Non-Vertical Descent of Missiles", Schellenger Research Laboratories, Texas Western College.



II-3 TABLE 2

<u>Missile</u>	<u>Array</u>	<u>Wave</u> <u>No</u>	<u>Estimated</u> <u>Warrrt</u>	<u>Warrrt</u>
AF 104	Salt	2	x + 458 sec	x + 463 sec
AF 37	NW 30	7	x + 584 sec	x + 585 sec
AA 3.124 C	NW 30	5	x + 603 sec	x + 602 sec
	Motel	3	x + 671 sec	x + 671 sec
NRL 60	Pat	4	x + 585 sec	x + 584 sec

APPENDIX

Table A-1 lists the following data for each of the waves received from the eight events:

Array: The name given to the array of microphones receiving the front.

Wave No: The order of arrival of the front at the array.

Az: The azimuth angle.

ϵ : The elevation angle.

R-C: A reliability ("R") designation based upon the fact that the travel time of a plane sound front between one pair of microphones in the square array should be the same as for another pair. Since the break times read from the field tape upon which these data are recorded are affected to some degree by wind noises, etc., these measured time differences are not always the same. The designations range from 4x to 1x, the larger integers signifying the greater accuracy in reading the tape. A "3M" (three mike) designation means that one of the microphones was inoperative and normal precision was not possible.

The number from 1 to 10 inclusive following the "R" factor is a grading of the wave expressing an overall confidence "C" factor in reading the wave. Sharp, clear breaks which can be read with confidence are indicated by the higher integers.

Strength: Strengths of waves are indicated by W, M, or S, meaning weak, medium, or strong in relative intensity when received at the array.

Warrt: Wave arrival time where x is the firing time.

Range: Horizontal distance from array to the projection on the ground of the event point

$\frac{c}{\sin \epsilon'}$: c is the speed of sound at the altitude of origin and ϵ' is the corrected angle of elevation. This ratio is the speed of the missile in usual SOTM analysis.

Altitude: Altitude of wave origin.

Origin time: Time of wave origin where x is the firing time.

II-3 TABLE A-1

Array No	Az	ϵ	R-C	Str	Warrt (sec)	Range (ft)	$\frac{c}{\sin \epsilon'}$ (ft/sec)	Altitude (ft)	Time of Origin (sec)
Air Force 104									
Salt 2	345.1°	76.7°	3x-8	W	x + 463	25,000	1,100	125,000	x + 342
Army 2	96.8	72.7	4x-9	S	x + 464	32,000	1,100	123,000	x + 341
SW 70 2	174.2	57.1	4x-8	W	x + 476	66,000	1,200	124,000	x + 339
Tula 2	312.8	45.3	4x-10	S	x + 498	100,000	1,400	125,000	x + 340
ORC 2	207.6	34.2	3M-6	M	x + 515	131,000	1,600	122,000	x + 341
Air Force 109									
ORC 2	241.3	71.4	4x-9	W	x + 536	27,000	1,100	96,000	x + 440
SW 70 2	50.4	54.1	4x-8	W	x + 549	56,000	1,200	96,000	x + 441
Army 2	36.5	30.3	4x-8	W	x + 591	119,000	1,600	97,000	x + 442
IGY NN 3.23 F									
Tula 5	259.1	51.5	3M-3	W	x + 555	80,500	1,200	95,000	x + 432
Army 5	165.1	37.9	3M-2	W	None	92,000	1,500	96,000	-----
SW 70 6	181.5	19.4	3M-5	W	x + 562	148,000	1,900	96,000	x + 432
Air Force 37									
NW 30 7	230.3	79.3	4x-9	M	x + 585	17,000	1,100	108,000	x + 481
Van 6	331.6	40.3	4x-9	M	x + 621	94,000	1,400	109,000	x + 480
Salt 5	210.4	34.3	3M-7	M	x + 631	112,000	1,500	109,000	x + 480
Tula 6	247.0	28.0	3x-10	M	x + 646	134,000	1,700	111,000	x + 478

II-3 TABLE A-1 (Cont.)

<u>Array No</u>	<u>Az</u>	<u>ε</u>	<u>R-C</u>	<u>Str</u>	<u>Warrt</u> (sec)	<u>Range</u> (ft)	<u>c</u> <u>sin ε'</u> (ft/sec)	<u>Altitude</u> (ft)	<u>Time of</u> <u>Origin</u> (sec)
<u>AA 3.124C</u>									
NW 30 5	282.4	47.6	4x-5	S	x + 602	98,000	1,400	121,000	x + 455
Salt 4	241.1	36.3	4x-5	M	x + 641	161,000	1,700	125,000	x + 450
Van 4	313.1	31.5	4x-8	M	x + 655	166,000	1,900	126,000	x + 454
Motel 3	291.9	25.7	3M-7	W	x + 671	201,000	2,200	117,000	x + 451
Tula 3	262.0	28.1	3M-5	S	x + 676	209,000	2,100	120,000	x + 453
<u>AA 2.143 C</u>									
Salt 3	97.1	66.4	3x-7	M	x + 479	47,000	1,100	125,000	x + 349
Tula 4	331.3	66.4	3x-5	M	x + 480	49,000	1,200	128,000	x + 348
Army 4	111.5	44.8	4x-6	M	x + 503	91,000	1,400	114,000	x + 358
NW 30 4	47.6	39.6	4x-7	M	x + 521	125,000	1,600	127,000	x + 348
<u>NRL 60</u>									
Van 3	335.4	54.6	4x-4	W	x + 572	62,000	1,200	106,000	x + 453
Pat 4	327.3	43.7	3M-7	W	x + 584	82,000	1,300	99,000	x + 459
Salt 9	194.5	29.3	4x-7	M	x + 671	132,000	1,700	106,000	x + 453
Tula 3	231.3	29.7	4x-8	M	x + 619	134,000	1,800	107,000	x + 453
<u>AA 1.126</u>									
Tula 4	212.6	30.5	4x-3	W	x + 475	152,000	1,800	124,000	x + 295
Salt 3	184.8	26.1	4x-1	W	x + 492	171,000	2,000	123,000	x + 296

ACOUSTICAL DETERMINATION OF WINDS
BY MEANS OF A
CIRCULAR MICROPHONE ARRAY
Robert O. Olsen
U. S. Army Signal Missile Support Agency
White Sands Missile Range, New Mexico

In the last few years a need has been generated by the missile development people, for a different method of wind measurements.

With a standard type aerovane, one is limited to a wind measurement at a discrete point in space; also, these instruments have a slower response time. Another method is to use pilot balloons, but this is limited because of the time and space differential of the balloon trajectory in relation to the missile trajectory.

One approach to this wind measuring problem is to use acoustics. With this method, the wind is not measured at a discrete point in space, but is integrated over an area, and the response time is decreased. However, the positioning of the sound source, and its coordinates is required.

A circular microphone array was set up to determine how well the wind could be measured over an area. The terrain chosen was level and free of obstacles which could disturb the generated sound patterns. A diagram of the array is shown in Figure 1.

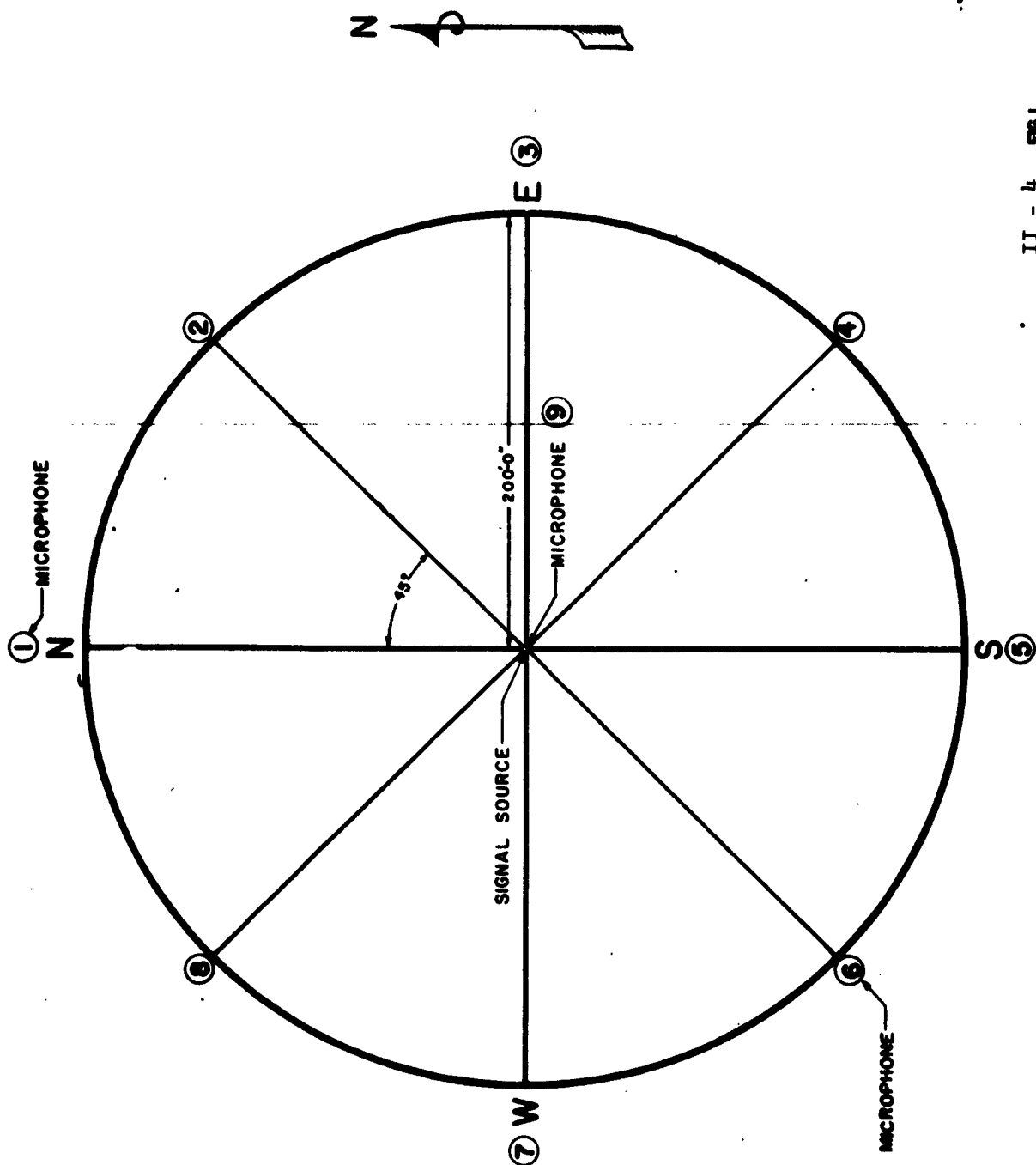
The microphones were set on 6-foot stands at eight evenly spaced points on a 200-foot-radius circle, and each stand was adjusted so that the microphones were on the same plane. The array was oriented with the number one microphone at a true north position. A ten-gauge salute cannon was placed on the same plane as the microphones, at the center of the array, and was used to generate the sound energy. A ninth microphone was placed next to the cannon, so that a zero time for the origin of the blast could be recorded.

Five three-bladed propeller-type aerovanes measured the wind at different points on the array. They were placed adjacent to the microphones at the center and positions 1, 3, 5, and 7, and at a height of seven feet above the surface. The aerovanes were wired to an RO-2 recorder, with a circuit for marking the chart at the time of the blast. A mercury thermometer was placed at the center of the array and was read at each cannon firing.

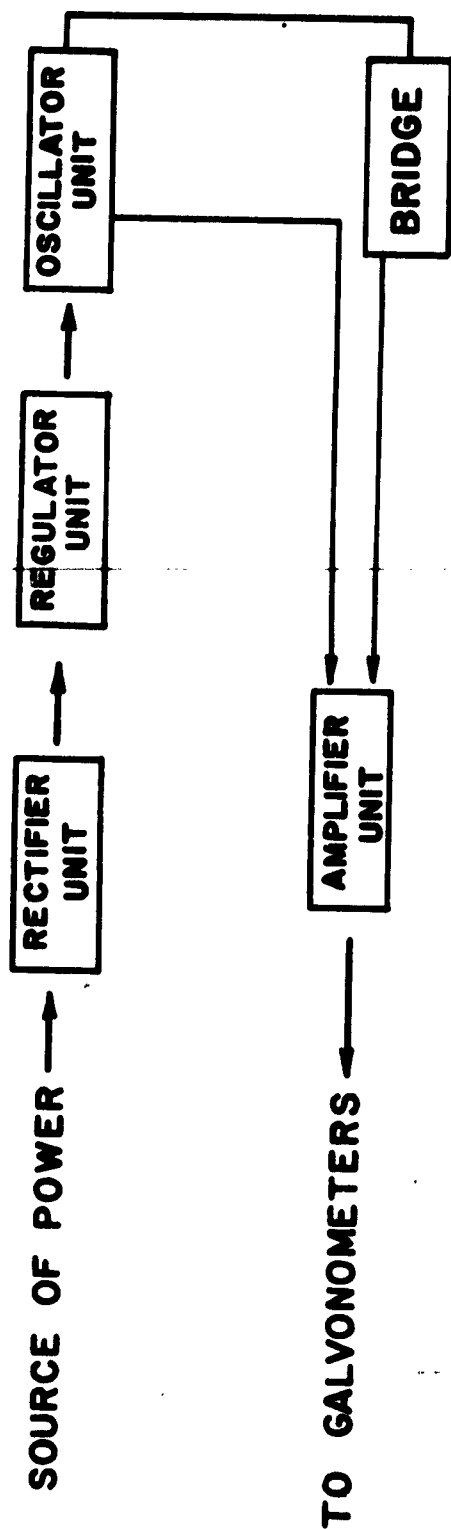
The data were recorded on a direct-write recording oscillograph. For these tests it was necessary to run the recorder at a paper speed of 50 inches per second, to be able to differentiate the various arrival times of the signals at the microphones.

Figure 2 is a schematic of the various components of the microphone recording system. The oscillator unit supplies a 5000-cycle carrier to the bridge circuit and any time the bridge becomes unbalanced a voltage is generated, then amplified, after which it is recorded by the galvanometers.

DIAGRAM OF CIRCULAR ARRAY



MICROPHONE RECORDING SYSTEM



The microphones used were the T-23B, a hot wire element microphone, in the form of a double Helmholtz resonator, and containing an amplifier and acoustical filter. These microphones had to be modified to be compatible with the carrier amplifiers of the recording system. The amplifiers were removed from the microphones and the carrier output from the oscillator was hooked across the hot wire element.

In Figure 3, the resistors A and B are the hot wire element which form two legs of the bridge circuit and resistors C and D are the other two legs placed in the bridge circuit by the amplifier assembly. This type of recording system had an advantage in that all the microphones were powered from a central source, so that the response characteristics of the microphones were approximately the same.

Timing was placed on both sides of the record by a 1000-cycle oscillator. With these timing traces the sound arrivals at the microphones could be read to a part of a millisecond.

By placing the cannon on the same plane as the microphones and firing it with the muzzle in an upright position, it was assumed that the sound was propagated in a circular wavefront, and that the refraction of sound was negligible because of the elevation of the microphones and the short distance over which it propagated. If, sound is being propagated in a homogeneous moving medium, Schotland* has shown that the wind along a particular axis can be determined by the following expression:

$$V_x = \frac{\Delta t \cdot C^2}{2X} \left[1 - \frac{V_x^2 + V_y^2 + V_z^2}{C^2} \right]$$

V_x = wind along x axis

V_y = wind along y axis

V_z = wind along z axis

Δt = time difference of sound arrival at 2 sensors on the same axis

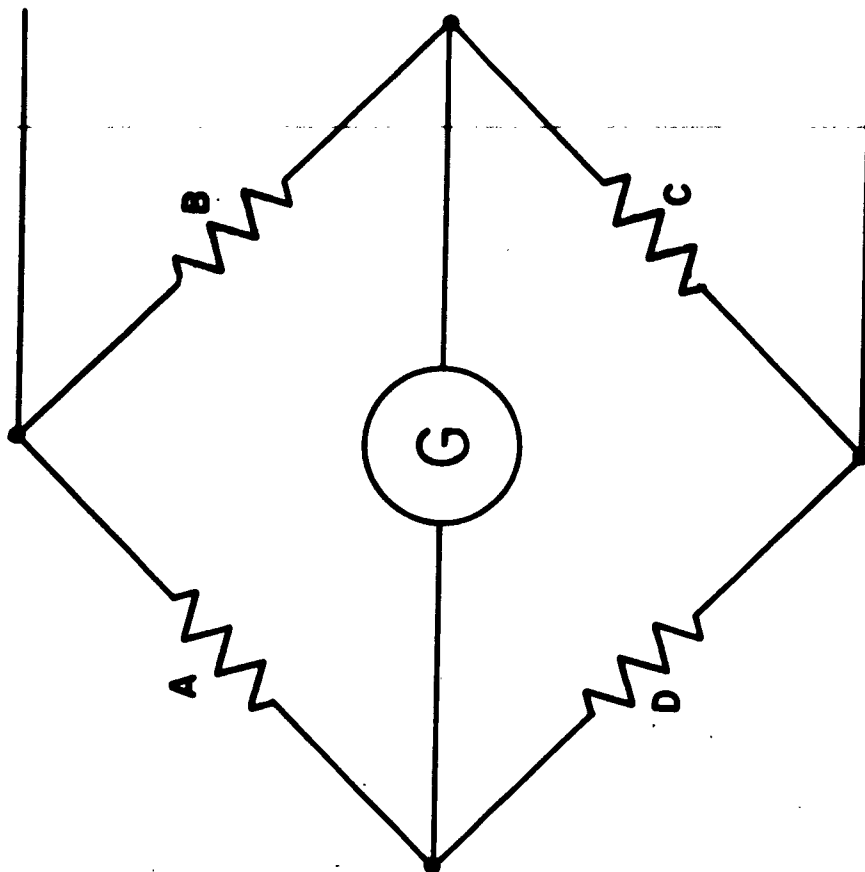
C = speed of sound

X = distance from source to receiver

He also states that by omitting the second term in the brackets an error is introduced in the measurement of V_x . This error depends upon the ratio of the square of the total wind speed to the square of the velocity of sound. For wind speeds less than 35m/sec., the error in the measurement of a component velocity is less than 1 per cent of the true value.

* Schotland, R. M., Journal of Meteorology. Vol. 12, No. 4, pp 386-390, 1955.

BRIDGE CIRCUIT



A&B - HOT WIRE ELEMENT OF T23 MICROPHONE
C&D - AMPLIFIER ASSEMBLY RESISTORS

Since the wind measurements are to be made over an area, it cannot be assumed that the sound is being propagated through a homogeneous moving medium and to compensate for these conditions it becomes necessary to average the various winds by a least squares method.

The wind speed from the center along the path to each microphone is determined by the following expression:

$$V_1 = \frac{\Delta t_1 \bar{c}^2}{D}$$

V_1 = wind speed from source to each microphone

Δt_1 = time difference between average travel time of sound to the microphone and the actual travel time

\bar{c} = average sound velocity

D = distance from source to microphone

The wind speeds are resolved by averaging the speeds along the same axis and then plotting these speeds on a graphical representation of the array. The resolution of these vectors usually results in a triangular intersection rather than a point of intersection. This area of intersection indicates a general direction and magnitude of the wind. The results of this method can be seen in Figure 4. Having determined the general magnitude and direction a mean wind vector is found by a reiteration process and a least squares method.

The wind vectors which have been determined are a component of the total wind along a given path. Therefore, it is necessary to find each of these winds and rotate them into one direction. This is done by using the following expression:

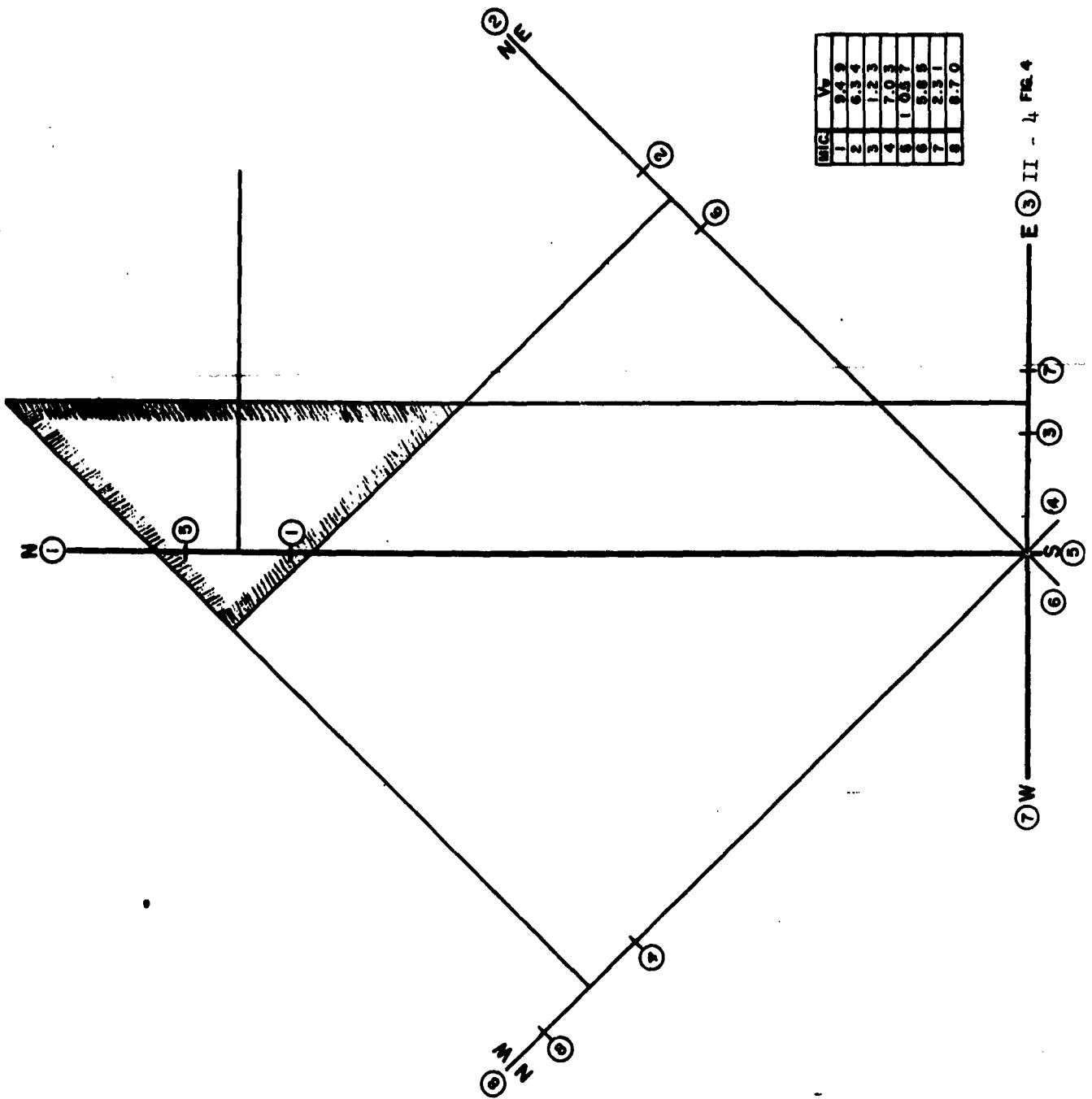
$$V_1 = \sec \theta V_1$$

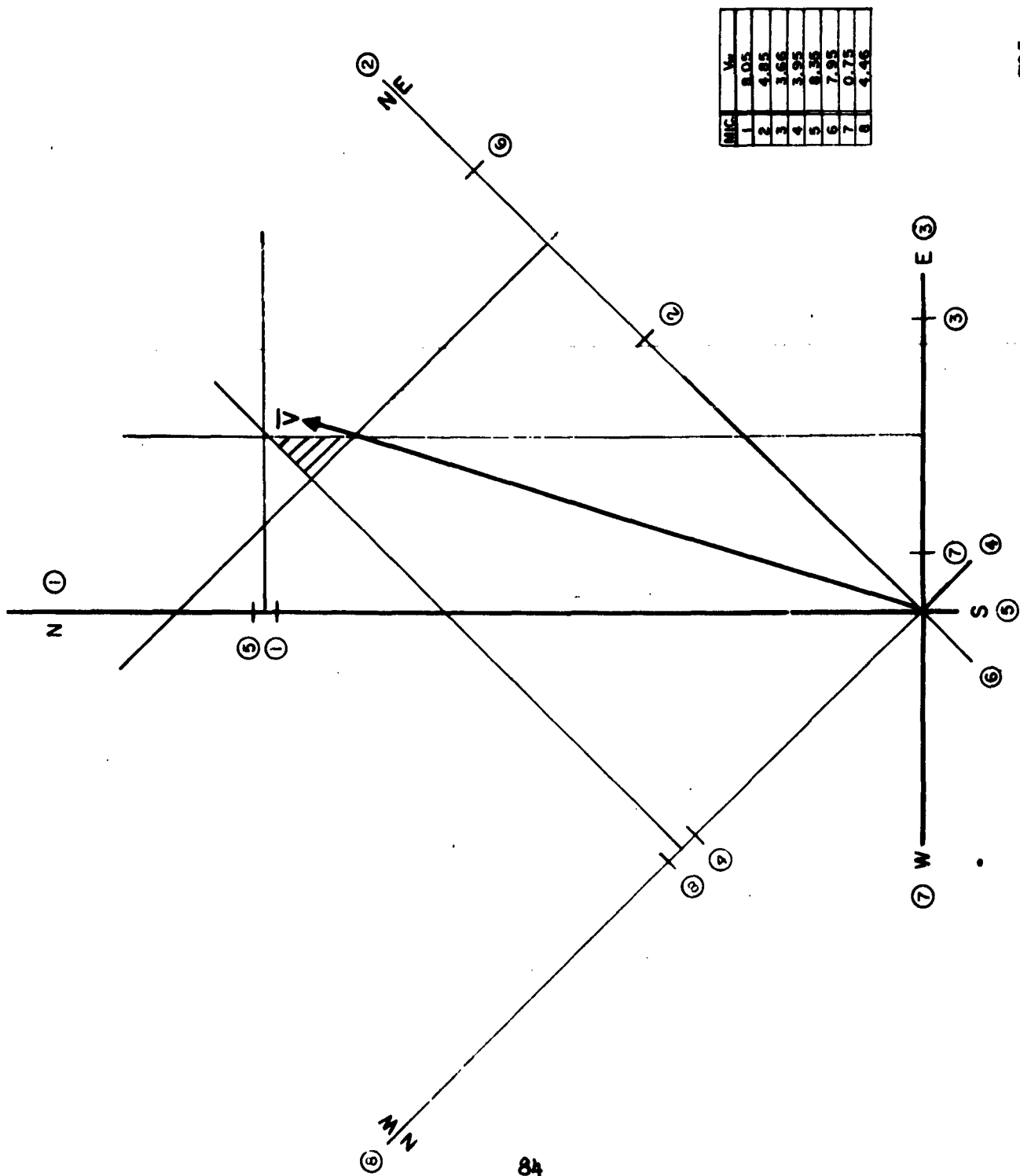
where V_1 is the wind component and secant θ is the angle between the component and the total wind vector. The best estimate of the total wind vector is determined when the sum of the squares of the residuals is a minimum for a given angle θ .

$$\sum (V_1 - \bar{V}_1) = \text{minimum residual}$$

when \bar{V}_1 is the best estimate. In using the least squares method it is assumed that variations are of a random nature and have a normal distribution about a mean.

In Figure 5, the wind vector falls outside the intersected area, because in the graphical representation the wind vectors on the same axis are averaged; while in computing the mean wind vector all eight vectors are used.





II - 4 FIG. 5

From the minimum residuals, the probable error on the mean estimate of the wind is computed. The variation in the probable error may indicate the amount of turbulence in the array area. Another factor contributing to the probable error is the T-23 microphone which has a long rise time, making it difficult to determine the exact time of the initial sound arrival at the microphone.

The wind data from the aerovanes were averaged over a 10 second interval, with the data indicating a steady condition during these tests. The thermometer temperatures were taken at the time of the cannon blast. These measurements were put into table form with the acoustical measurements. These results are summarized in Table 1. Table 2 indicates the estimated mean wind and the size of the probable error associated with that wind measurement.

Conclusions:

The data indicate that the wind can be measured over a given area by means of acoustics. This measurement is the result of averaging the wind vectors from different points on the array and making them fit a uniform laminar flow in the same direction. To fully evaluate the turbulence in the array area, it would be necessary to use microphones with high frequency response characteristics and an electronic means of determining the sound arrivals. With this equipment the instrument error could be more easily determined and the variation from the instrument error would be a measurement of the turbulence.

In the comparison of the data, the wind measurements indicate good agreement, but the temperatures determined by the average sound velocity when compared to the thermometer temperatures do not agree as well. This may be due to taking thermometer measurements at the surface and at one point, and the acoustical measurement five or six feet above the surface, over the entire array. The data from an acoustical array may be more meaningful in determining the flight of a missile during the launch phase, because the measurement is made over an area, and a mean wind is determined with a measure of the turbulence present. The response time of this system is faster than that of the conventional measurement systems.

II - 4 TABLE I
MEASUREMENTS FROM

STANDARD AND ACOUSTICAL EQUIPMENT

Event No.	Acrosvanes				C	Acoustical Measurement \bar{V}	Mercury Thermometer $T (^{\circ}F)$	Acoustical Measurement $\bar{T} (^{\circ}F)$
	I	V	H					
1	DD 197° 6.0 Kts	192° 2.0 Kts	195° -----		200° 4.0 Kts	197° 4.8 Kts	61.5	68.0
3	DD 198° 7.0 Kts	194° 2.7 Kts	190° 6.0 Kts		203° 5.8 Kts	190° 6.2 Kts	61.0	60.0
4	DD 195° 7.0 Kts	190° 3.0 Kts	188° 2.8 Kts		200° 5.0 Kts	194° 5.6 Kts	61.0	55.5
5	DD 193° 7.3 Kts	192° 3.0 Kts	185° 5.5 Kts		192° 5.2 Kts	195° 6.9 Kts	61.0	60.8
6	DD 193° 6.2 Kts	185° 2.0 Kts	----- 4.0 Kts		192° 4.7 Kts	174° 4.7 Kts	60.3	52.0
7	DD 185° 6.0 Kts	183° 2.0 Kts	183° 4.0 Kts		185° 4.0 Kts	190° 4.5 Kts	59.8	56.0
9	DD 192° 6.0 Kts	193° 2.5 Kts	190° 6.0 Kts		200° 4.0 Kts	184° 5.3 Kts	59.3	56.2

II - 4 **TABLE II**

Event	Minimum Residuals	Mean Wind Speed	Probable Error on Estimate of Wind Speed
1	58.34	4.3 Kts	.41 Kts
3	64.03	6.2 "	.43 "
4	149.85	5.6 "	.65 "
5	67.95	6.9 "	.44 "
6	171.65	4.7 "	.69 "
7	72.49	4.5 "	.46 "
9	35.96	5.3 "	.32 "

An Acoustical Technique for Calibrating
High Altitude Temperature Sensors
Harold Ballard
Texas Western College
El Paso, Texas

I. INTRODUCTION

Experimental tests were performed on VECO bead thermistors¹ coated with Krylon Glossy White No. 1501 Spray Enamel,² carbon black, and aluminum.³ The bead was .01 inch in diameter prior to coating. Dimensions of the beads and their cross-sectional areas after coating with the various substances were as follows:

THERMISTOR BEAD DIMENSIONS AFTER COATING*

Coating	Length (mm)	Diameter (mm)	Area (mm ²)
carbon black	5.0×10^{-1}	3.0×10^{-1}	$12. \times 10^{-2}$
aluminum	3.5×10^{-1}	2.5×10^{-1}	7.0×10^{-2}
Krylon ₂	5.0×10^{-1}	3.2×10^{-1}	$12. \times 10^{-2}$
Krylon ₃	4.5×10^{-1}	2.0×10^{-1}	7.0×10^{-2}

*Uncoated diameter: .01 inch (2.5×10^{-1} mm)

NOTE: Subscripts designate test series numbers rather than a difference in the Krylon coating.

TABLE I

Tests were run in an environmental testing chamber at pressures of 670, 87, 8, and 1 mm Hg, corresponding to altitudes of 4,000, 50,000, 100,000,

¹
Mfg's. Nos. 43A6, TX819C, and 55A5, Manufactured by Victory Engineering Corp., Union, N. J.

²
Manufactured by Krylon, Inc., Norristown, Pa.

³
An evaporated aluminum coating.

and 150,000 ft respectively. Temperatures were varied between +20°C and -70°C at each of the above pressures, reproducing as nearly as possible the environmental conditions expected during the descent of a parachute-supported temperature telemetry system.¹

II. ACOUSTIC THERMOMETER

A small speaker was placed within the environmental chamber and acoustically isolated from the chamber. A microphone was placed at the maximum distance from the speaker that was allowed by the size of the chamber. This distance was of the order of one-half meter. The speaker was pulsed from an external source. This pulse also triggered the sweep on an oscilloscope. The output of the microphone was connected to the vertical plates of the oscilloscope. The difference in time between the initiation of the sweep and the arrival of the pulse at the microphone was determined from the calibrated sweep on the oscilloscope. The temperature in °C can be calculated from the equation:

$$t^{\circ}\text{C} = 273 \left(\frac{v_t}{v_0} \right)^2 - 1$$

where

v_t = speed of sound at the temperature, $t^{\circ}\text{C}$, and

v_0 = speed of sound at 0°C.

Rather than calculate the temperature from the determination of the speed of sound, the temperature within the chamber was lowered in increments of 10°C between the limits of 20°C and -70°C while the chamber pressure was maintained at 670 mm Hg. At this pressure the thermocouple correctly read the air temperature. The elapsed time between the pulsing of the speaker and the arrival of the sound front at the microphone was determined from observation of the oscilloscope sweep. This was done at each temperature increment. The distance interval from the beginning of the oscilloscope sweep to the leading edge of the pulse from the receiving microphone was plotted as a function of temperature of the thermocouple used to determine the air temperature within the chamber. This procedure was followed at pressures of 670, 87, 8 and 1 mm Hg, corresponding to altitudes of 4,000, 50,000, 100,000 and 150,000 ft respectively.

From these data, the air temperature as a function of indicated thermocouple temperature was plotted in Figure 1.

III. DETERMINATION OF R_0 (670 mm Hg)

The resistance of the thermistor was determined as a function of air temperature. This was accomplished in two ways:

METHOD 1: By placing a high-impedance ohmmeter across the thermistor to measure the resistance directly.

METHOD 2: By determination of the resistance from voltage-

¹ On the basis of data taken from scheduled firings of the Meteorological Rocket Network.

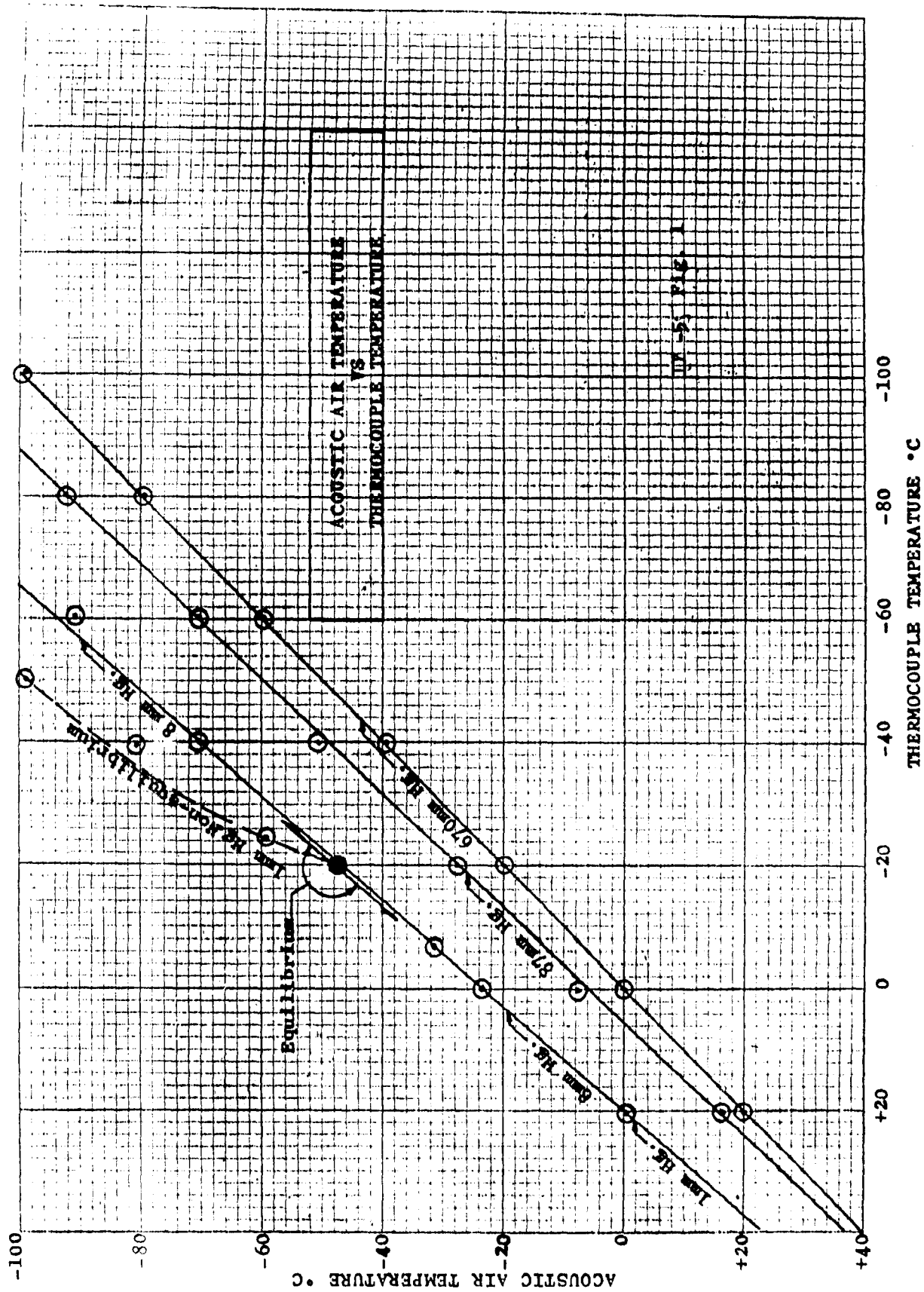


Fig. 5, Fig. 1

current calculations at constant powers of 1, 5, and 10 microwatts. It was found that the resistance characteristics of the thermistor were the same at powers between 1 and 10 microwatts. When this was determined, Method 1 was used for subsequent tests.

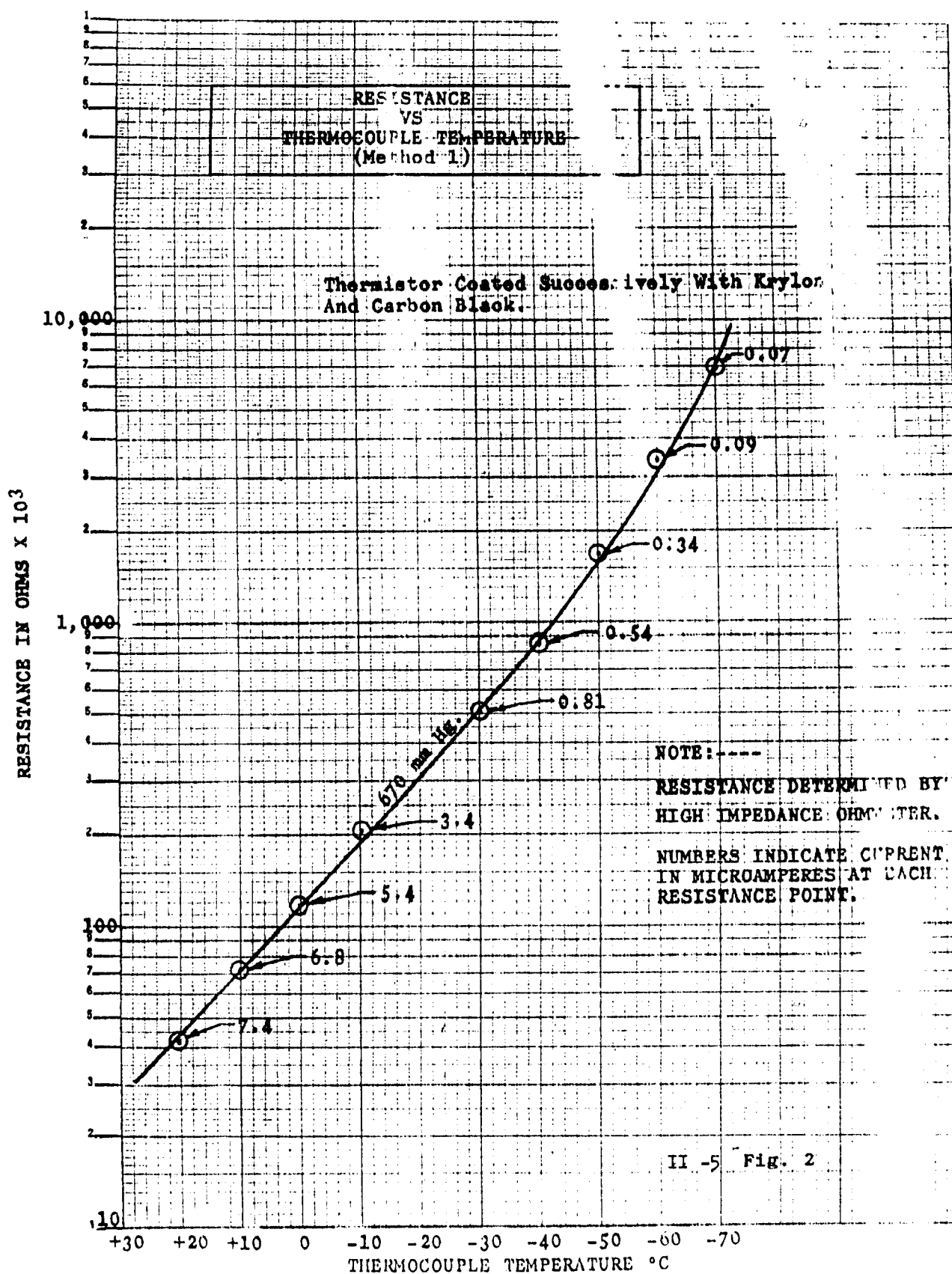
These data are presented in Figures 2-6, inclusive. The numbers beside each point in Figure 2 indicate the current that flowed through the thermistor when its resistance was determined by use of the high-impedance ohmmeter. The type of coating used in each case is indicated on each figure. Each test was run at 670 mm Hg pressure. Sufficient time was allowed between each determination of resistance to allow the chamber to reach equilibrium temperatures and pressure. The wall temperatures of the chamber were determined by thermocouples. The resistance of the thermistor was essentially the same when coated with Krylon white enamel as when coated with carbon black or aluminum.

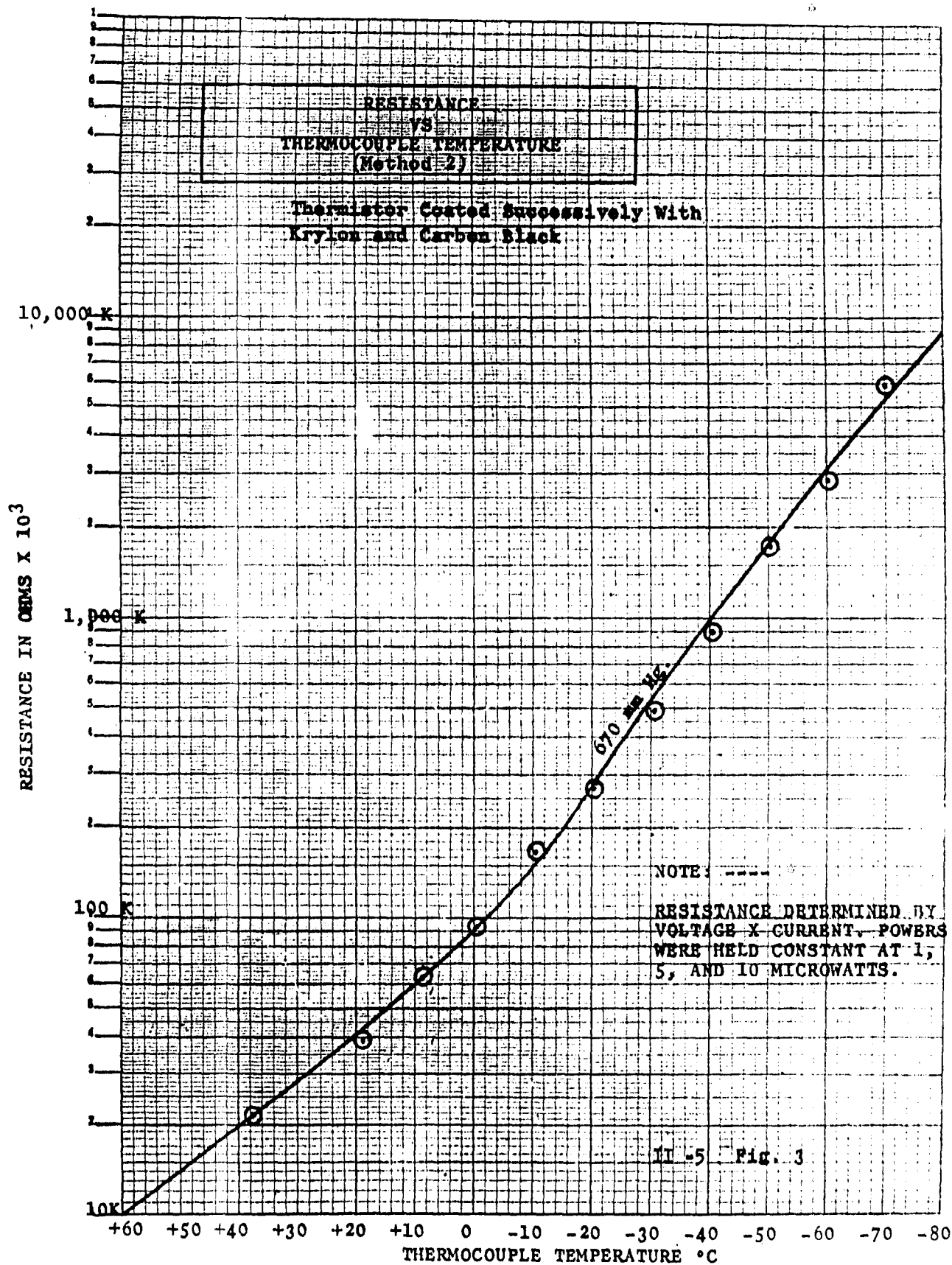
IV. DETERMINATION OF R_0 (1 mm Hg)

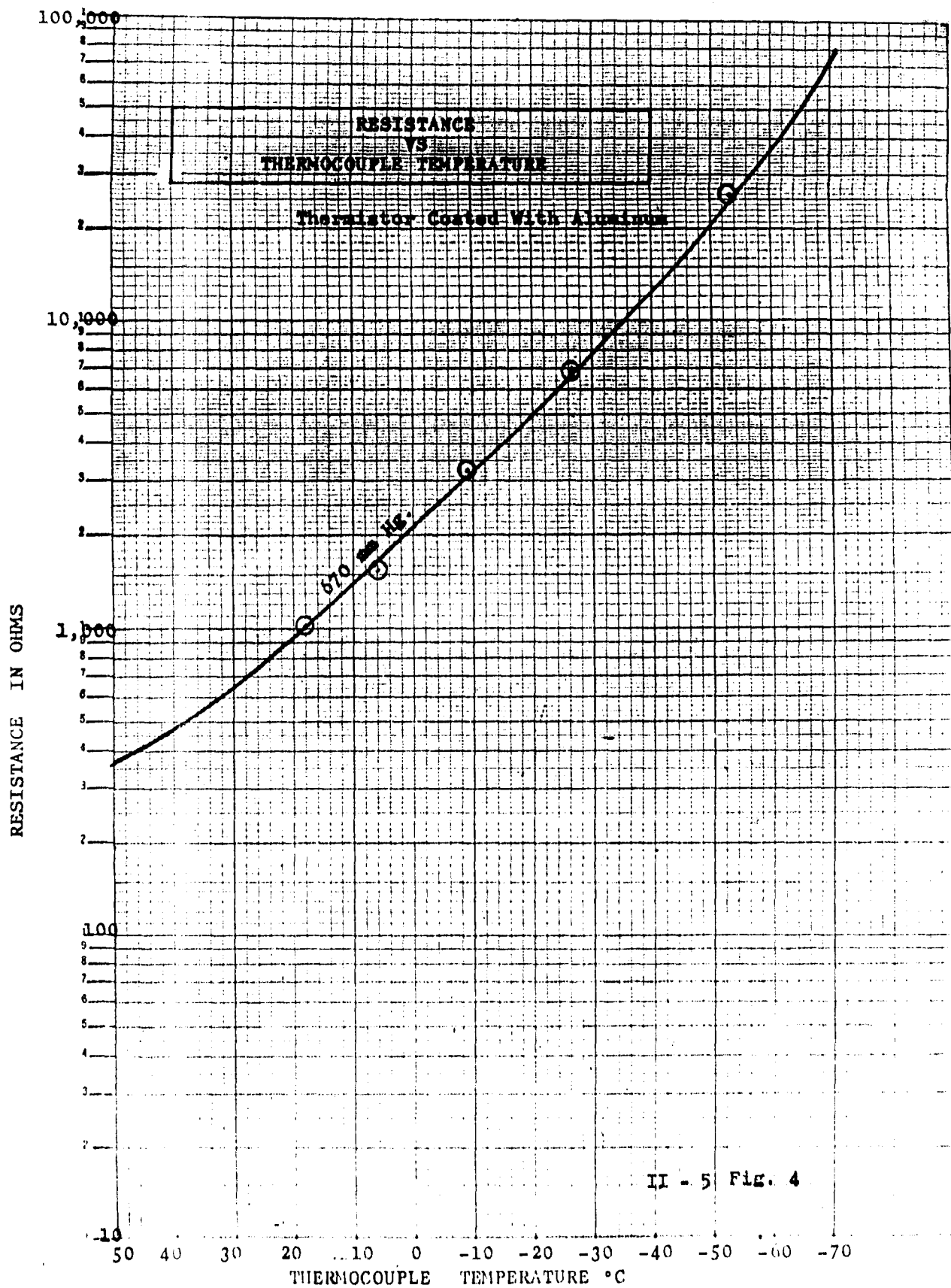
The resistance of the thermistor was determined as a function of temperature in the same manner as described for the determination of R_0 at 670 mm Hg. A difficulty was experienced here in that equilibrium temperatures could not be reached within the chamber at air temperatures below -50°C. Nevertheless, it was determined that the thermocouple and the thermistor, both of which were supposedly reading the air temperature, were in radiative equilibrium with the walls of the chamber.

V. CHAMBER WALL EFFECTS

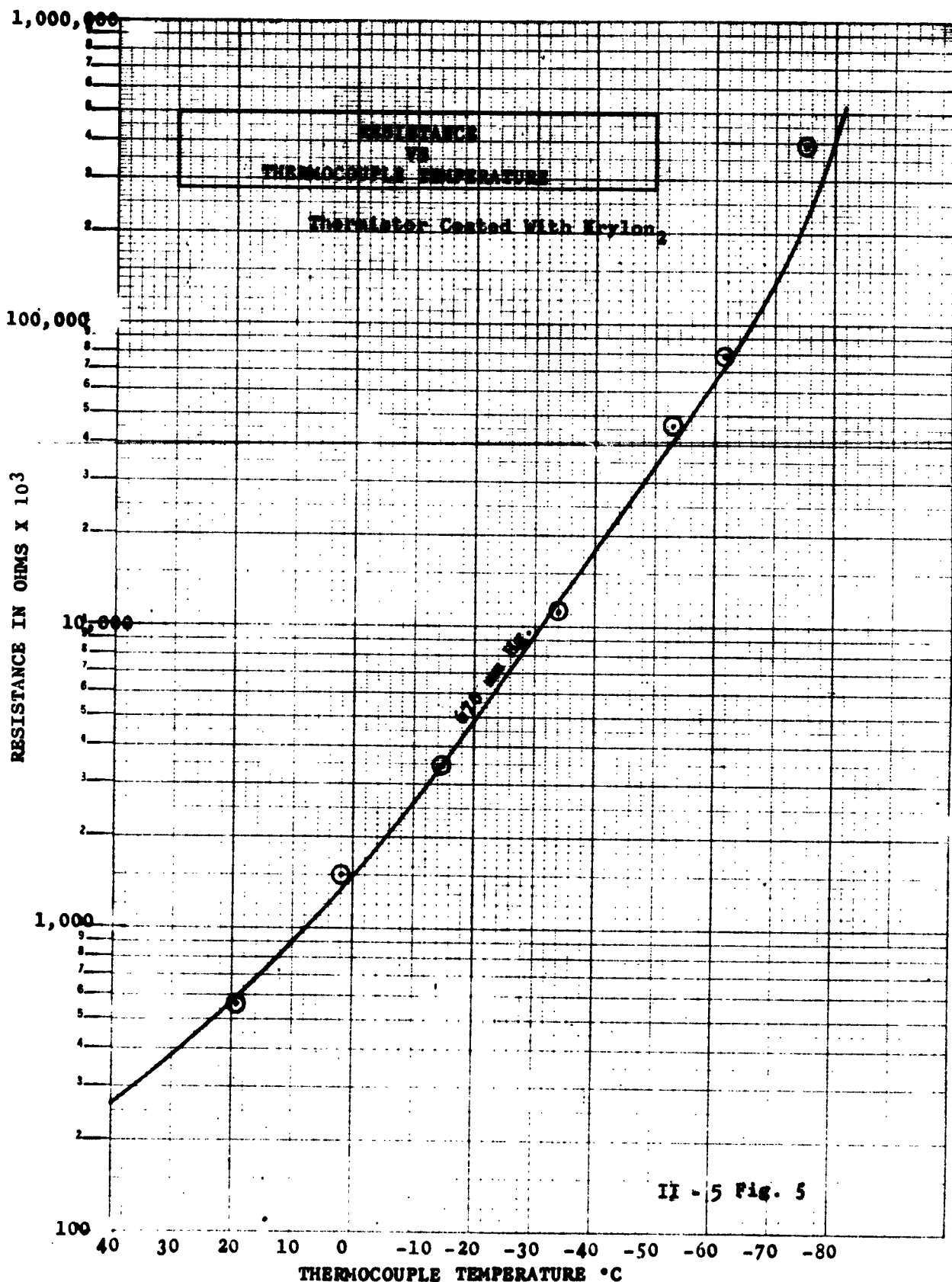
When it was noted that the thermistor was not reading the air temperature within the test chamber at a pressure of 1 mm Hg, a study was made of the effect of the walls on the thermistor and thermocouple. These tests were performed at 670, 87, 8 and 1 mm Hg. Thermocouples were placed on the six walls of the chamber, and one was placed in the air at the center of the chamber. The chamber was brought to equilibrium temperatures and pressure before each determination of air temperature. An elapsed time of approximately three hours was necessary for the chamber to reach equilibrium at pressures of 8 and 1 mm Hg. The air temperature was determined by the acoustic thermometer described above. Since each wall had essentially the same area, an average of the wall temperatures was determined and plotted as a function of the air temperature in Figure 7 and as a function of thermocouple temperature in Figure 8. The thermistor temperature as a function of thermocouple temperature was determined and plotted in Figure 9. The data presented in Figures 7, 8, and 9 indicate that the thermocouple and thermistor were in thermal equilibrium with the walls of the test chamber at a pressure of 1 mm Hg.



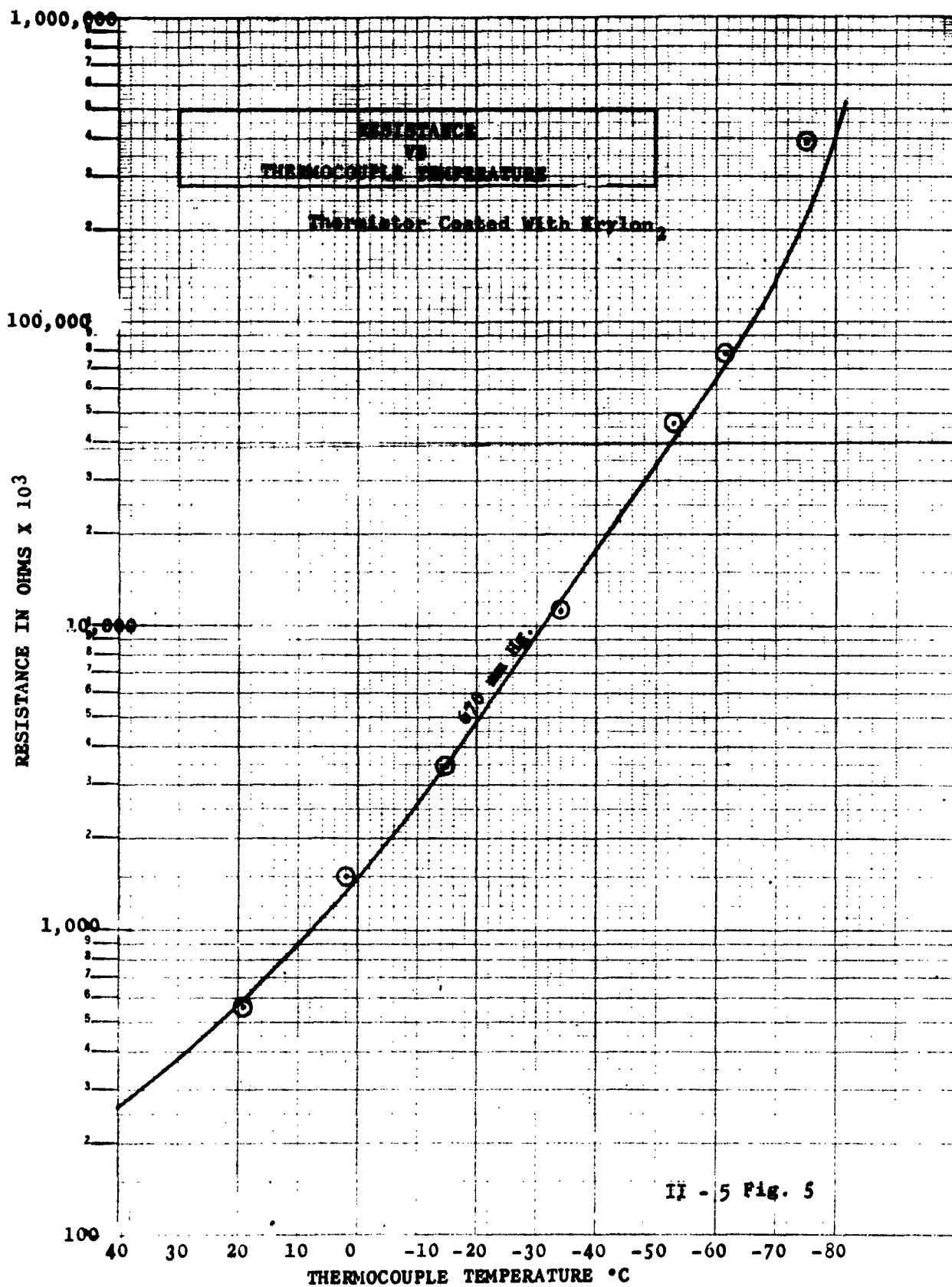


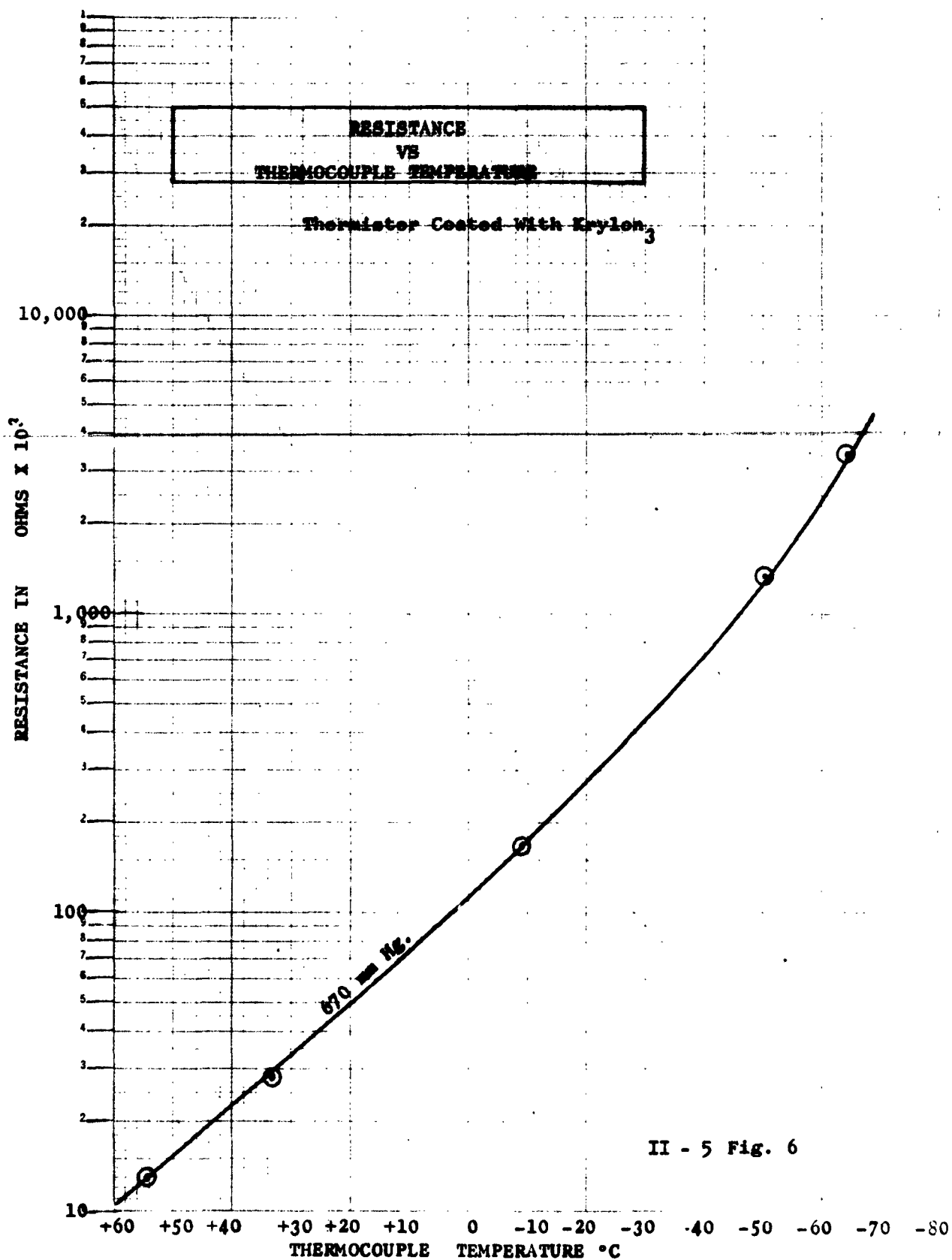


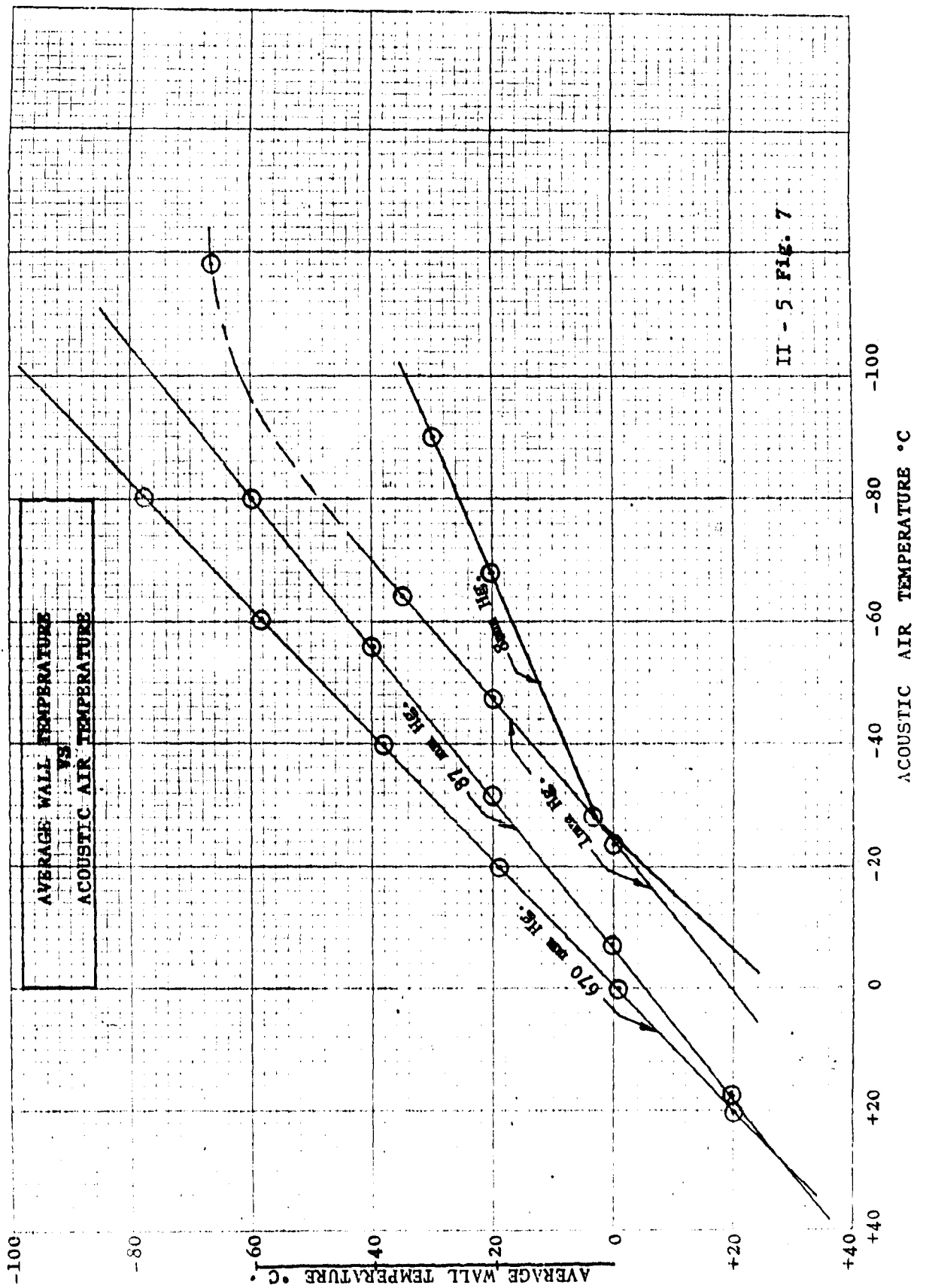
II - 5 Fig. 4



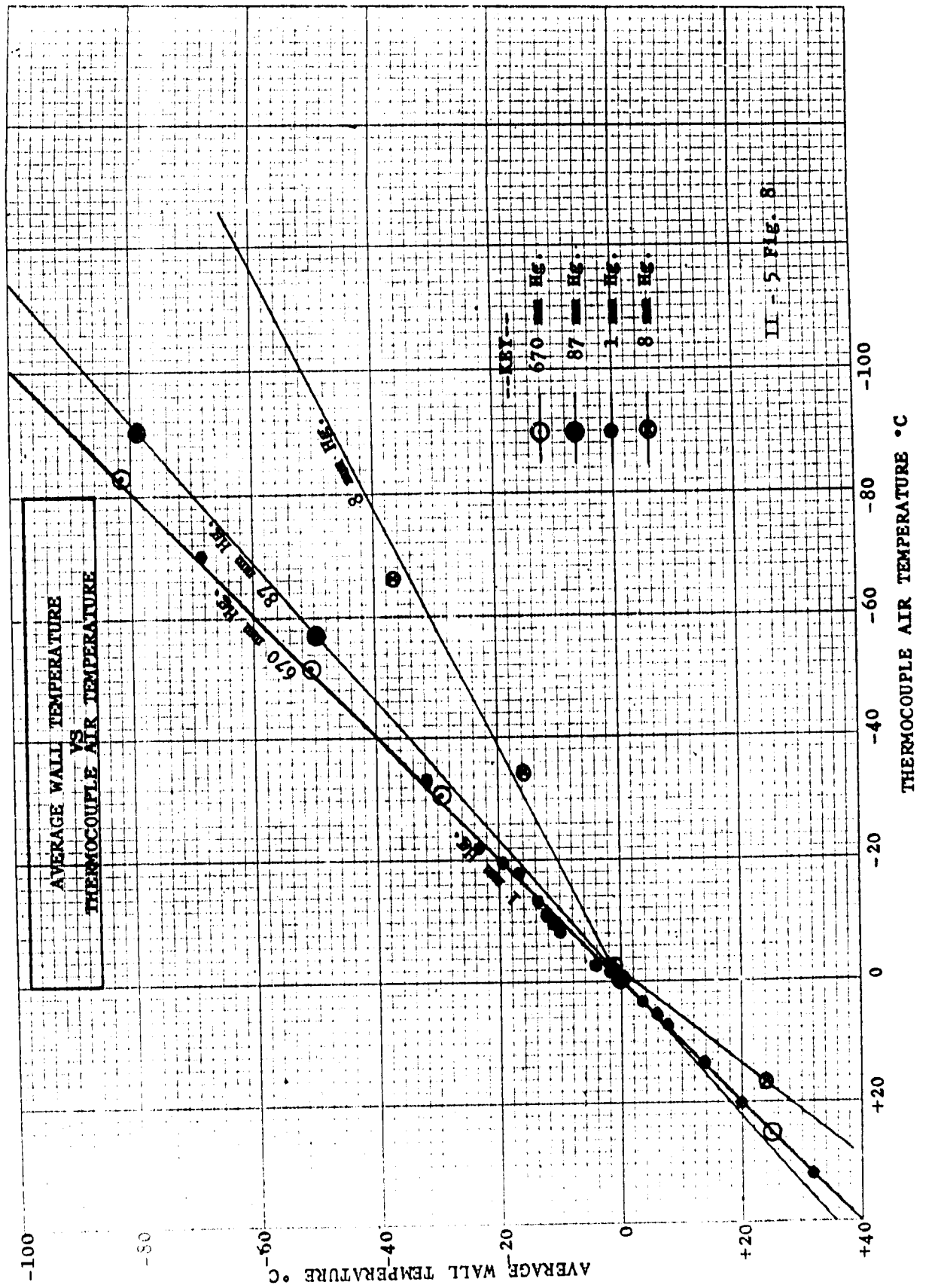
II - 5 Fig. 5

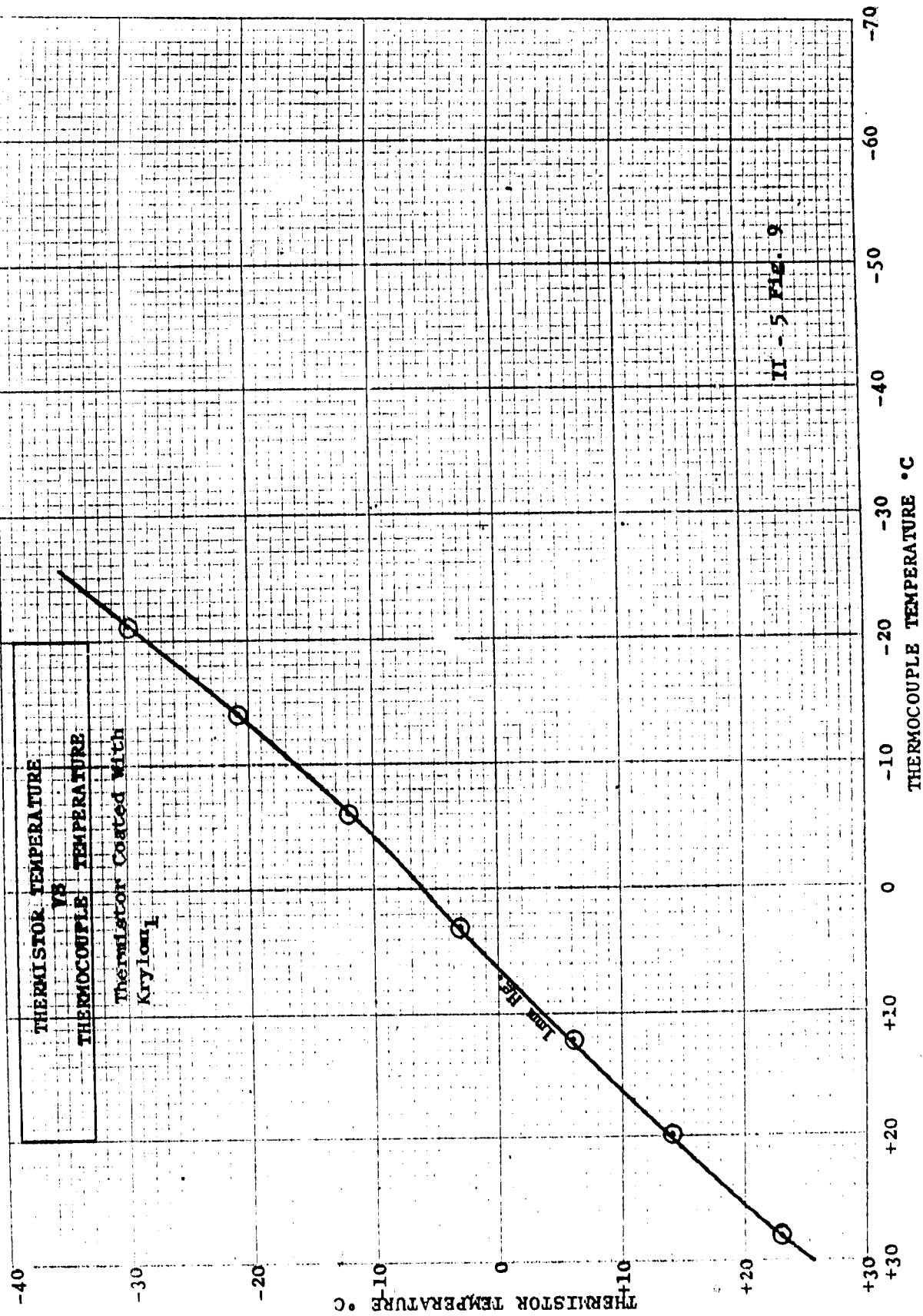






II - 5 FIG. 7





DETAILED ACOUSTIC STRUCTURE ABOVE THE TROPOPAUSE

Willis L. Webb

U. S. Army Signal Missile Support Agency
White Sands Missile Range, New Mexico

I. INTRODUCTION

Sufficient data on atmospheric thermal and flow structure now exists between the surface and 60,000 feet to permit a realistic analysis of sound propagation parameters. In many atmospheric acoustical problems the pressure perturbation energy passes through higher levels of the atmosphere which have only recently come under observational scrutiny. Mean profiles of reasonable accuracy have been obtained for several geographic locations (1). An understanding of mesospheric sonic structure is just becoming possible as the sensitivity and accuracy of available sensing techniques become established.

Theoretical and experimental studies of the response characteristics of wind and temperature sensors which are currently available for application in the mesospheric region indicate error values which are smaller than spatial and time variations. In view of the gross scale of most atmospheric acoustical problems, the data appear to be adequate for most detailed studies. An obvious exception to this conclusion is found in the acoustical data needed for local analysis of the drag experienced by a supersonic vehicle or the coupling of transducer energy into the acoustical environment. Improvements in current measuring techniques may well prove to be desirable, and are generally considered possible. The more difficult problem very likely centers around the selection of an observation program which will furnish adequate data.

Atmospheric acoustical scientists have long studied the complex wave forms which are observed at distances of the order of hundreds of kilometers from relatively simple acoustical inputs such as explosions. These environmental alterations of the propagation pressure waves are undoubtedly associated with the spatial acoustic structure of the atmospheric region involved, and there is reason to expect a maximum modifying influence at the levels where wave frontal propagation rays approach or leave the horizontal. One must, therefore, even in a preliminary survey, have data from the earth's surface to the sonic mesopeak, since the occurrence of grazing incidence ray paths is to be expected at all levels. The scale of the detail which will prove to be most interesting is not clear. We will proceed, therefore, from the lower major atmospheric duct (surface to mesopeak), which has been delineated in an earlier paper (1), to smaller scale features until the limits of resolution of our sensors are reached.

A cursory examination of the available atmospheric acoustic structure profiles indicates that a considerable degree of variability exists. Large scale deviations from the mean occur occasionally, with sub-ducting features reaching magnitudes of the order of one-half the strength of the

major duct and several tens of thousands of feet thick. Numerous smaller excursions are observed, and it is undoubtedly true that some of the fine scale sonic structure is lost in the inability of the sensors to adequately depict the actual situation.

II. APPLICABILITY OF THE AVAILABLE DATA

The atmospheric speed of sound data used in this study were determined primarily from flow and temperature data. The most active atmospheric variable which affects the speed of sound is the flow. Winds of the order of several hundreds of miles per hour have been observed and are known to be highly variable in space and time. The temperature structure of the atmosphere, while complex, is generally much more conservative with regard to extreme values. Other parameters, such as atmospheric composition, will undoubtedly have an effect on the local sound speed. For purposes of this report the latter effects are neglected, chiefly because of the lack of suitable instrumentation for data acquisition.

No single system currently exists which is capable of obtaining wind data over the entire region of interest (surface to 200,000 feet) with any reasonable efficiency. The technique thus far employed consists of a balloon sounding (approximately 1000 feet per second ascent rate) from the surface to balloon burst, which occurs near 100,000 feet in the most efficient systems. Meteorological data in the upper portion of the atmospheric acoustic duct are obtained through use of rocket systems, the more desirable of which involves a coherent radar reflector which accurately drifts with the wind and carries a temperature sensing system.

The principal problem involved in sensing the wind accurately centers around the fall rate. It is desirable to attain a fall rate of the order of 250 feet per second or less. If the particular sensor does have such a characteristic at 200,000 feet, the gross increase in density (decrease in fall rate) serves to prolong the fall to unusable proportions below 75,000 feet. The data published by Beyers and Thiele (2) indicates a probable fall rate of 375 feet per second at 200,000 feet, 210 feet per second at 165,000 feet and 60 feet per second at 100,000 feet for the system used to obtain the data analysed in this report. Further losses in sensitivity are encountered in the system tracking and data processing. These factors obscure details of the acoustic structure which have dimensions of less than 10,000 feet in the region above 150,000 feet, with resolutions of less than 5,000 feet the rule from 150,000 feet to the bottom of the sounding.

The measurement of temperature at altitudes of 150,000 and 200,000 feet presents a number of new problems in sensing and telemetry techniques. These problems have been carefully considered by Clark, Wagner and Ballard (3, 4, 5) with the conclusion that the data are reliable to within five degrees over the region of interest. Much of the error is absolute magnitude in character, and the observed gradients over small height differences can be relied upon to much greater accuracy. The speed of response of the sensors is adequate to provide over 90% response to a 1000-foot interval step function at the least sensitive point of interest (base of the sonic mesopeak).

III. TYPICAL DATA

Particular attention will be devoted to the nature of the observed details of atmospheric acoustic structure in the newly invaded lower mesosphere. Design criteria for the meteorological rocket system called for sensor deployment at 200,000 feet or above when launched from sealevel. Inadequate rocket performance or difficulties in the deployment technique occasionally resulted in a lower peak data acquisition altitude, although at White Sands Missile Range (elevation 4000 feet) the peak altitudes are frequently 250,000 feet or higher. The data are considered adequate for our purposes from 180,000 feet down, with the lower limit of data from the rocket borne sensor generally around 60,000 feet, established principally by the time which can be devoted to observation.

A few typical examples of the atmospheric acoustic structure evaluated from the rocket data are presented in Figures 1 through 4. The thermally induced speed of sound distribution, representing the vertical sonic components, and the structure for a horizontally propagating sound front from the east and the west are included in these figures. The vertical components are found to be illustrative of the more conservative case, at least in the gross characteristics. The east-west components illustrate the extreme of large scale variability. The north-south components have been omitted in this presentation because they generally fall between these extremes, although this assumption may prove unwarranted in the very fine scale structure.

The data obtained on 22 July 1961 (Figure 1) at White Sands Missile Range are more or less typical of the acoustic structure in the lower mesosphere in mid-latitudes in summer. We find a weak sonic inversion for a sound front coming from the west, a moderately increasing speed of sound with height for a vertically propagating sound front, and a strong sonic inversion for a sound front approaching from the east. One should immediately note that Figures 2 through 4 exhibit the inverse situation in the east-west components with a favorable ducting structure observed for an eastbound sound front during the winter season. These observations are treated in somewhat greater detail in reference 1.

Inspection of the thermally induced sonic profiles (center curves) confirms the expected rather conservative character of these data relative to gross differences. They do exhibit, however, marked differences in details. The data for White Sands Missile Range on 22 July 1960 (Figure 1) at about 120,000 feet present an unusual degree of complexity. All of the thermally induced profiles show a smoothing trend at higher altitudes. This trend undoubtedly is a combined result of increasing atmospheric homogeneity (which seems reasonable theoretically) and a deteriorating capability of the temperature sensor to respond to small scale changes which becomes important at the extreme high altitudes.

The east and west component profiles, which result from combined temperature and wind effects on the sonic profiles, are frequently several

Meteorological Effects on the Speed of Sound in the Atmosphere from Rocket Sounding Data

SUMMER SERIES - 1960

Altitude
(x 10³ ft. MSL)

140

220

300

380

460

540

620

700

780

860

940

1020

1100

1180

1260

1340

1420

1500

1580

1660

1740

1820

1900

1980

2060

2140

2220

2300

2380

2460

2540

2620

2700

2780

2860

2940

3020

3100

3180

3260

3340

3420

3500

3580

3660

3740

3820

3900

3980

4060

4140

4220

4300

4380

4460

4540

4620

4700

4780

4860

4940

5020

5100

5180

5260

5340

5420

5500

5580

5660

5740

5820

5900

5980

6060

6140

6220

6300

6380

6460

6540

6620

6700

6780

6860

6940

7020

7100

7180

7260

7340

7420

7500

7580

7660

7740

7820

7900

7980

8060

8140

8220

8300

8380

8460

8540

8620

8700

8780

8860

8940

9020

9100

9180

9260

9340

9420

9500

9580

9660

9740

9820

9900

9980

10060

10140

10220

10300

10380

10460

10540

10620

10700

10780

10860

10940

11020

11100

11180

11260

11340

11420

11500

11580

11660

11740

11820

11900

11980

12060

12140

12220

12300

12380

12460

12540

12620

12700

12780

12860

12940

13020

13100

13180

13260

13340

13420

13500

13580

13660

13740

13820

13900

13980

14060

14140

14220

14300

14380

14460

14540

14620

14700

14780

14860

14940

15020

15100

15180

15260

15340

15420

15500

15580

15660

15740

15820

15900

15980

16060

16140

16220

16300

16380

16460

16540

16620

16700

16780

16860

16940

17020

17100

17180

17260

17340

17420

17500

17580

17660

17740

17820

17900

17980

18060

18140

18220

18300

18380

18460

18540

18620

18700

18780

18860

18940

19020

19100

19180

19260

19340

19420

19500

19580

19660

19740

19820

19900

19980

20060

20140

20220

20300

20380

20460

20540

20620

20700

20780

20860

20940

21020

21100

21180

21260

21340

21420

21500

21580

21660

21740

21820

21900

21980

22060

22140

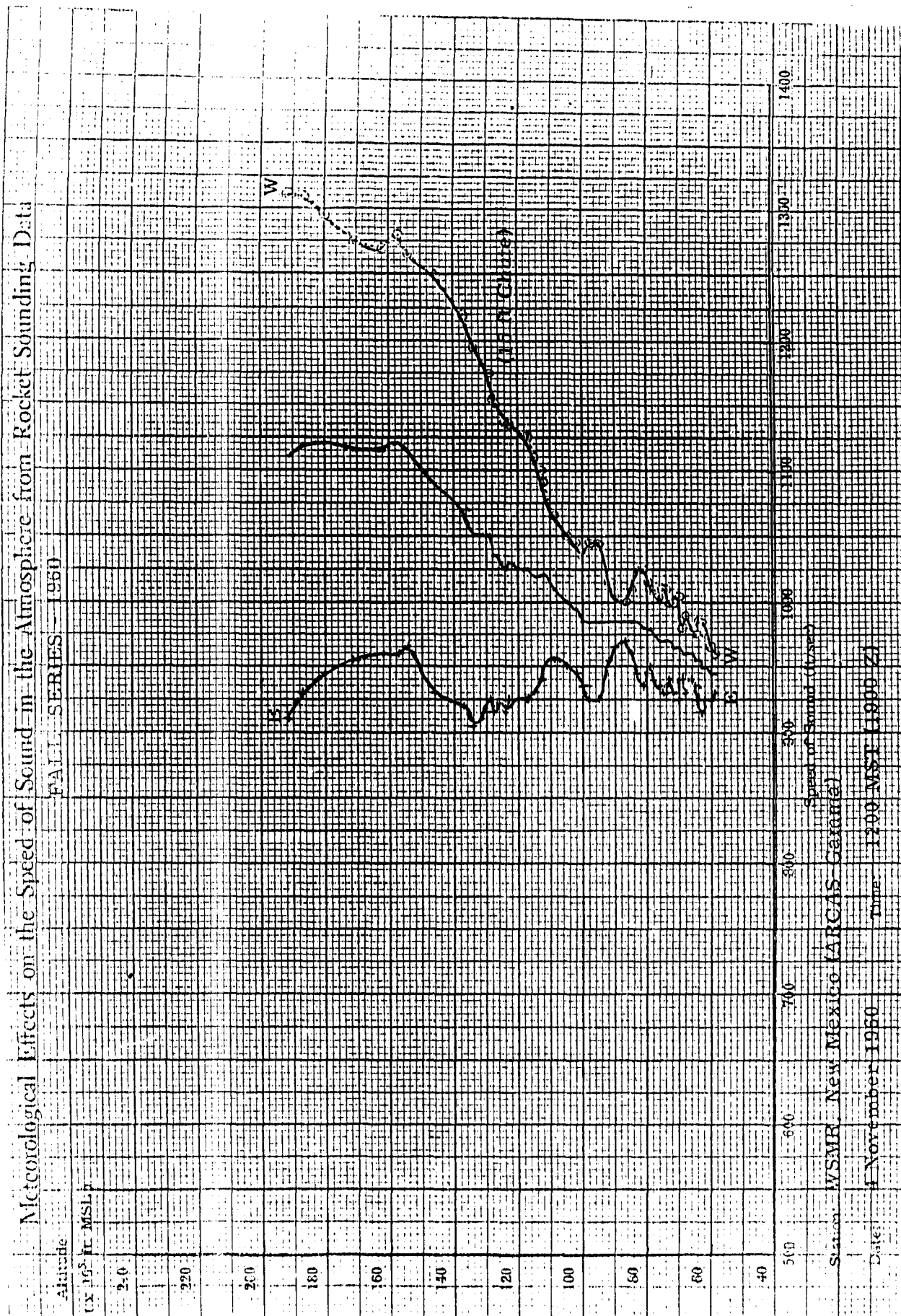
22220

22300

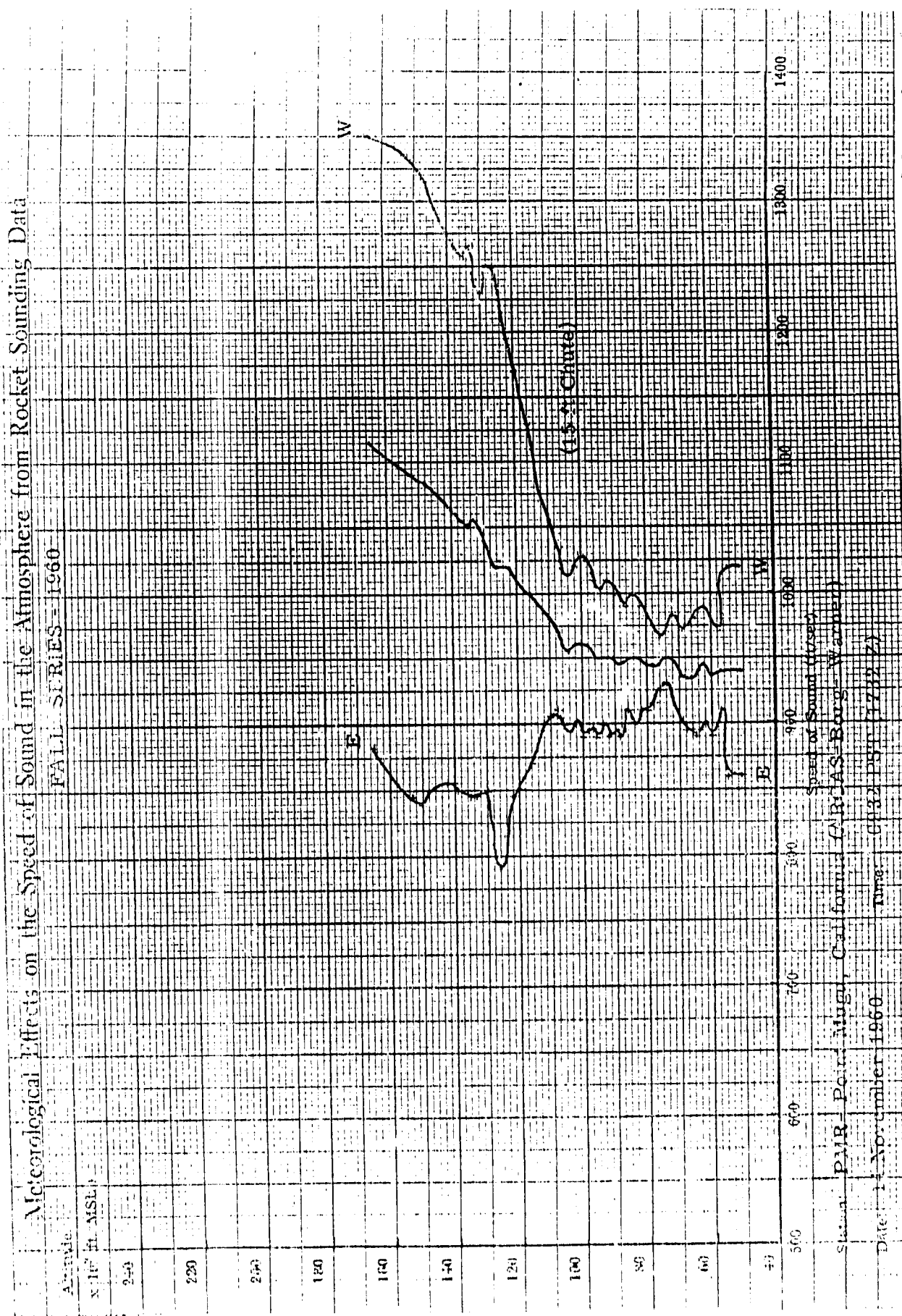
22380

22460

22540



II-6 FIGURE 2. An example of the type of meteorological Rocket Network data obtained in winter at mid-latitudes for the vertical, east and west components.



II-5 FIGURE 3. An example of the type of meteorological rocket network data obtained in winter at mid-latitudes for the vertical, east and west components.

Meteorological Effects on the Speed of Sound in the Atmosphere from Rocket Sounding Data



FIGURE 4. An example of the type of meteorological rocket network data obtained in summer in sub-polar regions for the vertically, east and west components.

tens of feet per second over restricted height intervals (of the order of thousands of feet). One would expect, therefore, that the stronger gradients will be found in restricted height intervals as the generating influences happen to favorably combine.

Frequent reversals of the temperature and wind induced sonic gradients result in the formation of sub-ducts which can be expected to exert a profound influence on a propagating sound front. Thermal gradients produce relatively minor sub-ducts, generally less than 10,000 feet thick and the order of ten feet per second in intensity. An example of the more pronounced class of thermally induced sub-ducts is centered around 144,000 feet in the Fort Churchill sounding of 17 November 1960 (Figure 4). This sub-duct is approximately eight thousand feet thick and has a strength of about 10 feet per second. An extreme case is found in the 22 July 1960 (Figure 1) sounding at White Sands Missile Range at an altitude of 124,000 feet. The duct is quite thin, approximately 3000 feet thick, and has an intensity of some 20 feet per second.

The sub-ducts formed by wind shears exhibit structures which range from the smallest scale discernable to gross features several tens of thousands of feet thick and several tens of feet per second in intensity. In general, the larger sub-ducts appear in the near isosonic profiles as is illustrated in the east component of the sounding obtained at White Sands Missile Range on 4 November 1960 (Figure 2). This sub-duct has an intensity of about 50 feet per second and a thickness of some 44,000 feet centered about a duct minimum of 905 feet per second at 134,000 feet.

A more typical example is represented by the sub-duct centered at 97,000 feet on the same graph or the sub-duct centered at 88,000 feet on the west component of the same sounding. A more extreme case is found in the east component of the sounding obtained at Pacific Missile Range, Point Mugu, California, on 14 November 1960 (Figure 3). The sub-duct is some 60 feet per second in intensity and about 9000 feet thick, centered about a minimum of 790 feet per second at 126,000 feet.

IV. SEASONAL COURSE OF THE SONIC INVERSION GRADIENT

It is clear from the data presented in reference (1) that a marked seasonal and latitudinal variability exists in the sonic structure of the upper portion of the principal atmospheric duct. This variability is induced primarily by the circulation pattern in the lower mesosphere. Immediately above the tropopause one generally finds increasing westerly winds with height in winter, while in the summer the reverse situation of increasingly easterly winds with height is the rule. The seasonal changes in these flows are of major interest, as are the details which are a part of the day-to-day atmospheric structure.

Observational problems have severely limited the atmospheric structure data available in the region from the tropopause to the mesopause. The Meteorological Rocket Network began in 1960 the routine sounding of thermal

and wind structure from which the speed of sound can be evaluated (6). The data which have been acquired to date are considered adequate for a gross inspection of the space and time variability of the general sonic gradient above the tropopause.

As is illustrated in Figure 5, the lower mesospheric sonic gradient experienced by a sound wave approaching in the horizontal plane from the west is a strong function of the season. The mid-latitude gradient varies from a maximum of 5 to 6×10^{-3} per second in January to a minimum of 1×10^{-3} per second just after the middle of July. The curve is characterized by a relatively moderate slope during the spring months, while the fall period shows a quite rapid change.

The regime in the sub-polar regions is decidedly different from the mid-latitude case. The peak amplitude reaches a value of only 4×10^{-3} per second in the winter while the summer minimum falls to $.8 \times 10^{-3}$ per second. The time of occurrence is considerably earlier in the sub-polar case with the minimum in mid-June, over a month earlier than the corresponding mid-latitude case.

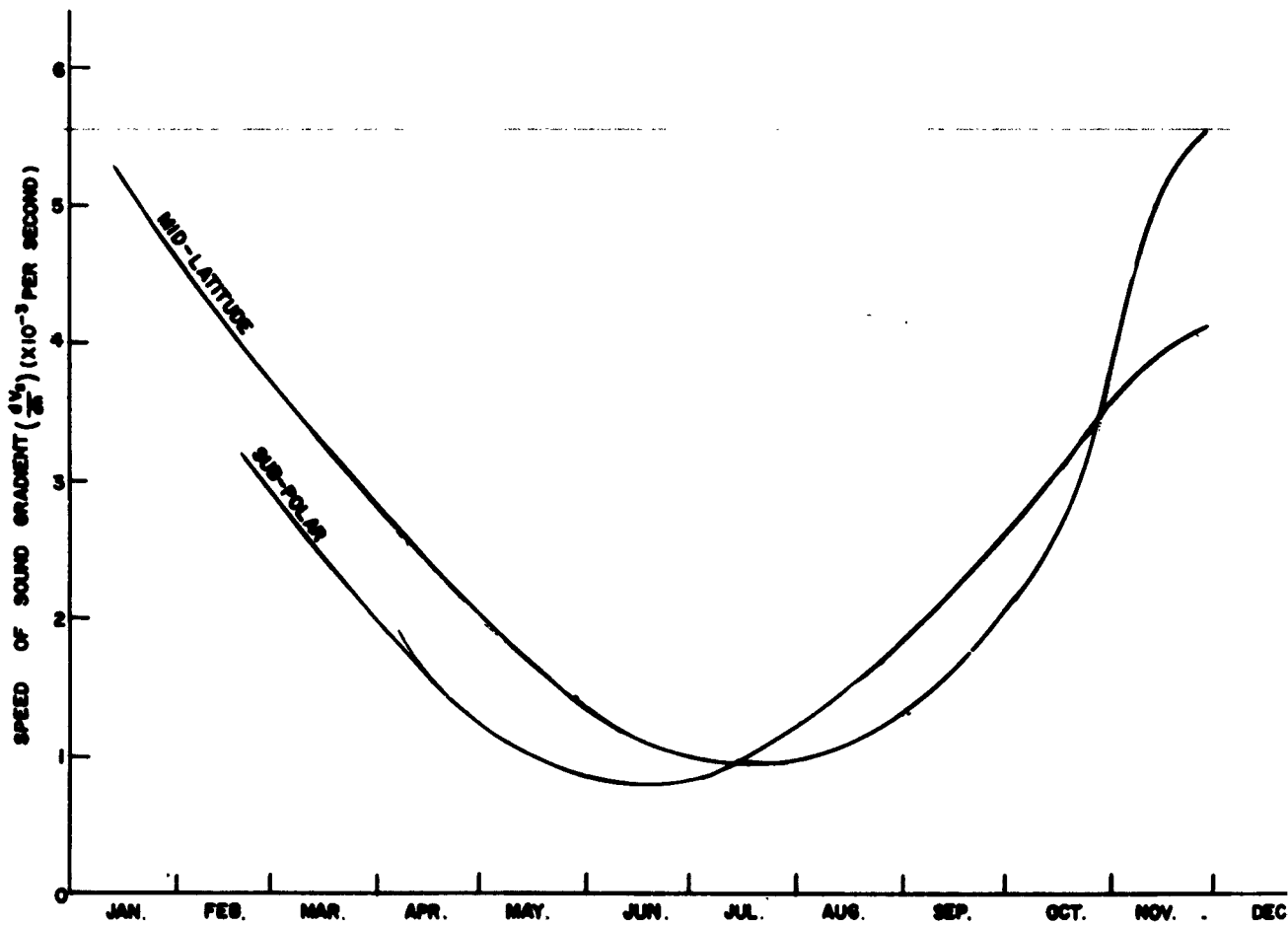
The significance of these data is indicated by the curves presented in Figure 6. The dashed curves indicate the range of values observed thus far. The data are of markedly different character during the spring and fall seasons, with cross-over periods during early winter and summer, during which times the data are quite similar.

One should view the data presented here with a certain amount of caution. The curves represent mean values based on data which were obtained over relatively short intervals of intensive observation, with appreciable interpolation required during the interim periods. One can expect that the curves will show considerable detail when sufficient data are available for daily, weekly or monthly means are obtained, or when the means are made up of more restricted latitude belts.

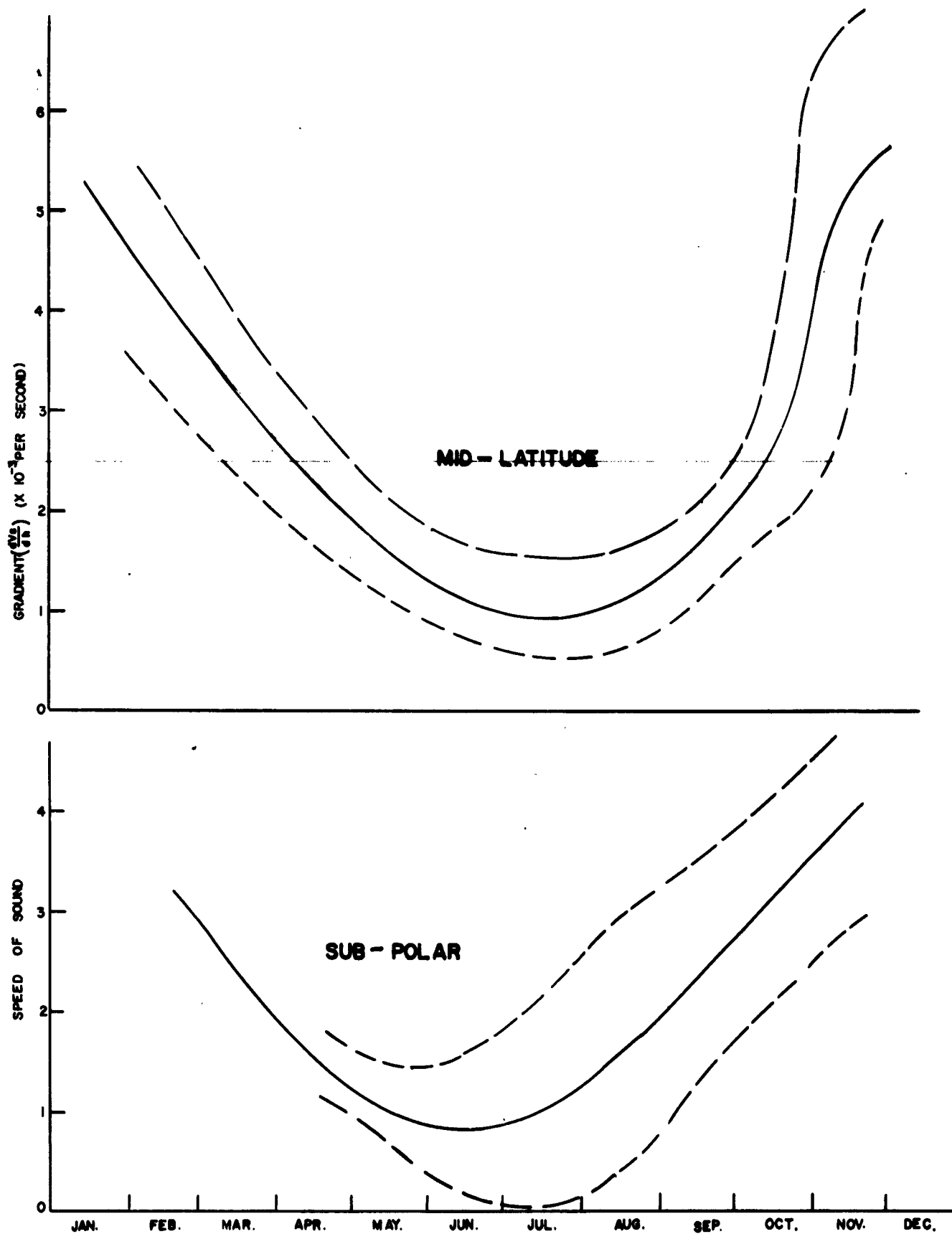
V. THE VERTICAL EXTENT OF SOUND GRADIENT LAYERS

The significance of a gradient in a sonic profile is directly affected by the parametric interval over which it is effective. The atmospheric processes which establish the sonic gradient at a point may combine to give a wide variety of values, but physical considerations relative to the permissible extreme values of these contributing factors limits the total change in sound velocity, which serves to define the sonic gradient over a particular height interval. The magnitude of the overall sonic inversion in the lower mesosphere has been indicated in Figure 6. It is of interest to inspect the available data for relations between the strength and the depth of the observed gradients.

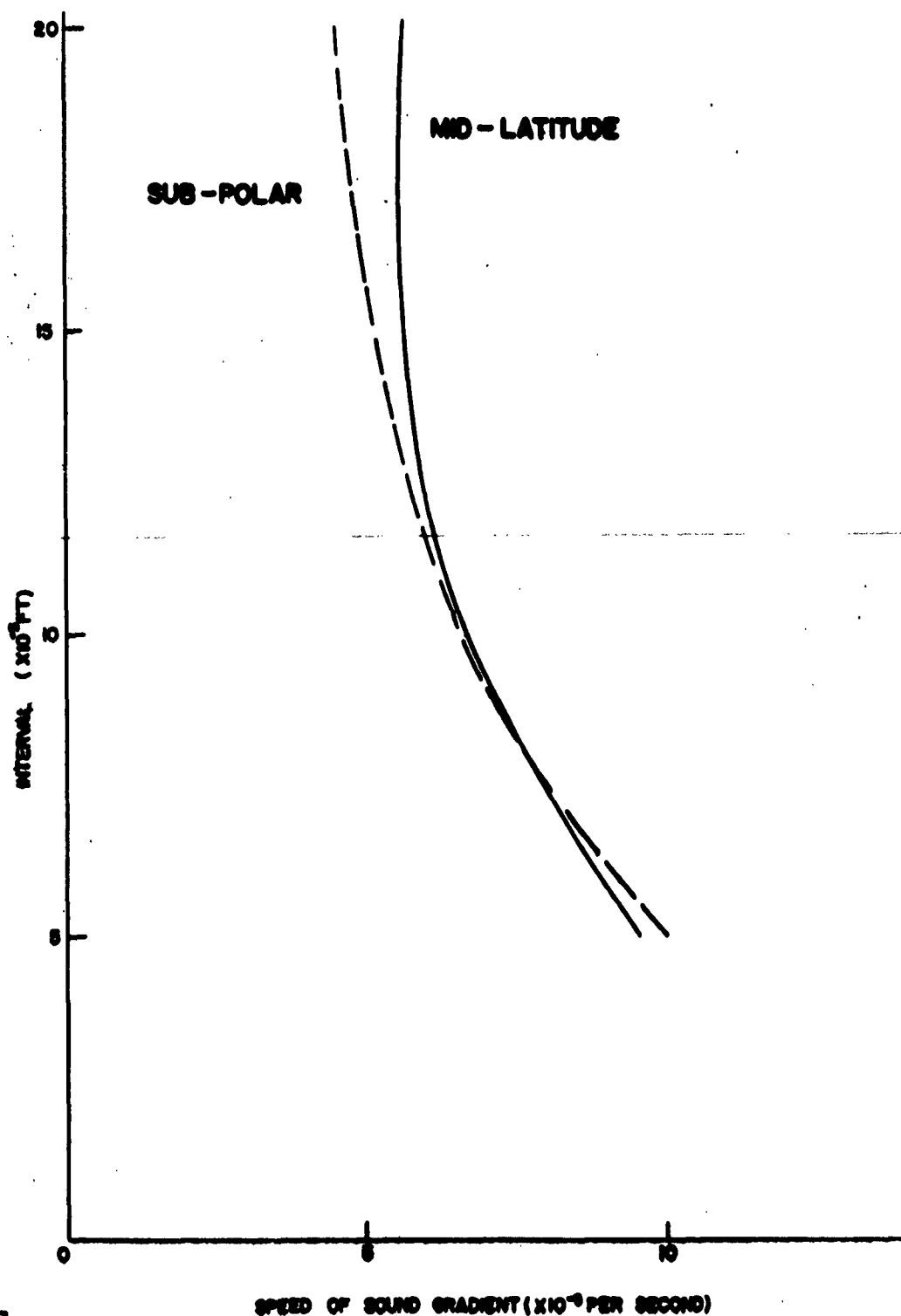
Figure 7 presents the results of an analysis of the average values of the maximum sonic gradients observed over various height intervals. In view of the data contained in Figure 6, the data presented in Figure 7 have been separated into sub-polar and mid-latitude cases. One should note that



II-6 Figure 5. The mean general sonic gradient of the lower mesosphere for a sound front propagating horizontally from the west is plotted against date for the year 1960.



II-6 Figure 6. Extremes of the observed data are illustrated for the mean curves presented in Figure 5.



II - 6 Figure 7. The average values of maximum speed of sound gradient observed as a function of the sample thickness interval. The vertical component data was reduced in 5 feet per second intervals, the west component data was reduced at 10 feet per second intervals, and points were obtained for thickness intervals of less than 5,000, 5,000-10,000, and 10,000-20,000 feet.

the average of the maximum gradients presented here are in general agreement with the average values of the curves in Figure 6, with the sub-polar inversion significantly weaker than the mid-latitude case.

As the height interval is decreased the maximum observed gradient exhibits an increasing trend. The data shows a doubling of the value by the time the interval has diminished to 5000 feet. The difference in sub-polar and mid-latitude data at gross intervals is absent when the interval is reduced to 10,000 feet, and the sub-polar case shows slightly stronger gradients at 5000 feet.

VI. SUB-DUCTS IN THE LOWER MESOSPHERE

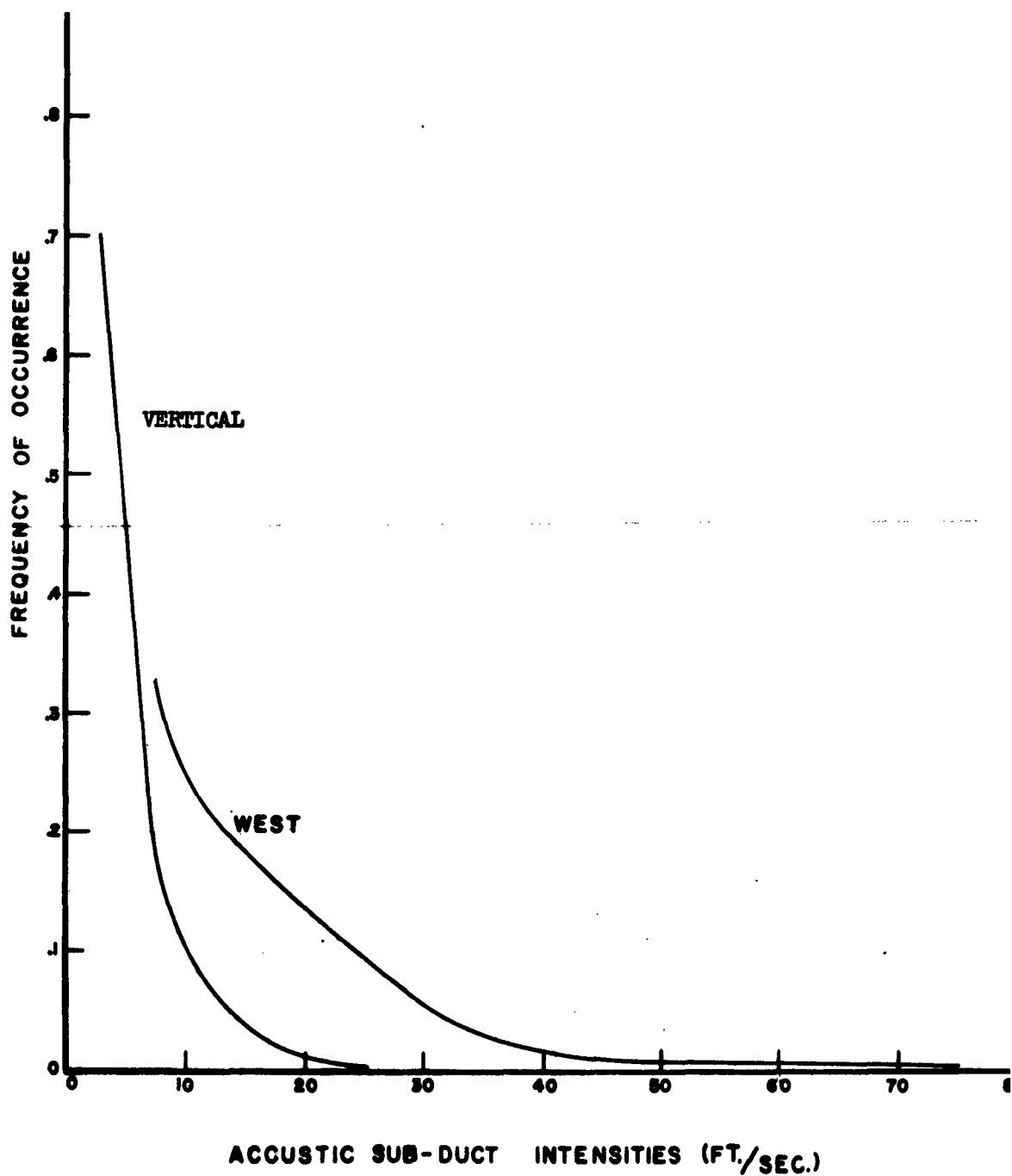
The occurrence of sub-ducts, defined as a region bounded by increasing speed above and below a speed minimum, is comparatively common in the lower mesosphere. They are most effectively formed by the meteorological variables when the general sonic gradient is minimal. We would, then, expect them to be most plentiful in the extreme lower mesosphere, immediately above the tropopause, and throughout the lower mesosphere for the east component in the winter and west component in the summer.

An examination of the data indicates a relatively narrow spectrum of thermally induced (vertical components) sub-ducts, with a strong predominance of weak ducts. The stronger sub-ducts occur frequently in the horizontal component cases, although the smaller scale phenomenon are still more prevalent. The strength of a particular sub-duct, from the acoustical point of view, is a function of the gradients involved and the depth of the layer over which they are active.

A summary of the frequency of occurrence of various intensity sub-ducts for the vertical and west components is presented in Figure 8. The data were obtained by observing the difference between the minimum sound speed in the sub-duct and the weaker of the duct defining higher sound speeds above or below the duct center. A total of 228 cases were employed in developing the vertical component curve; 363 cases were used in the west component. These sets of data represent all of the observed component sub-ducts in a total of 80 observations.

The small scale of temperature variations which serve to produce sub-ducts is illustrated in Figure 8. Practically no cases are noted where the intensities are greater than 25 feet per second, and a large majority of the observed features are less than 5 feet per second in intensity.

The curve obtained for the west component exhibits a distinctly different character. Intensities as high as 75 feet per second occur, although instances of data in excess of 40 feet per second are relatively rare. One should remember that the temperature induced sub-ducts contribute to the west component data, although the wind imposed gradients may serve to reduce the effectiveness of particular thermal gradients in sub-duct production. The increase in frequency observed at intensities below 25 feet per second is partially due to the thermally induced sub-ducts maintaining their identity in the west component profile.



II - 6 Figure 8. Frequency of occurrence of sub-ducts of various intensities for the vertical components (temperature) and the west component. Data were reduced at 5 foot per second intervals for the vertical components and 10 foot per second in the west component.

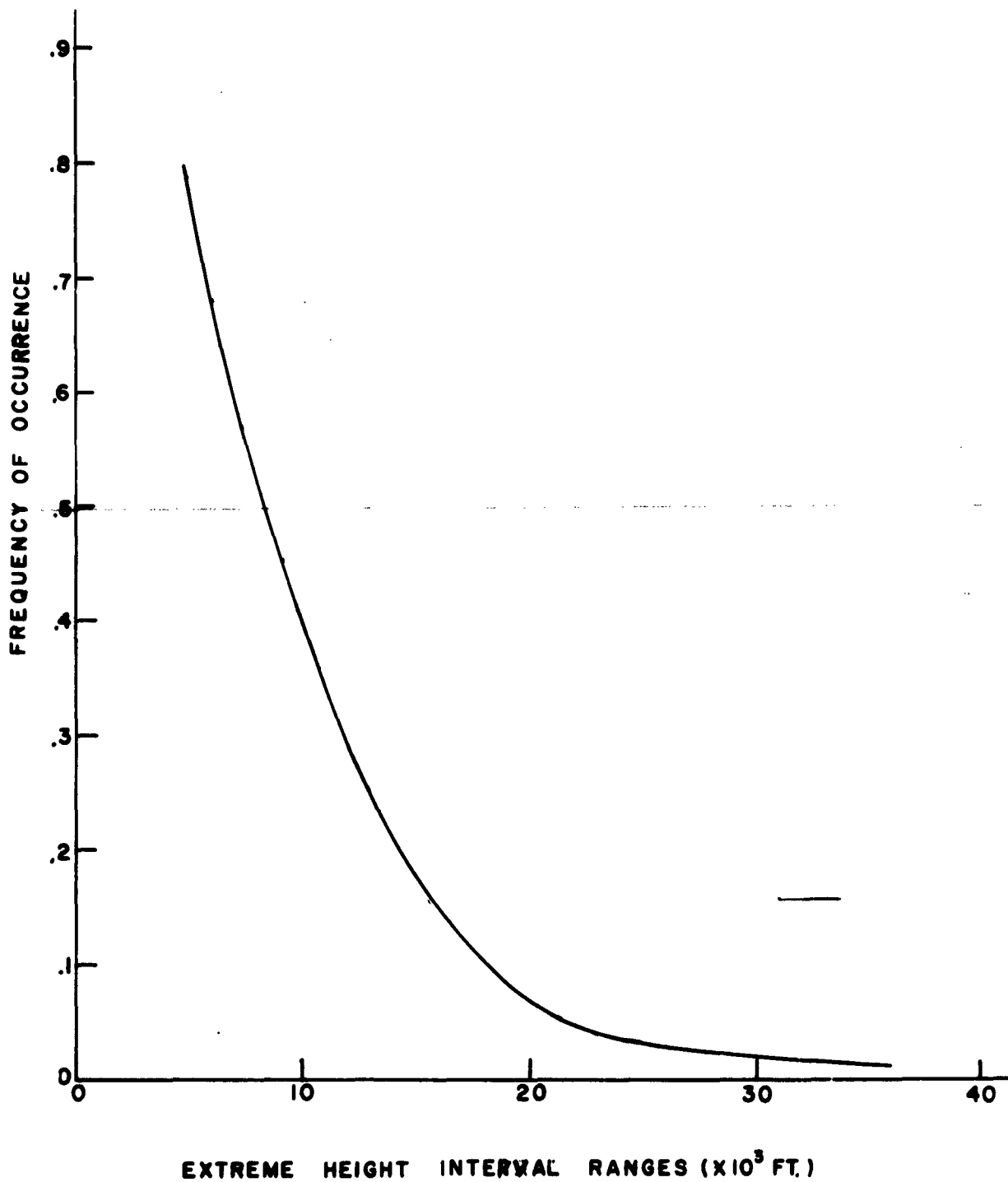
The frequency of occurrence of sub-ducts as a function of thickness is presented in Figure 9. Occurrences were evaluated for 10,000-foot intervals and the data plotted at the midpoints; 836 cases were observed in the 80 soundings analysed. It is clear that a large majority of the sub-ducts are less than 10,000 feet thick, and that sub-ducts greater than 30,000 feet thick are uncommon.

An understanding of the vertical distribution of sub-duct centers is required before we possess adequate knowledge relative to the detailed structure of the lower mesosphere. The distributions of vertical and west component minor sub-duct centers in relation to height are presented in Figure 10. Those sub-ducts that were less than 10,000 feet in thickness were given primary consideration in this summary, with data on sub-ducts in 10,000 - 20,000-foot range included. A total of 299 cases were used in 10,000-foot height intervals to develop the vertical component curve, 252 cases in the same height intervals were employed in the west component case, and 74 cases were included in the 10,000 - 20,000 curve.

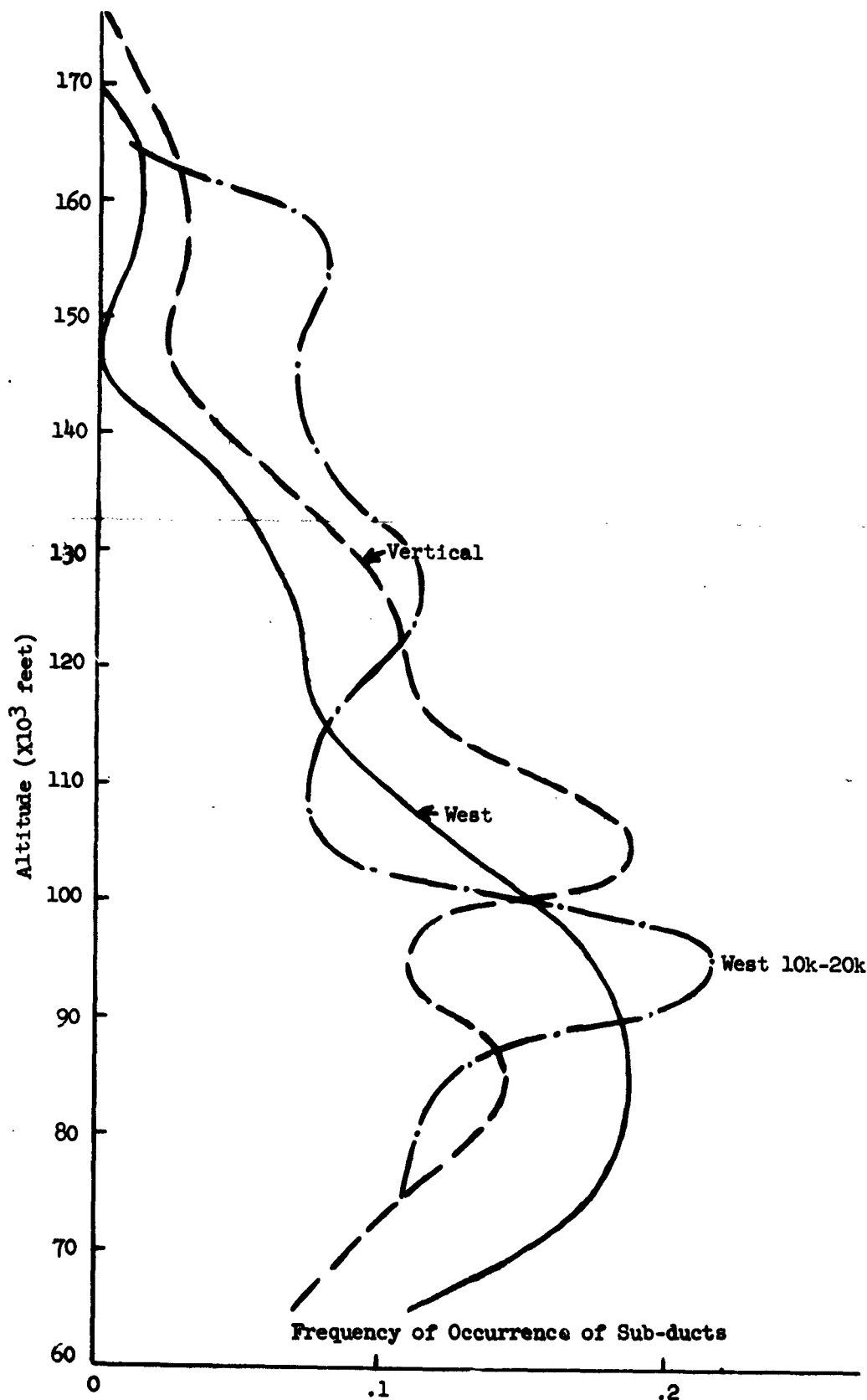
The amount of data available below 80,000 feet decreases due to abandoning of the rocket deployed parachute as the winds drift it away and the available observation time is exhausted. Therefore, the data do not conclusively prove the existence of a maximum in the distribution curve in the 80,000 - 100,000-foot height interval. It would be interesting to include the radiosonde data, since there is some reason to accept the indications of a more uniform atmospheric acoustic structure in the vicinity of the tropopause.

The general trend of the curves above 100,000 feet is toward a more stable atmospheric acoustic structure. This trend is well established before one gets into the regions where one can seriously question the ability of the system to detect the presence of such details. The data presented for the 10,000 - 20,000-foot interval curve indicate a loss of sensitivity in the smaller (10,000-foot) interval data in the 140,000 foot region, but furnishes support for the decreasing frequency trend which is apparent in all of the data. It seems likely that the variations in the vertical component curve at about 100,000 feet is partly due to the relatively small amount of data available. If one smooths the vertical component curve to the general shape of the west component curve the maximum in the vertical component curve will appear around 95,000 feet, some 10,000 feet above the maximum in the west component curve.

The curves are essentially similar over the remainder of the altitude range considered. It may well be significant that this maximum occurs in the altitude range which is characterized by strong positive temperature gradients and strong gradients in the flow. The situation at 150,000 feet represents a generally more isosonic distribution. One would surmise that regions of the mesosphere in which the maximum amount of detail is to be found are the regions of maximum sonic gradient. This is not particularly surprising to the meteorologist.



II-6 Figure 9. Frequency of occurrence of sub-ducts of various thicknesses. The data were reduced at ten thousand foot thickness intervals.



II - 6 Figure 10. Frequency of occurrence with height of vertical and west component sub-ducts less than 10,000 feet thick. The dashed-dot curve presents data on west component sub-ducts between 10,000 and 20,000 feet thick.

The meteorological factors which serve to establish the thermal and flow gradients in the 100,000-foot region are not uniquely related. The local temperature may be the result of radiational processes, while the larger scale adjustments in the pressure field have a controlling influence on the local flow profile.

VII. CONCLUSIONS

The gross atmospheric acoustic structure variations result primarily from changes in the atmospheric circulation. The principal effect is observed in the sonic profiles for sound fronts approaching from the west and the east. The lower mesospheric sonic gradient in mid-latitudes is positive and strong in the winter season, with a minimum in late summer. The sub-polar curve is about 10% behind in phase.

The magnitude of the sonic gradient demonstrates its maximum value as the height interval is decreased. Lower average gradients which are found in the sub-polar regions when viewed on the gross scale approach the mid-latitude value as the height interval is decreased. The data indicate similar physical processes are concerned with small scale sonic structure at all latitudes, while significantly different situations must exist relative to the gross features.

Sub-ducts occur frequently in the atmospheric acoustic structure. Small sub-ducts, of the order of 10 feet per second in intensity and a few thousand feet thick, are most plentiful, although occasionally a sub-duct will have dimensions approaching one half those of the major duct. Frequency of occurrence of sub-ducts with height decreases above 100,000 feet, by an order of magnitude at the sonic mesopeak in the case of the vertical components, and by a factor of two in the case of the west component.

The atmospheric acoustic structure exhibits a large amount of detail. The nature of these details is such that they will exert a pronounced effect on numerous atmospheric acoustical problems. Accurate speed of sound structure data appears to be a necessary part of any comprehensive study of acoustic propagation in the atmosphere, as well as other projects which include the use of sound velocity as a significant parameter.

ACKNOWLEDGEMENTS

The authors are indebted to all of the individuals and organizations participating in the Meteorological Rocket Network Committee of the Meteorological Working Group, Inter-Range Instrumentation Group. These individuals and organizations have furnished extensive facilities of great value, and have invested funds and personnel without which the Network could not have been initiated. Credit is also directed toward Mr. Norman Beyers of U. S. Army Signal Missile Support Agency for his activities in handling the data, and to Prof. Robert Schumaker, Mrs. Aurora Bustos, Miss Alice Marie Parra and others of the Schellenger Research Laboratories for data reduction and computation work in determining the sonic profiles.

REFERENCES

1. Webb, Willis L. and Kenneth R. Jenkins, 1961: SONIC STRUCTURE OF THE MESOSPHERE, Special Rpt 50, April, U. S. Army Signal Missile Support Agency, White Sands Missile Range, New Mexico
2. Beyers, Norman J. and Otto W. Thiele, 1960: METEOROLOGICAL ROCKET WIND SENSORS, Special Rpt 41, August, U. S. Army Signal Missile Support Agency, White Sands Missile Range, New Mexico
3. Clark, George Q., 1961: DEVELOPMENT OF A ROCKET TELEMETRY PACKAGE FOR THE METEOROLOGICAL ROCKET NETWORK, Proposed version of IRIG Document Nr. 105-60, Initiation of the Meteorological Rocket Network, Secretariat, White Sands Missile Range, New Mexico
4. Wagner, N. K., 1961: THEORETICAL TIME CONSTANT OF THE METEOROLOGICAL ROCKET NETWORK THERMISTOR, Submitted for publication in the Journal of Meteorology
5. Ballard, Harold N., 1961: RESPONSE TIME OF AND EFFECTS OF RADIATION ON THE VECO BEAD THERMISTOR, Schellenger Research Laboratories, Texas Western College, El Paso, Texas, April

INFRASONIC CAPACITOR MICROPHONE SYSTEMS
Carlos McDonald
Texas Western College
Schellenger Research Laboratories

I. Introduction

The capacitor microphone is one of the most useful and efficient acoustic transducers in the infrasonic range, particularly when used in conjunction with balloon borne telemetry systems.

In a capacitor microphone, sound pressures produce variations in microphone capacitance. For telemetering and recording purposes, these variations in capacitance have to be transduced to variations of some electrical parameter such as voltage, current, or frequency.

The objective of this discussion is two-fold: first to present the characteristics of the systems that can be used to convert low-frequency microphone capacitance variations to variations of some electrical parameter; and second, to discuss the requirements of balloon-borne telemetry systems best suited for these capacitor microphone systems. The analysis will stress the following requirements: (1) The system must have a flat frequency response from 100 cps down to at least 1 cps. (2) The telemetering system requirements will be based on the criteria that variations of microphone capacitance corresponding to sound pressures from one dyne/cm² (rms) to 0.01 dynes/cm² must be detectable.

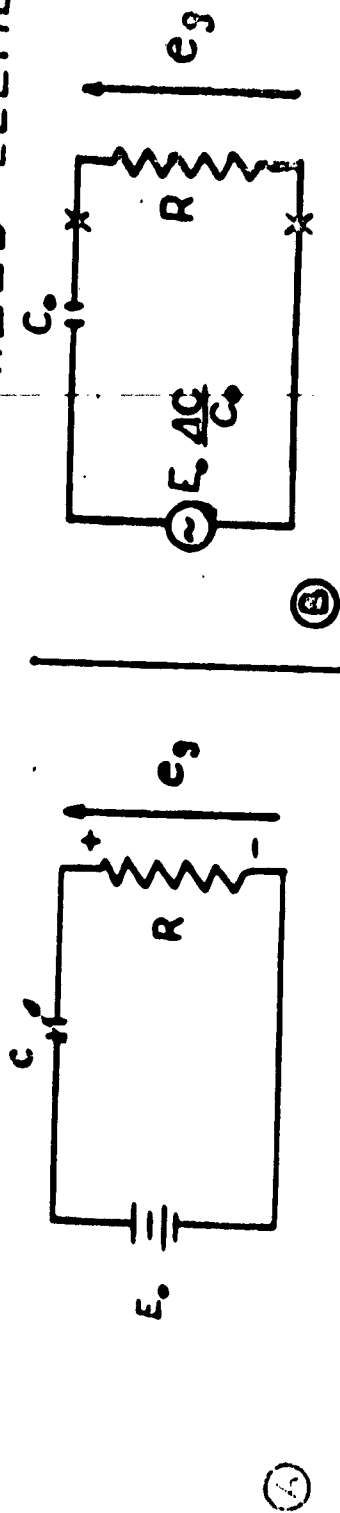
II. Capacitor Microphone Systems

A. Description

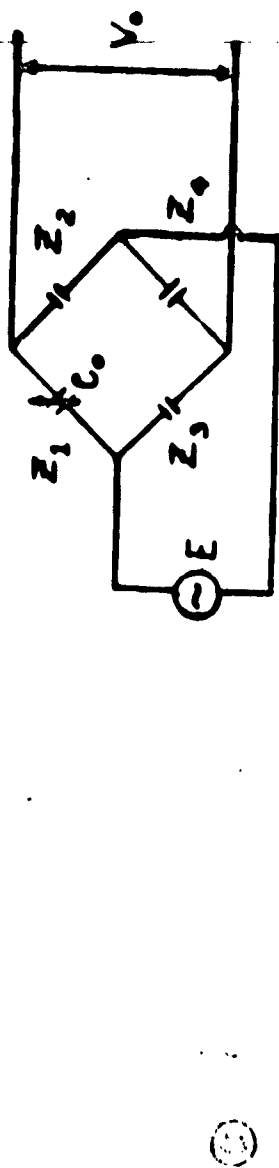
In order to convert capacitor variations to variations of some electrical parameter, the capacitor element of the microphone can be used as a polarized element, as a bridge impedance element, or as an element of a tuned circuit.

Figure 1-a shows the system when the microphone capacitance is used as a polarized element. In this case, the microphone capacitance is charged to a polarizing voltage E_0 through the resistor R from a DC voltage supply. Variations of microphone capacitance will cause variations of the polarizing voltage, and these voltage variations will also appear across the resistor R . In practical applications, the resistor R can be the input impedance of a vacuum tube. For small variations of microphone capacitance, the equivalent circuit shown in Figure 1-b can be derived.¹ This circuit consists of a generator operating at the frequency at which the microphone capacitance varies, and having an internal impedance equivalent to that offered by the steady state microphone capacitance, C_0 . The voltage magnitude of the generator is directly proportional to the product of the polarizing voltage E_0 and the percent change in microphone capacitance, $\Delta C/C_0$.

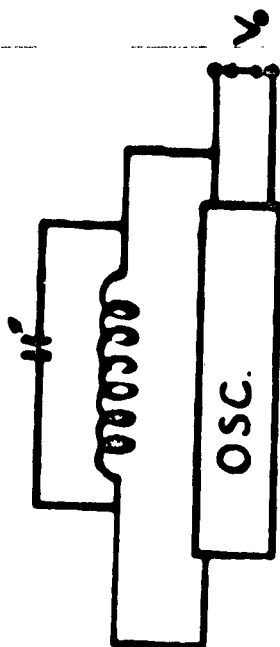
CAPACITOR MICROPHONE AS A POLARIZED ELEMENT



CAPACITOR MICROPHONE AS A BRIDGE IMPEDANCE ELEMENT



CAPACITOR MICROPHONE AS AN OSCILLATOR ELEMENT



The second method, shown in Figure 1-c, utilizes the capacitor element of the microphone as the impedance of one arm of an AC bridge. For simplicity, we have assumed that the other arms of the bridge are composed of similar capacitances.

In this type of system, any variation of the microphone capacitance will vary the impedance of the bridge resulting in an output at the frequency of the generator with an amplitude proportional to the change in microphone capacitance. Rectification and filtering of this output results in a voltage that varies at the rate of the microphone capacitance and is proportional to the change in microphone capacitance. In actual operation, the bridge is off-balance since, otherwise, frequency doubling will occur. The degree of unbalancing depends on the magnitude of the change in capacitance expected. Another method of detection that can be used is phase comparison between the input and output voltage of the bridge.² However, this method will not be considered since it requires balancing of the bridge in the steady state, and consequently, complicates the system when used for balloon-borne operations.

In the last method considered, (Figure 1-d), the microphone capacitance serves as one of the tuning elements of an oscillator. Consequently, variations in microphone capacitance result in a variation of the frequency of oscillation. A voltage output which is a function of the change in microphone capacitance can be obtained by limiting the oscillator output voltage and applying the limited output to a frequency discriminator.

B. Frequency Response

The electrical frequency response characteristics of these systems will now be considered.

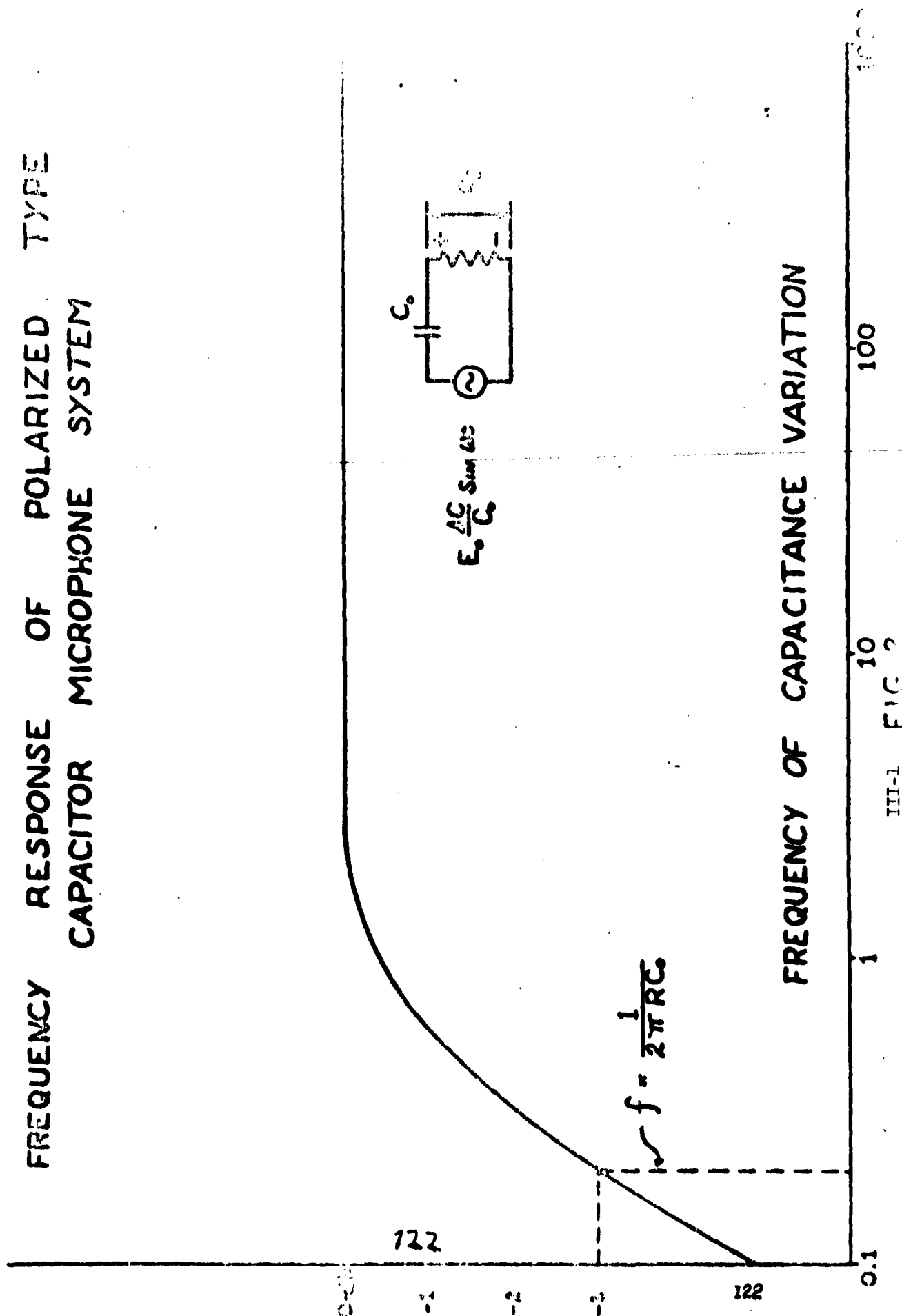
Figure 2 shows the frequency response of the system when the microphone capacitance is used as a polarized element. The relative voltage across the resistor R is plotted as a function of the frequency at which the microphone capacitance varies, while keeping the change in capacitance constant. As expected from the equivalent circuit, the frequency response is that of typical RC circuit: at low frequencies, the voltage across R decreases at a rate of 6 db per octave. At high frequencies, this voltage is essentially independent of frequency. The output drops to -3 db at the frequency f given by the relation

$$f = \frac{1}{2\pi RC_0}$$

where the product RC_0 corresponds to the RC time constant of the circuit in the steady state. The zero db reference corresponds to the voltage across R at high frequencies. The low frequency response can be extended by increasing R, or by paralleling a fixed capacitor to the capacitor microphone. However, the latter method reduces the sensitivity of the system.

For the system in which the microphone capacitance is used as a bridge impedance element, the output voltage of the bridge is essentially independent

FREQUENCY RESPONSE OF POLARIZED TYPE CAPACITOR MICROPHONE SYSTEM



III-1 FIG. 2

of the rate at which the microphone capacitance varies. The low frequency response is only limited by the stability of the system. The high frequency response is limited by the carrier frequency and the low-pass filter used to filter the carrier after rectification.³

For the system where the microphone capacitance determines the frequency of an oscillator, the frequency of oscillation is again essentially independent of the rate at which the microphone capacitance varies. The low frequency response is limited by the stability of the oscillator, and high frequency response is limited by the oscillator frequency and the low pass filter in the frequency discriminator.⁴

C. Sensitivity

The sensitivity characteristics of the capacitor microphone systems discussed will now be considered. Figure 3 shows an outline of the sensitivity relations of each of the systems discussed. The relationships shown are only valid when the change in microphone capacitance is much smaller than the nominal capacitance of the microphone. This assumption is based on the fact that the most sensitive capacitor microphones that have been constructed for balloon-borne applications⁵ have nominal microphone capacitances of about one-tenth picofarad change in microphone capacitance per dyne per cm² (rms).

For the system in which the microphone capacitance is used as a polarized element, it was previously shown that the voltage, V , of the equivalent generator, resulting from a small variation in microphone capacitance, is given by the relation

$$V \cong E_0 \left(\frac{\Delta C}{C_0} \right)$$

where E_0 and C_0 corresponded to the polarizing voltage and microphone capacitance, respectively.

For the system in which the microphone capacitance is used as a bridge impedance element, the output of the bridge, V , for small change, ΔC , in microphone capacitance, is given approximately by the expression

$$V \cong \frac{E}{4} \left(\frac{\Delta C}{C_0} \right)$$

where E and C_0 correspond to the input voltage to the bridge and the steady state microphone capacitance, respectively. The above expression was obtained by finding the relation between the output and input voltage as a function of the arm impedances of the bridge. The assumption was also made that the impedances were capacitances, that the bridge was near the balance position in the steady-state, and that the internal impedance of the generator was low.

Finally, for the system in which the microphone capacitance is used as the tuning element of an oscillator, the frequency of oscillation, due to a small change, ΔC , of microphone capacitance, can be expressed by the relation

$$f \cong f_0 \left(1 - \frac{\Delta C}{2C_0} \right)$$

where f_0 corresponds to the center frequency as determined by the steady-state capacitance, C_0 . The above expression was found by assuming that the frequency of oscillation is given by the expression

$$f = \frac{1}{2\pi\sqrt{LC}}$$

where L and C correspond to the oscillator inductance and microphone capacitance, respectively. The frequency of oscillation as a function of variation in capacitance was also investigated for other types of oscillators. However, the expressions obtained were found to be either equivalent to the expression shown above, or, less sensitive to the variation of capacitance.⁶

The last column of Figure 3 shows typical numerical values of the variation in electrical parameters of the microphone systems for an assumed sound pressure of one dyne/cm². A capacitor microphone with a nominal capacitance of 100 picofarads and a sensitivity of one-tenth picofarad change of microphone capacitance per dyne/cm² was assumed.

For the case when the capacitor microphone is used as a polarized element and a polarizing voltage of 50 volts is assumed, the output voltage corresponding to a sound pressure of one dyne/cm² is 0.050 volts peak-to-peak.

For the bridge-type microphone system, where the input voltage to the bridge is assumed to be 50 volts peak-to-peak, the output of the bridge varies 0.0125 volts peak-to-peak.

For the oscillator type of microphone system if a center frequency of 1.4 MCS is assumed, the frequency deviation, corresponding to a sound pressure of one dyne/cm², is ± 700 cps. This center frequency was assumed since, if the oscillator is used as a subcarrier (see section III) of an FM telemetry system, the maximum frequency deviation corresponds to that allowed by IRIG (Inter-Range Instrumentation Group) standards.

With the sensitivity and frequency response characteristics for each of the capacitor microphone systems known, the requirements of balloon-borne telemetry systems best suited for each of the above systems will now be outlined.

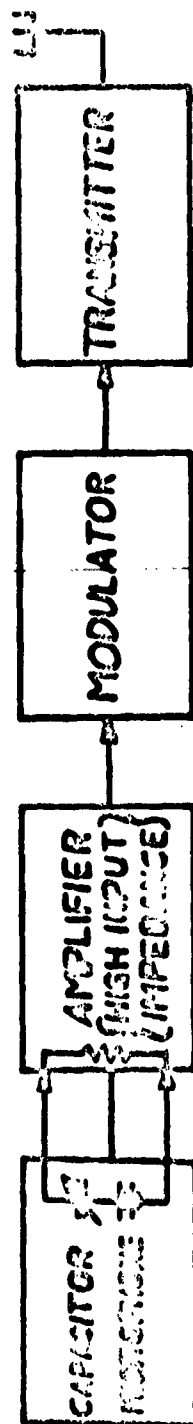
Figure 4 shows a telemetering system for the case when the capacitor microphone is used as a polarized element. As previously mentioned, the output of this system consists of a voltage that varies at the rate of the microphone capacitance and is proportional to the change in capacitance. If the system is to have a flat frequency response below 100 cps, the input impedance to the amplifier must be high. However, the input impedance requirement to the amplifier can be reduced by paralleling a fixed capacitor to the capacitor microphone, as previously mentioned, or if the same input impedance is maintained, the low frequency response can be extended. The rest of the telemetry system consists of a modulator and transmitter in the flight unit, and a receiver and demodulator in the ground system. The response requirements of these components are easily met by an FM or Pulse modulation type telemetry system.

SENSITIVITY — CAPACITOR MICROPHONE SYSTEMS			
TYPE	SENSITIVITY	TYPICAL NUMERICAL VALUES	
		$\left\{ \begin{array}{l} C_0 = 100 \text{ pico f} \\ \Delta C = 0.10 \text{ pico f} \end{array} \right\}$	
POLARIZED	$e \approx E_0 \left(\frac{\Delta C}{C_0} \right)$	$E_0 = 50 \text{ VOLTS}$ $e \approx 0.50 \text{ VOLTS P-P}$	
BRIDGE IMPEDANCE	$V \approx \frac{E_0}{4} \left(\frac{\Delta C}{C_0} \right)$	$E_0 = 50 \text{ VOLTS P-P}$ $V \approx 0.0125 \text{ VOLTS P-P}$	
OSCILLATOR	$f \approx f_0 \left(1 - \frac{\Delta C}{2C_0} \right)$ $f = \frac{1}{2\pi\sqrt{LC}}$	$f_0 = 1.4 \text{ MCS.}$ $\Delta f = \pm 700 \text{ C.P.S.}$	

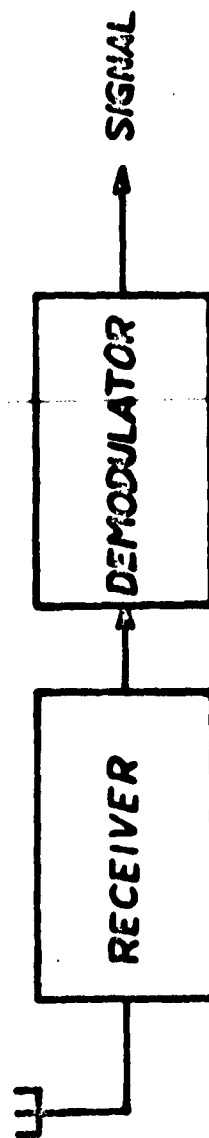
III-1 FIG. 3

CAPACITOR MICROPHONE TELEMETRY SYSTEM (POLARIZED TYPE)

FLIGHT UNIT



GROUND SYSTEM



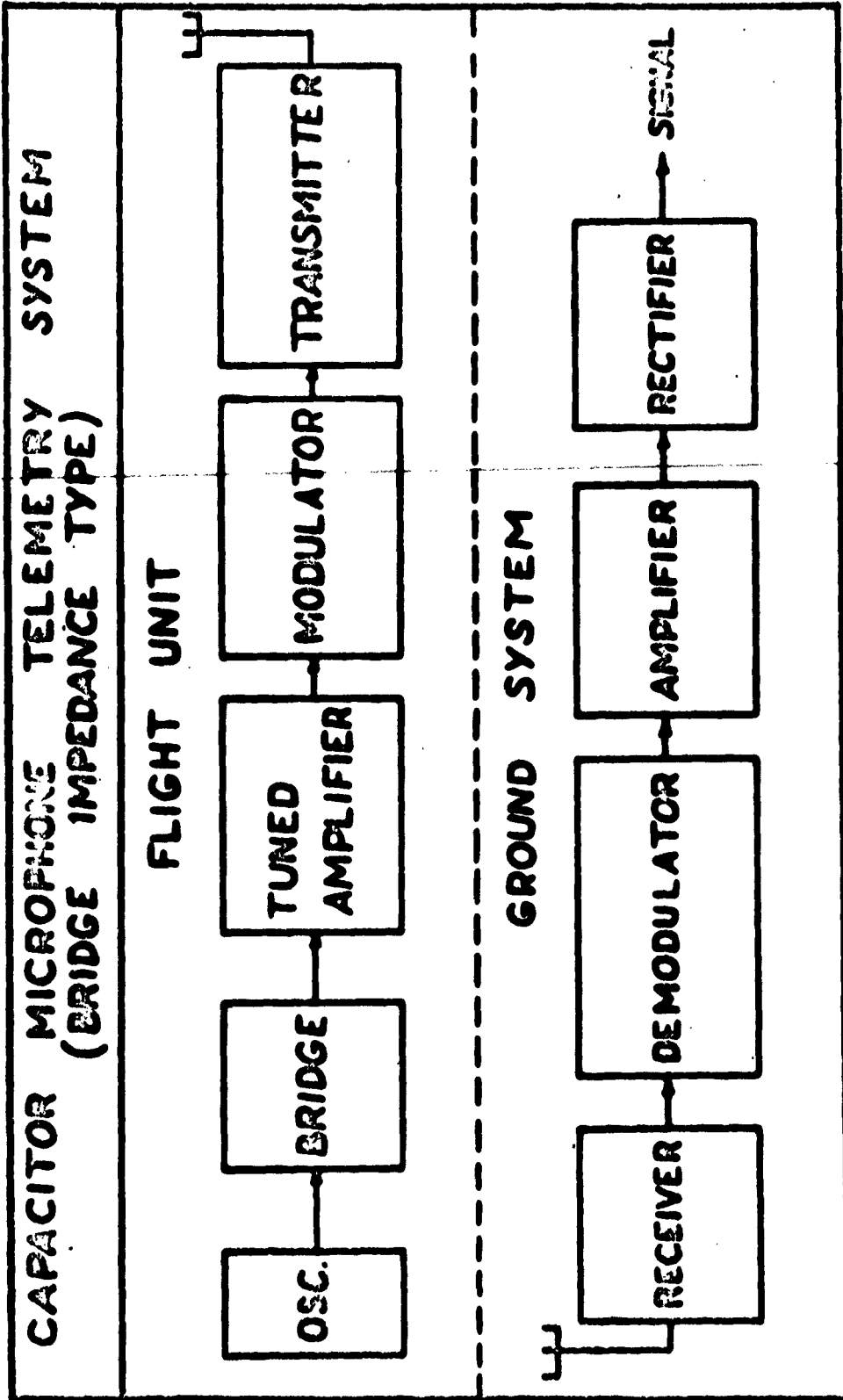
III-1 FIGURE 4

Figure 5 shows an FM telemetry system for the case when the capacitor microphone is used as a bridge impedance element. The flight unit requires an oscillator for the bridge and an amplifier to amplify the output of the bridge. The output of the amplifier is used as the subcarrier which frequency modulates the transmitter. The ground system detects the subcarrier which is then rectified, resulting in a voltage that varies at the rate of the microphone capacitance and is proportional to the change in microphone capacitance. If an FM telemetry system is not used, rectification of the bridge output can be accomplished in the flight unit.

Finally, Figure 6 shows the telemetry system best suited for the case when the capacitor microphone is used to vary the frequency of an oscillator. Essentially, the system is an FM-FM telemetry system. The flight unit simply consists of a subcarrier oscillator whose frequency is controlled by the microphone capacitance. This subcarrier in turn frequency modulates the transmitter.

The ground system is more complicated since the maximum frequency deviation of the subcarrier is only ± 700 cps as previously mentioned. Consequently, a sharp FM discriminator is required to demodulate the subcarrier. In order to accomplish this, the original subcarrier has to be heterodyned with a local oscillator in order to yield an intermediate frequency carrier that can be automatically controlled. The resulting IF carrier is amplified, limited, and applied to the FM discriminator. Automatic frequency control (AFC) is used to control the local oscillator frequency in order to obtain a stable IF center frequency. The response time of the AFC control has to be slower than the period of the lowest rate of frequency deviation to be detected. Frequency multiplication of the subcarrier can increase the sensitivity of the system.

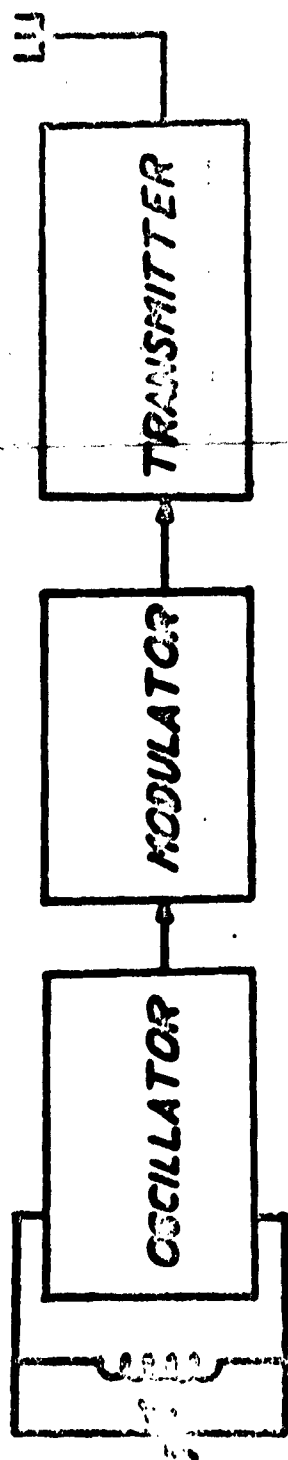
The telemetry systems considered vary in complexity. One important factor in determining the type of telemetry system used depends on the characteristics of the transmitter and receiver. Another factor that has to be considered is cost. For example, if the number of flight units greatly exceeds the number of ground systems, the FM-FM telemetry system utilizing the capacitor microphone to determine the frequency of a subcarrier would prove most economical since the telemetry system results in simple flight unit and a more elaborate ground system. On the other hand, if very low-frequency microphone capacitance variations are to be telemetered, say below one-tenth of cps, the bridge-type telemetry system would prove the most practical.



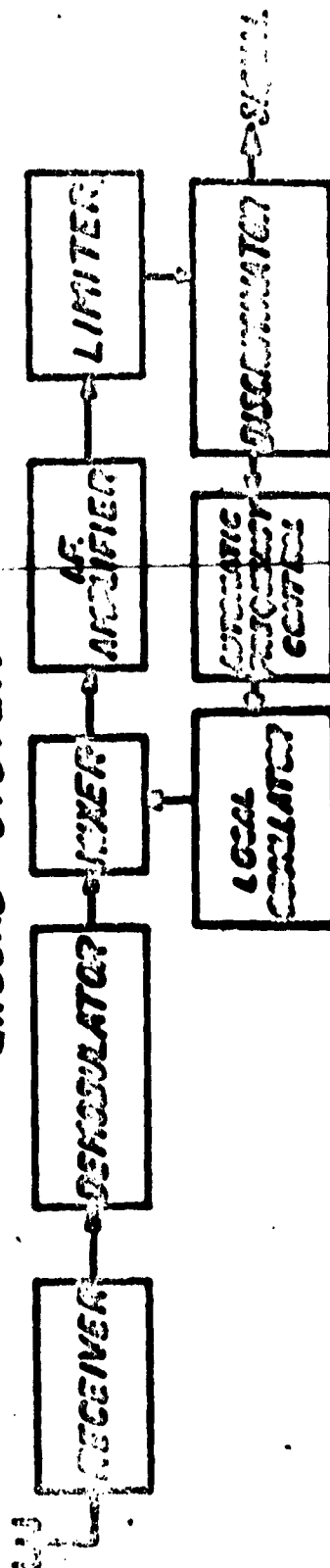
III-1 **FIG. 5**

CAPACITOR MICROPHONE TELEMETRY SYSTEM (OSCILLATOR TYPE)

FLIGHT UNIT



GROUND SYSTEM



III-1 FIGURE 6

LITERATURE CITED

1. KIMMER, L. E. and A. R. FREY. Fundamentals of Acoustics, Sec. 12.3, New York: John Wiley and Sons, (1950).
2. Extract of Mark III Equipment, U. S. Army Signal Operations Agency, Fort Monmouth, New Jersey.
3. NICHOLS, H. M. and L. L. RAUCH, Radio Telemetry, Sec. 4.4 New York: John Wiley and Sons, (1956).
4. NICHOLS, H. M. and L. L. RAUCH, Radio Telemetry, Sec. 4.5, New York: John Wiley and Sons, (1956).
5. McDONALD, C. and M. IZQUIERDO. Design, Development, and Production of Infrasonic Capacitor Microphones, (Unpublished).
6. McDONALD, C. Infrasonic Capacitor Microphone Systems. (Unpublished).

Problems in the Construction of Infrasonic Microphones
Mike Izquierdo
Texas Western College
Schellenger Research Laboratories

I. Introduction

The following discussion is a summary of the problems and solutions found in the production of Infrasonic Microphones using the capacitor microphone as a polarized element. The procedures outlined here have been applied directly to the Pulsonde, in the production of 3,000 units, and in performing over 10,000 acoustical calibrations.

The result of the techniques applied, has been:

- 1st--An increase in the acceptance rate of Pulsonde units from 10% to 90%.
- 2nd--an extension of the low frequency 3 db point from 5 cps to 1 cps.
- 3rd--the possibility of extending the system frequency response below 0.1 cps.

Objectives

It was decided that, for satisfactory performance, the microphone systems would have to meet the following requirements:

- 1. An acoustic response of ± 3 db from 1 to 100 cps.
- 2. A sensitivity of one volt P-P per dyne per cm^2 .
- 3. Proper operation in RF fields.

II. Methods of Production Testing

To achieve the requirements outlined above, it was decided that two tests would be necessary:

A. Electronic Acceptance Test

Since the input grid impedance of the microphone tube determined the low frequency response, a production technique had to be developed in order to measure this impedance. Instead of measuring the impedance by direct methods, it was decided to run a frequency response (Figure 1) by using the microphone capacitor and the grid impedance as impedance elements in series with a low frequency oscillator. The output voltage at the plate of the microphone tube was monitored as the frequency of the oscillator was varied. This procedure made it possible to analyze the overall system response without determining individual component values.

B. Acoustical Acceptance Test

Frequency response and sensitivity were determined using a low frequency acoustical source, the acoustical pistonphone. It was found that this testing procedure allowed quick detection and isolation of unsatisfactory responses, whether electrical or acoustical.

III. Problems of Production

A. Grid Input Impedance

It was found that while units constructed without special precautions had a low frequency 3 db point of 5 to 8 cps, the response could be extended to 3 to 5 cps by the following procedures:

1. Extra care in cleaning the mounting board,
2. cleaning the microphone tube,
3. floating the connection from the grid of the tube to the capacitor microphone back plate, and
4. spraying the circuit with acrylic resin.

It was also found, experimentally, that by selecting tubes with a low emission, the 3 db frequency could be lowered to 0.8 cps. This result led to lowering the plate and screen voltages, by inserting R_4 (Figure 1), which lowered the frequency response by an octave.

The final result of the modifications outlined was that the low frequency response changed from the 5 to 8 cps, mentioned above, to 0.4 to 0.6 cps, which was considered sufficient.

B. Blocking

In lowering the frequency response, a very high grid impedance of the microphone tube was obtained. This created a problem of blocking of the microphone tube when intense sound pressures were incident on the microphone diaphragm. The voltage magnitude on the grid of the microphone tube would cut off. In this case, the microphone capacitance could only discharge through the large leakage resistance. Consequently, blocking was from 35 minutes to 5 hours.

This problem was eliminated by using a neon tube between the grid and plate of the microphone tube (Figure 1) as a switch. Under operating conditions, the neon tube was close to an open circuit since the voltage from grid to plate was much lower than the ionization voltage of the neon tube. As soon as the microphone tube blocked, the plate voltage would rise, and the neon tube would conduct, thus discharging the grid immediately.

Three precautions were taken when using neon tubes in the microphone circuit:

1. Shielding of the neon tube from the RF field.
2. Shielding of the neon tube from the light.
3. Checking the neon tube for leakage resistance.

C. Acoustical Response

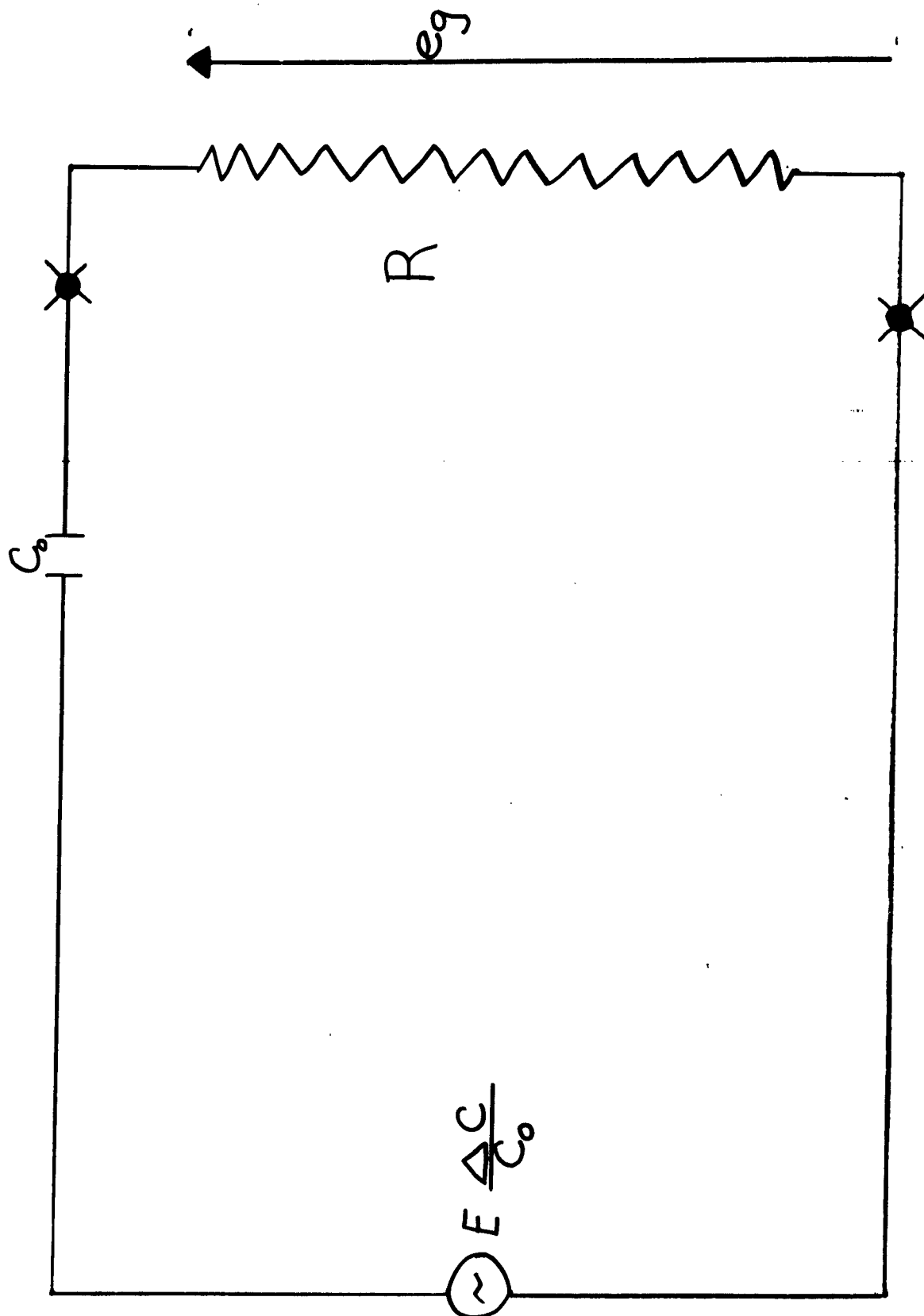
After passing the electronic response test, an acoustical frequency response check on the microphone was performed. The main problem encountered in obtaining the required frequency response was traced to uncontrolled leakage around the seal of the baffle and the seal of the diaphragm. In order to eliminate this problem in production, test procedure using a Manometer to detect the leakage was developed. Once the leakage was corrected, the response curves would follow the electronic response curve, thus indicating that the acoustical response went lower than the electronic response.

D. RF Detection

Another problem that had to be overcome was the loss of sensitivity due to the fact that the microphone was exposed to an RF field. The cause of the trouble was found to be due to lack of metallized coating of the mylar diaphragm. By selecting the diaphragms and by proper shielding, this problem was eliminated.

IV. Conclusions

With the procedures developed by the Schellenger Research Laboratories on the production and testing of infrasonic capacitor microphones, mass production of thousands of Pulsonde flight units was made possible. These developed techniques also made possible the construction of infrasonic capacitor microphones with an acoustic flat frequency response characteristic below one tenth cps.



III-2 Figure 1

PULSONDE TELEMETRY SYSTEM
George Q. Clark
U. S. Army Signal Missile Support Agency
White Sands Missile Range, New Mexico

The pulsonde telemetry system was developed to satisfy the need for a balloon-borne system with sensitivity in the infrasonic region.

After consideration of various types of modulation, such as AM, FM, and FM FM, it was decided that some type of pulse modulation offered the most potential for undistorted data transmission. Availability of the Ravin set AN/GMD-1, which utilizes a PDM-AM type of modulation, led to the selection of that unit for the ground receiver. However, because of the nature of the intelligence to be transmitted, it was necessary to use a pulse rate of 3000 pps to obtain the fidelity required instead of the 200 pps maximum rate employed with radiosonde balloon operation.

Figure 1 is a schematic representation of the modulation technique employed. Proceeding from top to bottom one can see how the pulses generated by a blocking oscillator, the repetition rate of which is a function of the intelligence to be transmitted, are used to cut off the carrier radiation. When this carrier is detected on the ground with a standard AM detector, negative pulses are observed with the intelligence contained in the repetition rate. The trailing edges are now used to trigger another pulse generator and if the level of triggering is set appropriately, the "grass" may be left behind and only pulses with a large signal-to-noise ratio are applied to a frequency sensitive filter. The intelligence is recovered in the form of a varying DC level at the output of the filter.

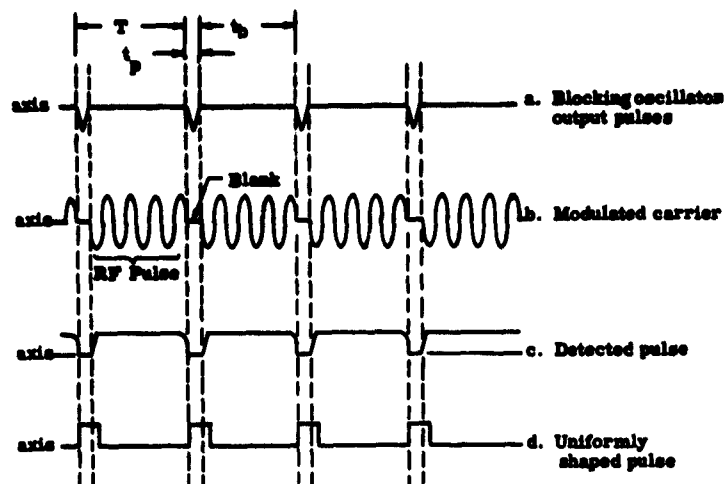
A block diagram of the ground system is shown in Figure 2. The output signal from this system is suitable for recording on standard recording devices such as magnetic tape or chart recorders.

Figure 3 is a presentation of the frequency response characteristics of the flight unit showing the 3 db points at approximately 0.14 cycle per second and 150 cycles per second. The upper limit is built in while the lower limit is determined by the microphone characteristics.

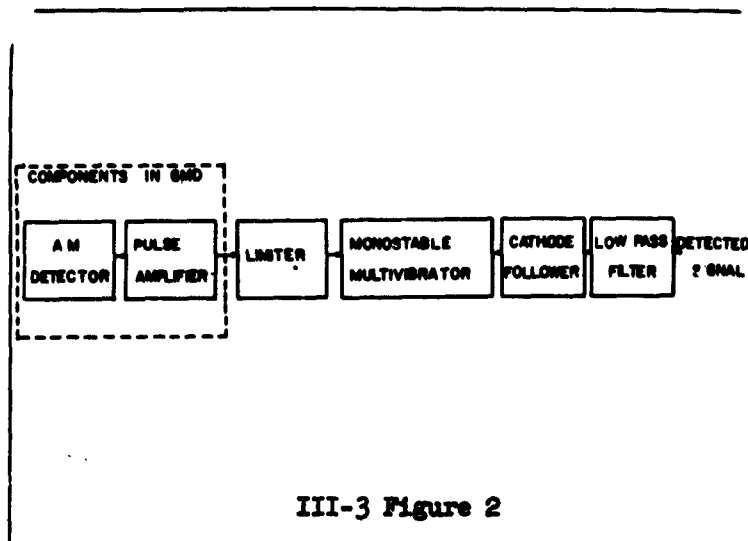
In Figure 4 one may observe the modulation characteristics of the flight instrument noting that quite large percentages of deviation can be tolerated with no loss in linearity of the modulation, hence a large dynamic range of pressure variations can be sensed with good fidelity.

The overall system frequency response is shown in Figure 5. Note that the upper limit has been decreased slightly. This is due to intentional limiting in the ground system. Even though the characteristics of the capacitor microphone are markedly better as frequency increases, it was decided that 100 cycles per second would include the area of interest.

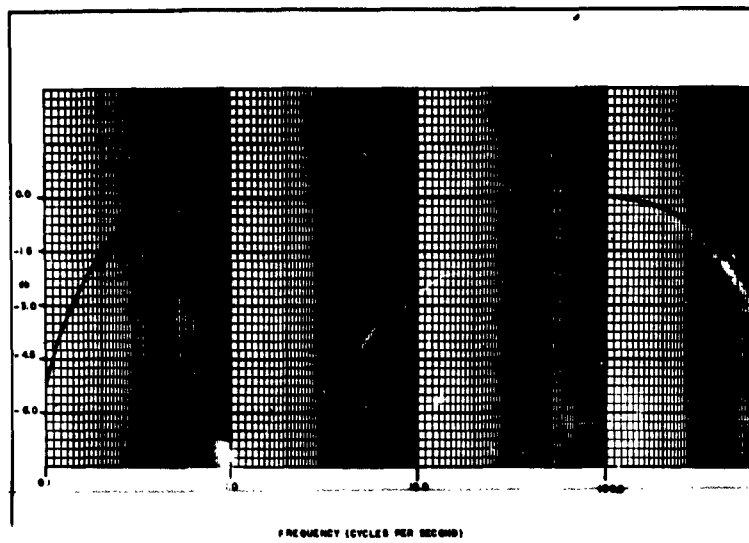
The filter system used to recover the intelligence has a linear voltage output (Figure 6) as a function of percent of deviation in frequency. Quite large coupling capacitors are employed to preserve this linearity in the lower frequency region.



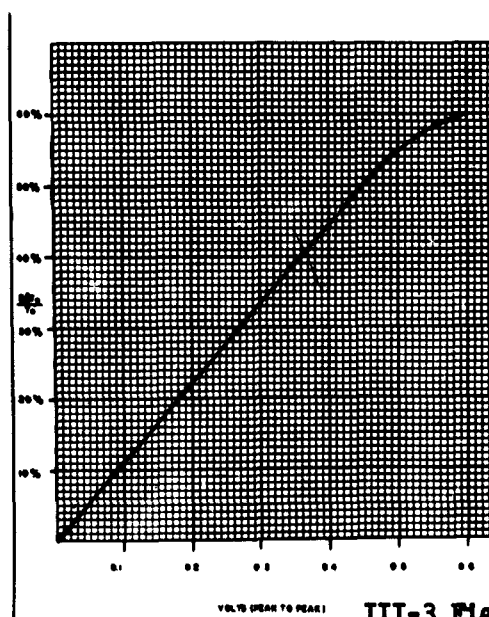
III-3 Figure 1



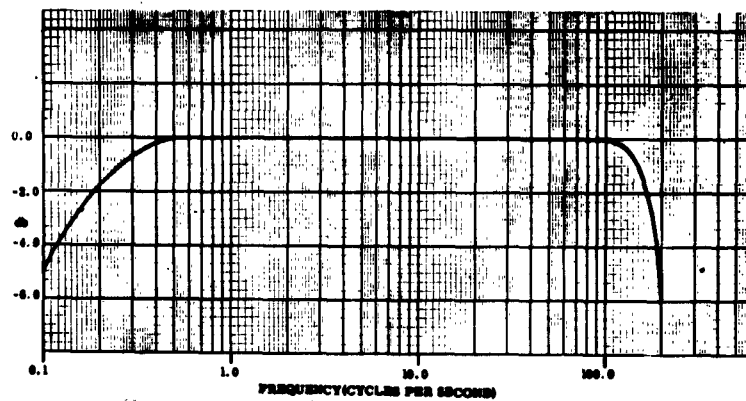
III-3 Figure 2



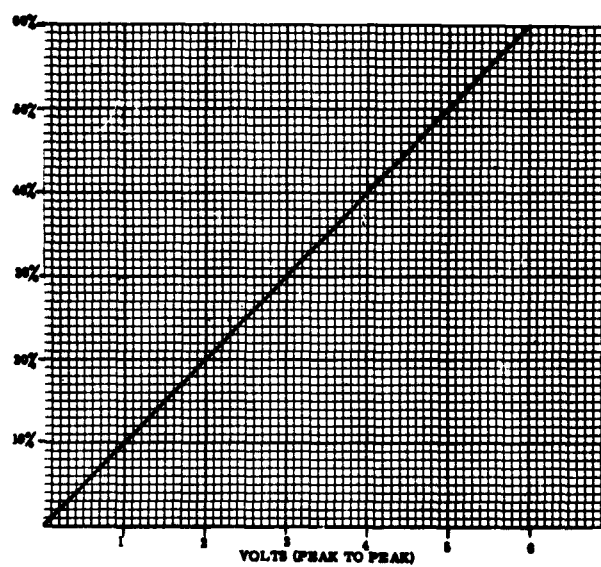
III-3 Figure 3



III-3 Figure 4



III-3 Figure 5



III-3 Figure 6

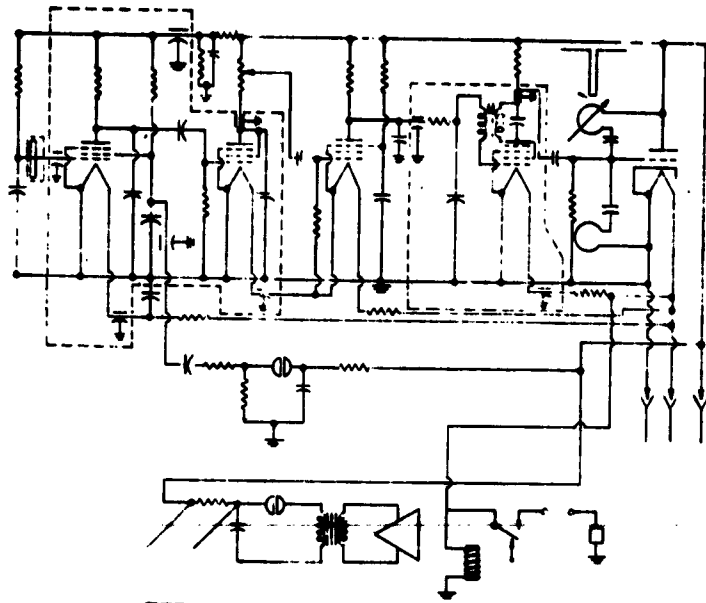
A schematic circuit drawing of the flight instrument is presented in Figure 7. The upper portion of the drawing presents the sensing and telemetering part of the instrument. This includes the capacitor microphone and associated hard tube, two amplification stages, the blocking oscillator, and the carrier frequency output stage. The capacitor microphone and its associated tube comprise a 0 db sensitivity microphone (one volt per dyne per cm²).

The lower portion of the drawing presents two calibration devices and a relay arrangement. One calibration device consists of a calibrated speaker and relaxation circuit which periodically supplies an acoustic signal to the microphones. The other calibration circuit supplies an electronic pulse to the input of the amplifiers. With these two devices it is possible to observe any change in sensitivity of either the sensor or the related circuitry during flight. The relay arrangement allows the instrument to be cut free from the balloon when the battery voltages fall to a level low enough to terminate the useful life of the instrument by applying the remaining battery power to activate a small explosive charge which operates a guillotine-type device on the attaching line.

Pulsonde prototypes were designed and tested by the U. S. Army Signal Missile Support Agency at White Sands Missile Range and the development of the final model was done under contract by the Schellenger Research Laboratories at Texas Western College in El Paso, Texas. The developmental work included improvement in microphone design, circuit design, and environmental testing to enhance long term stability in a thermal environment of approximately -70°C.

REFERENCES

1. Barnes, T. G., H. N. Ballard, G. Q. Clark, D. McCarty, A. Villegas, "Fundamentals of Capacitor Microphone Design," Schellenger Research Laboratories. Undated
2. McDonald, Carlos, and George Q. Clark, "Modification of Radiosonde AN/AMT-4 to Monitor Acoustic Data," Schellenger Research Laboratories, March 1960



III-3 Figure 7

A THEORY FOR METEOROLOGICAL CORRECTIONS TO ARTILLERY
SOUND RANGING DATA

Donald M. Swingle

U. S. Army Signal Research and Development Laboratory
Fort Monmouth, New Jersey

The techniques which have been used for correction of artillery sound ranging data for varying meteorological conditions have developed over a number of years by the process of accretion and adjustment. In an effort to study improved meteorological techniques for application to Army problems, this important meteorological application was investigated.

Stated very simply, the standard technique consists of weighting the wind speed, direction and temperature within the lower levels of the atmosphere according to a set of established criteria. The resulting correction is applied to received sound data without further explicit consideration the precise path of the sound ray reaching any particular microphone.

The basic nature of the meteorological data available to most users in most countries provides a real, if sometimes unrecognized, limitation to the degree of sophistication which it is prudent to employ in the application of such data to practical problems. In general, the atmosphere is described in terms of observations which represent finite difference computations, which are thus averaged over layers of the atmosphere, or they are originally sensed by elements which possess lag, and which are sometimes sampled at intervals. In the case of sound propagation through the lower atmosphere, wind data, as normally obtained by theodolite or rawinsonde tracking of an ascending sounding balloon, is taken in terms of average wind over specified height or time zones. Temperature and humidity data are alternated, with occasional time out for reference data, in accordance with changes of pressure as sensed by an aneroid baroswitch.

For the purposes of the present study, it was determined that no consideration should be given to the vertical gradients of wind and sound speed, but, rather, the investigation was deliberately limited to the use of the layer-mean winds and sound speeds. This was done because it was felt that, while more detailed treatments are possible, they can be expected to yield only slight improvements unless correspondingly better techniques for determining the state of the atmosphere are available.

An additional very important problem which is also eliminated by assumption, is the fact that the atmosphere varies in the horizontal. That is, we have assumed horizontal homogeneity within each layer of the atmosphere. In the present case this was done in order that the resulting meteorological correction method would be applicable to the typical situation in which data from a single rawinsonde or "pibal" station is readily available. The weaknesses of this assumption were later dramatically demonstrated. However, a large amount of progress in the elimination of the assumption of horizontal homogeneity cannot be expected until

either vast quantities of meteorological data are available throughout the volume of atmosphere through which received sound rays pass, or a much improved understanding of the meso-scale in the atmosphere is achieved. The latter development appears to be the more likely.

In the development which follows, it is assumed that the atmosphere consists of layers which are horizontally homogeneous, but whose properties vary in the vertical. Within each layer, the wind and sonic speed (which is principally determined by the temperature) are constant.

Consider a basic configuration for determining a line of position using two microphones. (Figure 1) The sound source is at G, while the two microphones are at M_1 and M_2 , respectively.

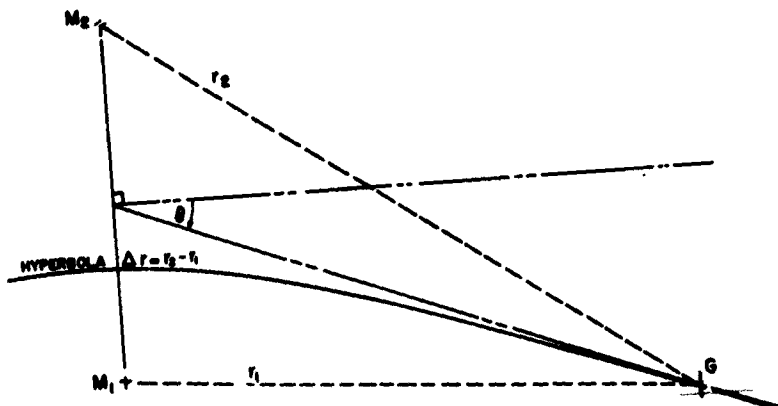
Under "standard" conditions of zero wind and 50°F temperature, sound velocity in all directions is V_0 . Then the time of sound travel from G to M_1 and M_2 is (Figure 2).

If we now consider a situation having a vector wind $W \neq 0$, a temperature $T \neq 50^\circ\text{F}$, and consequently sound velocity $V \neq V_0$, this equation could still be used if T_{02} and T_{01} could be expressed in terms of T_2 and T_1 and the meteorological conditions, there T_2 and T_1 are the actual times required for sound to travel from the source to the two microphones. We shall use V_e to represent the effective sound speed from sound source microphone. Then we have the equations in Figure 3.

To proceed further, we require at least an approximate method for finding the proper hyperbola $\Delta r(\Delta T_0)$. This can be done by finding approximate values of r_1 and r_2 . If one seeks more than a single line of position, he must, naturally use more than two microphones. This yields a multiplicity of approximate lines of position, when "standard" conditions are assumed, which give at least a first approximation to the true values of r_1 and r_2 . These approximate values can be used in an iterative procedure to find the improved estimate of the ΔT which would have occurred had "standard" propagation conditions obtained i.e. ΔT_0 . (Figure 4)

If we designate the first estimate of r as r' , we obtain equations 15 and 16. (Figure 5). Note that we can, if we desire, also iterate this process to obtain (Eqn 17, Figure 5) and similar successive approximations.

Our principal problem now is to find V_e which is appropriate to each sound path. This can be shown to be given by the following (Figure 6). Strictly, V should be multiplied by $\sin \alpha$, to give the horizontal component of sound velocity in each layer. However this factor is very close to unity in the relatively short range sound ranging with which we are particularly concerned. This is not true of propagation over distances of hundreds of miles, and account would have to be taken of the departure of this factor from unity in calculations for such problems.



III-4 Figure 1

Under "standard" conditions of zero wind and 50°F temperature, sound velocity in all directions is V_0 . Then the time of sound to travel from the given position to microphone is

$$T_{01} = \frac{GM_1}{V_0} = \frac{r_1}{V_0} \quad (1)$$

and

$$T_{02} = \frac{GM_2}{V_0} = \frac{r_2}{V_0} \quad (2)$$

Then G lies on a hyperbola for which $(r_2 - r_1)$ is constant.

$$\Delta r_0 = r_2 - r_1 = V_0 (T_{02} - T_{01}) = GM_2 - GM_1 = V_0 \Delta T_0 \quad (3)$$

III-4 Figure 2

$$Q_{12} = T_2 V_{02} \quad (4)$$

$$Q_{11} = T_1 V_{01} \quad (5)$$

$$\Delta r = Q_{12} - Q_{11} = T_2 V_{02} - T_1 V_{01} \quad (6)$$

Note. however, that

$$T_2 - T_1 = \Delta T = t, \quad (7)$$

III-4 Figure 3

$$\text{LET } T_0 = T + \partial T \quad (8)$$

$$\text{THEN } \frac{r}{V_0} = \frac{T V_0}{V_0} \quad (9)$$

$$\partial T = T_0 - T \quad (10)$$

$$= \frac{T V_0}{V_0} - T \quad (11)$$

$$= \frac{T(V_0 - V_0)}{V_0} \quad (12)$$

$$= \frac{T \Delta V_0}{V_0} \quad (13)$$

$$\text{WHERE } \Delta V_0 = V_0 - V_0 \quad (14)$$

III-4 Figure 4

$$\Delta T = c_0 \frac{\Delta T}{V_0} \quad (15)$$

$$= \frac{c_0}{V_0} \frac{\Delta T}{V_0} \quad (16)$$

Note that by iteration we can (if we desire) obtain

$$\Delta T' = \frac{c_0}{V_0} \frac{\Delta T}{V_0} \quad (17)$$

III-4 Figure 5

$$V_0 = \sqrt{V^2 - V^2 \sin^2 \omega} = V \cos \omega \quad (18)$$

$$V \left[1 - \frac{V^2}{c_0^2} \sin^2 \omega \right] = \frac{V}{V_0} \cos \omega \quad (19)$$

where

V is the velocity of sound in still air at temperature T ,

V is the wind speed,

ω is the angle between wind direction and the direction from the gun to microphone.

Then,

$$\Delta T_0 = V_0 - V_0 \frac{V}{V_0} = V_0 - V \cos \omega = \frac{V^2 \sin^2 \omega}{V_0} \quad (20)$$

Equation (16) then becomes

$$\Delta T = \frac{c_0}{V_0} \left[V - V_0 + V \cos \omega - \frac{V^2 \sin^2 \omega}{V_0} \right] \quad (21)$$

III-4 Figure 6

In cases where the sound is propagated through several layers, ΔT must be computed, using appropriate weighting factors $J(h)$. (Figure 7). The actual computation can be greatly facilitated by use of the "Criterion Curve", which is a simple plot of ΔV against height. (Figure 8). To a close approximation, the denominator of the last term of equations (20), (21), and (22) can be changed from $2V$ to $2V_0$.

With this, the effective ΔV_e is shown in Figure 9.

In order to parallel current practice as nearly as possible, successive ΔT_n ($n = 1, 2, 3, \dots$) may be subtracted to obtain a correction for each microphone pair in an array of microphones. Thus, we obtain the equation in Figure 10. This is added to the observed time difference of sound arrival, t , for the given microphone pair to yield a corrected time difference of arrival. The corrected ray is plotted. Doing this for each successive microphone pair will permit obtaining an "improved" fix point. If desired, the new ranges and angles may be again used to more accurately compute the corrections.

It will have been noted that the availability of a simple formula for the $J(h)$ was a major advantage in the above derivation. The development of the form used herein was due to Dr. Craig Crenshaw. As you will see in the following paper by Mr. Golden, this also permits a very simple graphical use of the criterion curve to determine the necessary weighting factors without computation.

As was mentioned at the beginning of this paper, there is a sizeable meso-scale fluctuation of the sonic propagation conditions, which leads to changes in actual time differences of sound arrival from successive sounds generated at the identical location. Within the given data of the problem, these fluctuations were a form of noise added to the other errors of determining the time of arrival of the sound.

We found that working with noisy data to develop techniques for the improvement of this data by application of small corrections for the known meteorological conditions was rather frustrating. Of particular significance is the standard by which one determines the degree of success of the trial method. In particular, some "fix" techniques utilize the centroid concept, giving as the estimate of the source location the centroid of intersections of the various rays. This is very sensitive to small errors in angles which are nearly equal.

A feature of the location by time difference of arrival is that, for angles departing much from the normal to the microphone base, the angular error resulting from a given error in time difference increases rapidly as the angle increases. This suggests that some form of "weighting" should be given the apparent sound rays, depending upon their angle and, perhaps, the range of the source. Several of these have been studied, but the details cannot be presented due to the limited time available in this symposium. However, considerable improvements are evidently possible in the fix technique. Unless a fix technique is used which does not magnify the errors arising elsewhere in the system it is very difficult to determine whether one is making progress in a practical sense or not.

$J(h) = [v_e^* - v_e(h)]^{-1/2}$ where v_e is the effective sound speed along the given sound ray in the layer for which $J(h)$ is being computed and v_e^* is the sound speed at the altitude of total refraction.

III-4 Figure 7

$$v_{crit} = v(h) - v_0 + W(h) \cos \omega(h) - \frac{W(h)^2 \sin^2 \omega(h)}{2v(h)} \quad (22)$$

III-4 Figure 8

$$\Delta v_e = v_e - v_o = \frac{\Sigma v_{ey1t} \cdot J(h)}{\Sigma J(h)} \quad (23)$$

and

$$\partial T = \frac{r^1}{v_o^2} \frac{\Sigma v_{ey1t} \cdot J(h)}{\Sigma J(h)} \quad (24)$$

III-4 Figure 9

$$\delta t_{21} = \partial T_2 - \partial T_1$$

III-4 Figure 10

EVALUATION OF METEOROLOGICAL CORRECTIONS FOR SOUND-RANGING

Abraham Golden

U. S. Army Signal Research and Development Laboratory
Fort Monmouth, New Jersey

In methods for sound-ranging, microphones are used to provide a number of apparent bearings to the sound source. Meteorological corrections to these bearings, calculated by using a single weighted wind, are then made which are intended to correct the measured difference between time of arrival at successive microphones to the time differences that the sound wave would have taken under standard conditions of no wind and a sonic temperature of 50°F. The theory of another way of making these corrections has just been described by Dr. Swingle.

This new method takes into consideration in greater detail than the single-wind method the state of the atmosphere along the sound paths from source to each microphone. It should, therefore, be expected to produce improved corrections. However, certain assumptions about the state of the atmosphere along the sound path must still be made. (Figure 1).

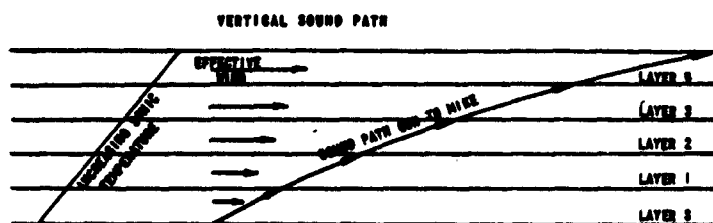
This method consists of obtaining the approximate range and angle from gun to each microphone from the difference of time of arrival of the sound wave at successive pairs of microphones. A determination of the vertical as well as the horizontal path of the wave is then made by the application of the law of refraction, the meteorological data, a minimum range graph, and a "criterion curve."¹ This is done for each ray from an approximated sound source to the individual microphones. Weighting factors are applied to the sound velocity in each layer according to the time it would be expected to spend in the layer.¹ Meteorological corrections are computed in terms of time differences. These time differences are added algebraically to the microphone-observed arrival times. This yields the meteorologically corrected time of arrival; the corresponding time differences lead to a new estimate of target location, and hence to a new range and a new angle. This entire process may be repeated again and again, each iteration coming closer, in principle, to the true target position.

The procedure for the step-wise method is as follows:

First, the path of the sound wave vertically and horizontally is determined from a plot of the meteorological information, consisting of a mean wind and a mean sonic temperature² for each layer. Figure 2 depicts a possible vertical sound path under the noted conditions of homogeneity in each layer. In order to trace the path, the sonic temperature and the wind speed along the path must be computed for each layer. The sum of the sonic and wind velocities along the path yields the effective sound velocity. (Figure 3)

1. The atmosphere is layered, with all layer boundaries being horizontal planes.
2. The atmosphere is horizontally homogeneous within each layer.
3. Sonic temperatures and winds are known as mean values of the layers.

III-5 Figure 1



III-5 Figure 2

$$V_0 = \sqrt{V^2 - V^2 \sin^2 \omega} + V \cos \omega$$

where

V_0 = effective sound velocity in the layer,

V = velocity of sound at ambient sonic temperature in the layer,

V = wind velocity in the layer,

ω = angle between wind and sound path in the layer.

Since $V \sin \omega \ll V$,

$$V_0 \approx V - \frac{V^2 \sin^2 \omega}{2V} + V \cos \omega.$$

III-5 Figure 3

$$\Delta V = V_0 - V_0 \approx V - V_0 - \frac{V^2 \sin^2 \omega}{2V} + V \cos \omega$$

where

V_0 = velocity of sound at standard conditions of sonic temperature equal to 30°F and no wind. This plot will yield a curve similar to Fig. 2.

III-5 Figure 4

A criterion graph is now plotted, consisting of effective sound velocity versus layer height. In order to save space, the deviation ΔV from the standard velocity is plotted as in Figures 4, 5, 5a, and 5b.

Next, the minimum range of a sound wave supported by a totally refracting layer is determined by the application of an overlay derived from the following equation (Figure 6).

The Minimum Range Chart, Figure 7, has overlayed the curve of Figure 5 so that the value of $V_S = 0$ is placed at the plotted value of the surface layer (layer S), and such that the abscissas match and the ordinates are parallel to one another. (Figure 8). The minimum range to which any layer will propagate sound may then be easily determined.

From Figure 8 it is noted that for layer 1 a minimum range of about 6200 yards for the propagation of the wave would be supported; for layer 2 a minimum range of about 9100 yards is possible; for layer 3 a minimum range of over 12,000 yards is found; and for layer 4 the minimum supportable range is over 12,000 yards. Therefore, if the approximate range determined from the initial plot were 10,000 yards, then layers S, 1, and 2 could all support the propagation of the sound wave to the microphone. Propagation is assumed to take place by a path through the highest layer supporting the estimated target range.

Weighting factors are then assigned to layers S, 1, and 2. A weight of 10 is assigned to the top refracting layer and a weight according to a weighting scale (Figure 9) to the remaining, S and 1 in this case.

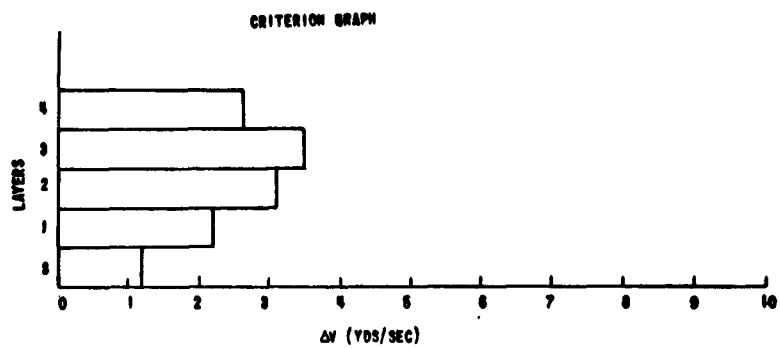
(Figures 10, 11, 12, and 13)

Another target fix is made, thereby providing a corrected sound-source location. Since the corrections computed above were based on an approximate location, these may now be computed more accurately by using a new range, new sound path, and new effective velocity. These new data in turn provide a new target location. In general, each new location should approach closer to the true target location. Limited experience with the method indicates that multiple iterations would rarely be required.

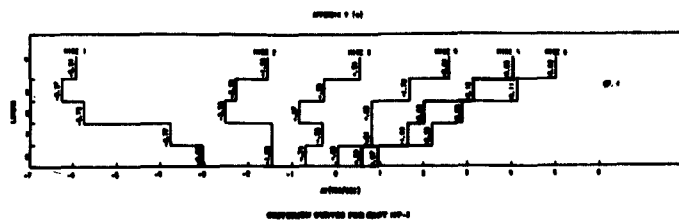
I will now present the results of the application of this method, using data from test firing of TNT. But first, a word about the data and data-processing techniques used.

The data were taken by detonating TNT charges at essentially two firing points. The time of arrival was recorded with the use of two different types of sound-ranging equipment at the same location. A weighted mean value was computed from the relationship shown in Figure 14.

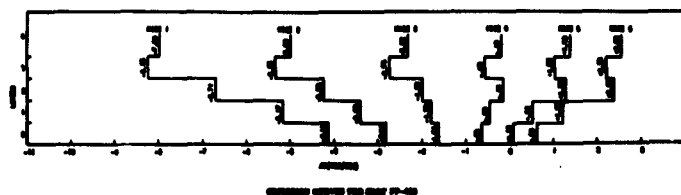
The wind data are averaged, separated into components, and plotted in Figures 14a, 14b, and 14c.



III-5 Figure 5



III-5 Figure 5a



III-5 Figure 5b

$$R_{min} = h (NV_0 / NV_1)^2$$

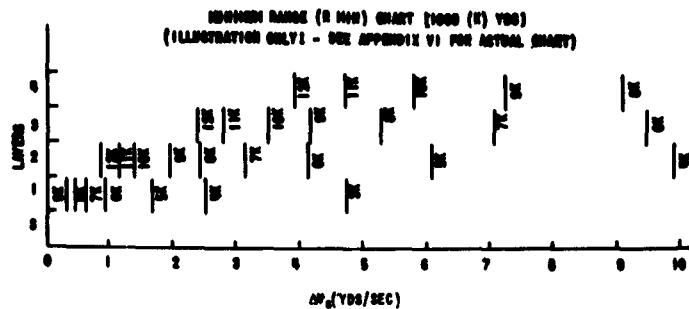
where

R_{min} = minimum range of a wave refracted back from a totally refracting layer from the value for the surface layer,

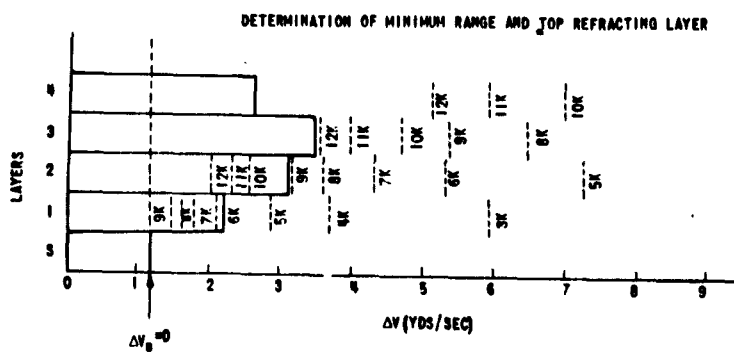
NV_0 = the deviation of the effective velocity of the top totally refracting layer from the value for the surface layer,

h = height of the top refracting layer.

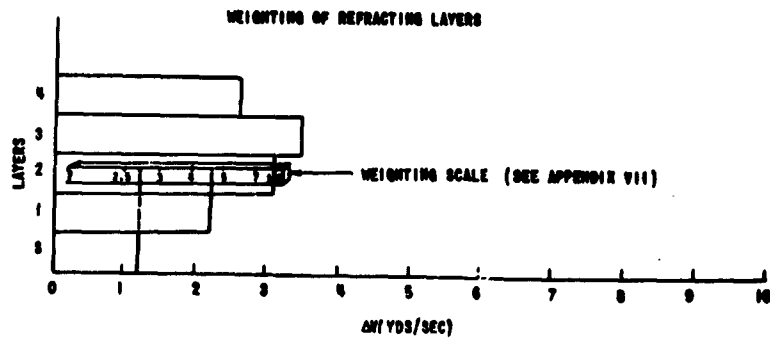
III-5 Figure 6



III-5 Figure 7



III-5 Figure 8 (VED FIG. 2)



III-5 Figure 9

$$\text{Weighting factor} = \frac{1}{\sqrt{\Delta V_0}}$$

where

ΔV_0 = difference between effective velocity of the top refracting layer and the effective velocity in each of the other layers. Thus, layer 2 is weighted 10, layer 1, 4.2; and layer 3, 2.7.

The weighted effective deviation from standard velocity ΔV_{we} is computed from the following relationship:

$$\Delta V_{we} = V_{we} - V_0 = \frac{\sum \Delta V \times \text{weighting factors}}{\sum \text{weighting factors}}$$

III-5 Figure 10

$$\delta t = \delta T_2 - \delta T_1 \approx \frac{r_2' \Delta V_{w_2} - r_1' \Delta V_{w_1}}{V_0^2}$$

$$\delta T \approx \frac{r_1' \Delta V_{w_1}}{V_0^2}$$

and

$$t_0 = \delta t + t_{\text{obs}}$$

where

t_0 = time difference of arrival of the sound wave at a pair of microphones under standard conditions,

t_{obs} = time difference of arrival under ambient conditions,

δt = time difference in successive δT_n , where $n = 1, 2$, etc.

III-5 Figure 11

$$t_{\text{curv}} = t_0 \sqrt{1 + \frac{V_0^2}{h_r^2} (s^2 - t_0^2)}$$

where

r = approximate range taken from the midpoint of the subbase S.

III-5 Figure 12

$$\sin \theta = \frac{t_{\text{corr}}}{s}$$

where

θ = angle between the normal to the surface and the sound path,

$$t_{\text{corr}} = t_{\text{obs}} + t_{\text{surv}} + \delta t,$$

s = the length of the surface in sound seconds (i.e., the length of the surface divided by standard sound speed V_0).

III-5 Figure 13

$$\frac{\sigma_1 \bar{T}_2 + \sigma_2 \bar{T}_1}{\sigma_1 + \sigma_2}$$

where

$$\sigma = \frac{\sum T^2 - \bar{T}^2 N}{N},$$

N = number of readings,

\bar{T}_1 = average difference in time of arrival at an adjoining microphone pair for OM-8 (U.S.) sound-ranging system,

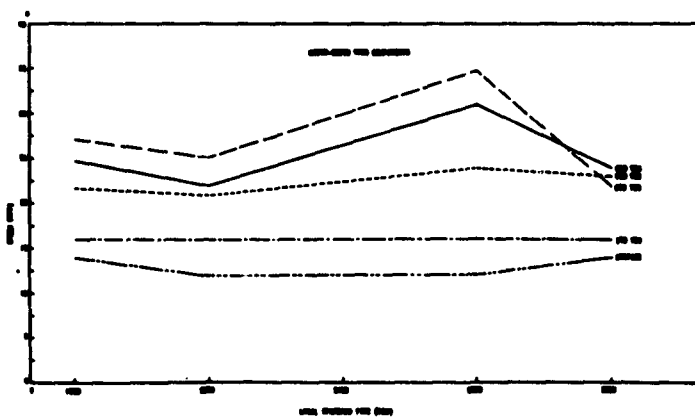
\bar{T}_2 = average difference in time of arrival at an adjoining microphone pair for MK-1 (British) sound-ranging system.

III-5 Figure 14

Wind Data for Station 127
Lower Wind Data

Height (ft)	Pressure	WPA	(a)	WPA	(a)	(a)	(a)
(Time: 1800 LST)							
surface	1.0	0.20	14	+0.005	+0.007	11.00	-1.17
100	329.1	0.20	14	+0.005	+0.007	11.00	-1.17
100	329.1	0.20	14	+0.005	+0.007	11.00	-1.17
100	329.1	0.20	14	+0.005	+0.007	11.00	-1.17
100	329.1	0.20	14	+0.005	+0.007	11.00	-1.17
(Time: 2000 LST)							
surface	1.7	0.20	14	+0.005	+0.007	11.00	-1.17
100	329.1	0.20	14	+0.005	+0.007	11.00	-1.17
100	329.1	0.20	14	+0.005	+0.007	11.00	-1.17
100	329.1	0.20	14	+0.005	+0.007	11.00	-1.17
100	329.1	0.20	14	+0.005	+0.007	11.00	-1.17
(Time: 2200 LST)							
surface	0.7	0.20	14	+0.005	+0.007	11.00	-1.17
100	329.1	0.20	14	+0.005	+0.007	11.00	-1.17
100	329.1	0.20	14	+0.005	+0.007	11.00	-1.17
100	329.1	0.20	14	+0.005	+0.007	11.00	-1.17
100	329.1	0.20	14	+0.005	+0.007	11.00	-1.17
(Time: 2300 LST)							
surface	1.4	0.20	14	+0.005	+0.007	11.00	-1.17
100	329.1	0.20	14	+0.005	+0.007	11.00	-1.17
100	329.1	0.20	14	+0.005	+0.007	11.00	-1.17
100	329.1	0.20	14	+0.005	+0.007	11.00	-1.17
100	329.1	0.20	14	+0.005	+0.007	11.00	-1.17

III-5 Figure 14a



III-5 Figure 14b

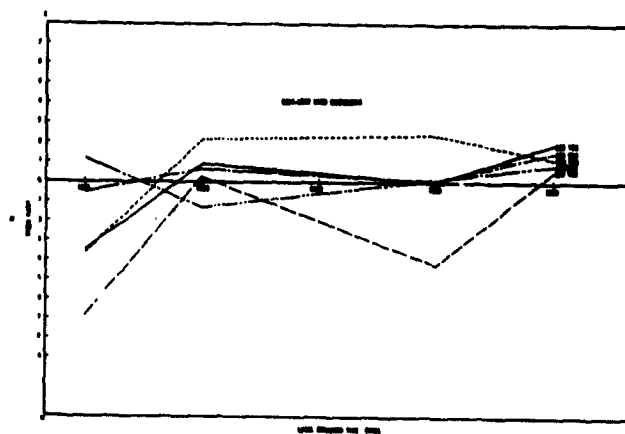
In order to compare the results of the application of this method with the single-wind method, computations were made, and the results are shown in Figure 15.

It should be expected that this detailed method would yield improved results in every instance. Such was not the case, as noted earlier in the discussion.

The reason for the two failures is not readily apparent. It should be noted, however, that the results are based on a very limited amount of data and that the effects of terrain and turbulence have not been accounted for. Substantially more calculations are required to be made in computing the meteorological correction as required by this method than by the single-wind method and, therefore, it is more suitable for machine processing than for manual computation.

REFERENCES

1. Unpublished Memorandum for File, "Meteorological Corrections for Sound-Ranging," by Dr. S. J. Bauer, USASRD, 1 Sep 56.
2. Gutenberg, B., Compendium of Meteorology, "Sound Propagation in the Atmosphere," American Meteorological Society, p 366, 1951.



III-5 Figure 14c

Comparison of Single Wind and USASNDL Methods for MP-3 Firings

<u>USASNDL Errors</u>	<u>Single Wind</u>
+0.10°	+0.43°
-0.30°	+0.40°
+0.46°	+0.25°
+0.26°	+0.40°
+1.73°	+0.18°

Comparison of Single Wind and USASNDL Methods for PP-426 Firings

<u>USASNDL Errors</u>	<u>Single Wind</u>
+0.02°	+0.54°
+0.09°	+0.61°
-0.09°	+0.47°
+0.41°	+0.49°
+0.16°	+0.41°

III-5 Figure 15

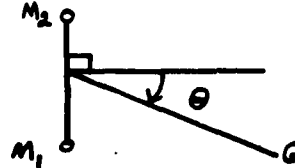
**ATMOSPHERIC AND GEOMETRIC CONSIDERATIONS
IN SOUND LOCATION DATA PROCESSING**

Donald M. Swingle

U. S. Army Signal Research and Development Laboratory
Fort Monmouth, New Jersey

In the well-known field methods of sound ranging using straight line arrays, one must assume the sound velocity V . For a plane wave

$$\begin{aligned}\sin \theta &= t/s \\ &= tV/M_2M_1\end{aligned}$$



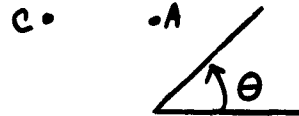
This poses the problem of determining the sound propagation speed in a variable atmosphere. A major portion of the propagation takes place in regions of the atmosphere which cannot be observed in detail. ~~We must usually assume horizontal homogeneity over the entire sound path.~~

One may partially solve this problem by the introduction of a two-dimensional array. Given three microphones, A, B, and C,

$$\sin \theta = (t_B - t_A)V/d_{BA}$$

$$\cos \theta = (t_C - t_A)V/d_{CA}$$

$$\tan \theta = [(t_B - t_A)/(t_C - t_A)] [d_{CA}/d_{BA}]$$



A common implementation of this approach takes the form of a square four-microphone array. Then

$$\tan \theta = (B-A)/(C-A) = (D-C)/(D-B)$$

$$= (D-C)/(C-A) = (B-A)/(D-B)$$



D - - B

As you can see, this is a redundant system. If the incoming signal is, in fact, a plane wave, the above relationships must be identities. Linear combinations of the several measures of $\sin \theta$ and $\cos \theta$ can be used. In particular,

$$\tan \theta = \left\{ \frac{[k(B-A) + \ell(D-C)]}{[m(C-A) + n(D-B)]} \right\} \cdot \frac{[m+n]}{[k+\ell]}$$

If we take $K = \ell = m = n = \frac{1}{2}$, then

$$\tan \theta = \frac{[(D-A) - (C-B)]}{(D-A) + (C-B)}$$

If A is taken as a reference time and set equal to zero, then

$$\tan \theta = (D-C+B)/(D+C-B).$$

A similar variety of forms can be derived for the elevation angle of the incoming plane wave if we know the velocity. Similarly, we can obtain a similar variety of forms for the apparent velocity if we know the elevation angle. I will not cover these today in view of the limited time available.

Returning to the measurement of azimuth angle, one may ask which of the several formulas given is the most accurate.

I have approached this problem with the assumption that the errors in determining arrival time of the idealized plane wave at each microphone are random and uncorrelated. Since identical microphones, circuits, and techniques are normally used for all microphones in the array, I have assumed equal standard deviations for each microphone. This results in a number of forms for σ_θ corresponding to the forms for θ itself.

θ	σ_θ
$\tan^{-1} (B-A)/(C-A)$	$\frac{\sqrt{2} \tilde{E}V}{d} (1 - \sin \theta \cos \theta)^{\frac{1}{2}}$
$\tan^{-1} (D-C)/(D-B)$	$\frac{\sqrt{2} \tilde{E}V}{d} (1 - \sin \theta \cos \theta)^{\frac{1}{2}}$
$\tan^{-1} (B-A)/(D-B)$	$\frac{\sqrt{2} \tilde{E}V}{d} (1 + \sin \theta \cos \theta)^{\frac{1}{2}}$
$\tan^{-1} (D-C)/(C-A)$	$\frac{\sqrt{2} \tilde{E}V}{d} (1 + \sin \theta \cos \theta)^{\frac{1}{2}}$
$\tan^{-1} [(D-A)-(C-B)] / [(D-A)+(C-B)]$	$\tilde{E}V/d$
$\pi/4 - \tan^{-1} (C-B)/(D-A)$	$\tilde{E}V/d$
$\sin^{-1} (B-A)V/d$	$\left[\left(\frac{\sqrt{2} \tilde{E}V}{d \cos \theta} \right)^2 + \left(\frac{\tilde{V}}{\tilde{V}} \tan \theta \right)^2 \right]^{\frac{1}{2}}$

The first six forms show σ_θ proportional to V, the ground track speed of sound over the array. No term for velocity error appears since this factor is a derived quantity.

The form using only two microphones is included above simply for general interest. It assumes perfect knowledge of the denominator term. \tilde{E} is the standard deviation of determination of time of arrival of the idealized plane wave at each microphone and \tilde{V} is the standard deviation in the value determined for effective propagation speed.

The form giving arbitrary weighting to the redundant differences was omitted from the above table, since it can be shown that equal weighting is as good or better than any other form if errors are random and independent.

You will note that similar results are obtained for each pair of forms. This follows from symmetry for the first four forms. For forms shown fifth and sixth in the table the same value of σ again appears. This must be, since the same data are used in each and the sixth form can be obtained from the fifth form by simple trigonometric transformation. The advantage of the sixth form is, however, that it is much simpler to use. In effect, the first pair of forms is superior to the second pair because errors in the common term in numerator and denominator appear with the same sign, rather than with the opposite sign. The third pair of forms, in effect, takes the time differences over the longer, diagonal baselines, thus achieving smaller percentage errors.

Now you will note that I assumed that departures of measured time of arrival from idealized plane wave arrival were not correlated between microphones. This is true with respect to errors in evaluating records, circuit noises, etc. However, the departures introduced by the atmosphere, which is not horizontally homogeneous in fact, will be partially correlated. The natural atmosphere supports a wide range of scales of variation ranging from small dust whirls and gusts up to major global circulations.

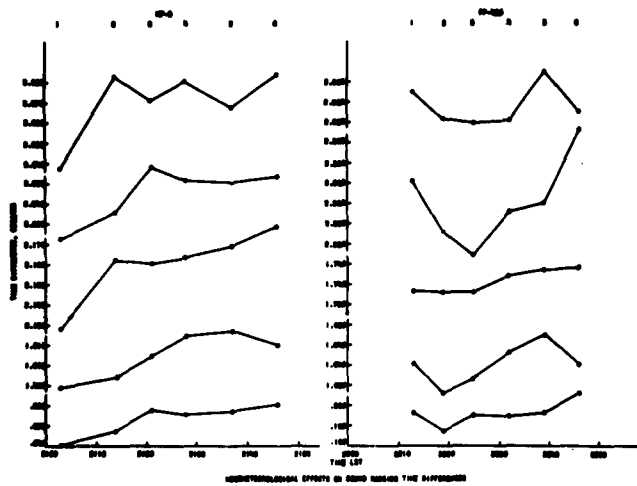
Propagation over long distance tends to average out the smallest scales. Under certain assumptions, we may expect this smoothing to become more effective in proportion to the square root of the path length. On the other hand, the gradients of large scale variations are very small. Over the dimensions of microphone arrays, the large scale differences usually prove to be negligible.

This problem has been treated by Blokhintsev in his book on ACOUSTICS OF A NONHOMOGENEOUS MOVING MEDIUM (1946, Leningrad), which has been translated and disseminated by the NASA. Based on the turbulence theory of Kolmogoroff, he shows that for a two microphone array, where

$$\sin \theta = tv/d, \sigma \theta = 0.3 d^{-1/6} (R/2\pi)^{1/2} (\bar{v}/2.7) = .044 \bar{v} R^{1/2} d^{-1/6},$$

where R is the range in meters, and \bar{v} is the mean wind speed in meters per second. When this is applied to long range propagation, which almost certainly includes portions of the propagation path at high altitudes, the value obtained is several times as large as the observed discrepancies.

The data considered by Golden in his paper on "Evaluation of Meteorological Corrections for Sound Ranging" showed well the variability of the atmosphere over short times. Two series of shots were made, with all shots of each series being from the same point (Figure 1). Tabulated are the time of firing, and the observed time difference between successive microphone pairs.



III-6 Figure 1

Shot Time	2103	2113	2121	2128	2137	2146	
Pair 2,1	640	648	658	656	657	660	milliseconds
3,2	1489	1494	1504	1514	1517	1510	
4,3	2128	2162	2160	2164	2169	2179	
5,4	2623	2636	2658	2652	2651	2654	
6,5	2940	2983	2971	2980	2968	2984	

Shot Time	2213	2219	2225	2232	2239	2246	
Pair 2,1	198	194	198	197	198	203	
3,2	1040	1033	1036	1043	1048	1040	
4,3	1938	1738	1738	1742	1744	1744	
5,4	2296	2283	2277	2288	2290	2308	
6,5	2692	2686	2685	2686	2698	2688	

We believe that much of this variation is due to small-scale changes in the atmosphere. In the more remote portions of the atmosphere, near the sound source, rays to the several microphones are close together and a small portion of the atmospheric variation affects the rays in a differential fashion. However, the longer the distance between microphones, the greater the portion of the variation which differentially affects the rays. Blokhintsev shows that this difference increases with the $5/6$ power of spacing and this largely nullifies the d^{-1} factor in the sine formula.

The error in a three microphone array would be somewhat greater, while in a redundant four-microphone array this value in turn might be reduced by a factor of the square root of two.

Now, this Kolmogoroff formulation assumes that we know only the mean value of V . Three obvious ways of improving our meteorological corrections are evident.

First, we can consider use of the corrections implied by a recent known shot. This, however, is particularly weak in that these data contain mostly small scale variations which are rapidly changing.

Second, we can use data from large scale meteorological analyses and predictions. The analysis process has smoothed out many of the small scale variations in the raw data sampled by sounding balloons. Air Weather Service studies have shown that stale observed data is more accurate than forecast data up to about six hours. Absence of observations over oceans, enemy areas, etc. may force a partial dependence on extrapolated or forecast data.

Third, local observations in the area of the array and forward of it could be analyzed to correct for differential conditions between ray paths.

The simple formulas used above assume a plane wave to be crossing the microphone array. In actuality, however, as shown by the studies at Denver Research Institute, the natural wave front appears to be rough or "corrugated". Mr. Chernetz will cover material which sheds more light on this problem.

Some years ago, Dr. Crenshaw carried out an extensive series of research studies in the Pennsylvania, New Jersey area. It is regrettable that he has not presented this material, which is unknown to most of you, at this meeting. In general, it underscores the significance of atmospheric variations in sound propagation, suggesting that determination of the effective speed of sound to closer than about one percent will require detailed observations or analyses of atmospheric conditions along at least a part of each sound path.

BLAST PREDICTION FOR SMALL-YIELD, HIGH-EXPLOSIVE SHOTS
Jack E. Chinn
University of California Lawrence Radiation Laboratory
Livermore, California

The daily routine for blast prediction is broken down into a number of steps which can be followed with the help of a close U. S. Weather Bureau R.A.O.B. and RAWIN reporting station.

1. The first step (Fig. 1) consists of getting the U.S.W.B. upper air sounding which includes pressure, temperature and dew point. This can be accomplished through teletype or by telephone and is then plotted (Fig. 2). The resulting plot gives one the pressure, temperature and dew point for each 1000 ft. level up through approximately 16,000 ft. of atmosphere.
2. The second step consists of following a pilot weather balloon with a theodolite up through approximately the same distance (Fig. 3). The 100 gram pilot balloon rises approximately 1000 ft. per minute. By taking readings of the vertical angle and horizontal angle and knowing the elapsed time or ascent, the distance out can be determined for each 1000 ft. elevation (Fig. 3). The horizontal angle and distance out is plotted (Fig. 4) for each minute. By using the same scale, the direction and velocity of the wind is reasonably accurately measured for each 1000 ft. elevation.

For blast prediction purposes, consider that the shock wave moves at sonic velocity. For practical purposes, humidity can be disregarded. Consider that the velocity of sound is 1088 ft. per second at 0° Centigrade and increases 2 ft. per second per 1° Centigrade rise in temperature. Now, by combining the sound velocity due to temperature, the wind direction and velocity for each 1000 ft. level and selecting a number of directions of interest, it can be determined whether the sound velocity increases or decreases with altitude. If there is no increase in sound velocity, with altitude toward any direction of interest, it can be concluded that sound should not return to the surface in amounts which would cause damage or complaints beyond two or three miles from the detonation point (Condition I, Fig. 5).

If there is a steady increase in sound velocity (Condition II, Fig. 5), it may be assumed that there will be no zones of silence under these weather conditions in our direction of interest.

Should there be a lapse in sound velocity and then an increase at some elevation above the surface, there may be several miles of silence; and then the sound may be focused back to the surface in a comparatively small area, much as the sun's rays are focused through a lens (Condition III, Fig. 5).

Figure 1

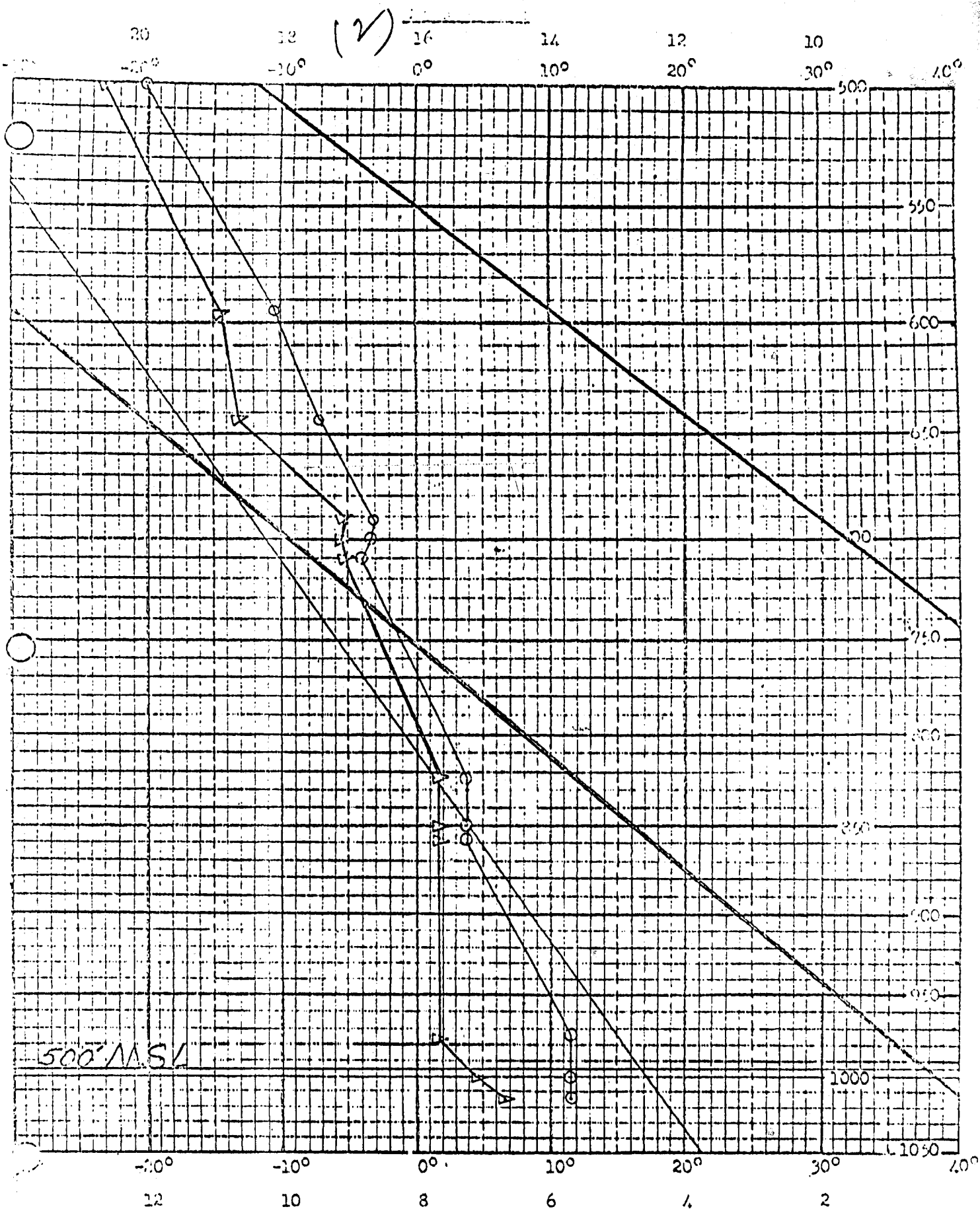
OAKLAND WEATHER STATION DATA

DATE 21 January 1960

RAWIN	RAOB	RAOB	RAOB
OAK	OAK 493		
1100			
51412	11037 11042 0 14 19	0	0
1 1433	85 478 03015 0 18 52	85 0	85 0
2 1536	70 989 53554 0 20 45	70 0	70 0
3 1640	50 839 70732 0 20 54	50 0	50 0
4 1750	40 371 81854 0 19 61	40 0	40 0
5 1850	55555 00013 11061	55555 00	55555 00
6 2050	11974 11013	11	11
7 2052	22858 01015	22	22
8 2053	33822 03015	33	33
9 2048	44710 54551	44	44
10 2043	55691 53554	55	55
12 2253	66642 57633	66	66
14 2162	77594 60646	77	77
16 2050	88 10171	88	88
18 2054	99 37920	99	99
20 2053	12373		
	06		

Zebra Time
 Pressure Millibars
 Elevation 4780 ft.
 Temp. °C
 Dew Point °C
 Tenths °C for each
 Wind Direction 1400
 Wind Velocity Knots

Wind Velocity Knots
 Wind Direction 20.°
 Elevation Kilofeet



III-7 Figure 2

DATE 1-21-60 BY 1100 STATION OAK

Figure 3

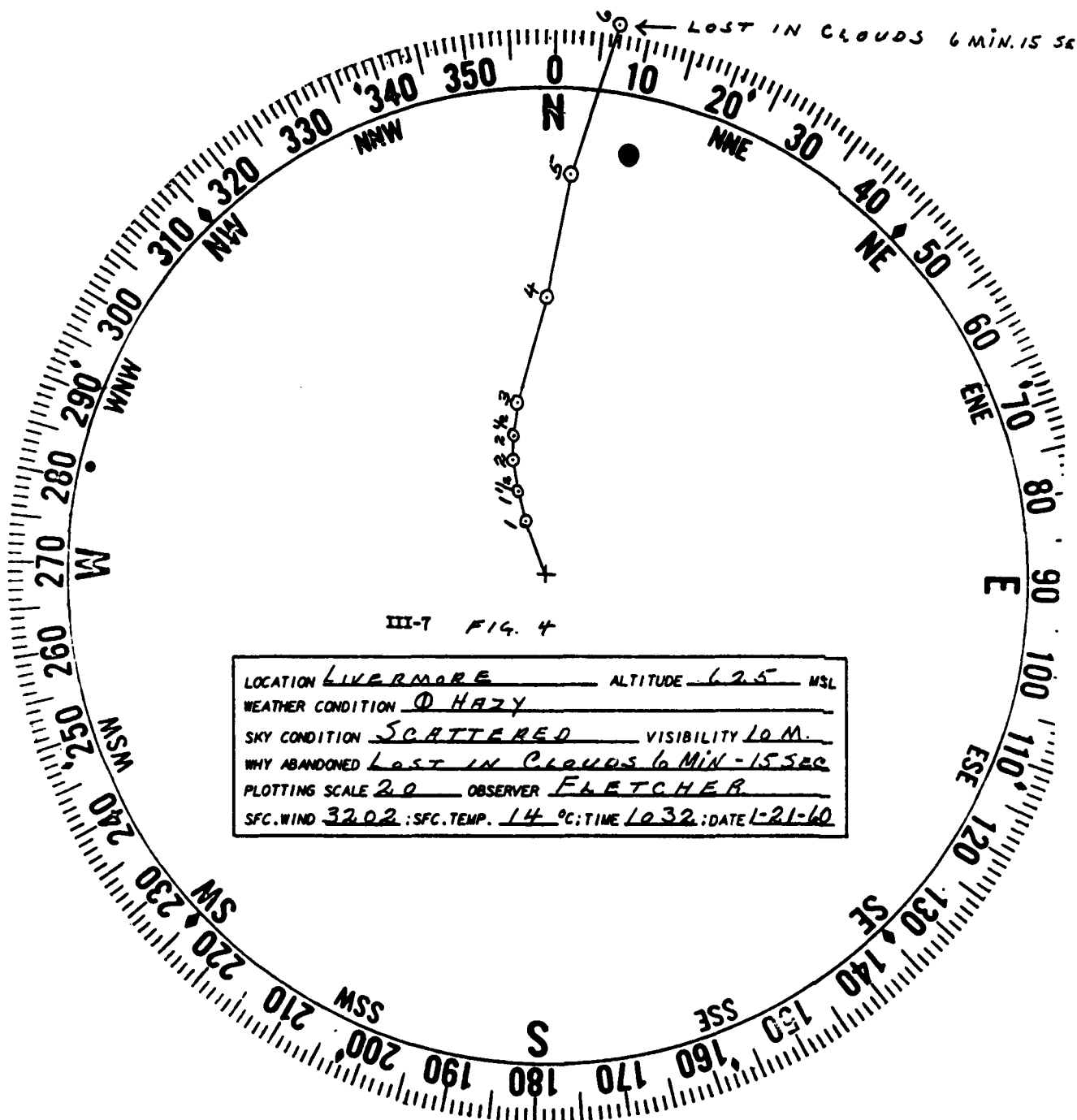
30 G Pilot Balloon

TIME STARTED 1032

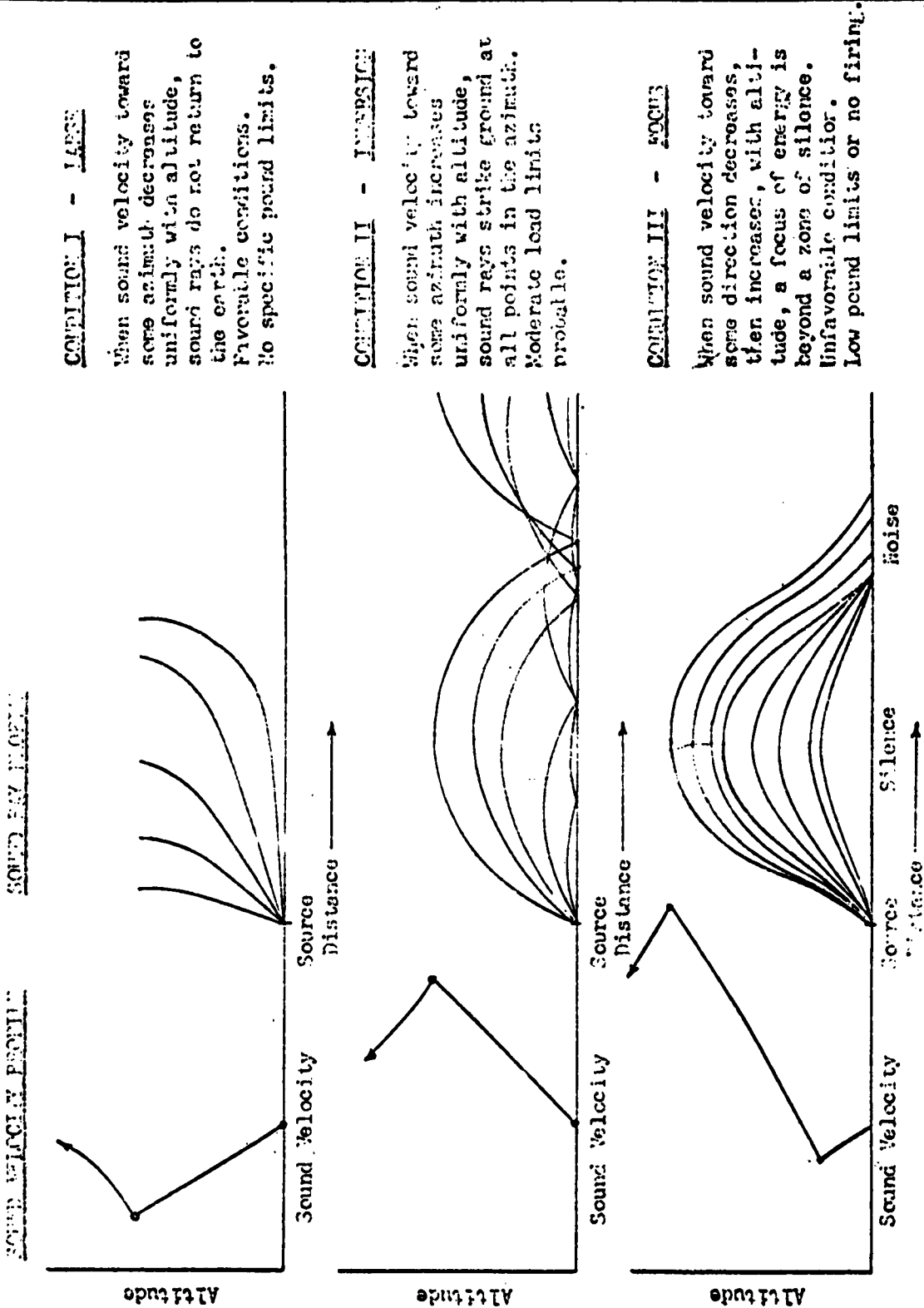
DATE 1-21-60

	Elapsed Time-Minutes	Vertical Angle	Horizontal Angle	Distance Out-Feet
T	V	H	DO	
1M	34.9	339.1	100	
1 $\frac{1}{2}$	32.7	341.5	159	
2	32.2	343.3	213	
2 $\frac{1}{2}$	32.8	346.5	258	
3	32.2	350.0	315	
4	27.3	359.4	502	
5	23.7	2.9	730	
6	20.5	6.9	1013	
7				← Lost in Clouds
8				6:15 Sec.
9				
10				
11				
12				
13				
14				
15				
16				
17				
18				
19				
20				

30 SECOND		
38	332	90
Elevation Feet		
Wind Dir.		
Velocity Knots		
LIVERMORE SITE LRL (625' MSL)		
8	-	15 09
.5	1	16 10
2.0	2	17 11
3.5	3	20 20
5.2	4	20 27
6.8	5	20 30
8.5	6	
10.2	7	
11.9	8	
13.6	9	
15.3	10	
18.7	12	
22.1	14	
25.5	16	



SUBJECT			<h1 style="text-align: center;">S K E T C H</h1> <p style="text-align: center;">LAWRENCE RADIATION LABORATORY UNIVERSITY OF CALIFORNIA - BERKELEY</p>			NO. NO.		TAG NO.						
DRAWN BY						SERIAL NO.		NO. RECD.						
DATE 2/1/50			BUILDING NO.			ROOM NO.			APPROVED BY			DATE		
									AS SHOWN INFORMATION			DATE RECD.		
									DELIVER TO			DATE RECD.		



The problem of sound velocity for each thousand-foot level up through 16,000 feet of atmosphere depending on temperature, wind direction and velocity, and direction of interest for 14 different directions of interest has been coded on the IBM 650 and 704 electronic computing machines. The velocities for all 14 directions are obtained in less than two minutes on the IBM 650.

Should there be a lapse of sound velocity and then an increase (Fig.6), then the resulting pressure and the distance at which it will return to the surface, under identical weather conditions, may be calculated by hand with the equations (Figs. 7 and 8). Figure 7 calculates the distance at which the sound rays may strike, and Figure 8 calculates the amount of pressure at that distance per 10 pounds of yield. This problem is also coded on the IBM and gives a complete answer on the 650 in approximately two minutes.

Considering the many variables in micrometeorology, it is felt that only the surface has been scratched concerning small-scale blast prediction. It can only be said that so far as can be determined, according to data received from a group of microbarograph stations located seven to ten miles east of the test site, the pressure in that area has been held under 300 microbars since the test site was opened in 1955.

Shots of as much as 1000 pounds have been fired at the site with no complaints and no record on the microbarograph grids. On the other hand, there are microbarograph records of as much as 60 to 75 microbars on shots of from 10 to 25 pounds of H.E.

The particular day illustrated in the slides shows the weather picture and calculations on which 150 microbars were picked up on microbarograph stations seven to ten miles distance, and complaints were received from 25 miles away from the site on a true course of 50° on an H.E. shot of 100 pounds.

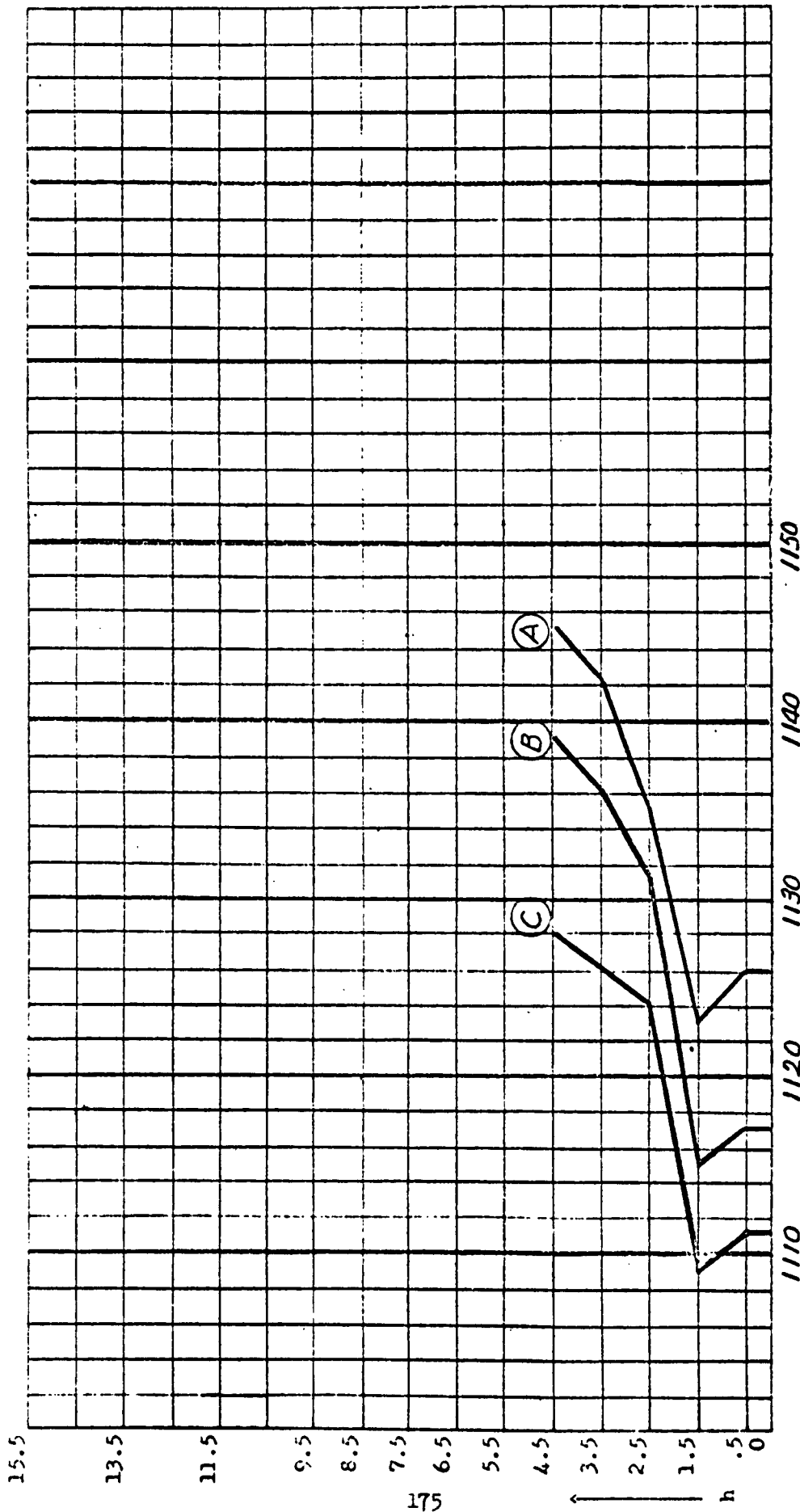
The day illustrated in the attached illustrations shows a weather condition giving a weight limit of 10 pounds due to a calculated focusing of seven to eight miles under the existing weather conditions at the time the calculations were made.

It is well known that wind direction, velocity and temperature, in the lower regions of the atmosphere especially, change considerably from moment to moment and from mile to mile, making blast prediction in the lower levels and for small-yield explosions extremely difficult and by no means infallible with the weather data presently available.

6

SOUND VELOCITY PROFILE - 02-11-60

DATE 21 JAN 60



V, ft/sec →

10° - 250 μBARS
 50° - 300 μBARS
 70° - 275 μBARS

RULE A-1 = 10° FCST

RW

Figure 7

Date _____
 Time _____
 Yield 10 lbs.
 Bearing _____

(1)	(2)	(3)	(4)	(5)	(6)	(7)	(8)	(9)	(10)	(11)
Level i	h_i ft. above 500' MSL	v_i ft/sec	v_i^2	$h_{i+1}-$ h_i $\Delta(2)$	$v_{i+1}-$ v_i $\Delta(3)$ +	m (5) (6)	$v_p^2 -$ v_i^2 from (4)	$\sqrt{v_p^2 - v_i^2}$	$\Delta(9)$ +	$m \Delta(9)$ $\Sigma = \frac{1}{2} R$ ft.

Figure 8

Date _____

W, Tons				$W^{1/3}$		$T=0.4W^{1/3}$		$\beta=5.7 \times 10^{14} \frac{W}{T}$		
.005				.171		.0684		4.17×10^{13}		
(12) R f.	(13) Level i	(14) m	(15) $\frac{1}{(9)}$	(16) $\Delta(15)$ +	(17) $\frac{n}{(14) \times (16)}$	(18) $v_p^2 \times \sqrt{\frac{n}{v_p^2 - v_o^2}}$	(19) $\sum = \frac{1}{2} \frac{dR}{d\theta}$	(20) $\frac{\beta}{R \frac{dR}{d\theta}}$	(21) $2\sqrt{\frac{P_s}{(20)}}$ bars	

Theory of Acoustic Background at High Altitudes
William C. Meecham*
University of Minnesota, Minneapolis, Minnesota

Introduction

We wish to discuss pressure fluctuations at high altitudes, up to 60,000 feet. We shall be primarily concerned with background measurements of such fluctuations. The experimental equipment will be described in a later paper together with the presentation of details of the results of measurements. It is the purpose of this paper to discuss some theoretical considerations relating to such effects.

The basic experiment consists of allowing a freely floating balloon to rise to an altitude of about twelve miles, after which the altitude is maintained. The balloon carries one or more microphones, whose pressure measurements are telemetered back to a ground station. The floating balloon platform eliminates much of the relative air motion with respect to the microphone and thus, as is well known, greatly reduces the effect of pressure fluctuations arising from local turbulence.

Using such a system the Michigan group has obtained some interesting pressure fluctuation background measurements (other groups have also been active in this area). For now we content ourselves with a brief description of the salient characteristics of such measurements. It is found that there is a relatively large pressure fluctuation, located mostly in the frequency range below 10 cps with a level of about 0.2 dynes per cm^2 . Superimposed on this persistent fluctuation are larger fluctuations occurring mainly in the frequency range of 1-3 cps with an amplitude of about 1.0 dyne per cm^2 . These larger effects last for several minutes and occur at intervals of from 20 minutes to an hour.

Such pressure effects have a number of possible causes. For the present purpose we divide these into three categories. First of all the larger sporadic disturbances might arise from single noise-producing events, for instance shock waves from airplanes, lightning, or any one of a number of such occurrences. It is difficult to see how the persistent lower level background could arise from such sources however. As a second possible explanation we might consider local hydrodynamic effects. If there were air motion, relative to the microphone, such motion would in general cause local turbulence which would in turn produce local pressure fluctuations. These fluctuations would in general be non-propagating. Thus, for instance, one would not expect a cross correlation due to them if there were a sufficient separation between the sensing elements involved in the correlation.

* Financial support for this work was furnished by the U. S. Army Signal Missile Support Agency through Contract DA-20-018-ORD-22840, with the University of Michigan.

Finally we might expect large regions of turbulent air, for instance, a jet stream, to generate sound which could propagate to great distance at low frequencies and perhaps give the observed pressure fluctuation background.

In what follows we discuss these possibilities in greater detail.

Characteristics of Source Mechanisms

We begin by discussing isolated sources. For any source whose characteristic time is less than a fraction of a second, we expect a flat frequency spectrum up to 5 or 10 cps, depending on the duration time of the phenomenon. For examples of such short time sources we could consider explosions, shock waves, and lightning. There are of course many other sources which one might think of, and the frequency characteristics of such effects are quite diverse.

More can be said concerning the characteristics of local pressure fluctuations and propagating fluctuations (sound); we turn to these effects now.

Local pressure fluctuations have been the subject of considerable study in controlled experiments in wind tunnels. In order to estimate the order of magnitude of such pressure fluctuations we apply Bernoulli's principle. (It is of course true that the principle cannot be applied exactly unless certain conditions are met, notably in the present case we should require the flow to be time steady. However, for purposes of estimating, the principle can be used as can be seen from dimensional arguments alone.) The strict statement of the principle asserts that the sum of the pressure and the kinetic energy per unit volume is constant. Thus, the pressure fluctuation from this source is

$$\Delta p \sim \frac{1}{2} \rho (\Delta u)^2$$

where ρ is the fluid density and Δu is the velocity fluctuation. In the cgs system, $\rho \approx 10^{-4}$ gms/cm³, and for the observed steady pressure background of about 0.2 dynes/cm², a velocity fluctuation of about 60 cm/sec or 1.5 miles per hour would be required. A relative air motion of a mile or two an hour does not seem impossible, although further experimental confirmation of this point is needed. The frequency spectrum for such pressure fluctuations has been measured by Reichardt and Motzfeld (Reference 1). The experiments were performed in a tunnel one meter wide by 24.4 cm high. The flow velocity was about one meter per second. They found a power spectrum for the velocity, which from Bernoulli's principle is the same as the frequency spectrum of the pressure fluctuation, as follows. The spectrum rises to a maximum at between 1 and 2 cps and falls at a rate of $f^{-1.7}$ where f is the frequency. This corresponds to about 10 db per octave for the pressure. The balloon measurements are still uncertain on the question of the power spectrum of the background. Early results for this quantity gave a fall off of 6 db per octave, somewhat

less than the measurements of Reichardt and Motzfeld. However the maximum of wind tunnel spectrum falls in the range where strong frequency components from the balloon measurements are observed.

Another characteristic of the background fluctuations which is of interest is the probability distribution of the pressure.* For local effects, one might expect the pressure to be non-Gaussian. In fact since in fully developed turbulence the velocity fluctuation is known to be Gaussian, the simple application of Bernoulli's principle leads to the prediction that the pressure would be very non-Gaussian. We shall see that turbulence-generated, and propagating, sound is quite different in this respect. No measurements of the probability distribution have yet been made.

We now turn to a consideration of turbulence-generated sound. The basic work on the problem of turbulence-generated sound was done by Lighthill (Reference 2). He found that the broad band noise produced was proportional to the eighth power of the turbulence Mach number. By using the formulas developed by Lighthill it seems reasonable to expect sound pressure levels of from 10^{-2} to 10^{-1} dynes per cm^2 . For this calculation a turbulence Mach number of 10^{-2} has been used, corresponding to a jet stream velocity of about 70 MPH, with an average fluctuation of about 7 MPH. The power spectrum of the sound from turbulence is difficult to arrive at. It depends on the turbulence model used. Kraichnan calculated from his theory (Reference 3) of turbulence that the power spectrum should fall off as the first power of the frequency. On the other hand Meecham and Ford (Reference 4) find, by using the Kolmogoroff inertial subrange theory of turbulence, that the spectrum should fall off like the 3.5 power of the frequency. If it is believed that the low frequency background pressure fluctuation observed at high altitude is due to propagating sound, then the tentative measurements favor the Kraichnan result.

Since sound from large turbulent regions can be thought of as coming from a large number of statistically independent source systems, it is expected that the probability distribution of such pressure fluctuations would be Gaussian. As stated above this distribution provides another means of distinguishing between local and propagating pressure effects. Local effects are probably quite non-Gaussian, as already explained.

Conclusions

It seems likely from the preliminary results available so far that one cannot yet rule out local effects as the cause of the steady background fluctuation observed in balloon systems. The results of cross correlation measurements involving two receivers located a few hundred feet apart so far show little correlation. There is however an interesting correlated component which occurs for a delay time of the order of the

* To the author's knowledge this criterion has not been used for experiments of the type discussed here. It seems a potentially powerful tool.

sound propagation time between the two receivers. Further investigation of this point is indicated. As the systems employed in these investigations become more sophisticated it is hoped that correlation techniques can be used to isolate local pressure fluctuation effects so that the propagating components alone can be examined.

At this time, and with the amount of information at present available, it seems that the sporadic pressure signals may be due to local effects. These signals, although they appear simultaneously on both channels of a two receiver system, are apparently not correlated, indicating again that they may not be propagating acoustic signals.

The power spectra at present available from these experiments are not yet conclusive, and further comment will be delayed on this point.

Finally the pressure probability distribution function is another interesting criterion to apply to high altitude pressure fluctuations.

BIBLIOGRAPHY

1. H. Reichardt and H. Motzfeld, ZAMM 18, 362 (1938).
2. M. J. Lighthill, Proc. Roy. Soc. (London) A211, 564 (1952).
3. R. H. Kraichnan, Phys. Rev 109, 1407 (1958).
4. W. C. Meeham and G. W. Ford, J. Acoust. Soc. Am. 30, 318 (1958).

Acoustic Background at High Altitudes

by
John W. Wescott

Institute of Science and Technology
The University of Michigan
Ann Arbor, Michigan

Introduction

This paper concerns the experimental phase of an investigation into the nature and sources of acoustic background noise at altitudes of about 60,000 feet above the earth. The investigation is not yet complete, but some relationships have already been established between high-altitude acoustic noise and the atmospheric phenomena which generate it.

One of the major sources of acoustic background at high altitudes has been found to be noise generated by the turbulent motion of air in and near the layer of maximum wind. This layer commonly lies at altitudes of 30,000 to 50,000 feet and moves at speeds of 50 to 150 knots, although higher and lower wind speeds and altitudes have been measured. The wind shear or gradient for the first 10,000 feet above and below this layer is usually about 5 to 10 knots per 1000 feet. The type of fluid motion which results is called "shear-flow turbulence". It is nonisotropic turbulence since the mean velocity of the flow is a function of altitude. This turbulence produces local compressions and rarefactions of air pressure and, therefore, radiates acoustic energy. In another paper W. C. Meecham has investigated theoretically the power spectrum of noise radiated by turbulence¹. Meecham's theory predicts that the amount of acoustic energy per cycle should fall off as the $7/2$ power of frequency (about 10.7 db per octave).

The experimental results to be reported here indicate that the power spectrum falls off as the second power of frequency or 6 db per octave measured on an energy per cycle basis. While theoretical and experimental results do not agree exactly, they are reasonably close. Furthermore, the measurements which produced the experimental results include not only noise radiated by turbulence but other background noise as well. A better understanding of what sort of noise background was measured can be had by considering the equipment and procedure that was used.

Equipment and Procedure

The essential feature of the method for sampling high-altitude, acoustic background noise lies in the use of free-floating balloons as quiet observation platforms. There is so little relative motion between a balloon and the air mass in which it floats that local flow noise at

Financial support for this work was furnished by the U. S. Army Signal Missile Support Agency through Contract DA-20-018-ORD-22840.

a microphone hanging from the balloon is reduced almost to the vanishing point. Under these conditions all acoustic background that has propagated to the microphone, and is above instrument self-noise, can be detected and transmitted by radio to a data recording station. It has turned out that acoustic background levels are usually at least 40 db above instrument noise for frequencies below 100 cps. Consequently, instrument noise has not been a serious problem in this work.

Figure 1 shows a pair of balloons and acoustic probes about to be launched.^{2,3} When the launching is completed, one probe hangs 300 feet below the other on the end of a nylon cord. The two-channel data thus obtained is cross-correlated to determine what portions have propagated from distant sources and what portions, if any, have been generated locally. Each probe contains a condenser microphone with a two-inch diameter diaphragm to develop relatively large electrical signals at low sound pressure levels. A diaphragm this large would never do for high-frequency work. Diaphragm resonances and directional effects would become objectionable at frequencies as low as 1000 cps. But acoustic background at high altitudes contains very little energy at frequencies above 200 or 300 cps, so that advantage can be taken of the extra sensitivity of a large diameter condenser microphone. Microphone sensitivity is about 40 db below one volt for a sound pressure level of 1 dyne per cm². Overall response of the microphone and three stage audio amplifier is flat from 1 to 300 cps with an intentional roll-off of 18 db per octave above 300 cps. Microphone response is sustained down to 1 cps by using a large chamber to isolate the rear of the diaphragm. The chamber is vented through a small diameter tube so that changes in air pressure can equalize on both sides of the diaphragm at high altitudes.

Using pulse modulation techniques, amplified data from the microphone is transmitted on an RF carrier frequency of 1680 MC to a tracking station shown in Figure 2. Only 1/2 watt of RF power is transmitted from each balloon-borne probe, but the servo-controlled parabolic antenna shown on top of the tracking van has such high gain that a useable RF signal-to-noise ratio is maintained until the probe drifts over the horizon. For a balloon altitude of 60,000 feet the line-of-sight range is 300 miles. Thus, depending on wind speed at 60,000 feet, up to ten hours of data may be acquired from one flight. Azimuth and elevation angles to the probe are determined by antenna position as it tracks, and are displayed and recorded automatically in the van.

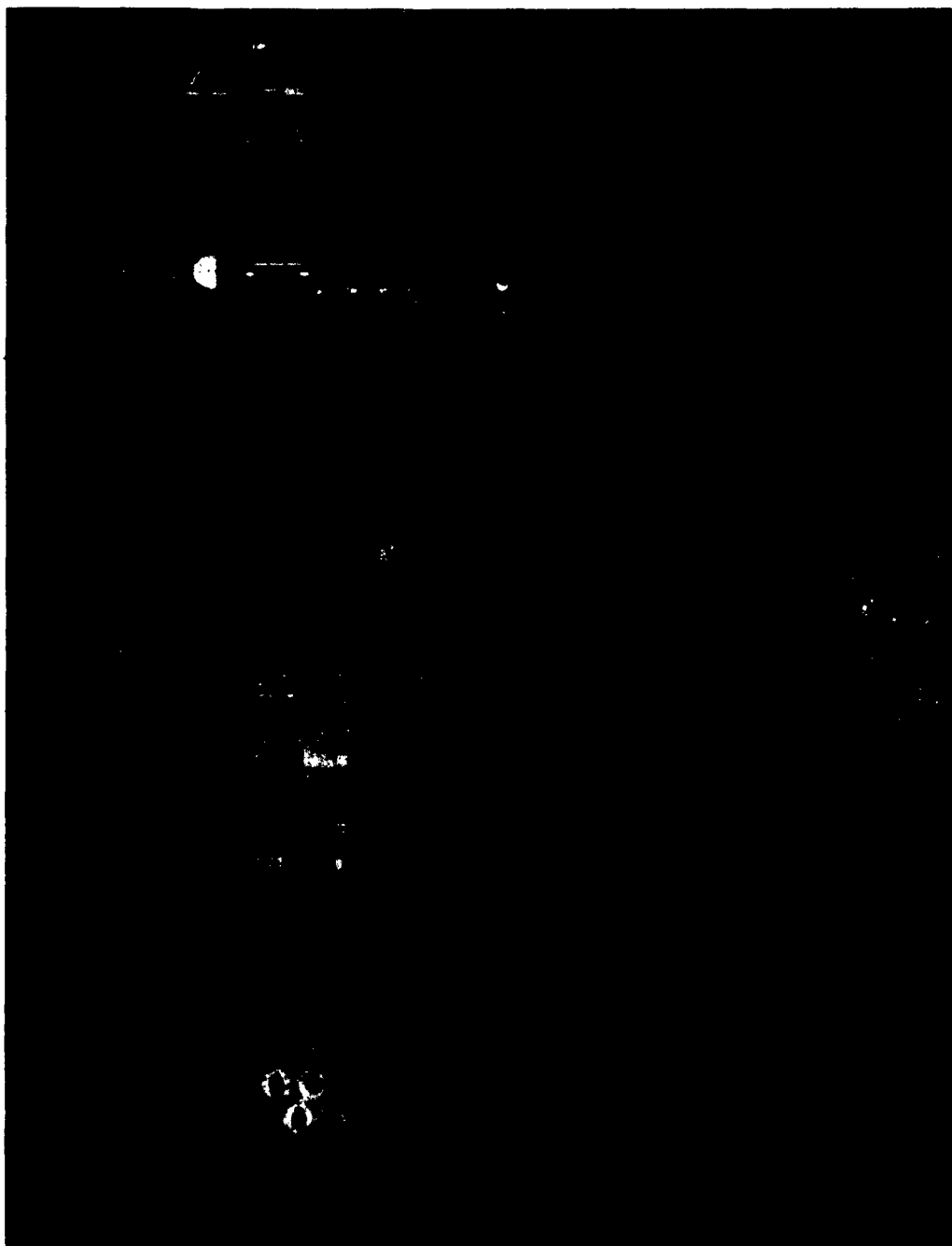
Figure 3 is an interior view of the van. Tracking information is displayed and recorded by the equipment bay on the right. The next bay contains equipment for recording meteorological data. Received acoustic data is demodulated and recorded on magnetic tape. An FM tape recorder shown in the next bay is used to preserve the low-frequency content of the original signal. An oscilloscope on the left is used for circuit checks and visual observation of incoming acoustic signals. The entire system from probe and transmitter through ground based receiver and tape recorder is calibrated prior to each flight. System response is held flat to within



III-9 Figure 1 Balloons With Acoustic Probes



III-9 Figure 2 Tracking Station



III-9 Figure 3 Interior View of Van

5 db or better from about 1/2 to 300 cps. System sensitivity is set so that when a tape recording is played back for analysis, an output signal of 1 volt is equivalent to an original sound pressure level of 1 dyne per square cm.

A block diagram of the two-channel receiving system is shown in Figure 4. The feature of this system is that it requires only one high-gain, automatic-tracking antenna. Advantage is taken of the fact that two different IF frequencies can be developed by one local oscillator and mixer circuit by merely tuning the probe transmitters to slightly different frequencies. The frequencies chosen are 1680 and 1695 MC. Both receivers contain rather elaborate electro-mechanical automatic frequency control systems to allow for drifting of the transmitter frequencies.

Experimental Results

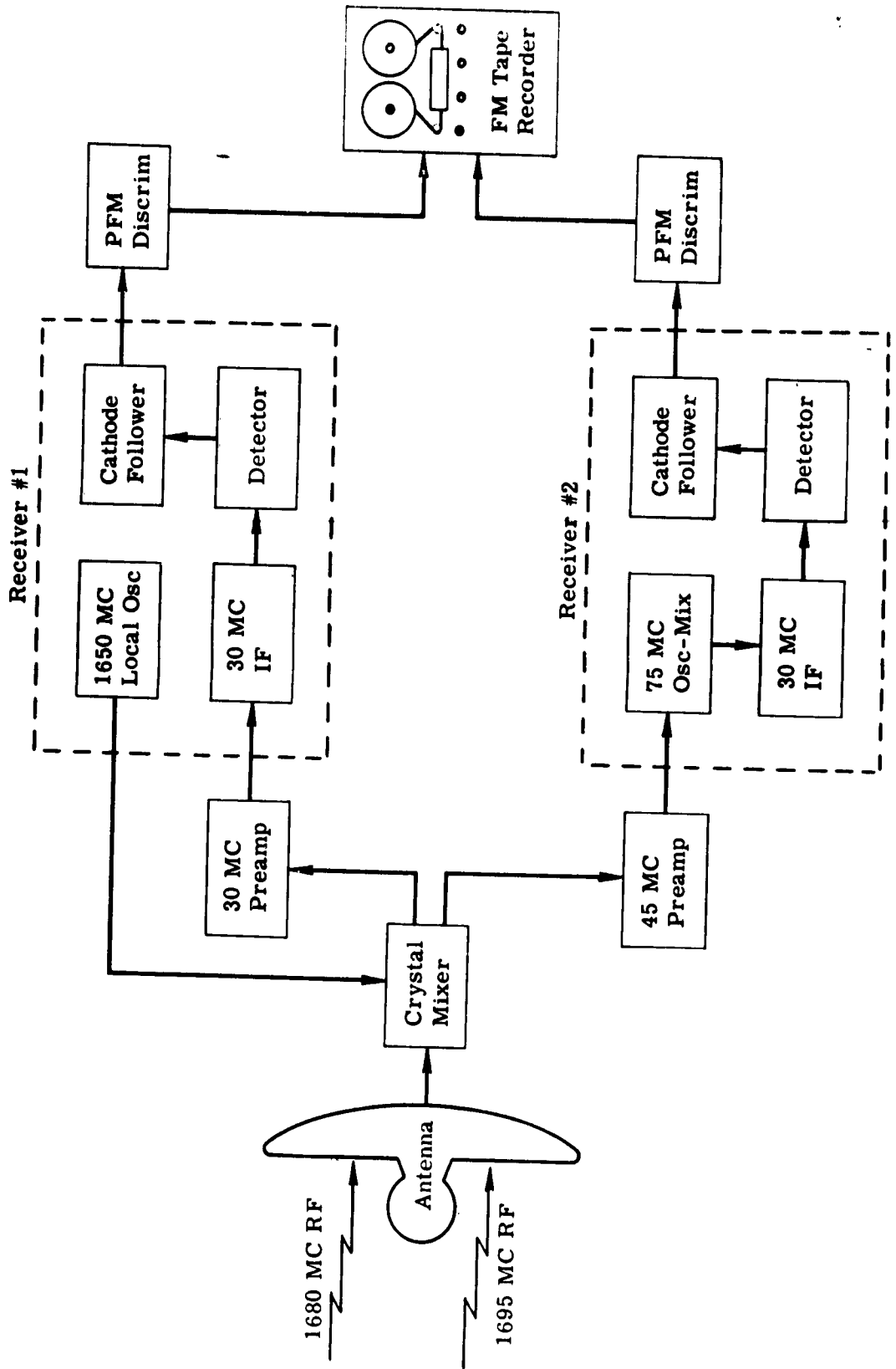
With the equipment described the following results have been obtained on the basis of 17 balloon flights made during the summer, fall and winter months of 1960 from Ann Arbor, Michigan. The average sound pressure level at 60,000 feet above the earth as measured over a bandwidth from 2 to 300 cps is about 0.2 dynes/cm². Frequency analysis of the quietest data samples shows that the acoustic power spectrum falls off as the second power of frequency (6 db per octave) when measured on an energy per cycle basis. This value is somewhat less than the seven halves power predicted by Meecham. Figure 5 shows some typical examples from the data analysis which led to the experimental result. These measurements were made over a frequency region of 1 to 150 cps with a spectrum analyzer having a constant bandwidth of 1 cps. This is fortunate since the output of the analyzer displays the spectrum directly on an energy per cycle basis. Each frame is a complete frequency analysis taken over a two-second period of time.

Several flights have been completed with two acoustic probes hanging from one balloon system; that is with one probe hanging below the other at the end of a long nylon cord. A magnetic tape recording of the two-channel data from one of these flights has been cross-correlated by using the electronic multipliers of a Pace Analog Computer, and delaying the playback of one data channel with respect to the other by various increments of time. The purpose of this was to determine whether or not a significant portion of the acoustic background at 60,000 feet propagates to these altitudes from lower altitude atmospheric turbulence. The result, as shown in Figure 6, indicates a pronounced cross-correlation of over 20% for a time delay between channels of 0.105 seconds. Microphone spacing was 150 feet for this flight. The average speed of sound in the altitude range from 35,000 to 60,000 feet was about 1000 feet per second. The apparent angle from the vertical at which the correlated portion of the acoustic background reached the microphones is calculated as,

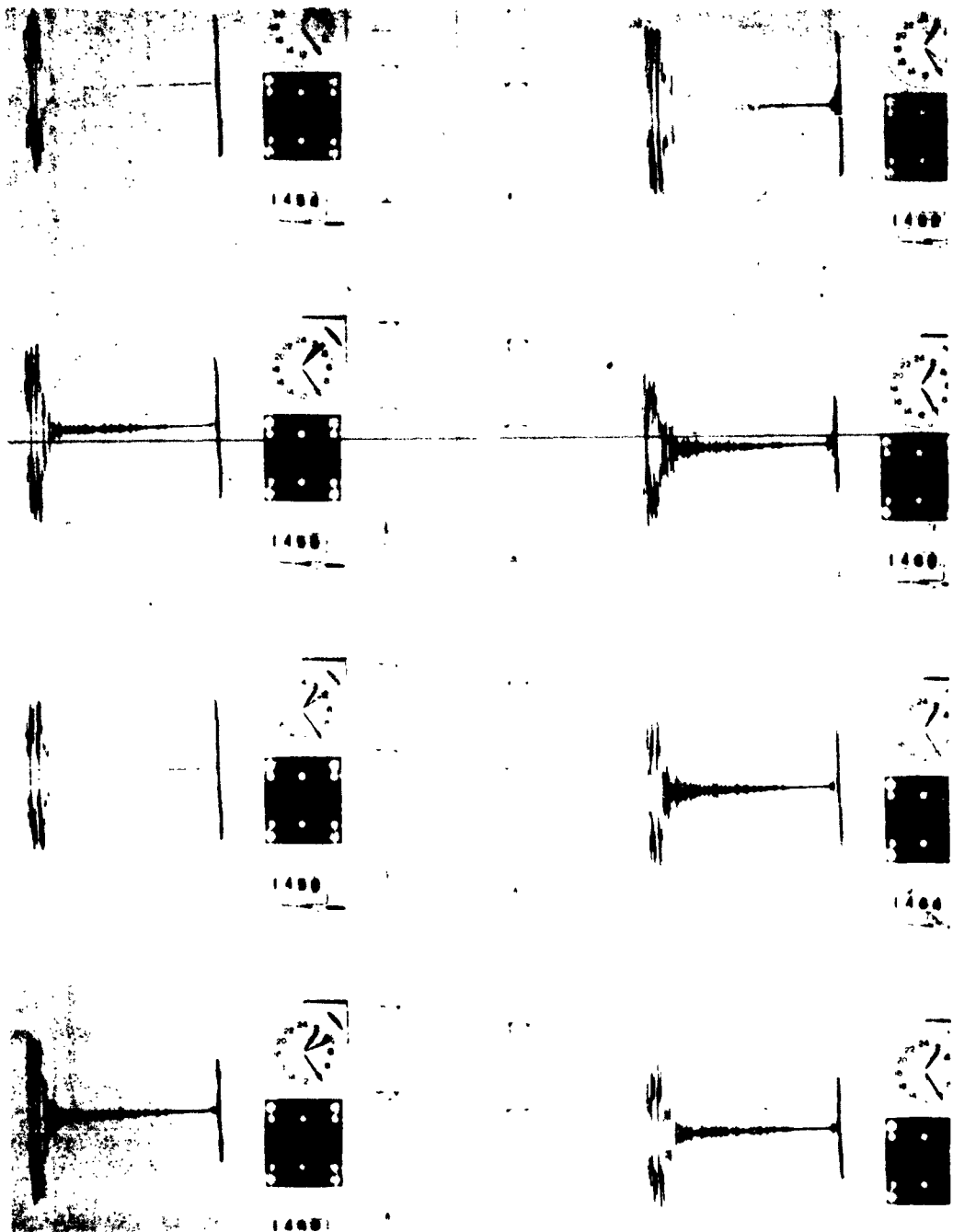
$$\theta = \arcsin \frac{0.105 \text{ sec} \times 1000 \text{ ft/sec}}{150 \text{ ft.}}$$

$$= 45^\circ \text{ (approx.)}$$

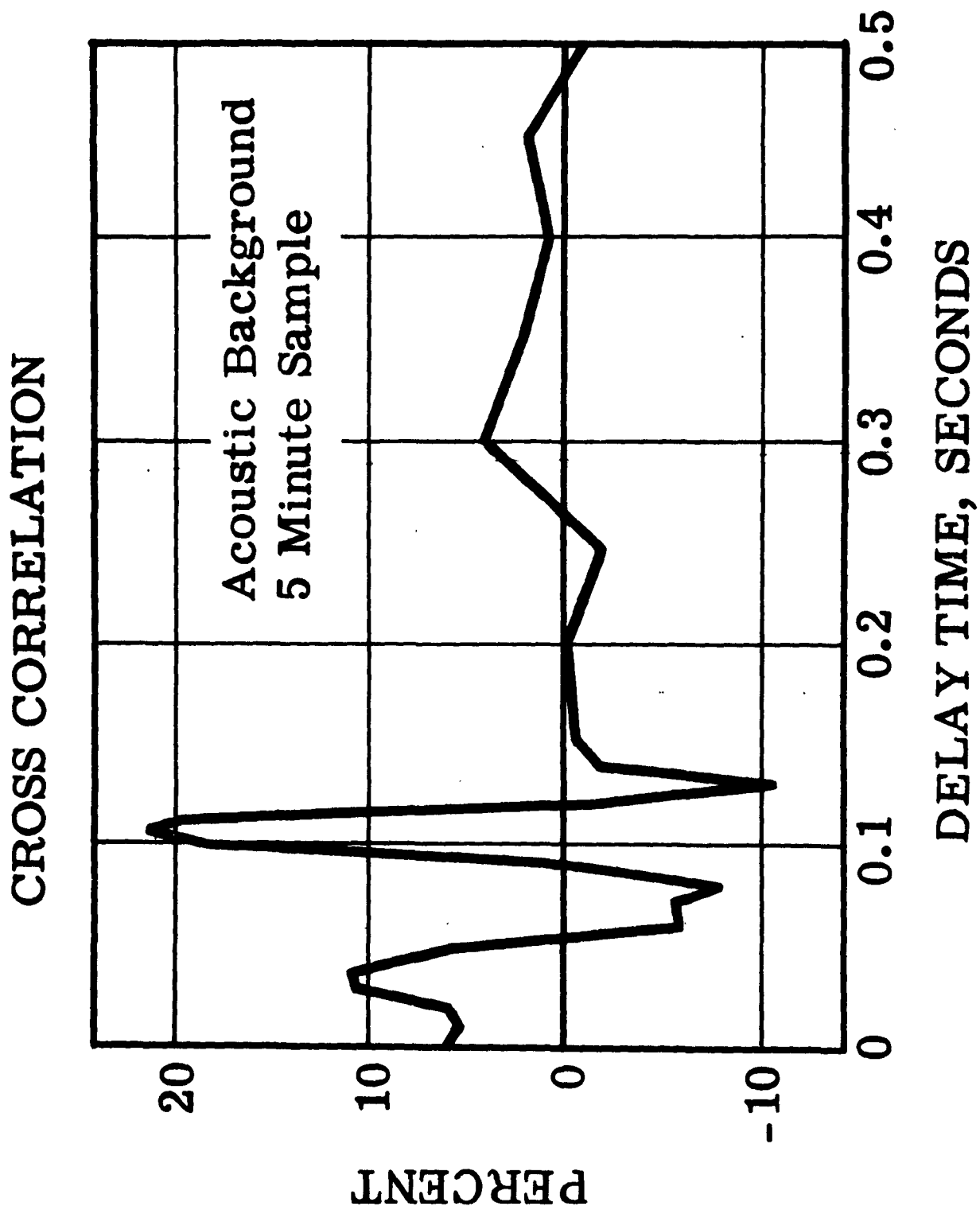
TWO-CHANNEL RECEIVING SYSTEM



III-9 Figure 4



III-9 Figure 5 Typical Example From the Data Analysis



III - 9 Figure 6

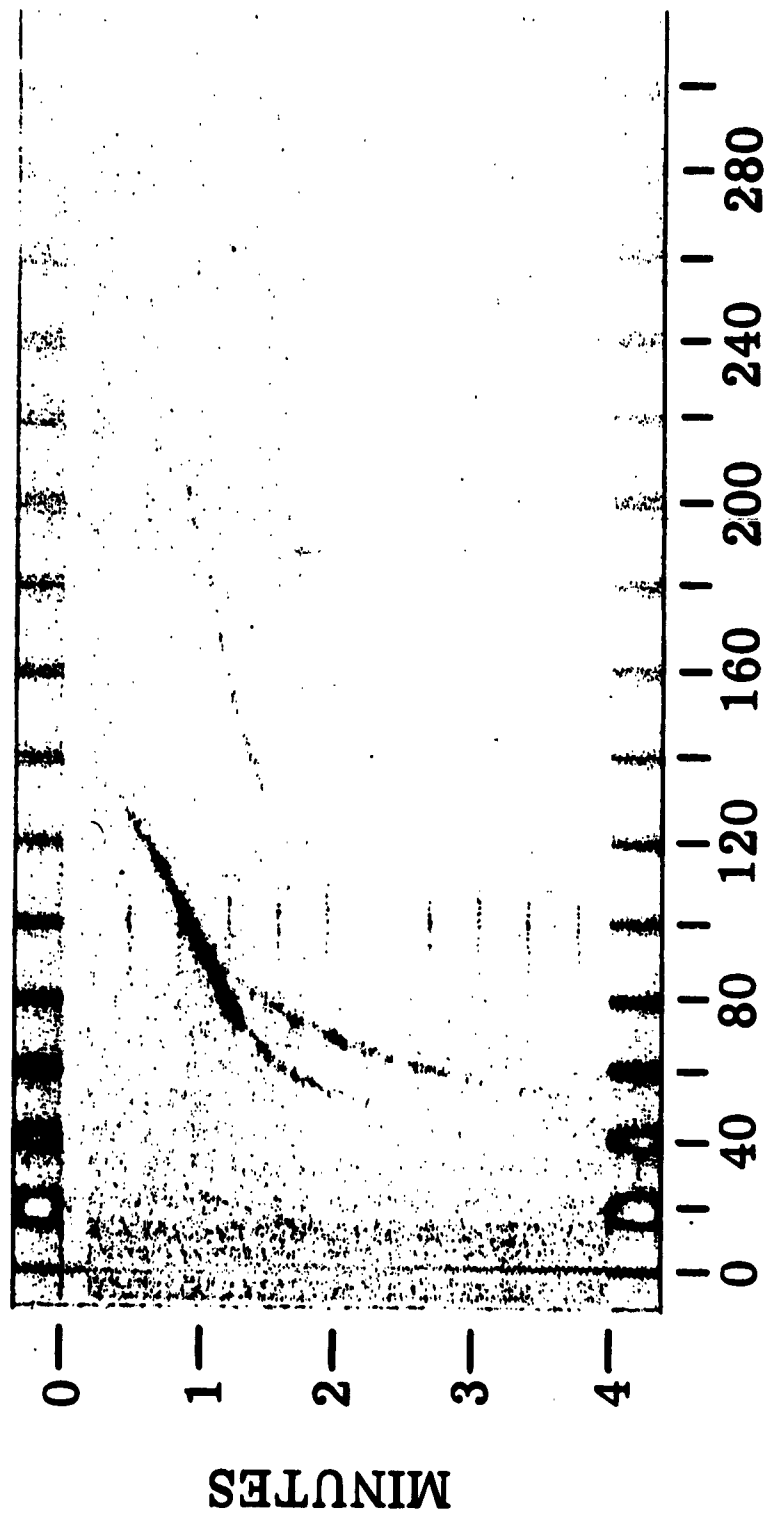
From this result it seems that an acoustic probe placed above a plane of uncorrelated sound sources, such as atmospheric shear-flow turbulence, will detect an apparent ring-shaped source of radius equal to the height of the probe above the plane. The main conclusion drawn from Figure 6, however, is that there is definitely a significant amount of acoustic background noise that propagates to 60,000 feet from some other altitude,-- enough to produce a 20% correlation peak. It seems likely, from meteorological considerations, that the major source of this propagating noise is lower altitude atmospheric turbulence.

In addition to the preceding results some interesting phenomena have been made evident by the form of data analysis shown in Figure 7. Here one can see the way in which the acoustic pressure spectrum varies with time. Sound pressure level is proportional to the darkness of the trace, frequency reads from left to right and time proceeds from top to bottom. This four-minute segment of data shows the Doppler effect that occurs whenever a piston engine aircraft comes within acoustic range of the balloon-borne microphone, passes by and then recedes in the distance. Note the double trace with the steeper sloped portion representing the Doppler shift of sound propagating directly from aircraft to probe. The trace having less slope represents a reflected path from aircraft to earth to probe.

If straight, constant speed flight is assumed, the range and speed of the aircraft can be calculated from the shape of the Doppler curve. What is challenging about this data is that it would be possible to measure the absorption per unit distance of low-frequency sound in air if the sound source were omnidirectional. Unfortunately, an airplane is not an omnidirectional sound source and, for sound pressure measurements along the Doppler curve to be useful, one would have to know the directivity of the source and the posture of the source relative to the receiver for each measurement.

In all of the flights launched so far there have been sporadic occurrences of strong, very low-frequency signals that persist from half a minute to several minutes. These events were detected at least once and often two or three times in one hour during the summer months. The rate of occurrence seemed to drop to once every hour or two during the winter, indicating that there may possibly be a seasonal effect. Data analysis shows these signals to lie in the frequency region below 5 cps and to have pressure amplitudes of about 10 dynes/cm². It has not yet been established what causes all of these disturbances, but a number of probable causes have been suggested. Any object, man-made or natural, that moves through the atmosphere at supersonic speeds generates shock waves. The high-frequency content of a shock wave is attenuated rapidly as the wave propagates in the atmosphere. This is due principally to molecular absorption which is severe at high frequencies. The shock wave degenerates, therefore, into a low-frequency pressure wave. A low-frequency disturbance can propagate over great distances with very little energy absorbed. Moreover, natural sound ducts caused by minimum temperature layers in the

AIRPLANE DOPPLER ANALYSIS



0-300 ~ Airplane from Flight 2420 25 August 1960 +6 db

atmosphere can channel a low-frequency acoustic signal and greatly increase the range over which it can be detected.^{4,5} Some of the possible sources of the strong signals detected are meteors, lightning bolts, tornadoes, supersonic aircraft, missiles, explosions and perhaps certain earthquakes which move the ground enough to radiate seismic energy into the air.

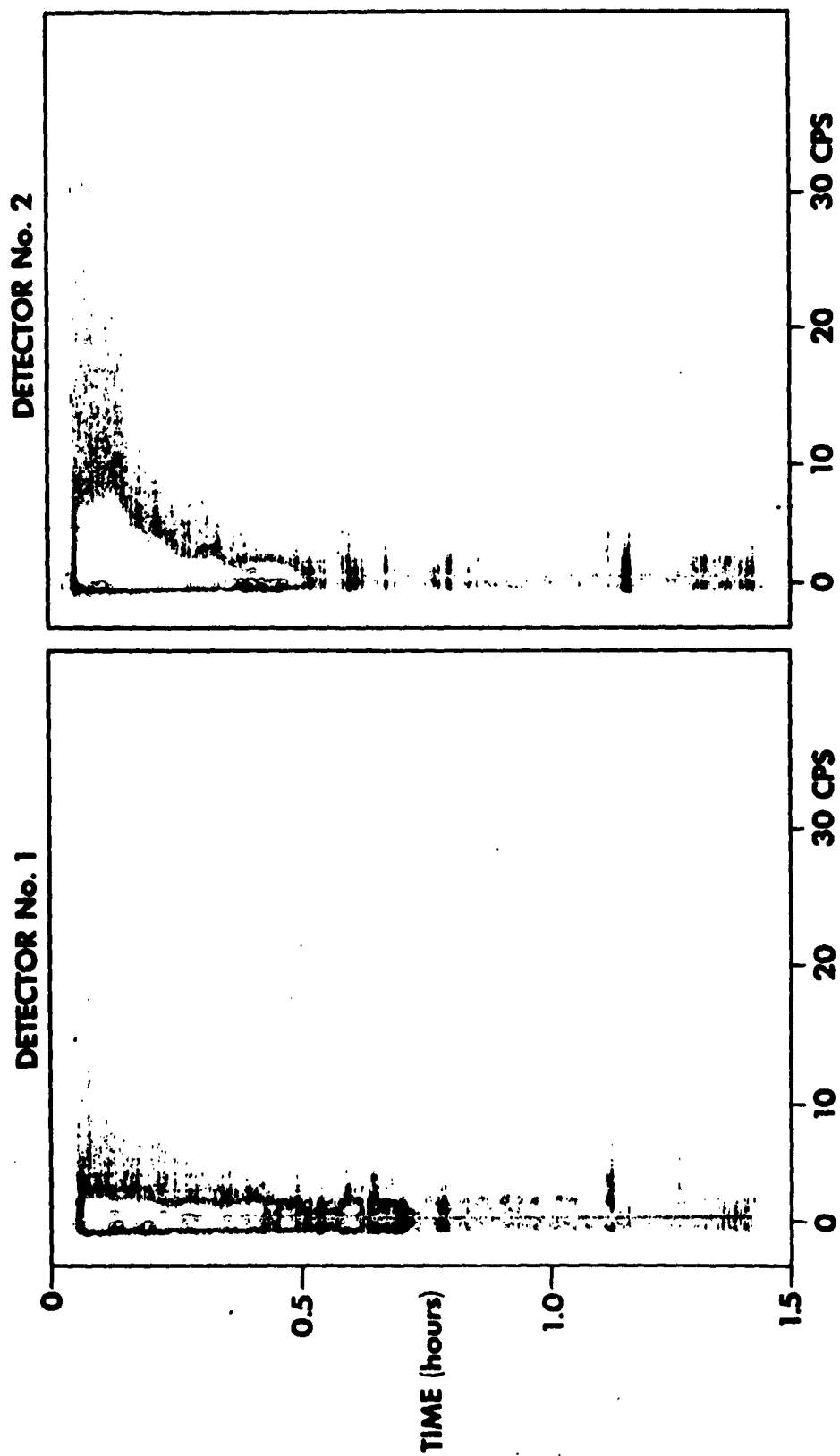
Some idea can be gathered about two-channel correlation of total events from Figure 8. The acoustic pressure spectrum as it varies with time is shown for two microphones spaced 300 feet apart at an altitude of 60,000 feet. Acoustic pressure is roughly proportional to the darkness of the trace. Figure 8 shows that in an hour and a half there were several infrasonic disturbances that correlated as total events.

An interesting sidelight shown in Figure 8 is the strong signal decaying with time at the beginning of each record. The balloon system carrying the acoustic probes which furnished the data was just completing its ascent prior to leveling off at this time. Maximum ascent rate was about 1000 feet per minute or 12 mph, and hydrodynamic flow past the microphones is clearly evident. The dynamic range for this type of analysis is about 12 db from black to white. Note how this transition occurs within about one octave indicating that local flow noise probably has a steeper roll-off characteristic with frequency than noise propagating from turbulence.

REFERENCES

1. Meecham, W. C., and Ford, G. W. (1958) ACOUSTIC RADIATION FROM ISOTROPIC TURBULENCE. J. Acoust. Soc. Am., 30, 318-22.
2. Webb, W. L., Coffman, J. W., and Clark, G. Q. (1959) A HIGH ALTITUDE ACOUSTIC SENSING SYSTEM. Missile Geophysics Div., U. S. Army Signal Missile Support Agency, White Sands Missile Range, N. Mex., Special Rpt. 28, 38 pp. AD-230, 726L.
3. Fugate, R. L. (1960) PULSONDE ACOUSTICAL SENSING DEVICE. Schellenger Research Lab., Texas Western College, El Paso, Texas, 96 pp.
4. Webb, W. L., and Jenkins, K. R. (1960) SPEED OF SOUND IN THE STRATOSPHERE. Missile Geophysics Div., U. S. Army Signal Missile Support Agency, White Sands Missile Range, N. Mex., Special Report. 37, 56 pp.
5. Webb, W. L., and Jenkins, K. R. (1961) SONIC STRUCTURE OF THE MESOSPHERE. Missile Geophysics Div., U. S. Army Signal Missile Support Agency, White Sands Missile Range, N. Mex., 24 pp.

INFRASONIC EVENT CORRELATION



III - 9 Figure 8

AMBIENT ACOUSTIC NOISE AT HIGH ALTITUDES

James C. Hart
Ray State Electronics Corporation
Boston, Massachusetts

As more and more investigation of acoustic phenomena at high altitudes is performed, knowledge of the acoustic noise spectrum gains the same relative import as that of its electromagnetic counterpart.

An opportunity to add to this knowledge was provided by the library of such data gathered in some sixty balloon flights made by the Applied Science Division, Melpar, Inc. from Rome Air Development Center in 1959. These flights employed a microphone and FM-FM telemetry system that enabled recording of audio and sub-audio signals at 62,000 feet.

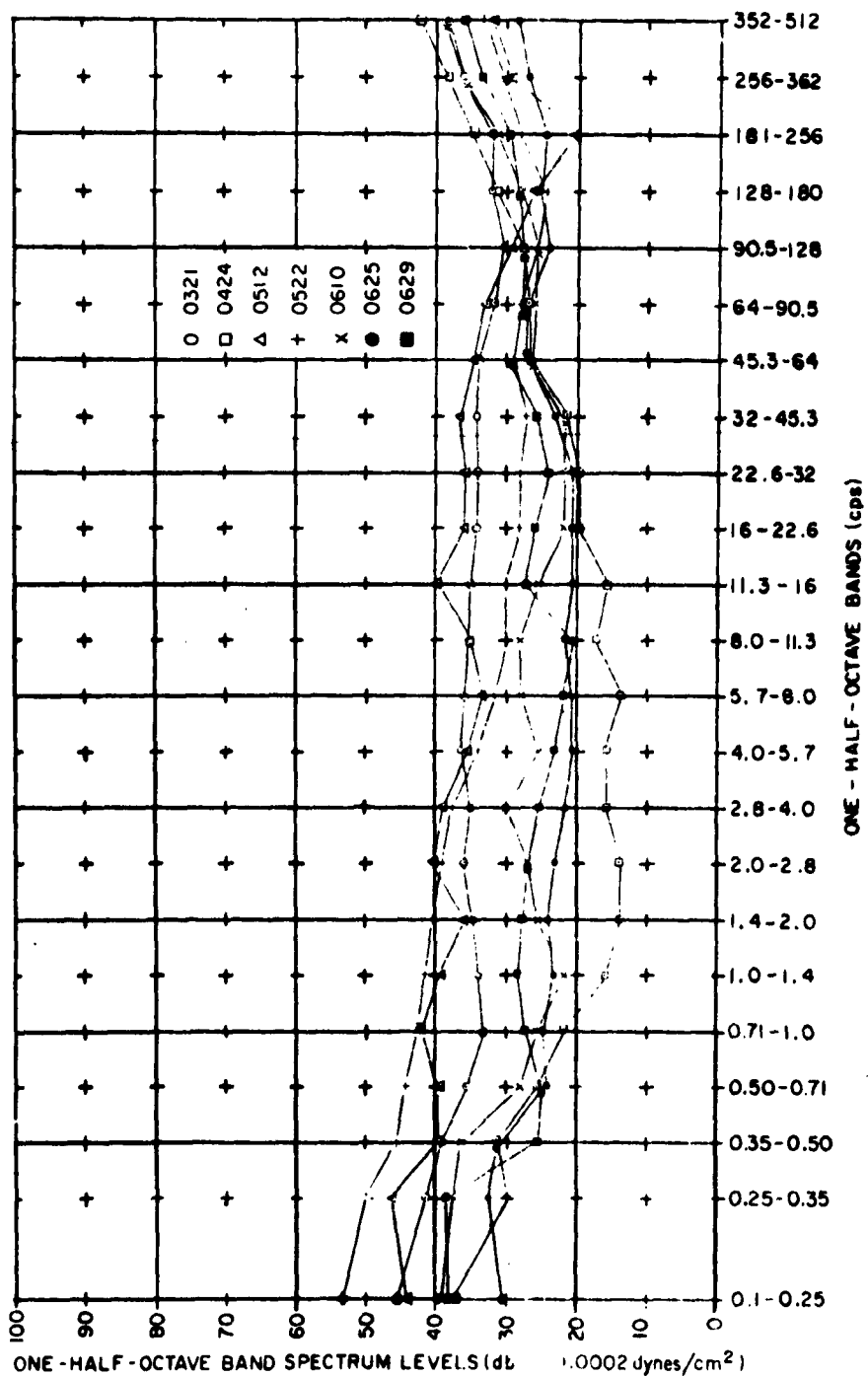
The sensor, a condenser microphone with a frequency response flat from 0.1 cps to 500 cps, modulated a voltage controlled FM oscillator at 200 kc. A radiosonde transmitter was, in turn, modulated by the 200 kc subcarrier; receiving and tracking were accomplished with standard Rawin gear whose output was translated to a 10.5 kc IRIQ FM subcarrier for magnetic tape recording.

It should be noted that in certain cases the sensor output was attenuated in order to require a larger acoustic input for a given change in the frequency of the subcarrier. Discarding these instances, only 32 of the 60 odd flights are deemed applicable to an analysis of the noise.

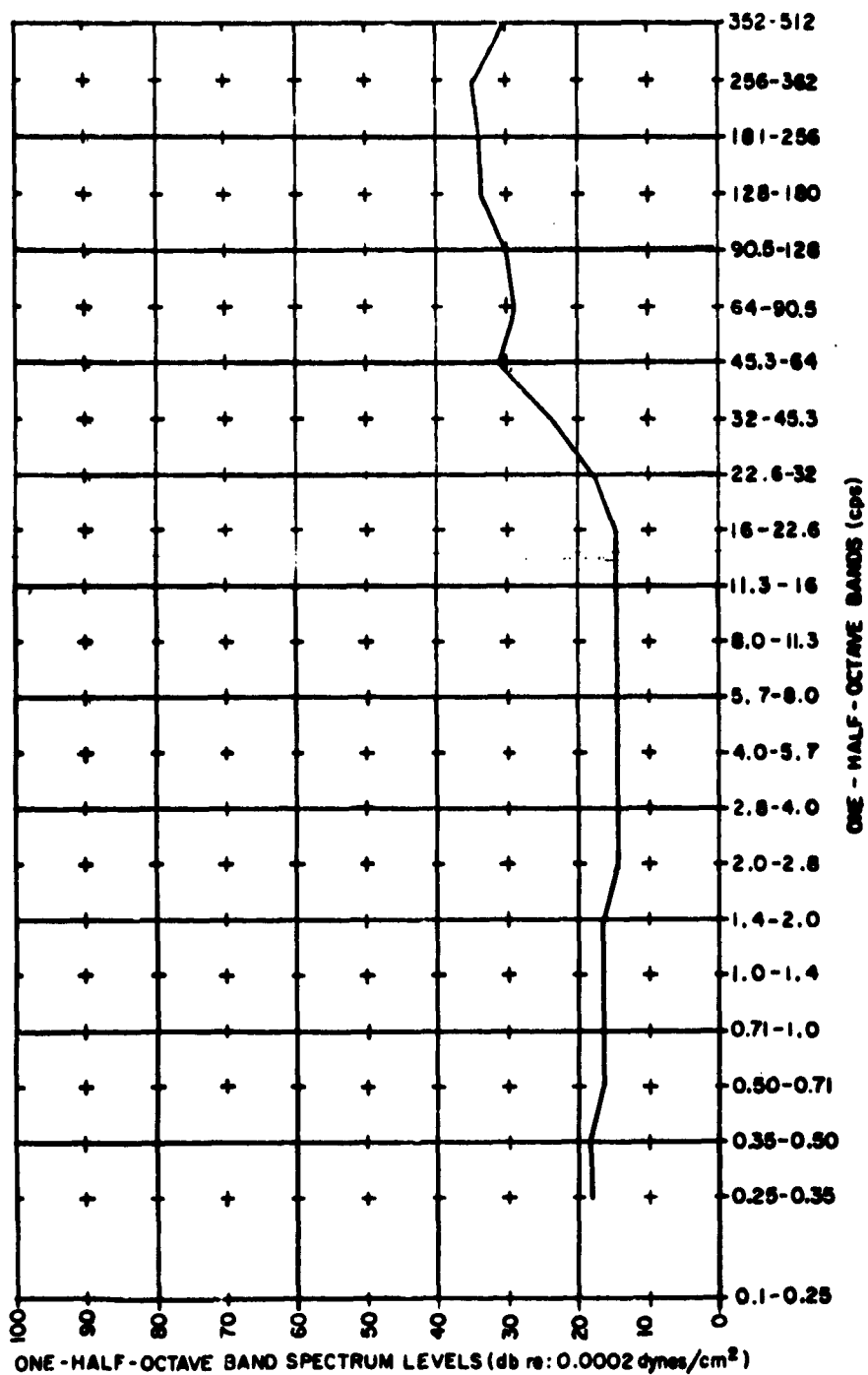
In the laboratory the 10.5 kc subcarrier was discriminated to obtain the original audio, or sub-audio, input. This, in turn, was passed through a series of half-octave bandpass filters, contiguous from 0.125 cps to 512 cps, producing an amplitude versus time display for each half octave; and by mounting these half octave charts in sequence, a "pseudo" three dimensional, i.e., frequency, amplitude, time, display may be obtained. For a selected time on this display, the noise level in each half octave was determined and plots of sound pressure level versus frequency produced for each balloon flight. Seven such plots are superimposed on the scale of Figure 1.

Assurance is granted that these are plots of acoustic rather than systemic noise by Figure 2. This is a record of systemic noise, obtained by flying the system with a disabled microphone electrometer, and of course, includes all noise sources of the transmission, receiving, discriminating, and data handling processes. The rise in level starting at 20 cps is attributed to a combination of the receiving antenna scan mechanism, power line pickup, and at the high frequencies, frequency modulation effects. Note that between 0.25 cps and 8.0 cps the average level is approximately 18 db. It is precisely because of the low noise in this frequency region that this discussion is confined to these five octaves.

For the 32 flights selected for analysis the range of pressure sound levels varied from 32.3 db referenced to 0.0002 dynes/cm² to 53.6 db.



III-10 Figure 1



III-10 Figure 2

Several rudimentary attempts were made to correlate the occurrence of these levels with the known meteorological data.

The first of these was an effort to correlate the values of the wind at 62,000 ft. with the sound pressure levels. See Figure 3. The circled points indicate local thunderstorm activity as reported by the tracking sites.

Second, correlation of the noise with maximum winds in the acoustic duct below the balloon was attempted; and the result is shown in Figure 4. The third correlation effort was to match noise with the average wind gradient, i. e., the difference between the values of wind speed at 70,000 ft. and 50,000 ft. Once again, as demonstrated in Figure 5, no significant positive result was obtained.

Several other efforts to determine the cause of the different noise levels were made, including attempted correlations with magnetic activity, temperature and sound velocities. None of these proved fruitful.

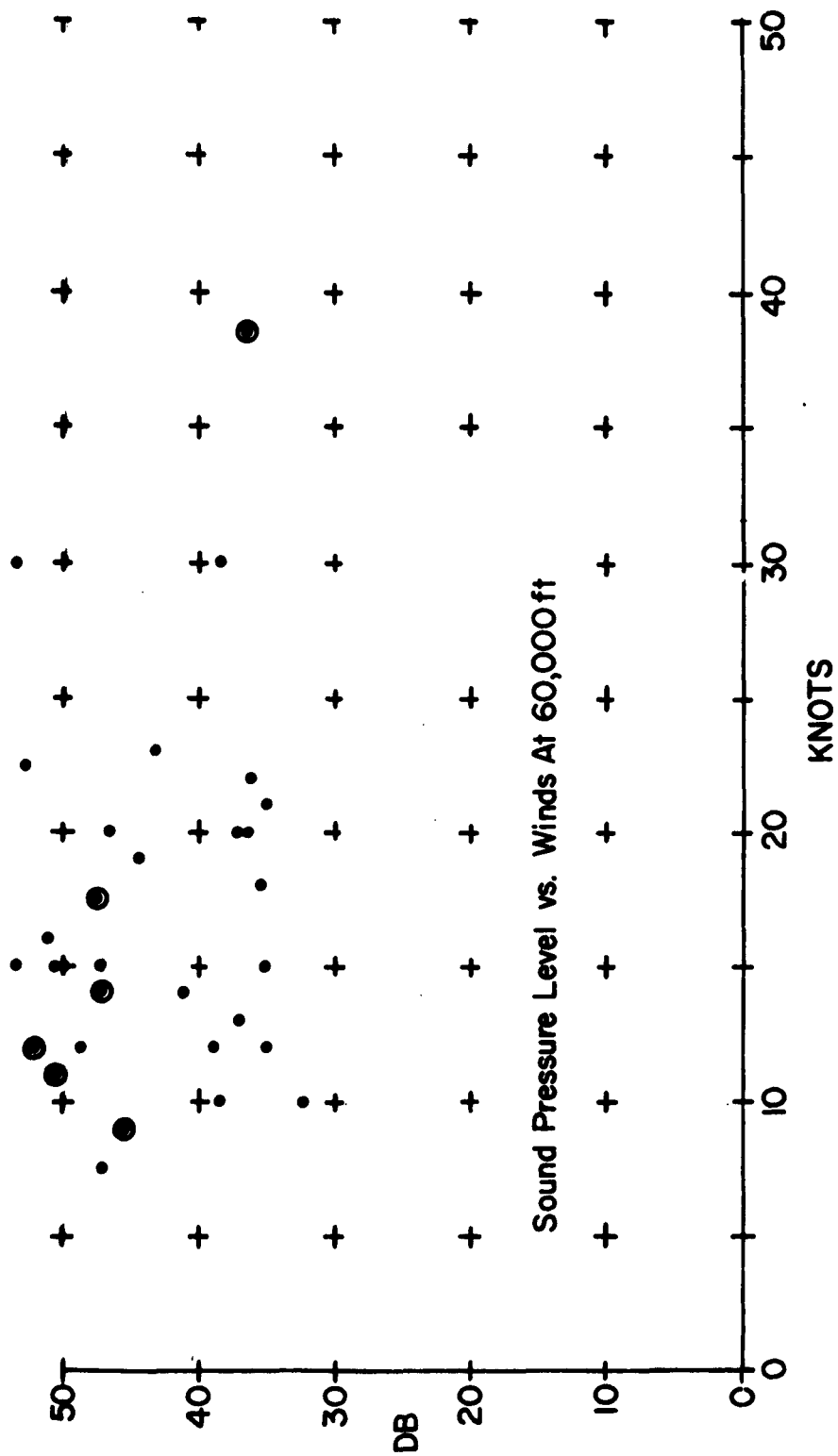
The lack of correlation produced by these efforts, disappointing though it is, may be shown as premature by the use of more sophisticated techniques. The thunderstorm reports available, may, at best, be incomplete. An attack on the problem using more complete data (believed available through the U. S. Weather Bureau) is suggested.

At this point it was felt that contrary to a previous conclusion the difference in noise level might be systemic; a correlation between the noise and the range of the telemetry link might have been possible. The endeavor was made to show this (see Figure 6); and once more, the outcome was negative. However, from the viewpoint of system performance, this result is a happy one.

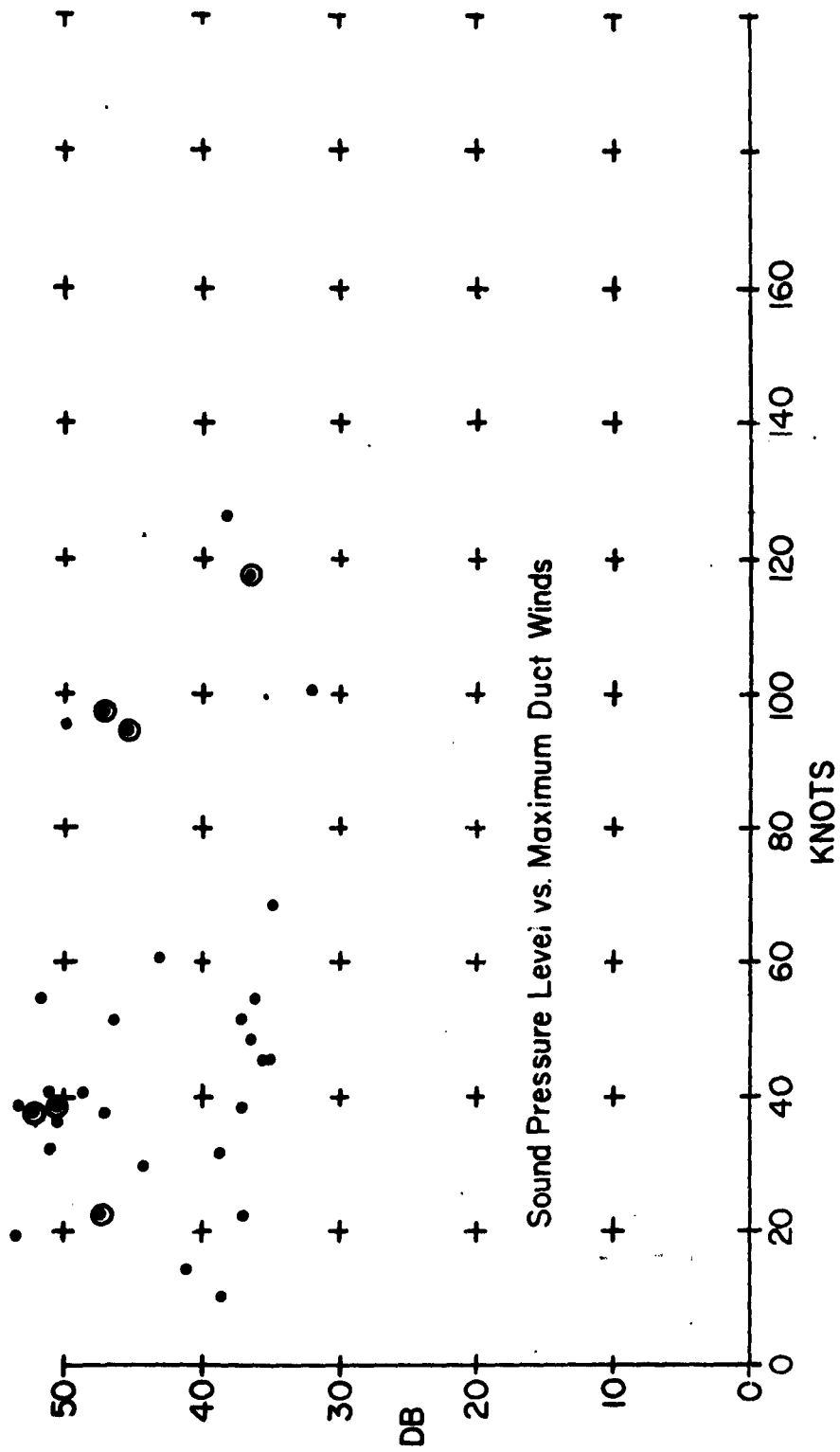
As correlative to increasing confidence in the actual measurements performed, an inspection was made of the data acquired during the same time period for widely separated sensors. In fact, there were several occasions when data was available from balloon-borne microphones separated by 200 to 300 miles for the same half hour period. When the spectra of the output of both sensors is plotted on the same scale, certain similarities in shape are evident. This similarity suggests that the mechanism responsible for the acoustic noise at 62,000 feet may not be a local one, but instead, some gross geophysical phenomena. Some examples of these dual spectra are shown in Figures 7-13.

The time has not been available, unfortunately, to pursue the hypothesis of a ranging effect of great magnitude; however, the hint of such a phenomena is made by these illustrations and should not be dismissed without continued investigation.

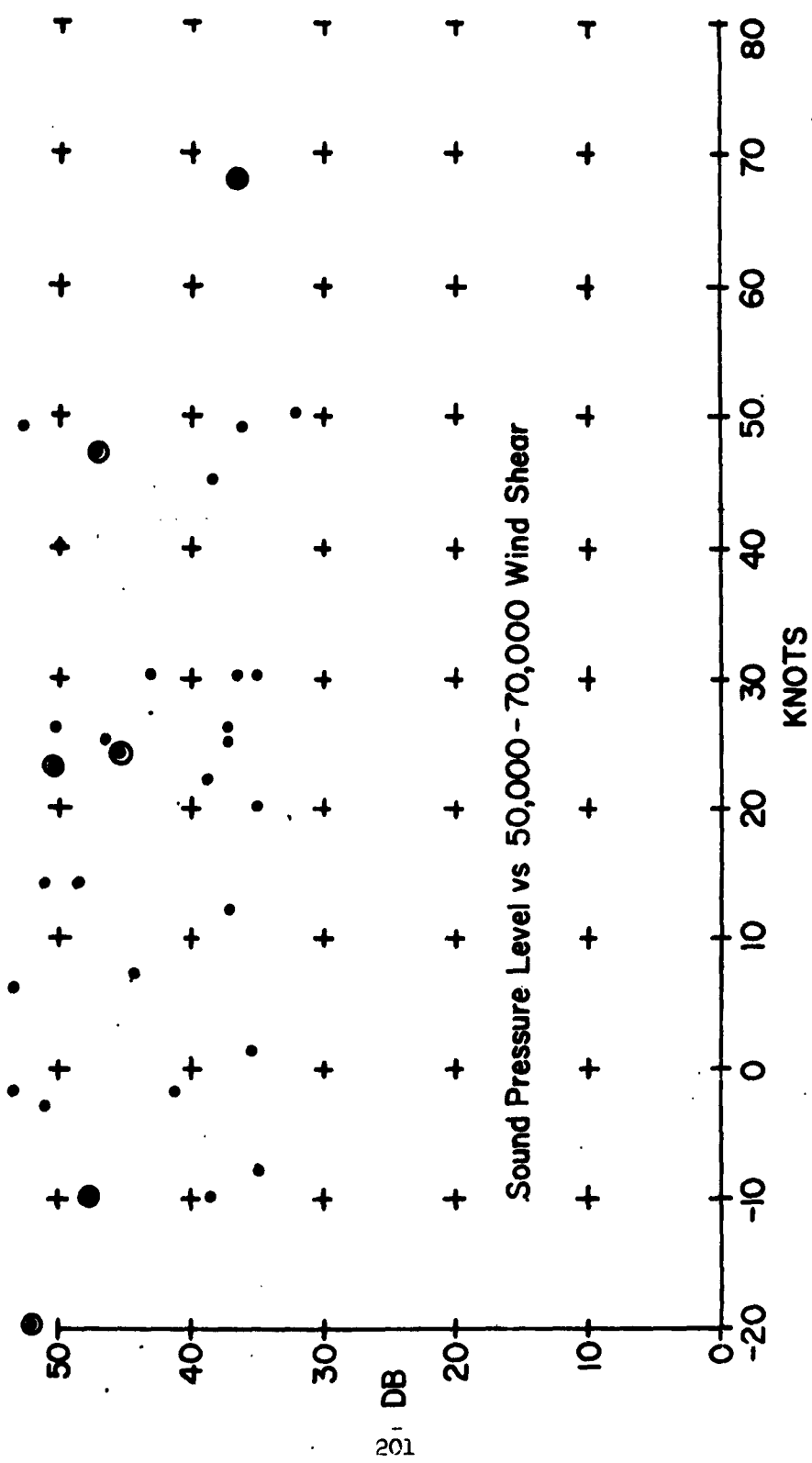
The average sound pressure for the 32 flights was found to be 0.03 dynes/cm² in the band from 0.25 cps to 8.0 cps, corresponding to a sound pressure level of 43.3 db referenced to 0.0002 dynes/cm². The associated standard deviation is ± 6.84 db. The variance of sound pressure level observed was as low as 32.3 db to as high as 53.6 db. This implies a range of pressures of less than 0.01 dynes/cm² in this frequency band.



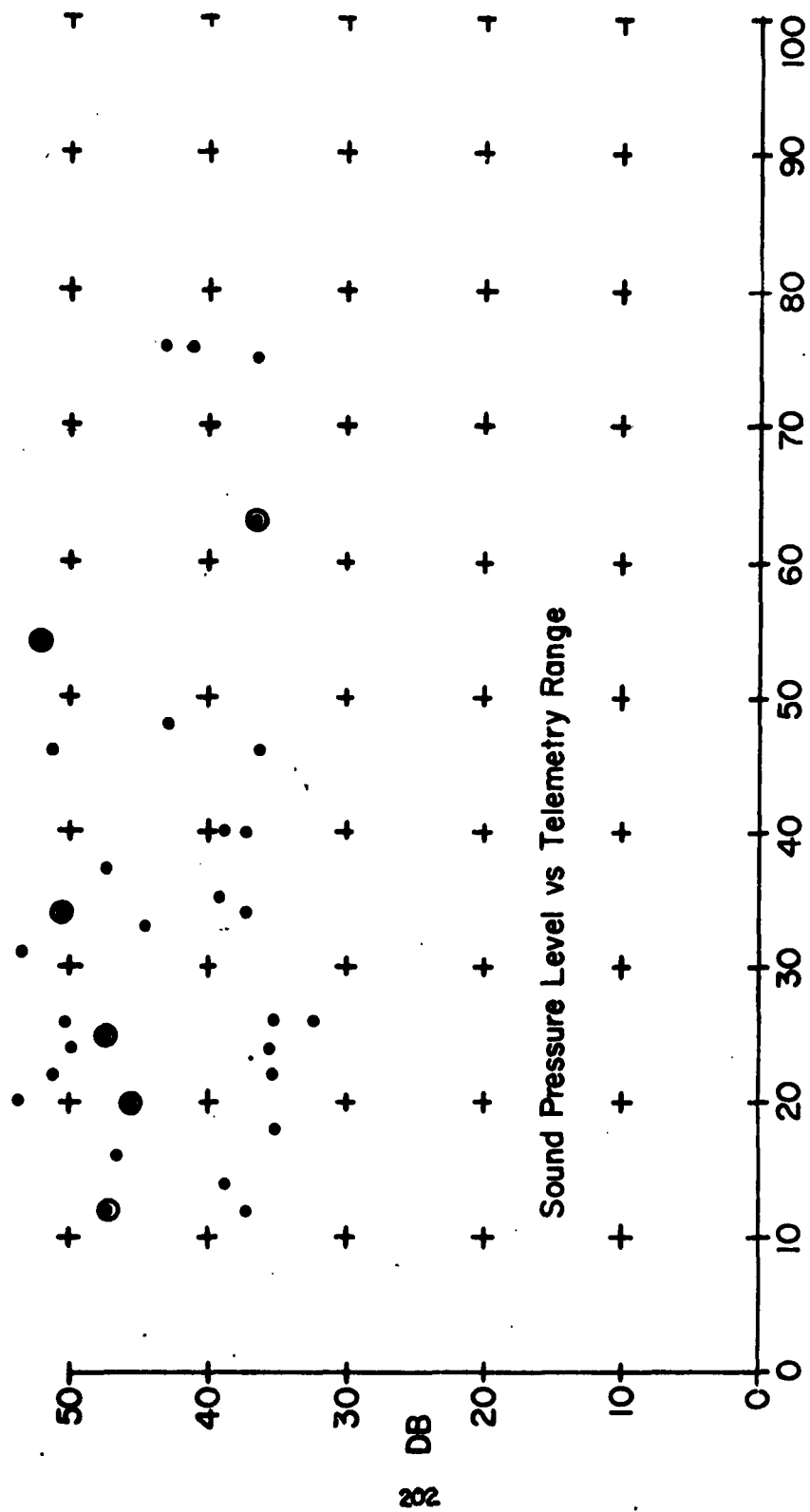
III-10 Figure 3



III-10 Figure 4



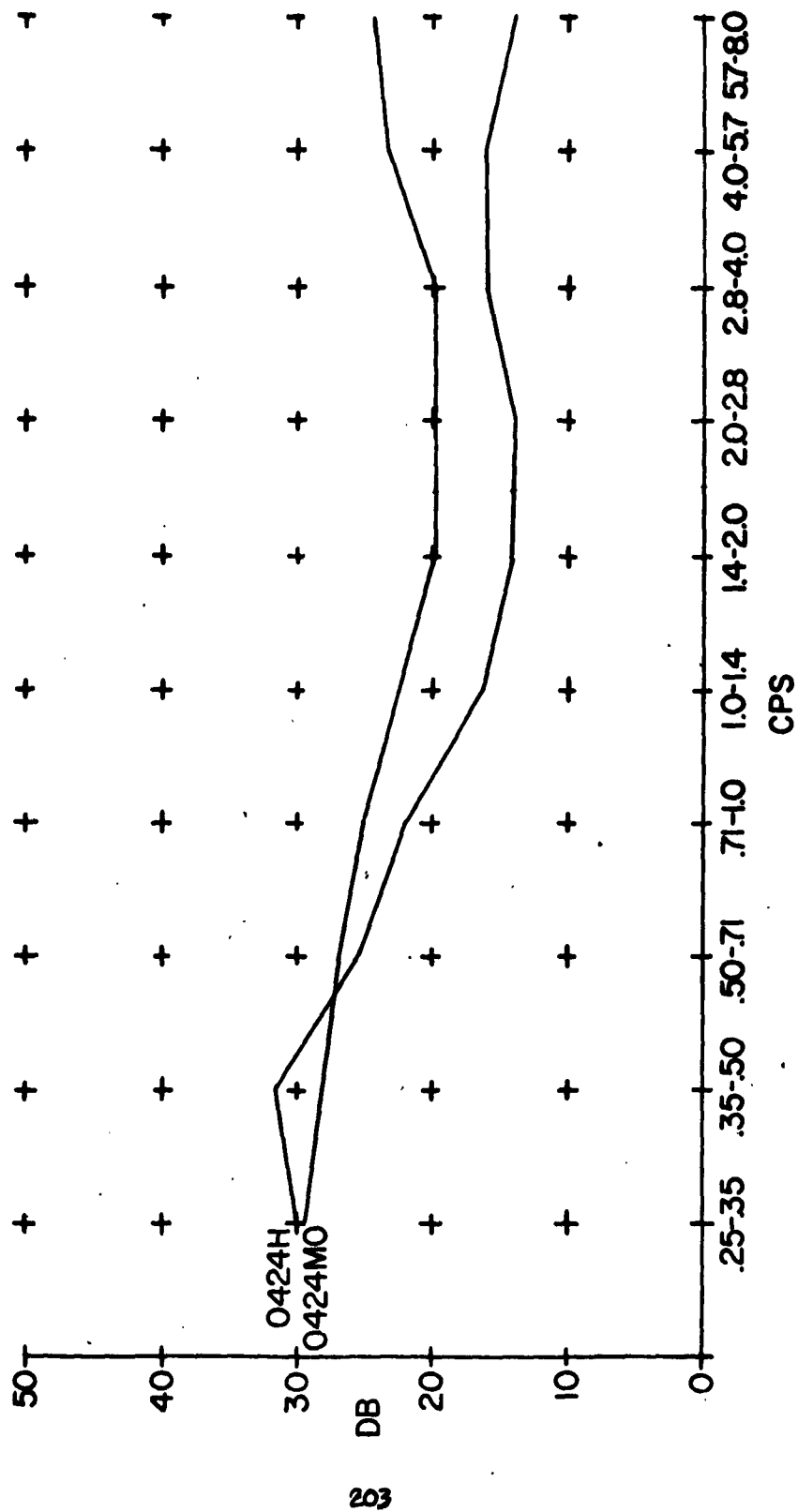
III-10 Figure 5.



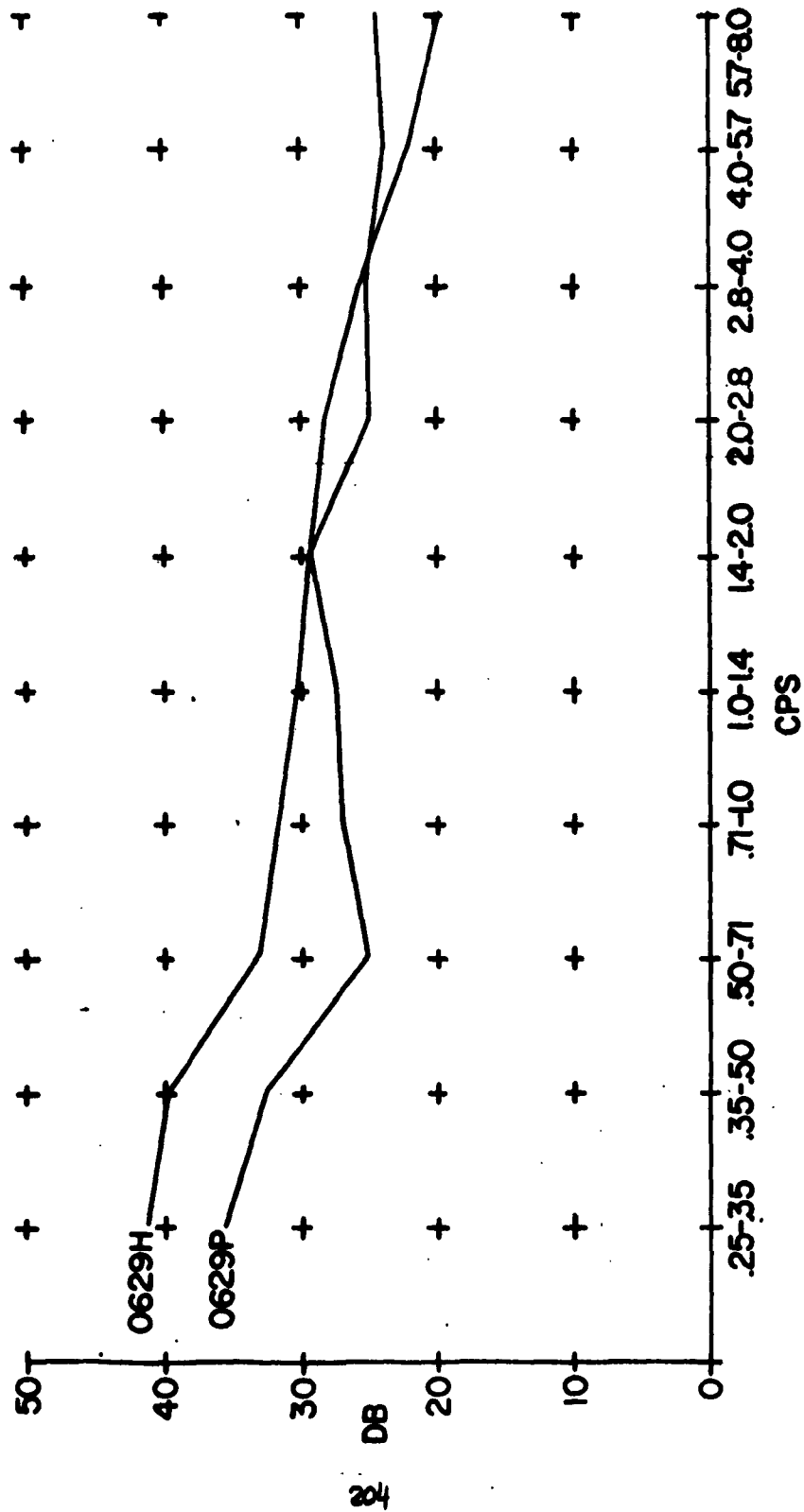
Sound Pressure Level vs Telemetry Range

NAUTICAL MILES

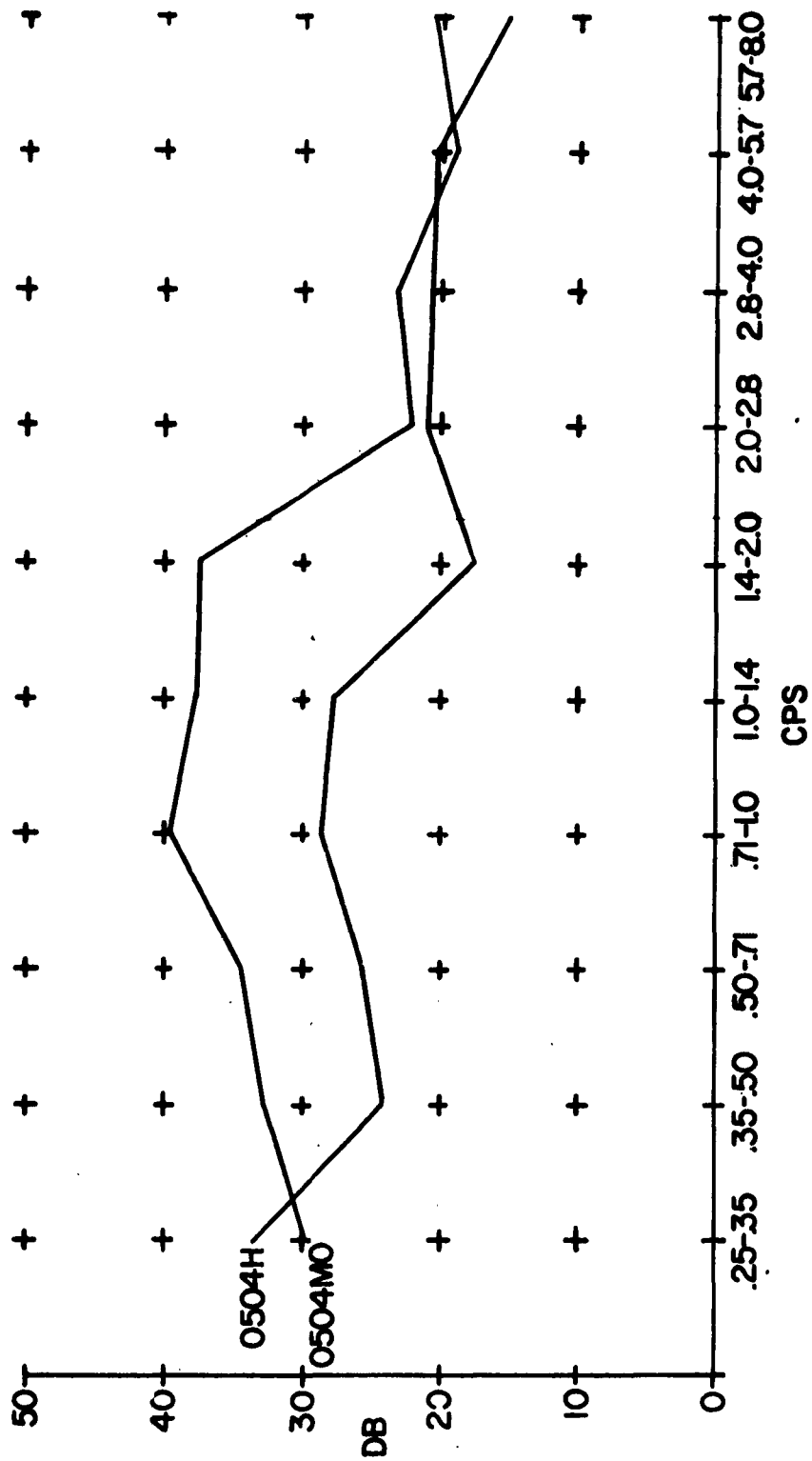
III-10 Figure 6



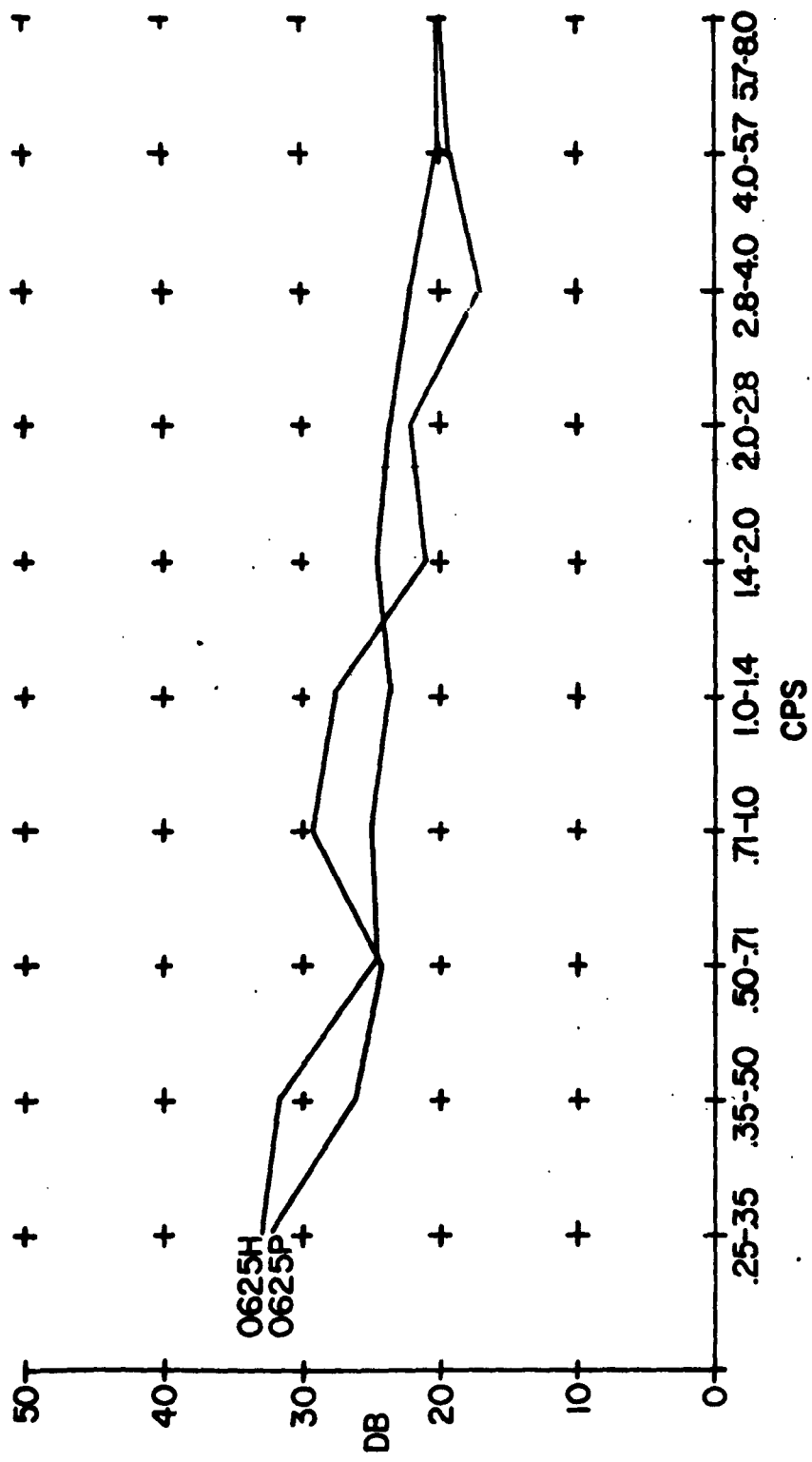
III-10 Figure 7



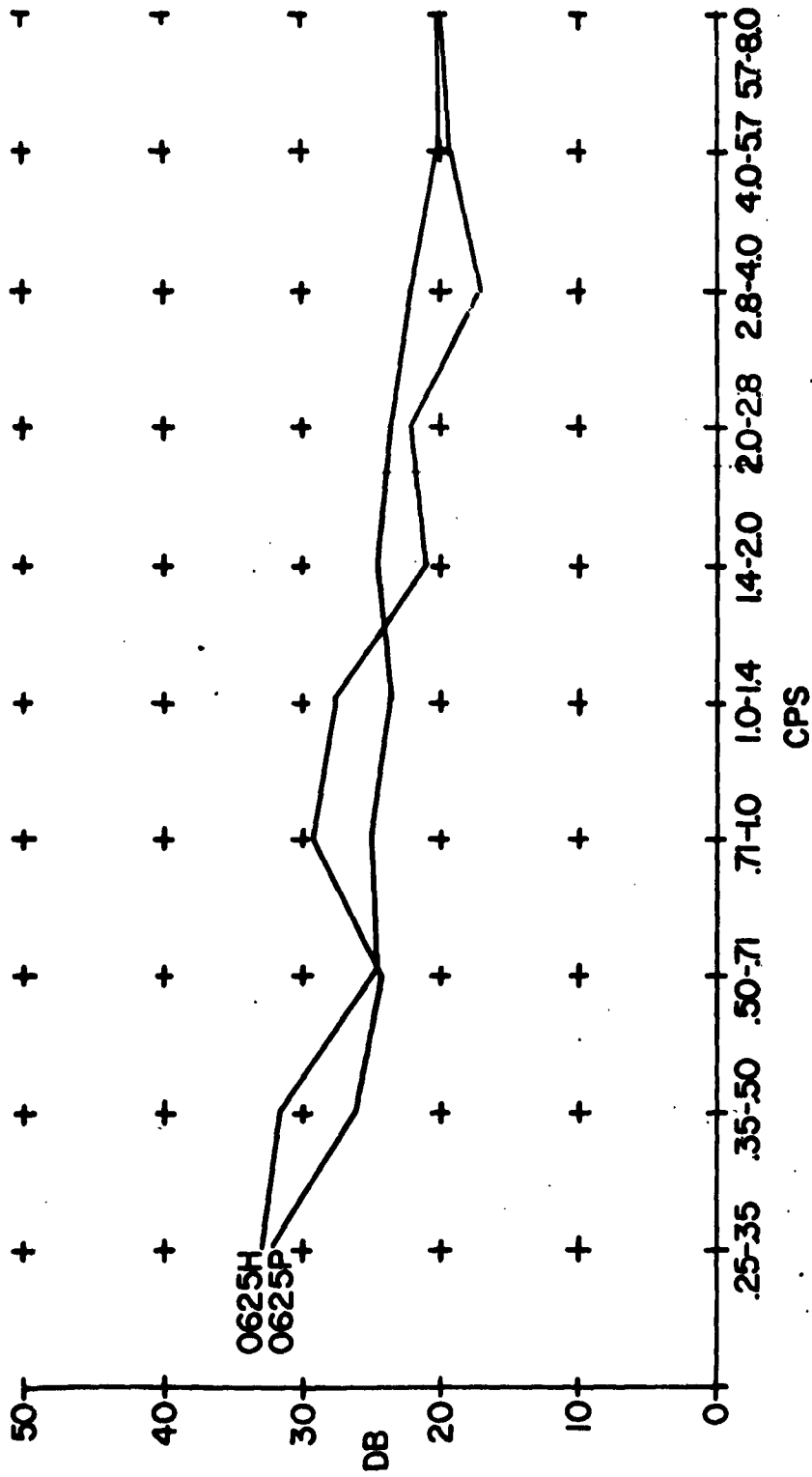
III-10 Figure 8



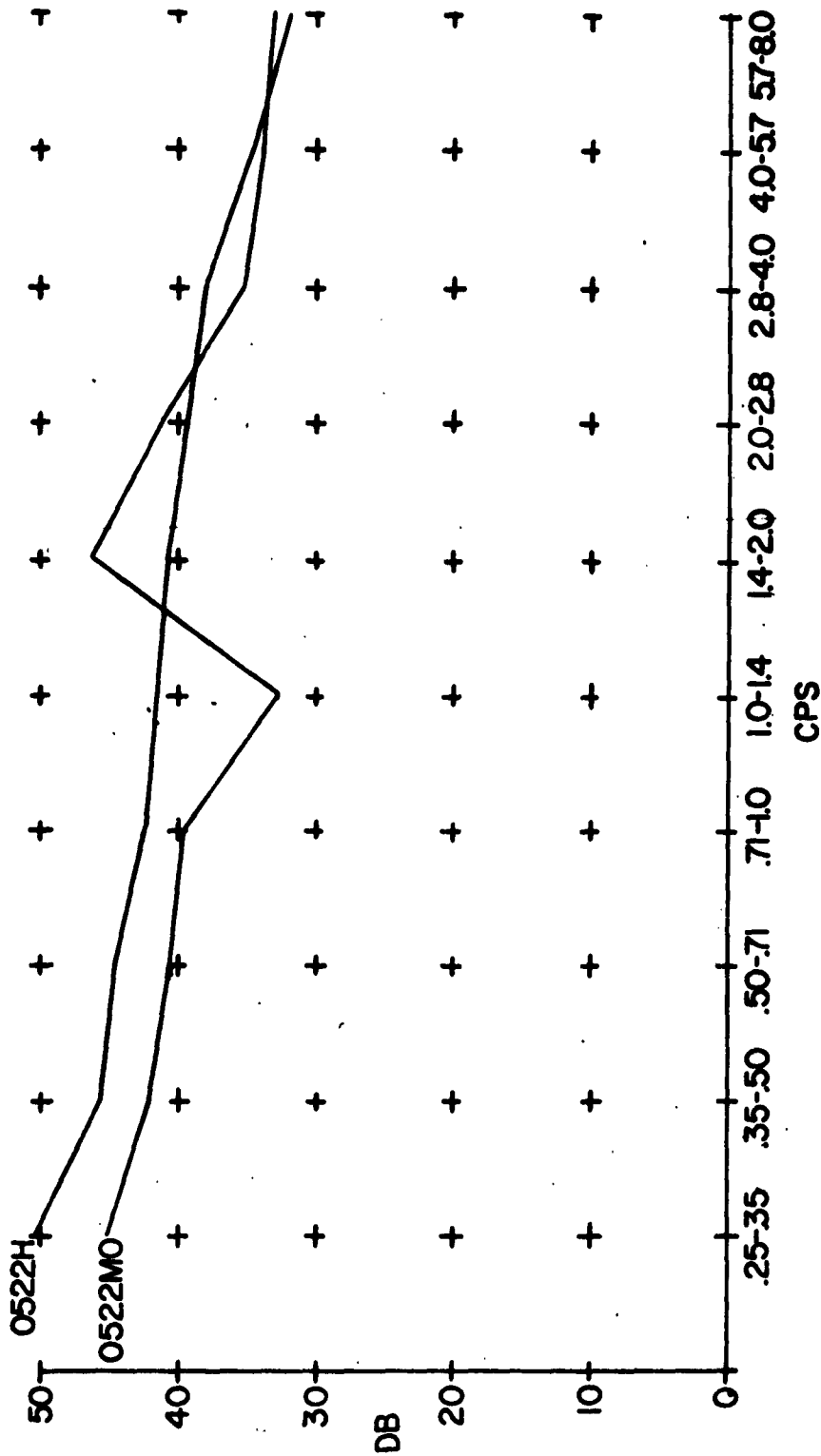
III-10 Figure 9



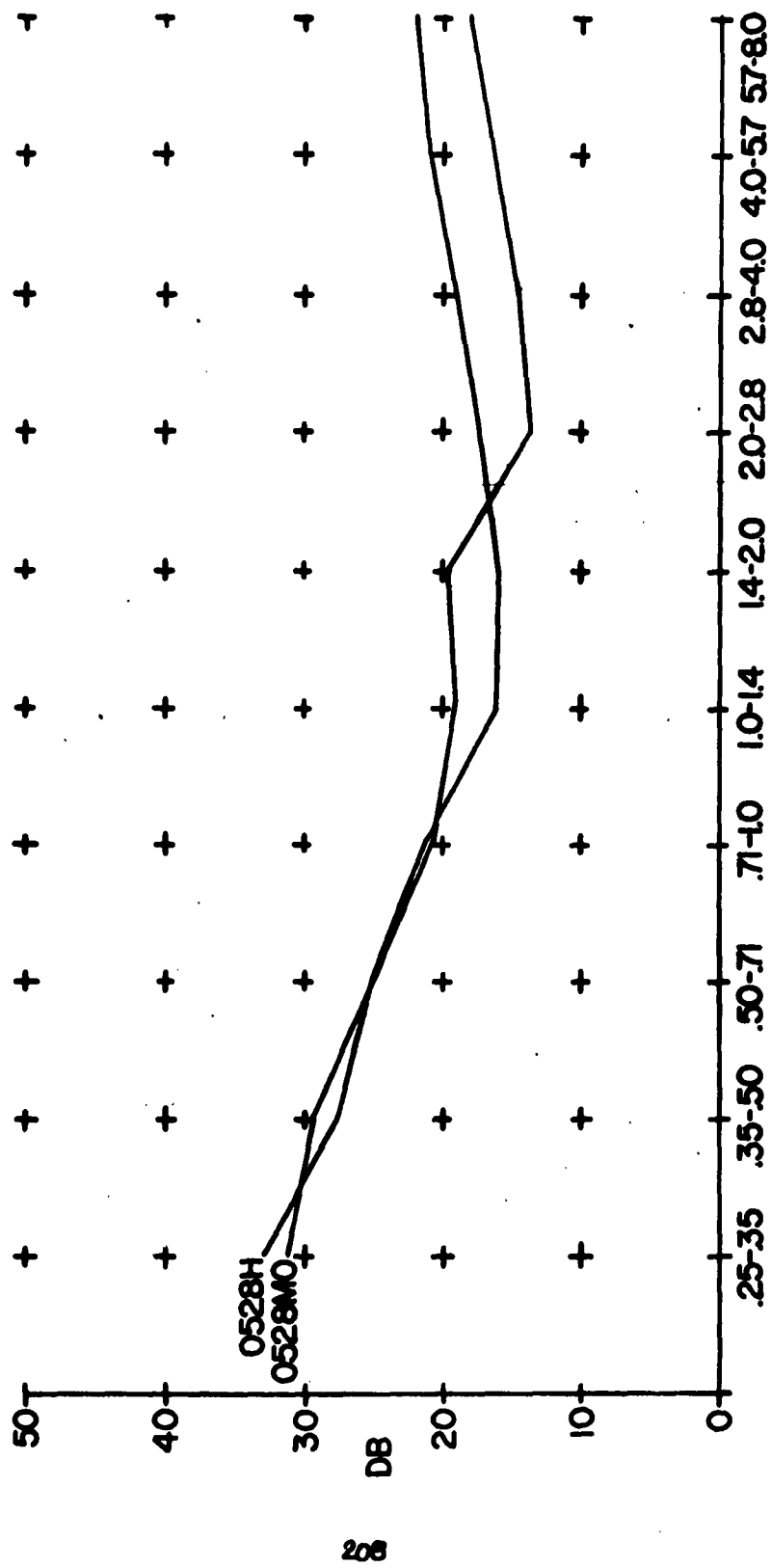
III-10 Figure 10



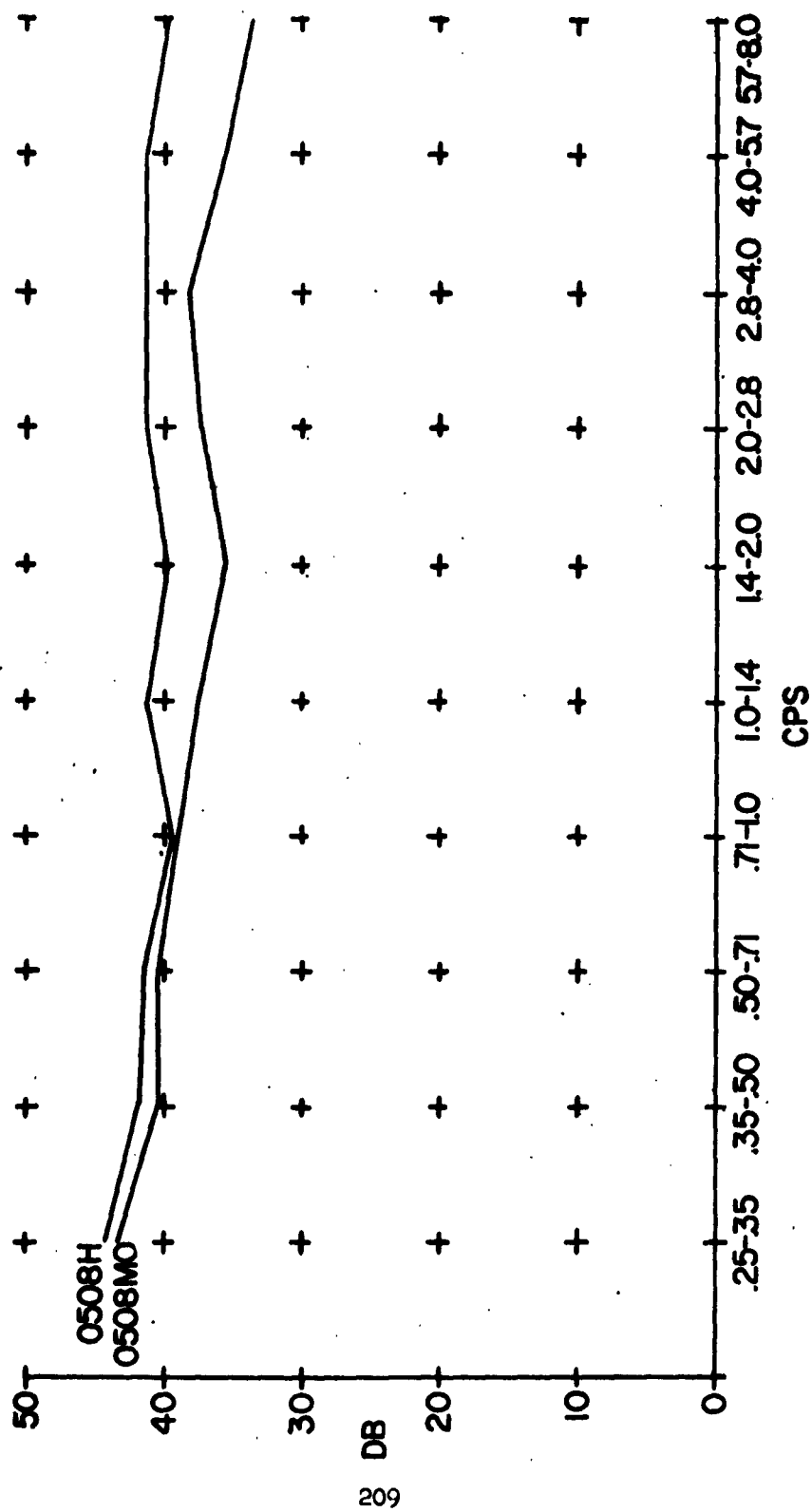
III-10 Figure 10



III-10 Figure 11



III-10 Figure 12



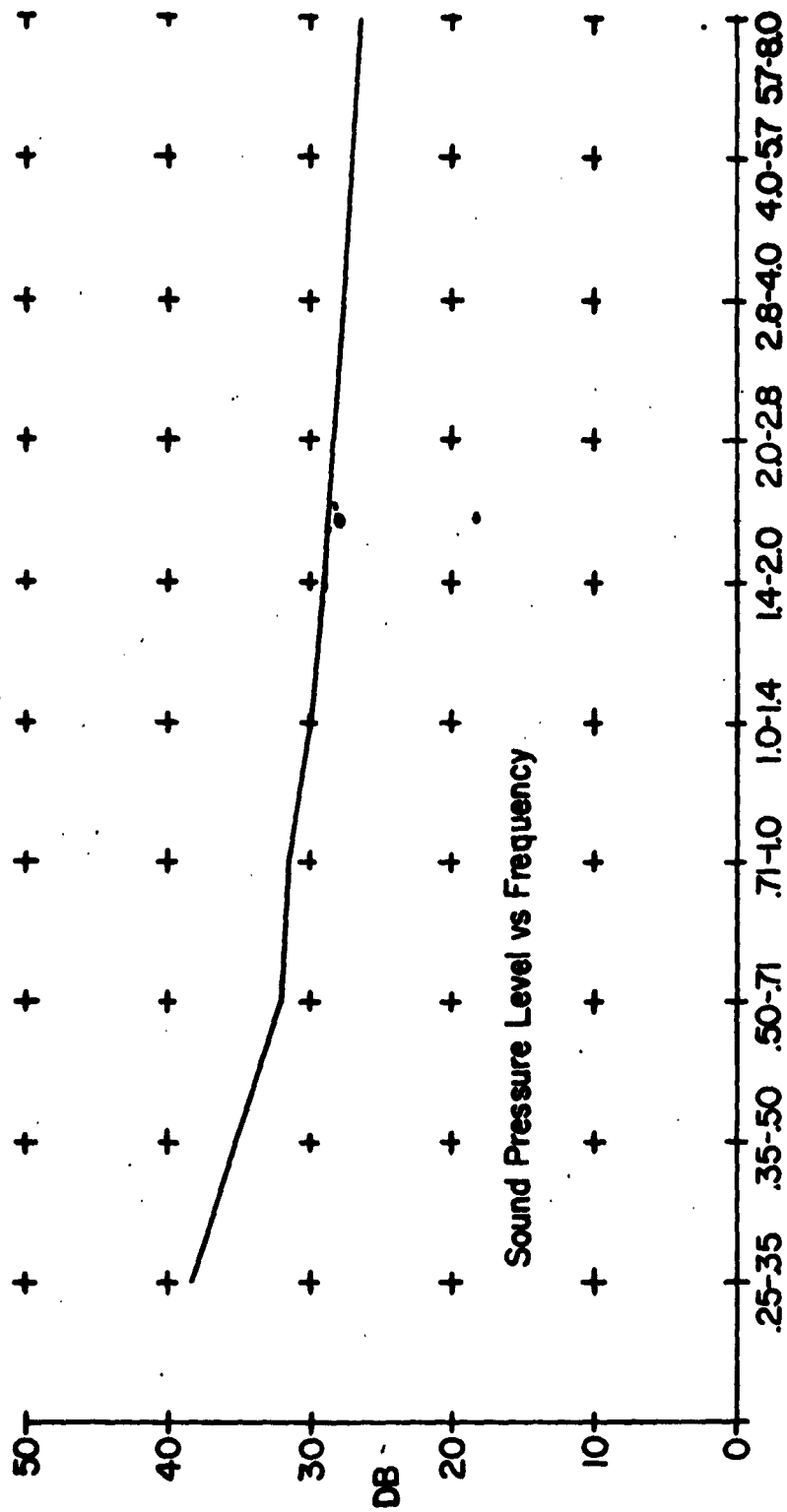
III-10 Figure 13

From an inspection of the noise curves at higher frequencies it seemed a plausible assumption that the noise contained in the next five octaves, namely 8.0 cps to 256 cps, is approximately equal in intensity to that of the five octaves below 8.0 cps. Notice that this would add only 3 db to the average figure given and hence the new average sound pressure for the band between 0.25 cps and 256 cps would be 0.4 dynes/cm².

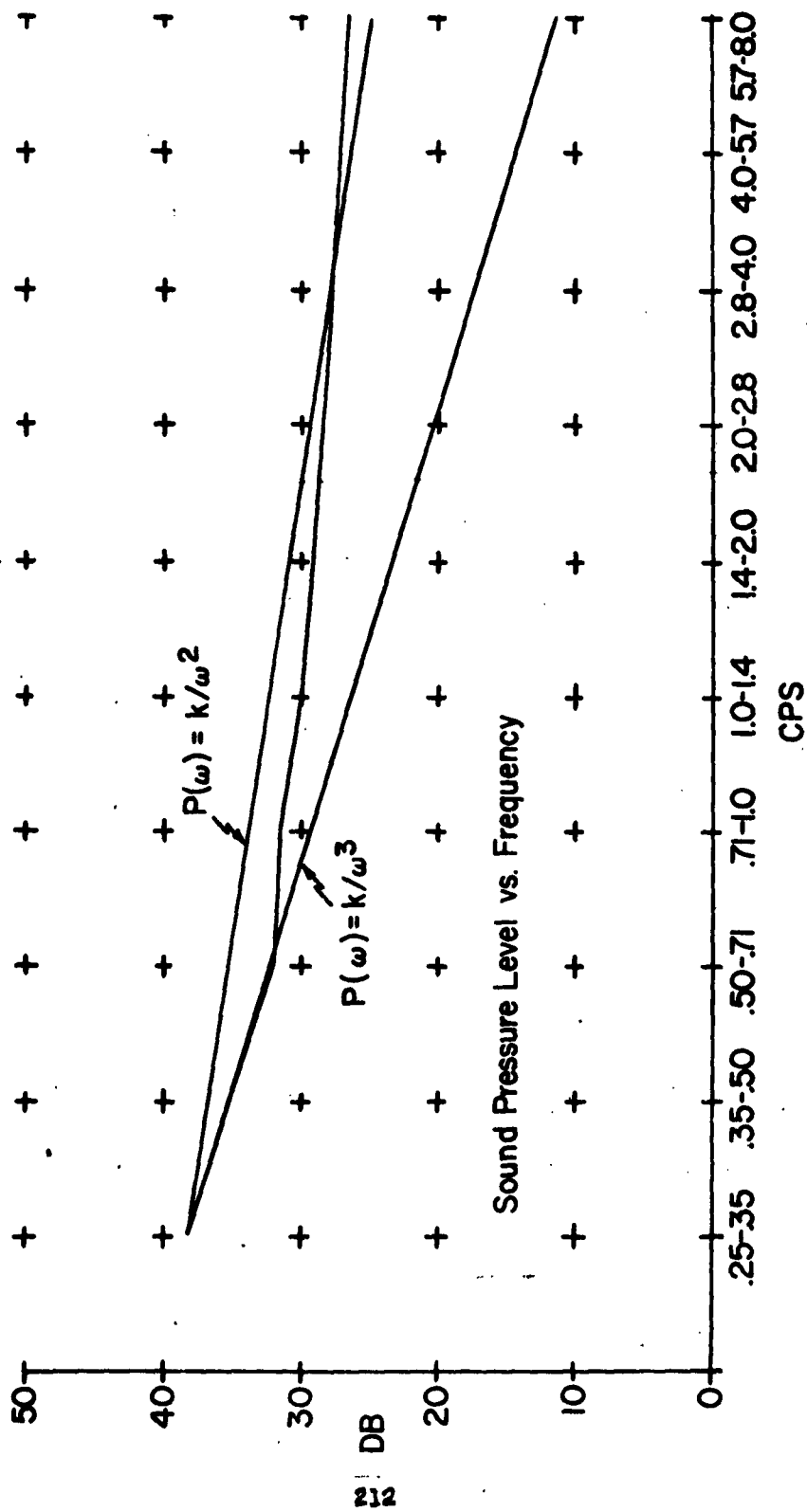
The sound pressure level for each half-octave band was averaged for the 32 flights and the resultant average spectrum is shown in Figure 14.

Of special significance here is the possibility of comparing this average spectrum with the theoretical spectrum developed by the University of Michigan group. Meecham, Westcott, and Jackson, in their paper for the Acoustical Society meeting of October 1960, suggested a power spectrum fall off on the order of $1/w^{3.5}$. Figure 15 shows the average spectrum for these 32 flights, a line corresponding to a $1/w^2$ fall off, and a line corresponding to a $1/w^3$ fall off. As can be seen in the figure, and the average fall off is closer to a $1/w^2$ dependence than that theoretically predicted.

ACKNOWLEDGEMENT: The author expresses his thanks to Rome Air Center, Melpar, Inc., and Bay State Electronics for their cooperation in making the data available for this discussion and for their support in its preparation.



III-10 Figure 14



III-10 Figure 15

PRELIMINARY ANALYSIS OF ACOUSTIC DISTURBANCES

GENERATED BY THE SCOUT ST-1

James F. Bettie

Schellenger Research Laboratories

Texas Western College

El Paso, Texas

BACKGROUND

Schellenger Research Laboratories, under contract to Missile Meteorology Division, White Sands Missile Range, New Mexico, designed and developed an airborne acoustic sensing telemetry system for investigation of atmospheric disturbances in the sub-audio range. This system is called the Pulsonde system and is capable of a flat response to detect disturbances in the range of 0.5 cps to above 50 cps.

This preliminary report is on the Pulsonde operation covering the Scout ST-1 rocket firing of 2 July 1960 at Wallops Island, Virginia. This operation was conducted under contract to Missile Meteorology Division in conjunction with Goddard Space Flight Center of the National Aeronautics and Space Administration at Wallops Island, Virginia.

This report presents only the first few events¹ received by the Wallops Island Pulsonde and is a detailed correlation of received events to those predicted.

CORRELATION

Ideally, the analysis of the Scout operation would be to account for every disturbance received at the Pulsonde during the expected times of arrival of the Scout noise generations. The necessary supporting information was available for this operation and an ideal situation could be approached. Some of the more important goals to be reached in the analysis are: to identify the origin time and location of the received events, to determine the types of sources received (motor and/or ballistic), and to determine the attenuation between event origin and event reception.

The solution of each step is dependent upon the results of each preceding step. Thus far, step one has been partially and successfully completed. That is, most of the events received at the Wallops Island Pulsonde during the first few minutes of reception² have been identified as to origin location and time. Job priority and time have prevented identification of the later events, nor has there been an opportunity to include pressure and frequency content of the received events. This will be presented in a later report.

1

An event is considered any irregular acoustic disturbance received at the Pulsonde.

2

Additional events of some type and origin were detected about 10 minutes after those presented here. As of this date they have shown no relationship to events that might have been generated by the Scout rocket.

BRIEF DESCRIPTION OF TELEMETRY SYSTEM

The Pulsonde³ is a balloon-borne electronic telemetry instrument which operates on the pulse position modulation method. The acoustic detection is by a capacitor microphone which modulates a 3,000 pulse per second sub-carrier which in turn amplitude modulates the 1680 mc RF carrier.

The circuitry of the Pulsonde is an adaptation of the standard radio-sonde so that the transmitted signal may be received by a slightly modified Ground Meteorological Detector (GMD). In addition to the GMD, the ground station consists of timing, communication, and recording facilities.

Acoustic data transmitted from the Pulsonde was recorded on magnetic tape using a multi-channel Precision Instrument tape recorder.

Essential information for successful operation and analysis on the Scout was: upper winds from surface to 70,000 feet for pre-setting of the constant level balloon; azimuth and elevation of Pulsonde during event arrivals for Pulsonde position determination; time of day to one second accuracy to correlate events; sound propagation profiles from surface to 400,000 feet MSL and complete rocket performance data.

ROCKET PERFORMANCE

The Scout ST-1 was a four-stage, 17 ton rocket. T-Zero for the 2 July 1960 firing was 0003:54 ZULU. The performance was satisfactory and very nearly that predicted prior to flight. The planned destination was 4,700 miles from the launch site, but because the rocket "appeared" to veer off course after 120 seconds of flight the range safety officer ordered that the fourth-stage should not fire. As a result the Scout impacted some 1,500 miles off the coast of Virginia after an otherwise well predicted trajectory.

The trajectory of the rocket with respect to the Wallops Island Pulsonde is shown in Figure 2. Other rocket performance data is shown in Figures 3 and 4.

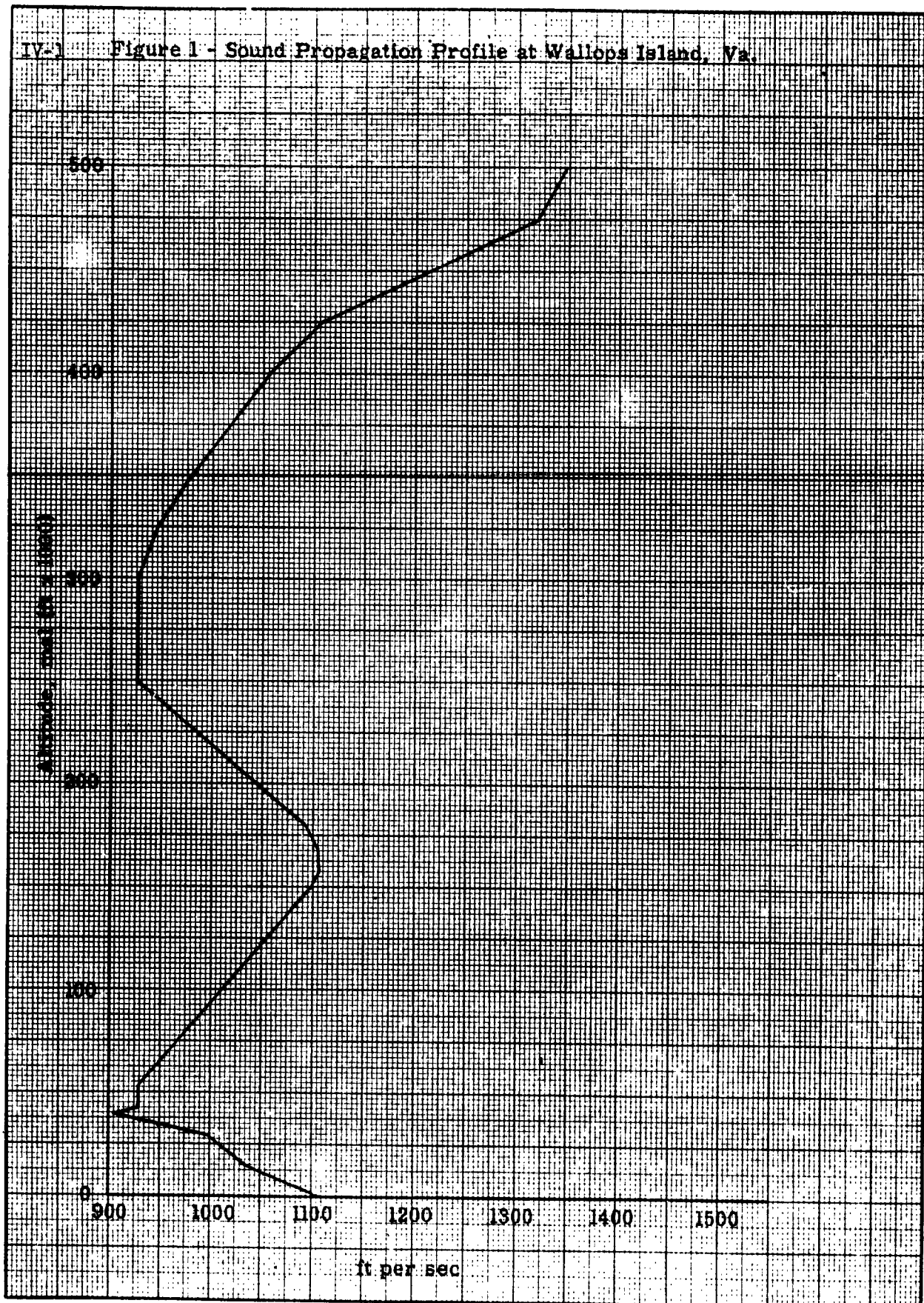
ANALYSIS AND RESULTS

In predicting the event arrivals, the rocket trajectory (Figure 2), sound profile (Figure 1), Rocket-Pulsonde separation distances (Figure 4), and rocket performance of the first, second, and third stages had to be known. The Langley Research Center of the National Aeronautics and Space Administration provided the necessary rocket information while the meteorological support group at Wallops Island supplied the weather data from which the lower portion (surface to 100,000 feet) of the sound propagation profile was calculated. The sound propagation above 100,000 feet was taken from the ARDC (1959) standard atmosphere model. These profiles are shown in Figure 1.

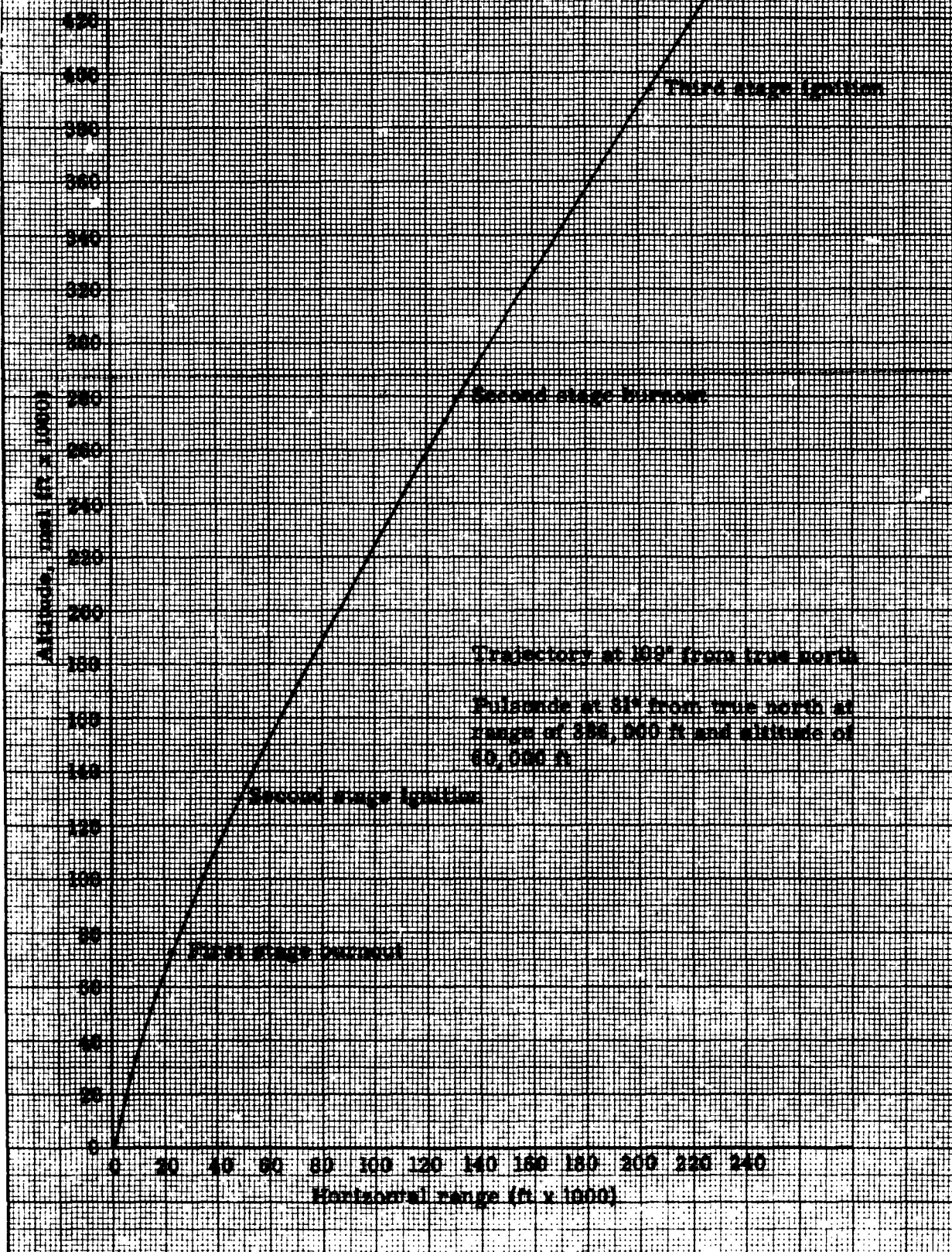
3

Fugate, Francis L., PULSONDE ACOUSTICAL SENSING DEVICE, Schellenger Research Laboratories, El Paso, Texas, April 1960.

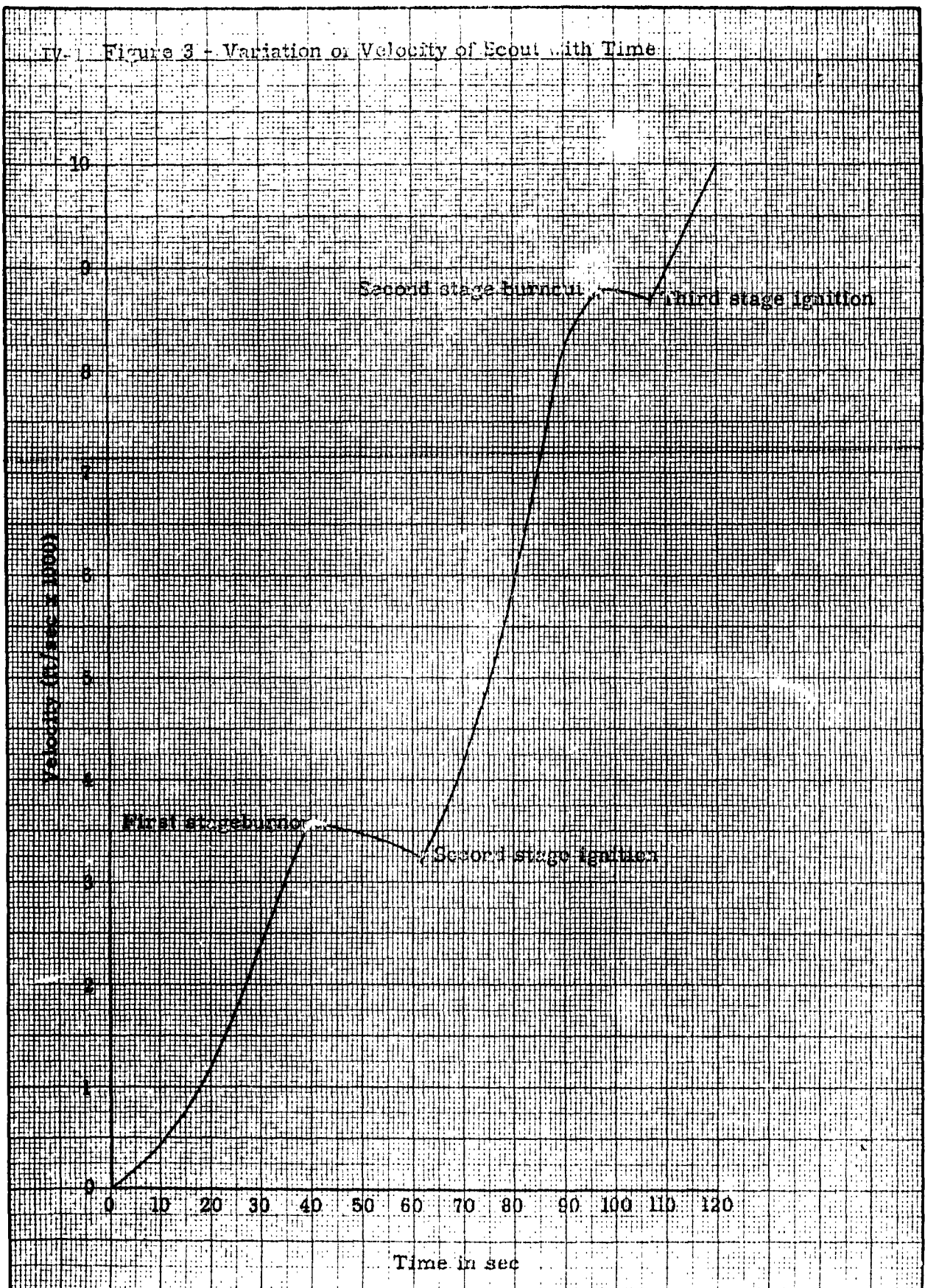
IV-3 Figure 1 - Sound Propagation Profile at Wallops Island, Va.

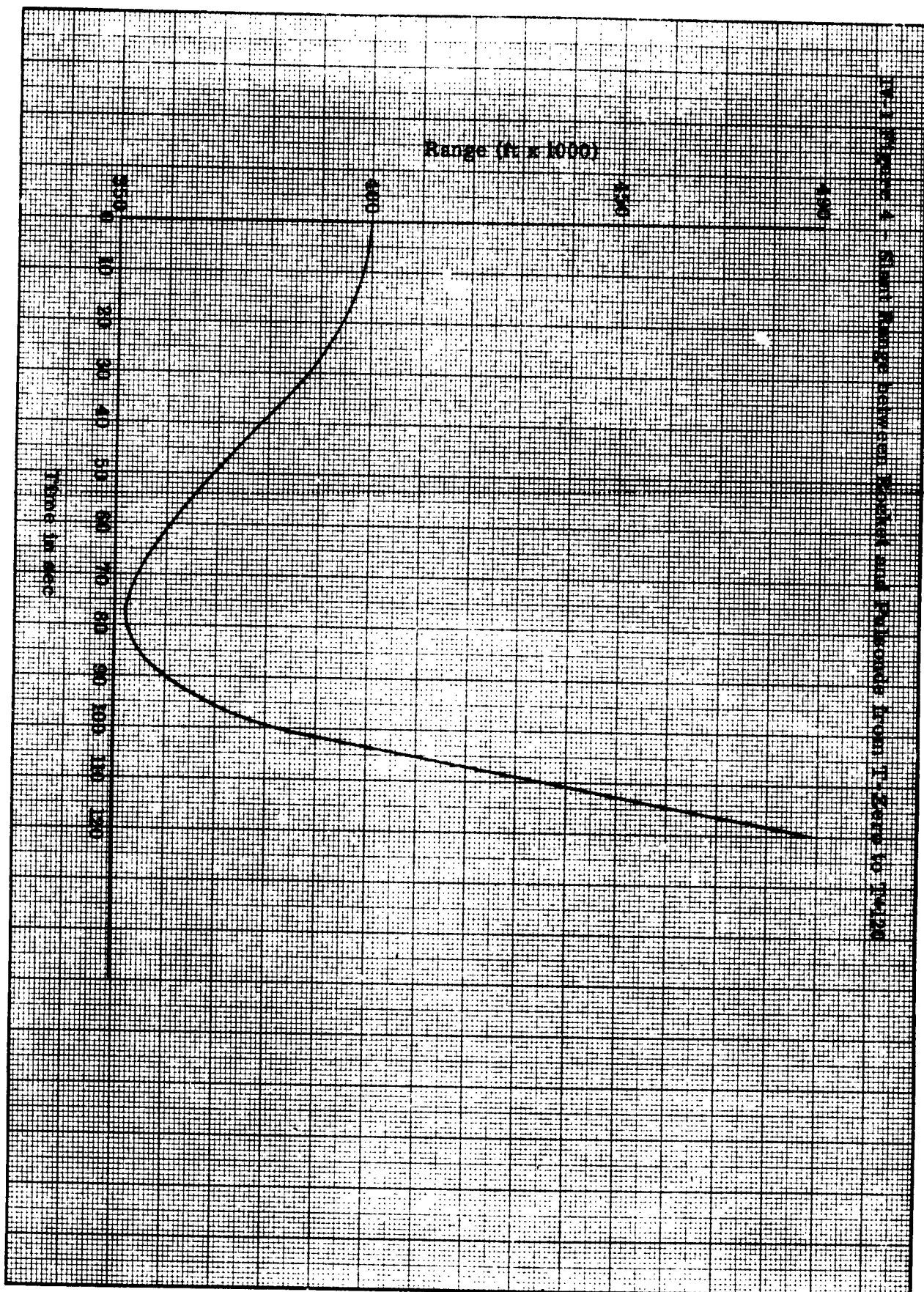


IV-1 Figure 2 - First 120 Seconds of Horizontal Range and Altitude of Scout



IV. Figure 3 - Variation of Velocity of Scout with Time





From all the combined data of the atmosphere and rocket-Pulsonde position in space, a mathematical model was constructed to determine the paths of sound from the rocket to the Pulsonde. Each succeeding second after T-Zero was considered as a new sound source along the rocket trajectory. Therefore, 120 sources of rocket motor noise were possible during the first 120 seconds of flight. However, no motor noise would occur between the burnout and ignition of various stages which were during the intervals of T + 44 seconds to T + 62 seconds (between first and second stages), and T + 98 seconds to T + 107 seconds (between second and third stages). There then remained 101 events to ray trace.

Rocket velocity and atmosphere data indicate ballistic waves should have begun forming at T + 13 seconds (Figure 3). This effect, although an important one, has not been considered in this preliminary analysis because a suitable mathematical model has not been prepared as of this writing.

The atmosphere from the surface to 400,000 feet MSL was divided into 18 sound propagation layers based upon regions of constant temperature gradient. For each second of rocket flight under consideration an average speed of sound was calculated along a straight line path between the rocket position and the Pulsonde position. From this speed of sound and the straight line distance, ray arrival times were predicted.

The possibilities of sound refraction and absorption along these paths were not considered. This was practically impossible in that the angle at which the events arrived at the Pulsonde could not be determined to facilitate ray tracing back to the source origin.⁴ Thus, the rays traced were from the source positions to the Pulsonde and along a straight line path with varying sound velocities.

Table 1 tabulates the resulting arrival times at the Pulsonde for 101 event origins. It will be noted that in many cases, especially during the first 90 seconds after T-Zero, there are events predicted to arrive simultaneously even though all have different origin times. It should be obvious from the rocket trajectory (Figures 2 and 4) and the sound propagation (Figure 1) between the rocket and Pulsonde that this is quite possible.

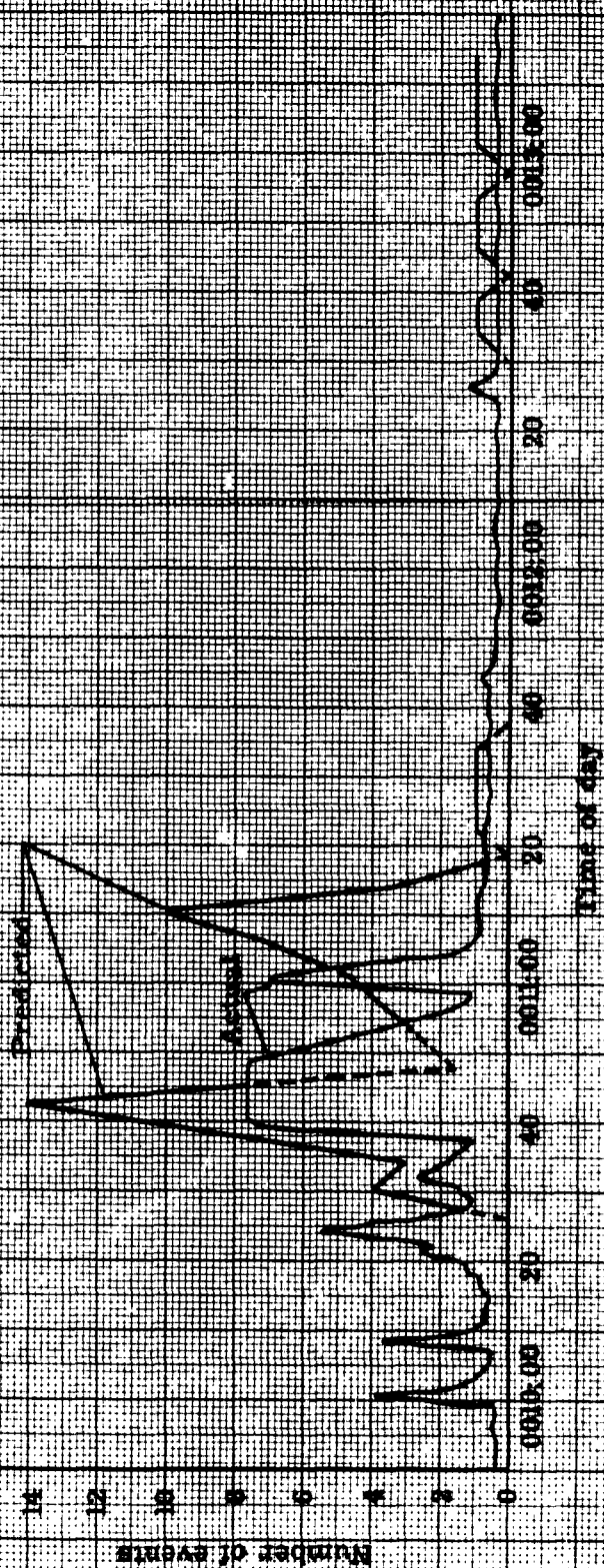
Figure 5 shows the envelopes that represent the number of events predicted to arrive to those that were actually received. The amplitudes of the two are independent since the actual events shown are DC amplitude as a function of time and were obtained from an infrasonic analyzer with a wide band amplifier (.01-1000 cps) and rectifier system with 1.0 second smoothing. The arrivals at about 0010:40 ZULU were of larger

⁴
Barnes, T. G., VELOCITY GRADIENT METHOD OF RAY TRACING IN THE ATMOSPHERE, Schellenger Research Laboratories, El Paso, Texas, August 1956.

IV-1 TABLE I			
Origin Time after T-Zero with Corresponding Predicted Arrival Times at Pulsonde			
Origin Time after T-Zero (sec)		Predicted Arrival Time (min and sec after 0000 Z)	
1		10:29-32	
2			
3			
4			
5		10:33-36	
6			
7			
8	73	10:37-40	
9	74		
10	75		
	76		
	77		
	78		
11	66	10:41-44	
12	67		
13	68		
	69		
	70		
	71		
	72		
14	63	10:45-48	
15	64		
	65		
16		10:49-52	
17			
18			
19		10:53-56	
20			
21		10:57-11:00	
22			
23			
24			
25	42	11:01-04	
	43		
26	38	11:05-08	
27	39		
	40		
	41		

IV-1 TABLE I (Continued)		
Origin Time after T-Zero (sec)		Predicted Arrival Time (min and sec after 0000 Z)
28	32	11:09-12
29	33	
	34	
	35	
	36	
	37	
30		11:13-16
31		
None		11:17-20
	94	11:21-24
	95	11:25-28
	96	11:29-32
	97	11:33-36
	108	12:29-32
	109	12:33-36
	110	12:37-40
None		12:41-44
	111	12:45-48
	112	12:49-52
	113	12:53-56
None		12:57-13:00
	114	13:01-04
	115	13:05-08
	116	13:09-12
	117	13:13-16
None		13:17-20
	118	13:21-24
	119	13:25-28
	120	13:29-32

Figure 8 - Predicted Events Compared to Actual Events



amplitude than those shown since the signal was of sufficient amplitude to block the Pulsonde. This blocked portion is believed to be that which corresponds to events originating closest to the Pulsonde as emphasized above. The first two peaks that appear are unaccounted for. They are presently believed to be shock waves and may be determined by future analysis.

CONCLUSIONS

It is always difficult to draw conclusions on only one experimental operation of this nature. The results, however, appear convincing enough to say that the correlation of the events are more than just coincidence.

Further investigations are being conducted at this time to fully confirm these results. Analysis of other operations of a similar nature (Pulsonde near the trajectory of a large rocket or missile) are expected to strengthen these examples.

The mathematical solution to the above analysis will be explained in a final report.

SOUND TRANSMISSION LOSS FOR NEAR-VERTICAL ATMOSPHERIC PROPAGATION*

E. Alan Dean

Schellenger Research Laboratories
Texas Western College

In the analysis of the signal amplitude received from upper atmospheric detonations as part of the rocket-grenade experiment, two facts became apparent:

1) It is impossible to receive signals from above about 95 kilometers, which qualitatively support Schrodinger's ** work based on classical absorption. The pressure of about a micron of mercury at this altitude increases the frequency-to-pressure ratio to 5 megacycles / atm, causing large absorption, even though the frequency is only 5 cps.

2) The amplitude vs. altitude function is not monotonically decreasing, and there is correlation between amplitude and temperature, suggesting refractive focusing.

In order to check this theory, calculations have been made for the transmission loss for near-vertical atmospheric propagation, and these calculations have been compared to the observed amplitudes. Although not fully analyzed, the results thus far have been inconclusive. The large spread of the data is consistent with other atmospheric propagation studies, although it was thought that less spread should result, since accurate meteorological data are obtained from the rocket-grenade experiment itself, and there is no reflection problem as with ground level measurements.

Thus far, only paper tape reproductions of the signals have been available. In the future, we hope to have magnetic tapes, which will allow transmission loss vs. frequency to be studied, thus improving the analysis.

In theory, the transmission loss has been divided into two forms, absorption losses, and losses due to divergence and refraction. The absorption loss does not consider the vibrational absorption, as the humidity is not known. The losses included are those due to viscosity, thermal conduction, and rotational relaxation, and as such, are about 35% greater than the classical absorption and used by Schrodinger. The empirical formula for the absorption coefficient used was

$$\alpha = \frac{3.32 \times 10^{-6} f^2 T}{P (T + 233)} ,$$

where P = ambient pressure in N/m^2 , f = frequency in cps, and T = temperature in $^{\circ}K$. One would expect this to be a minimum absorption and that there would be excess absorption due to vibrational rotation. After integration in a constant temperature layer having a sound speed c , height h , and

* Supported by National Aeronautic and Space Administration, contract NAS 5-556.

** E. Schrodinger. 1917. Zur Akustik der Atmosphere. Physik. Zeit. 18:445.

ray elevation angle ϵ , the absorption loss when summed over several layers, becomes

$$L_a = 8.686 \sum \frac{h_1 \alpha_1 \sinh X_1}{X_1 e^{X_1} \sin \epsilon_1},$$

where $X_1 = \gamma g_1 h_1 / 2c_1^2$.

The derivation of the divergent and refractive loss can be obtained with the help of Figure 1. Consider a source S at the top of layer s. Let dW be the power radiated by the source within the ray bundle defined by the differential pyramid having vertex angles of $d\epsilon_s$. The component of the intensity normal to the wave front at any point on the ray will be

$$I_n = \frac{dW}{dS}$$

where dS is the base area normal to the ray. Suppose the plane of Figure 1 is the azimuth plane of the ray, then the side of dS which is parallel to this plane at various boundaries is represented by AC, BE, etc. Let this side be denoted by dx, a function of height, z. At the boundary between layers s and s-1, this distance is

$$dx_s = \frac{h_s d\epsilon_s}{\sin \epsilon_s},$$

where ϵ_s is the elevation angle of the ray as it leaves the source, and h_s is the height of layer s.

To find dx_{s-1} , or BE, construct CD parallel to the refracted ray AB. But ray SC is refracted so that it takes the path CE. It follows that angle DCE is the change in refracted angle due to the change in incident angle $d\epsilon_s$. Then

$$dx_{s-1} = BD + \frac{h_{s-1} d\epsilon_{s-1}}{\sin \epsilon_{s-1}},$$

where $d\epsilon_{s-1}$ = angle DCE. Referring to the insert, and neglecting the fact that CD' is not parallel to SA (this difference for triangle ACD' is of second order in $d\epsilon$), one has

$$AC = AD' \sin \epsilon_s$$

and

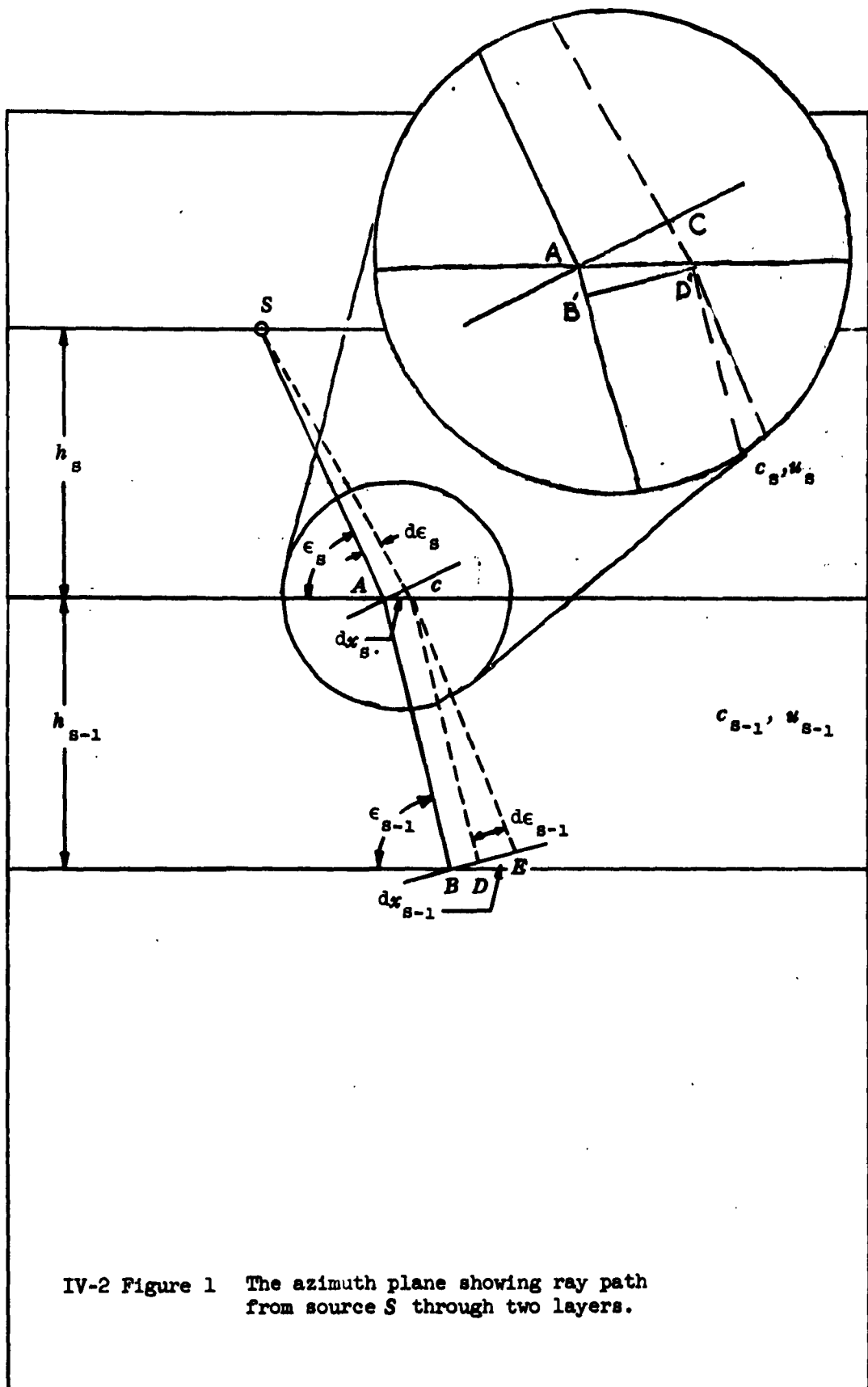
$$BD' = BD = AD' \sin \epsilon_{s-1},$$

so that

$$\frac{BD}{AC} = \frac{\sin \epsilon_{s-1}}{\sin \epsilon_s},$$

yielding

$$dx_{s-1} = \frac{\sin \epsilon_{s-1}}{\sin \epsilon_s} \cdot \frac{h_s d\epsilon_s}{\sin \epsilon_s} + \frac{h_{s-1} d\epsilon_{s-1}}{\sin \epsilon_{s-1}}.$$



IV-2 Figure 1 The azimuth plane showing ray path from source S through two layers.

Likewise,

$$dx_{s-2} = \frac{\sin \epsilon_{s-2}}{\sin \epsilon_{s-1}} \left(\frac{\sin \epsilon_{s-1}}{\sin \epsilon_s} \cdot \frac{h_s d\epsilon_s}{\sin \epsilon_s} + \frac{h_{s-1} d\epsilon_{s-1}}{\sin \epsilon_{s-1}} \right) + \frac{h_{s-2} d\epsilon_{s-2}}{\sin \epsilon_{s-2}},$$

which may be generalized to:

$$dx_{s-n} = \sin \epsilon_{s-n} d\epsilon_s \sum_{i=s-n}^s \frac{h_i}{\sin^2 \epsilon_i} \cdot \frac{d\epsilon_i}{d\epsilon_s}.$$

The value of the derivative $d\epsilon_i/d\epsilon_s$ may be obtained from the differentiation of Snell's law: this results in

$$\frac{d\epsilon_i}{d\epsilon_s} = \frac{c_s \sin \epsilon_s \cos^2 \epsilon_i}{c_i \sin \epsilon_i \cos^2 \epsilon_s},$$

and substitution yields

$$dx_{s-n} = \frac{c_s \sin \epsilon_{s-n} \sin \epsilon_s d\epsilon_s}{\cos^2 \epsilon_s} \sum_{i=s-n}^s \frac{h_i \cot^2 \epsilon_i}{\sin \epsilon_i}$$

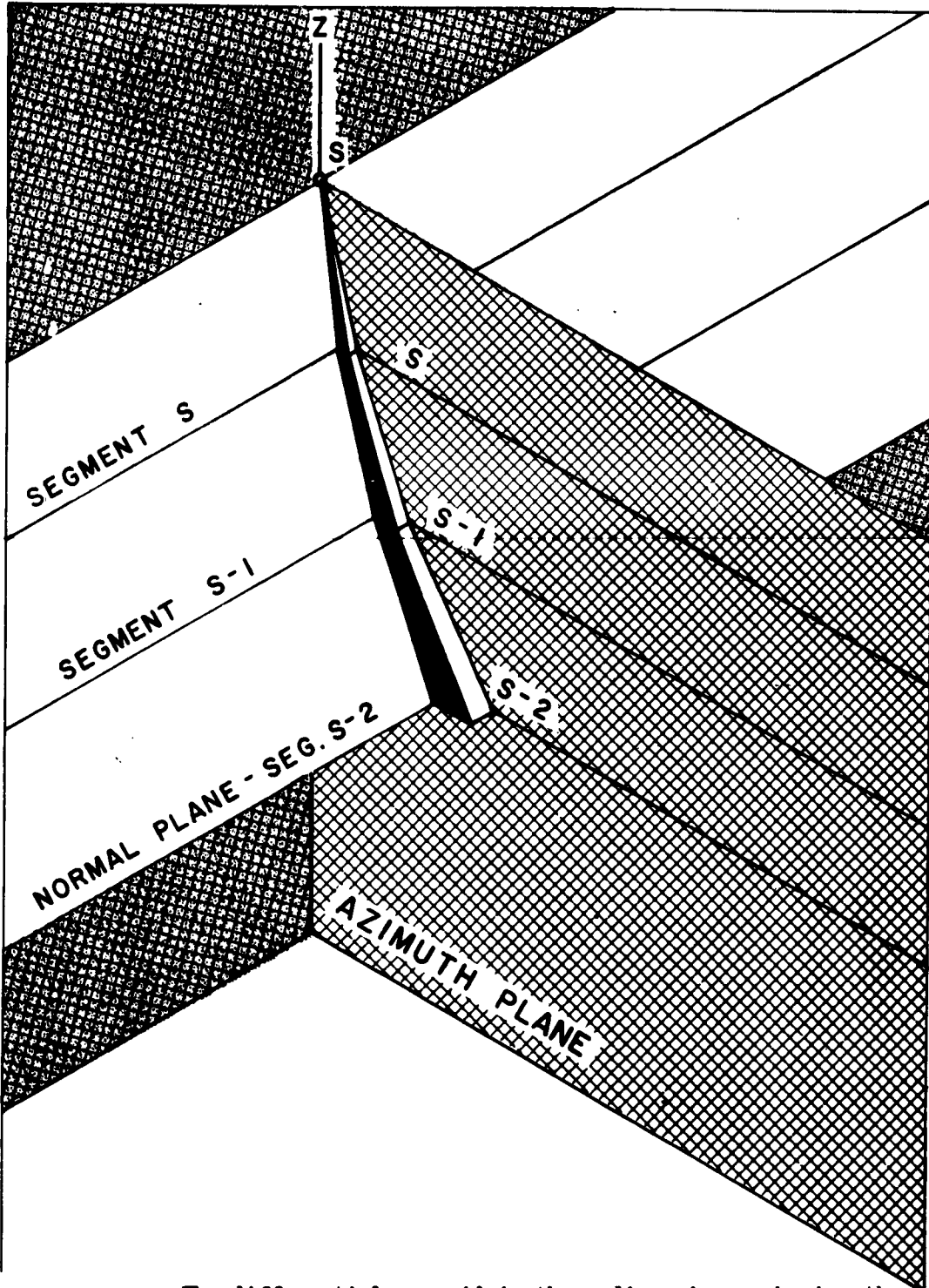
To find the adjacent side of dS , one must consider a ray which emerges at an angle $d\epsilon_s$ normal to the azimuth plane. This ray cannot move outside the azimuth plane, and the normal "plane" must be segmented and tilted to contain the ray. (See Figure 2) If this normal "plane" is so straightened, dy_{s-n} becomes

$$dy_{s-n} = d\epsilon_s \sum \frac{h_i}{\sin \epsilon_i}$$

It is apparent that the path length which determines both the flux and absorption losses is to be measured with respect to the medium, not a fixed frame such as the earth. It does not follow, however, that the intensity, a vector, is independent of relative velocity between the medium and the receiver. Wind causes the medium to be anisotropic, so that the intensity vector is no longer normal to the element of area $dxdy$. When consideration of this is made,* the element of area n layers down from layer s becomes:

$$dx_{s-n} dy_{s-n} = \frac{c_s \sin \epsilon_{s-n} \sin \epsilon_s (d\epsilon_s)^2}{\cos^2 \epsilon_s} \left(\sum \frac{h_i \cot^2 \epsilon_i}{c_i \sin \epsilon_i} \right) \left(\sum \frac{h_i (c_i + u_i' \cos \epsilon_i)}{B_i \sin \epsilon_i} \right),$$

* E. A. Dean. 1961. Sound transmission loss for near vertical atmospheric propagation. Schellenger Research Laboratories. Contract NAS 5-556. (Several mistakes in this report have been corrected in the present paper)



IV-2 Figure 2 The differential pyramid in three dimensions, showing the azimuth and normal planes. Note that the normal "plane" is segmented.

where

$$B_1 = \sqrt{c_1^2 + (v_1')^2 + c_1 u_1' \cos \epsilon_1}, \quad (v = \text{wind velocity})$$

$$v_1' = v_1 - v_{1-1}$$

and

$$u_1' = u_1 - u_{1-1} \quad (u = \text{wind component in azimuth plane of ray}).$$

If Ω is a solid angle, then

$$dS = r^2 d\Omega = r^2 (d\epsilon)^2,$$

or,

$$r^2 = \frac{dx dy}{(d\epsilon)^2}$$

is a measure of the effective path length, including refraction. Therefore, the transmission loss due to divergence and refraction, $L = 20 \log r$, becomes

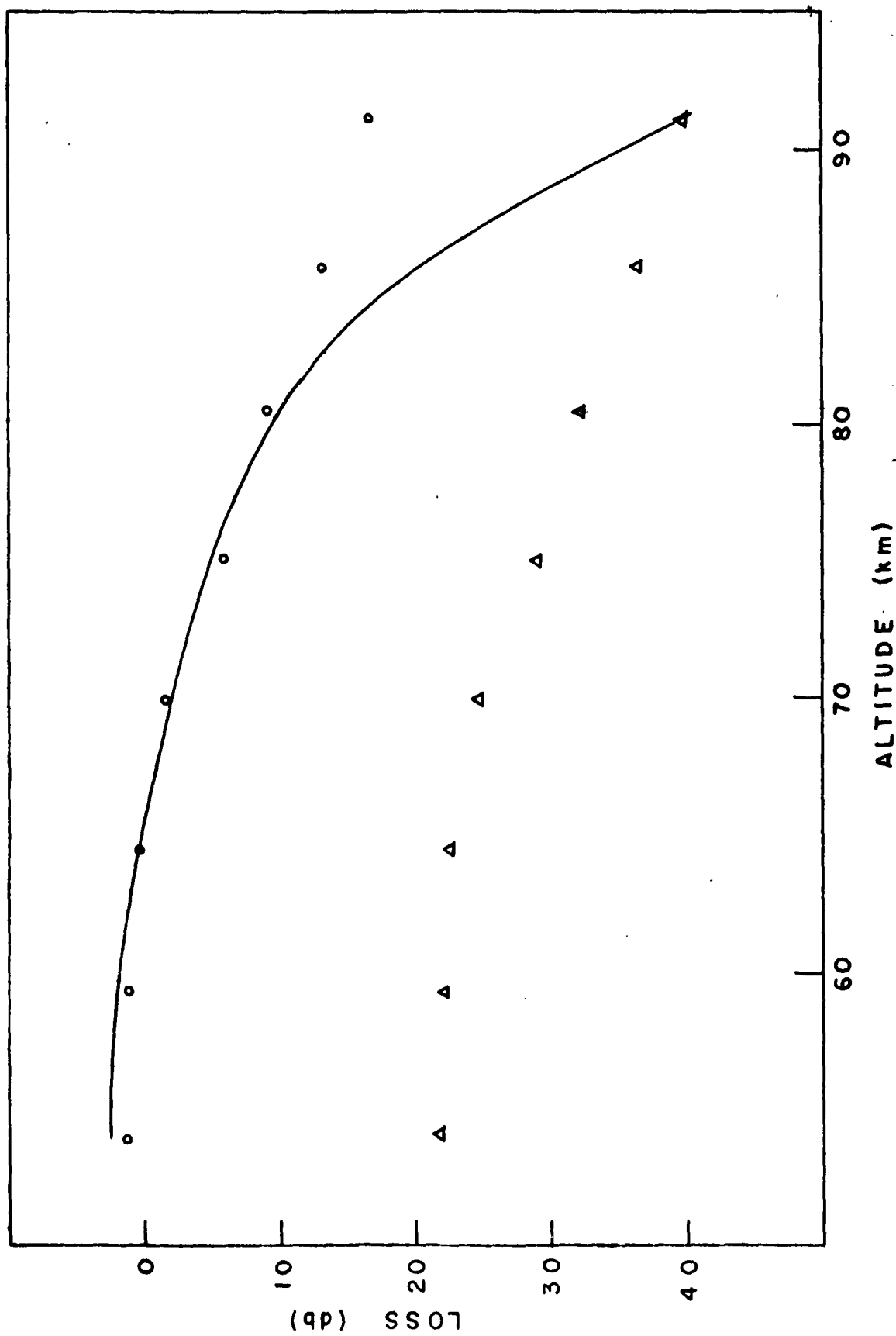
$$L = 10 \left[\log \frac{c_s \sin \epsilon_s \sin \epsilon_0}{\cos^2 \epsilon_s} + \log \sum \frac{h_1 \cot^2 \epsilon_1}{c_1 \sin \epsilon_1} + \log \sum \frac{h_1 (c_1 + u_1' \cos \epsilon_1)}{B_1 \sin \epsilon_1} \right]$$

when the summation is carried out from layer 0 (location of receiver) to layer s (location of source).

Thus far, calculations have been limited to within 5° of being vertical, and the divergent and refractive loss has been within a db or so of the homogeneous spherical propagation. Future plans include deviations from the vertical to obtain values for refractive focusing based on the above relation. This analysis breaks down if the propagation is far enough from the vertical to allow waveguide type propagation where more than one ray passes through a single point. Besides the problem of summing the individual ray intensity with due regard to interference, the constant gradient method of ray tracing, rather than constant velocity method, has to be used to skirt the singular point when $\epsilon = 0$.

The theoretical loss for grenade detonations has been calculated with the aid of a computer. Figure 3 shows an example of the high altitude cutoff which makes extension of the rocket-grenade experiment difficult. The slope of the loss curve is large at 90 km, and continues to increase. The experimental loss, (circles) calculated from the average signal reported by 9 T-23 microphones, is matched to the theory curve at about 65 km. The match is excellent to 80 km, then the loss is less than theory.

Since the theoretical and experimental losses are relative, and there is no good reason to believe the loss at higher altitudes is smaller than



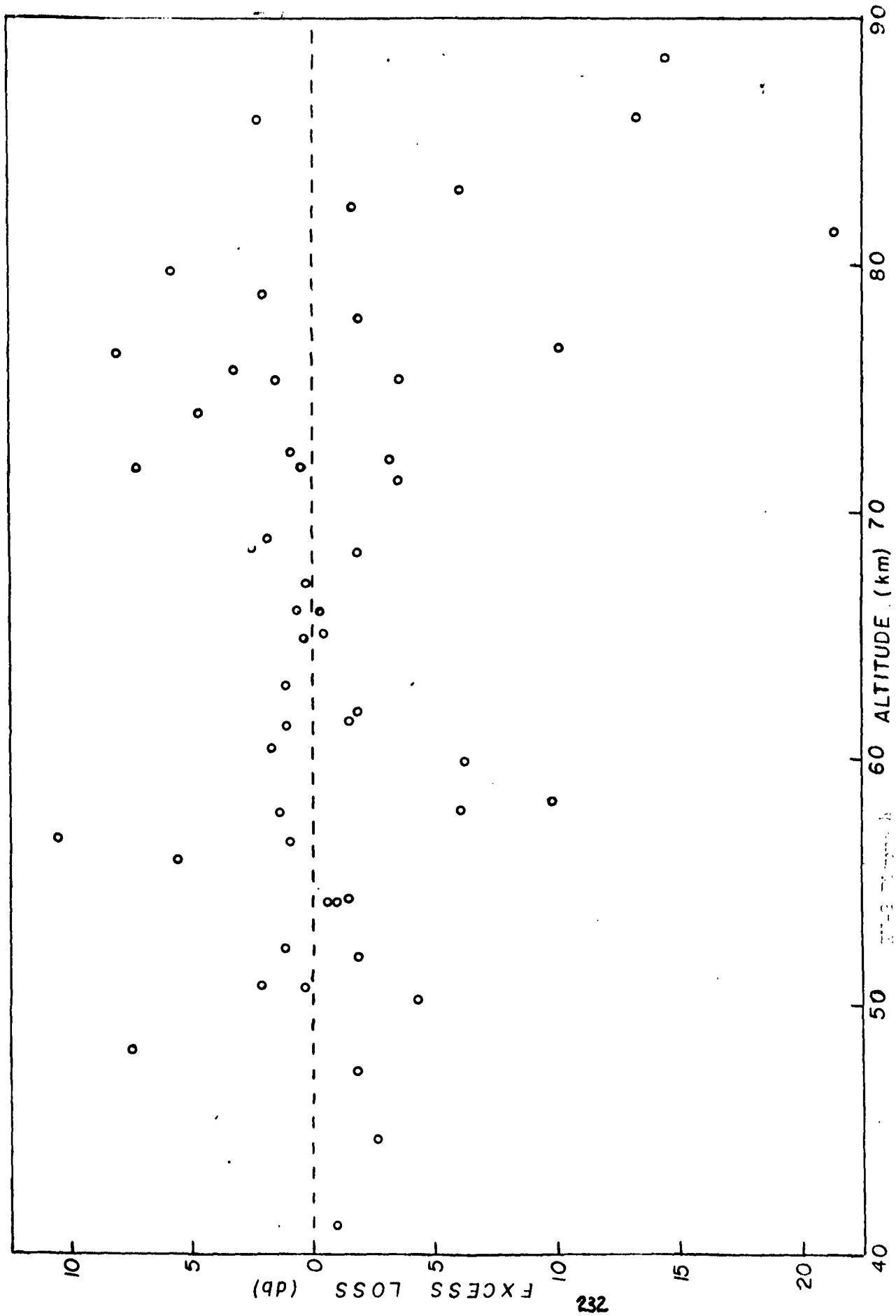
IV-2 Figure 3

calculated, the points can be fitted so that there is no difference at 90 km (triangles), which yields excess loss at lower altitudes.

There is no escaping the parallelism shown by the triangles or the fit shown by the circles at low altitudes. This is again brought out in Figure 4, a plot of the excess loss vs altitude for 52 pairs of grenade explosions. Here is shown the comparison between experimental and theoretical loss differences between successive grenade pairs, plotted vs the mean altitude of the pair. Although there is some spread in the data, the average for each 10 km region up to 80 km is 0 ± 1 db. Whereas the 80-90 km region averages to -7 db.

Three conclusions are being investigated:

- 1) The loss at higher altitude is less than that expected from divergence and absorption: (The method of measuring detonation frequency is questionable.)
- 2) To the contrary, the loss at the lower altitude is excessive, this excessive loss being constant (disregarding fluctuations).
- 3) The intensity from detonations is not constant, but is a function of temperature and/or height. (Finite amplitude effects have not been considered).



ACOUSTIC PHENOMENA OBSERVED ON ROCKET-BORNE HIGH ALTITUDE EXPLOSIONS

William Nordberg
National Aeronautics and Space Administration
Greenbelt, Maryland

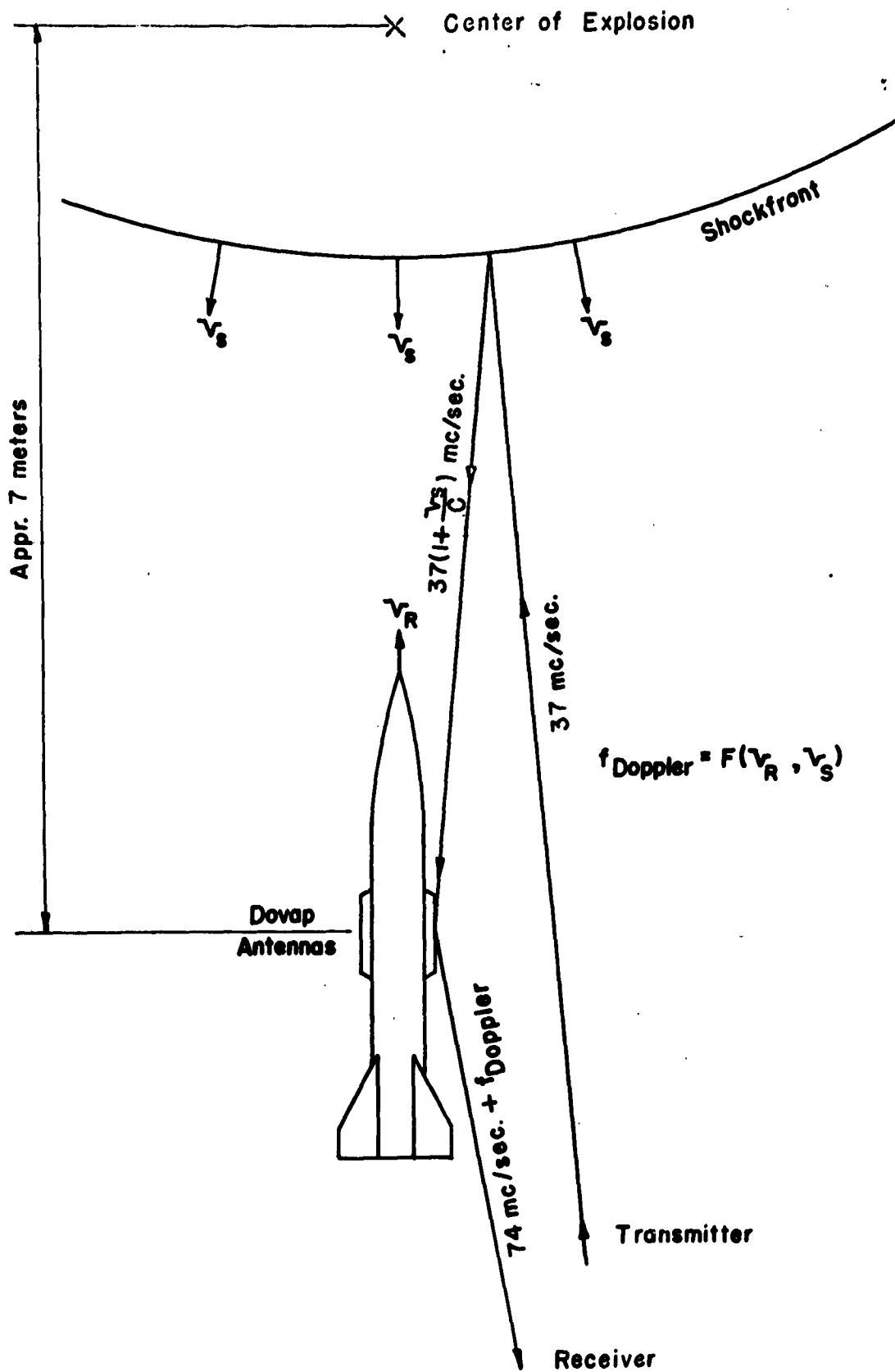
INTRODUCTION

A series of rockets instrumented with high-explosive charges were fired during the past years to measure temperatures and winds in the upper atmosphere. The charges were High Explosive, 45 percent TNT, 35 percent RDX, and 20 percent Aluminum, varying in weight from one to four pounds. They were cylindrical, approximately two inches in diameter and, depending on weight, from approximately 12 to 24 inches long. Upon ejection through the nose cone of the rocket they were exploded by means of a lanyard about 15 feet ahead of the rocket. The altitudes of the explosion were generally between 30 and 100 km. Excellent measurements of temperatures, winds, pressures, and densities were obtained over Fort Churchill, Canada, from 1956 to 1958 and over Guam, Mariana Islands, Pacific, in November 1958. These results as well as the method of the experiment have been published. (1,2)

In addition, however, a number of interesting phenomena not directly related to the main object of the experiment could be observed by studying the propagation of the acoustic wave from the exploding grenade to the ground. Two of these phenomena shall be the subject of this presentation. The first deals with the shock propagation in the immediate vicinity of the explosion and the second with unusual variations in the amplitude of the sound waves detected by microphones on the ground. It will be shown that the former phenomenon conforms well with existing theories on shock propagation; the latter cannot be explained by conventional absorption and refraction treatments.

THE SHOCKWAVE IN THE VICINITY OF A GRENADE EXPLOSION

A rather ingenious method of observing the shock front as it propagates from the grenade to the rocket was used by Bartman and Ottermann (3). It is demonstrated in Figure 1. A radio signal of 37 mc is normally received by the rocket from the ground, doubled and retransmitted. When received at the ground this signal is not exactly two times 37 mc because of the Doppler shift due to the moving rocket. The Doppler shift is recorded as part of the normal tracking operation. As the shock front emanates from the exploding grenade, part of the 37 mc signal reaches the rocket via reflection off the shock front. A Doppler shift due to the rapidly expanding shockwave will be superimposed on the Doppler signal from the travelling rocket. By analysing this superposition the velocity of the shock front relative to the rocket may be determined. And, since the rocket's velocity is known precisely, a space-time function for the shock front can be derived.



IV-3 Figure 1

The propagation of shocks from large charges (in comparison to our grenades) was calculated by Brode (4) and the dashed and solid lines in Figure 2 show some of the results of Brode's calculation. They give the scaled distance (λ) of a shock front from its origin as a function of a scaled time (τ) for an assumed spherical source and point source respectively. The dimensionless quantity λ is obtained by dividing the actual distance R of the shock front from the center by the cube root of the ratio between the energy content W of the explosion and the ambient pressure P_0 . The time t which the shock front takes to travel the distance R is also scaled by this ratio times the velocity of sound C_0 to obtain the dimensionless quantity τ .

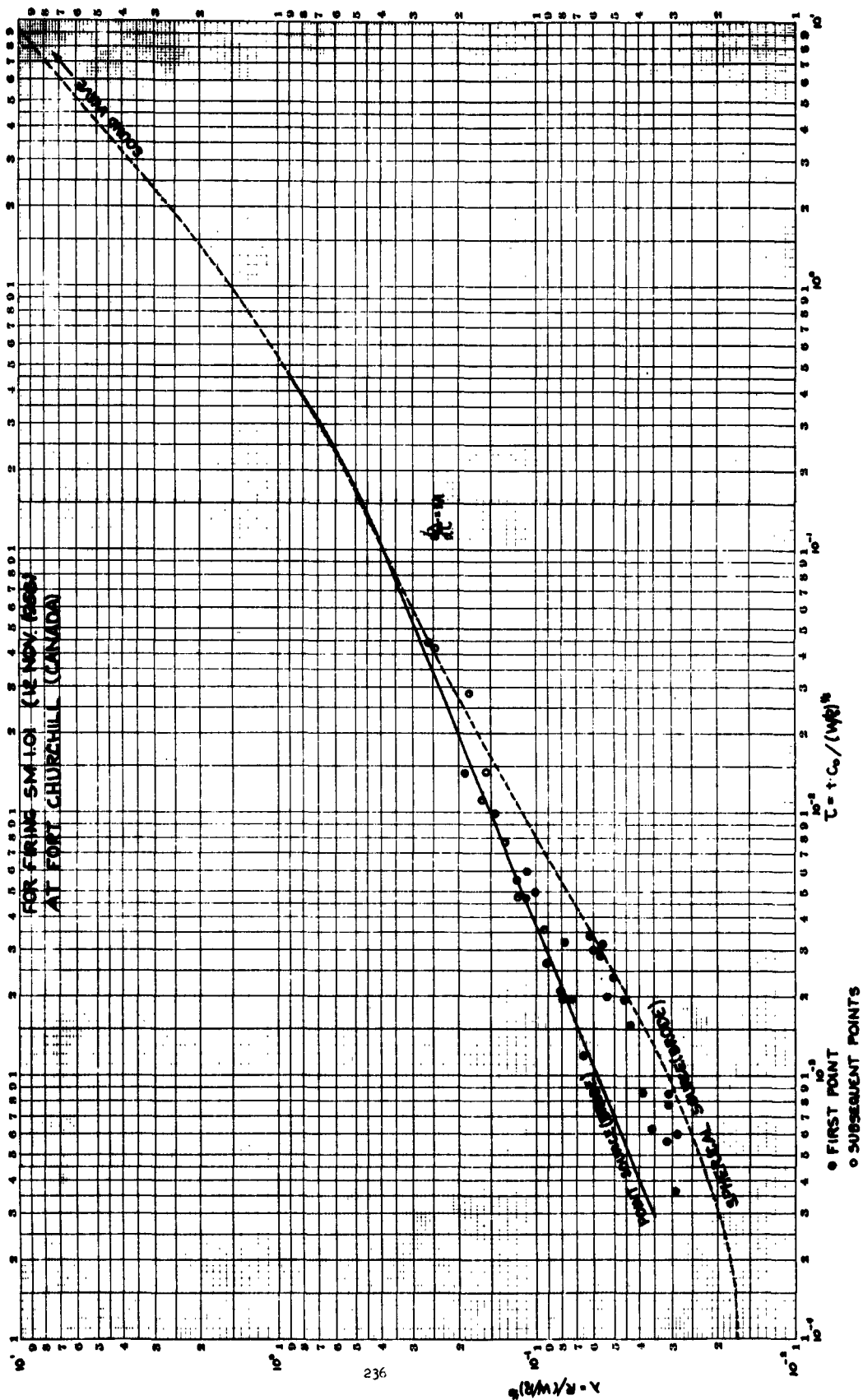
$$\lambda = R (E/P_0)^{1/3}$$

$$\tau = t C_0 (E/P_0)^{1/3}$$

τ and λ were computed for a number of grenades exploded at Fort Churchill and plotted on Brode's graph. Three to four points were plotted for the trajectory of each shock front. The earliest detectable point for each grenade, usually within less than three meters of the center of the explosion, is shown by solid circles, subsequent points further along on the trajectory are indicated by light circles.

It can be seen that all solid points follow closely the theoretically obtained curve for a spherical charge by Brode. The slight deviation at high Mach numbers may be due to the fact that our charge is cylindrical rather than spherical. The light points, further than about three meters from the explosion, show very good agreement with Brode's curve for a point source. The overlap of the solid and light circles indicates that the minimum distance at which the front can be considered originating from a point source rather than a spherical one is solely geometric consideration and does not depend on the scaled parameters λ and τ or Mach number which is expressed by the differential quotient $d\lambda/d\tau$. The distance from which the grenade can be treated as a point source is therefore three meters. Note that the only range where the shock front trajectory can be determined by this Doppler method is between the center of the explosion and the Dovap antennas on the rocket. Once the front has passed the point on the rocket where the Dovap antennas are located the superimposed Doppler shift disappears and no velocity for the shock front can be obtained. (Refer to Figure 1.) This limits the observation of the shock front to a maximum distance of about seven meters. At most altitudes the shock front has not reached sound velocity at this distance. The range where most of the circles in Figure 2 fall and in which the good agreement with the theory can be observed is from Mach 80 down to about Mach 3. It is a reasonable conclusion, however, that agreement will continue to lower Mach numbers until the shock can be treated as a sound wave. In Figure 2 this occurs where the slope of the curve approaches a maximum of about 45° with respect to the abscissa. This is the case in the upper right hand portion of Figure 2, from about $\lambda = 1.0$ on. Using the proper values for W/P_0 we find that at 30 km the shockwave

IV-3 Figure 2 SPACE-TIME DIAGRAM FOR
INITIAL SHOCK FROM GRENADE EXPLOSIONS
FOR FIRM SM-101 (12 NOV 1963)
AT FORT CHURCHILL (CANADA)



from a 4 lb. grenade can be treated as a soundwave after travelling only 10 meters from the center of the explosion. At an altitude of 90 km this distance is 400 meters.

The same phenomenon is demonstrated in Figure 3 where the observed Mach numbers of the shock front are plotted as a function of distance travelled. It can be seen that at 26 km the wave travels at Mach = 9 at a distance of 3 meters from the explosion while at 61 km the speed is Mach = 60 at the same distance. At 4.5 meters we find the wave in the 26 km case has slowed to Mach = 2 while in the 61 km case we still find a speed of Mach 25. If we extrapolate the data shown in Figure 3 to Mach = 1 to obtain a distance R at which the wave may be considered a sound wave, we find again that the values agree generally with the ones obtained theoretically from Figure 2. In summary, we conclude that the initial shock propagated from 4 lb. charges in a highly rarified atmosphere at altitudes up to 90 km can be treated quite satisfactorily by Brode's theory which was originally developed for the much higher ambient pressures at the earth's surface.

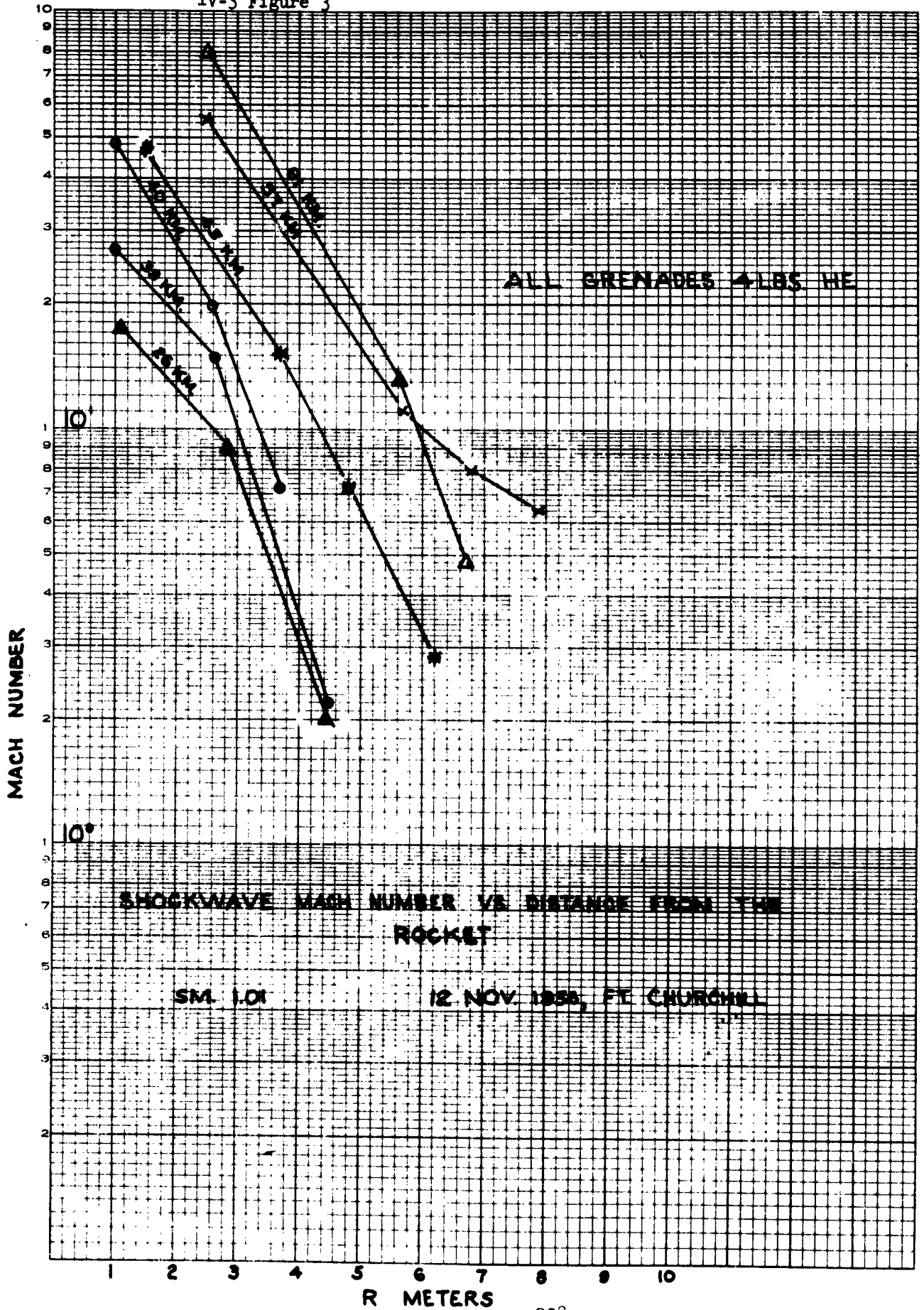
SOUND AMPLITUDES RECEIVED ON THE GROUND

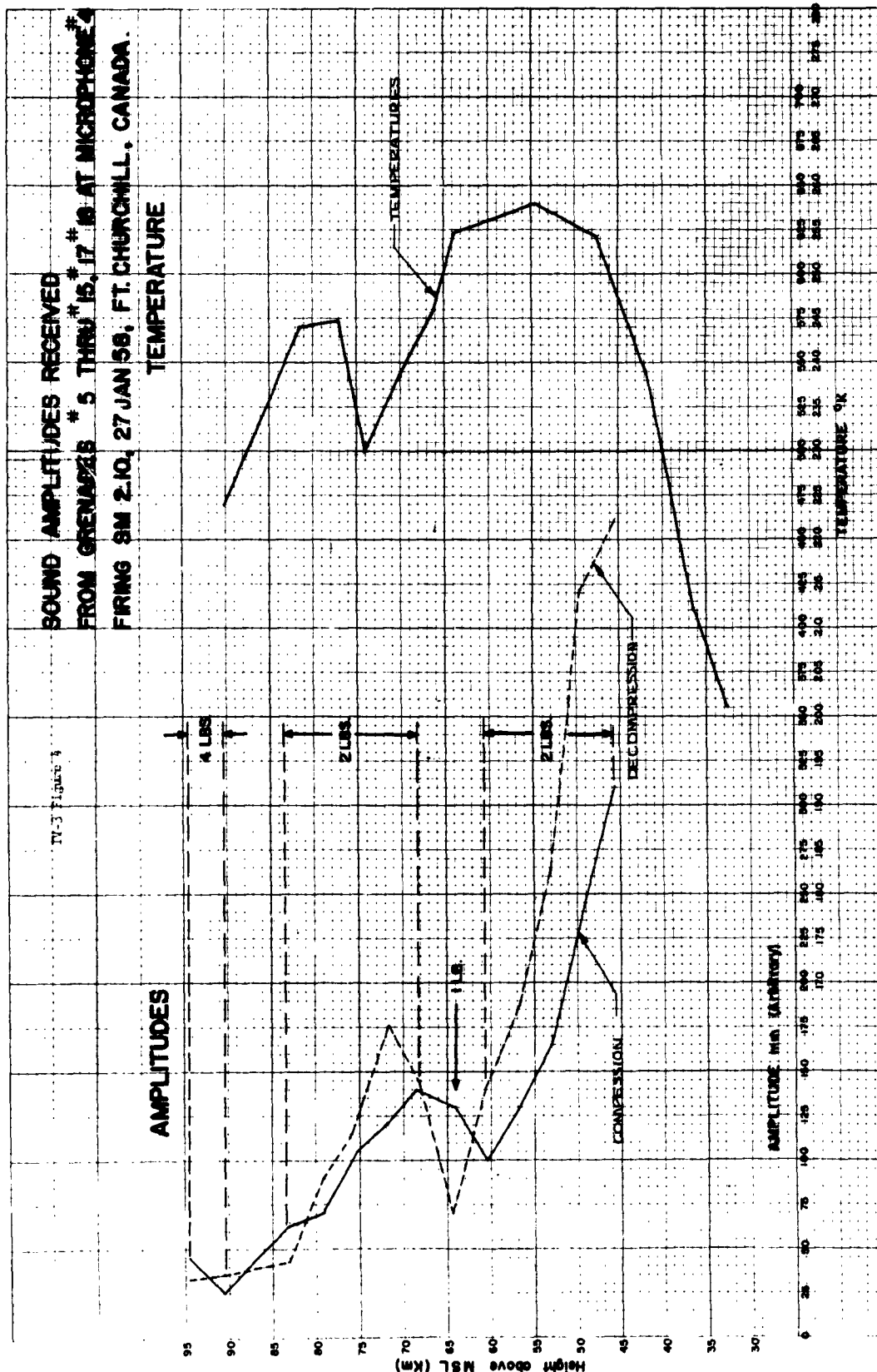
A series of hot wire microphones, U. S. Army Type T-23, were used to measure the times of the sound arrivals at the ground. Although these microphones cannot be calibrated to measure the amplitude of the received sound signal absolutely, an attempt was made to determine the relative attenuation of sound with increasing altitude of the exploding grenades.

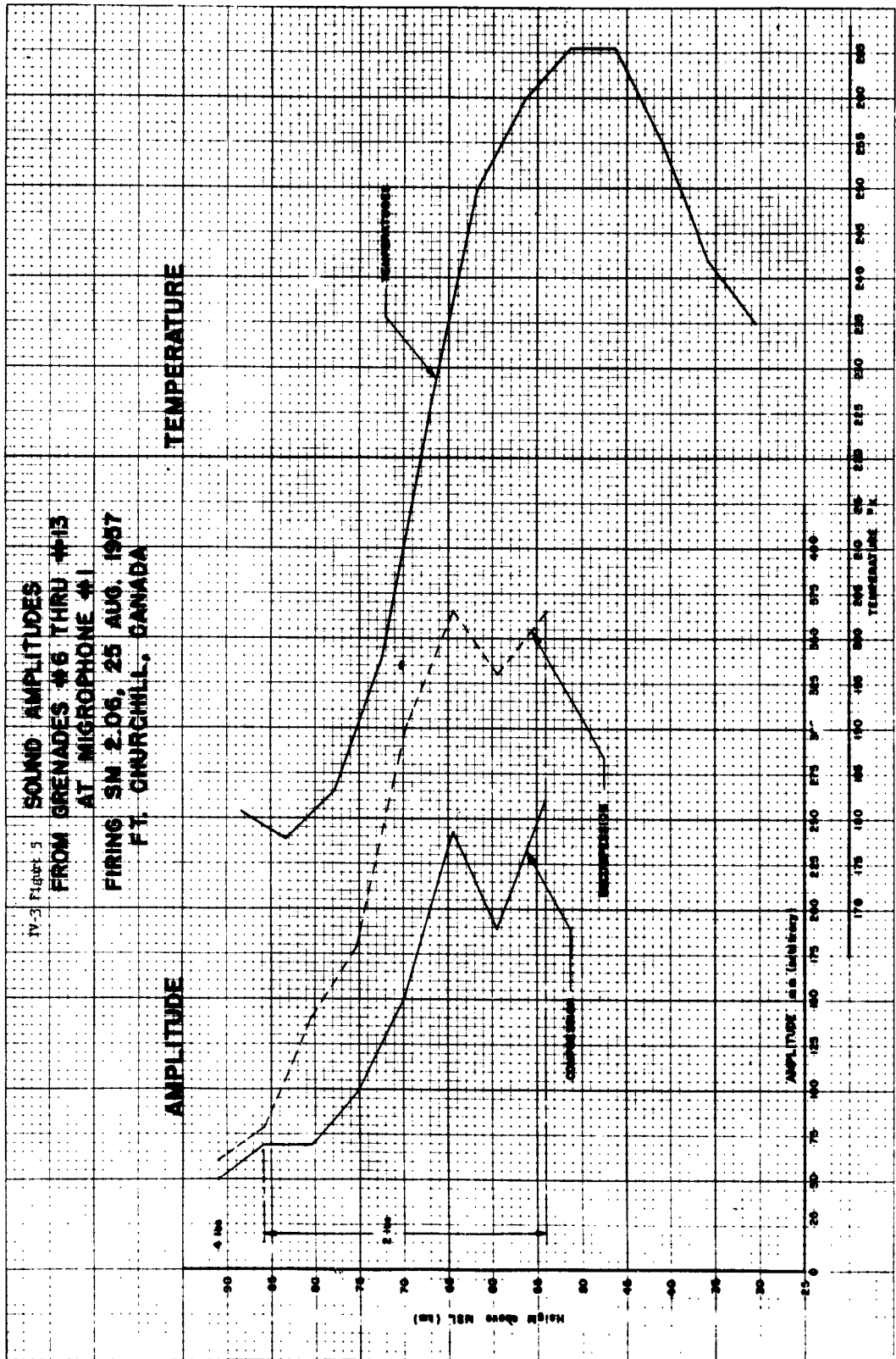
Theoretically the sound amplitude should be attenuated exponentially with distance travelled, with the mean free path and with the square of the frequency of the sound wave. Bandeen (5) attempted to explain the sound amplitudes shown in Figure 4 on this basis. He found that the average decrease in sound amplitude with altitude was somewhat greater than the theory called for and that amplitude increases such as are shown between 65 and 75 km in Figure 4 cannot be accounted for at all.

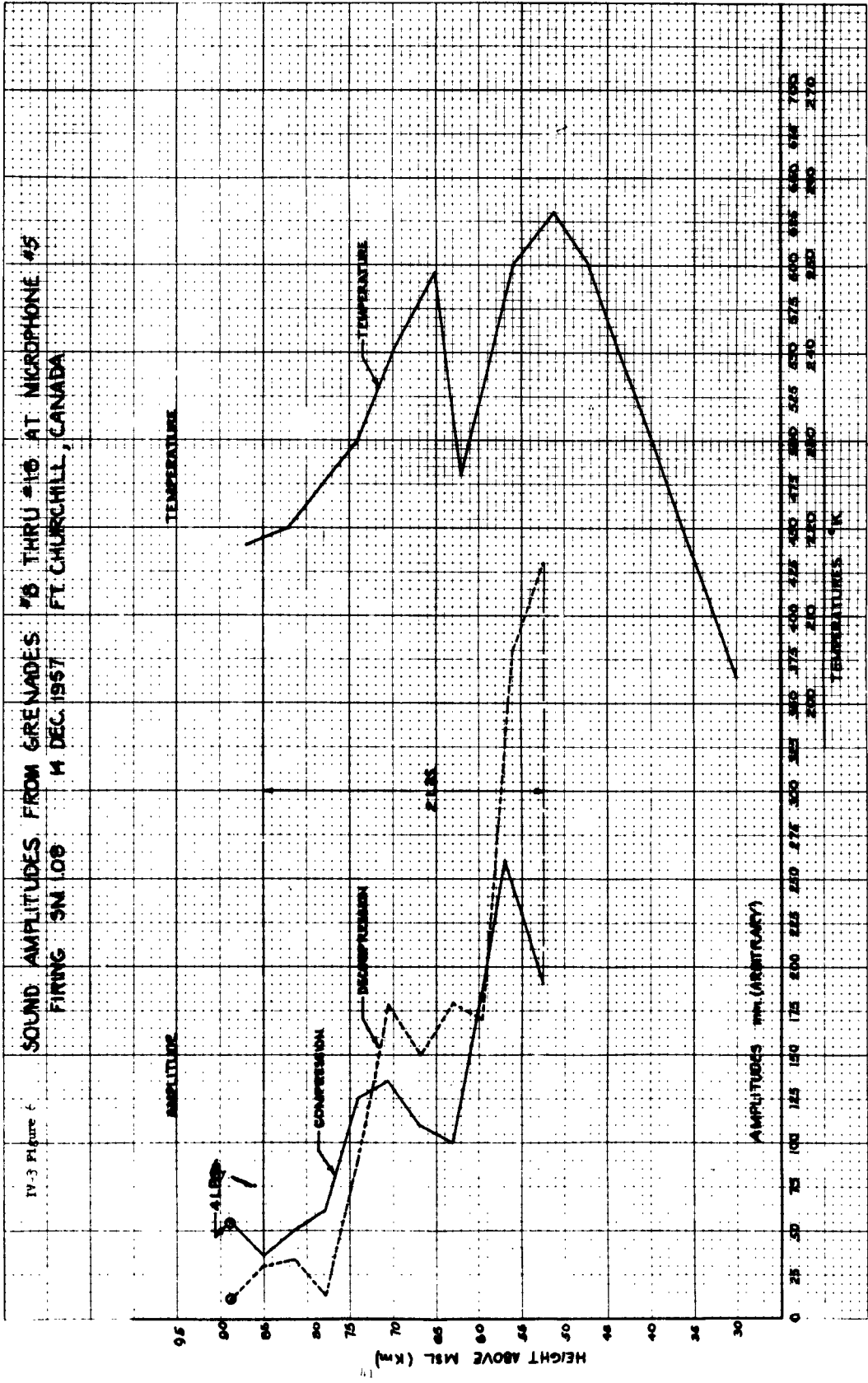
We investigated three more firings and found that such increases occurred in each of them (Figures 5, 6, 7). Note that the temperatures measured in each of these firings is plotted alongside the sound amplitude graph and that the amplitude increase in each case occurs at altitudes between 60 and 75 km just above the temperature peak which we usually find near 50 km. In Figure 7 we find that there is a second, abnormally high, increase of amplitude at about 80 km. This goes hand in hand with an unusually large secondary temperature maximum at about 70 km. In each case the abnormal sound amplitude increase with altitude occurs in a strong negative temperature gradient, i. e. just above a peak in the temperature distribution. This strong correlation with temperature gradients leads to the suspicion that the amplitude variations may be caused by refractive focusing of the sound wave. Such focusing could occur in a strong vertical thermal gradient in the vicinity of the explosion and could be enhanced by the fact that the wave undergoes a

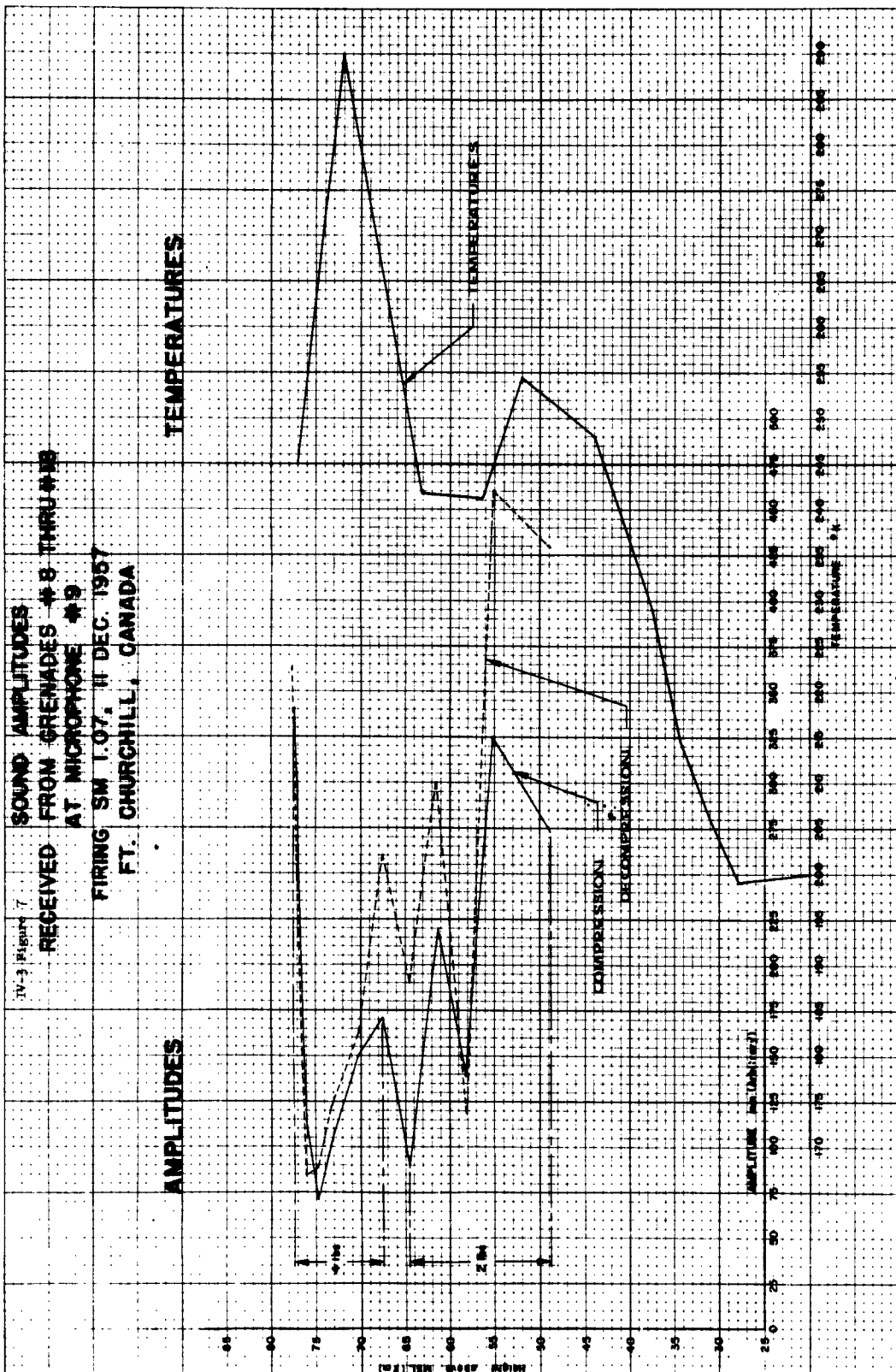
IV-3 Figure 3











tremendous velocity gradient in its transition from shock wave to sound wave, as pointed out in the first part of this presentation. Our calculations showed, however, that the amplitude variations cannot be explained by this approach and subsequent and more detailed calculations by Alan Dean seem to confirm this conclusion. We are quite confident that the sound output from one explosion to another is sufficiently constant so that a variation in the explosions themselves cannot explain this phenomenon. The frequency distribution of the generated wave could also greatly affect the amplitude of the sound arrivals since the attenuation is exponentially proportional to the square of the frequency of the wave. The principal frequency of the arriving soundwave can be measured and results show that this frequency decreases rapidly with increasing grenade altitude. It is not plausible, however, to assume that some explosions produce a larger share of low frequencies than others.

The only conclusion in this case is that in most of our firings the sound intensity of the grenades did not decrease exponentially with altitude as one might expect. There seems to be a preferred region between 60 and 75 km, from where sound returns are stronger than from altitudes just below. There is strong evidence that there is a relation between the sound amplitude increase and the strong negative temperature gradient in this region. Analytical treatment of this phenomenon so far has not produced any satisfactory explanation.

References

1. Stroud, W. G., W. Nordberg, and W. R. Bandeen. "Rocket-Grenade Measurements of Temperatures and Winds in the Mesosphere over Churchill, Canada," Journal of Geophysical Research, Volume 65, No. 8, August 1960, pp. 2307-2323.
2. Nordberg, W. and W. G. Stroud. "Results of IGY Rocket-Grenade Experiments to Measure Temperatures ~~and~~ Winds above the Island of ~~Green~~," Journal of Geophysical Research, Volume 66, No. 2, February 1961, pp. 455-464.
3. Bartman, F. L. and J. Otterman. "Atmospheric Phenomena at High Altitudes," Quarterly Report, Engineering Research Institute, The University of Michigan, Ann Arbor, Michigan, October 1957, p. 25.
4. Brode, Harold L. "Blast Wave from a Spherical Charge," The Physics of Fluids, Volume 2, No. 2, March-April 1959, pp. 217-229.
5. Bandeen, William R. "The Recording of Acoustic Waves from High-Altitude Explosions in the Rocket-Grenade Experiment and Certain Other Related Topics," U. S. Army Signal Research and Development Laboratory Technical Report 2056, 1 July 1959.
6. Dean, E. Alan. "Sound Transmission Loss for Near-Vertical Atmospheric Propagation," Progress Report on the Analysis of Rocket Grenade Experiment Transmission Loss, Schellenger Research Laboratories, Texas Western College of the University of Texas, January 1961.

PANEL DISCUSSION

Panel members: Dr. Craig Crenshaw
Dr. Cyril Harris
Dr. William Meechan
Dr. Alan Powell
Dr. Wayne Rudmose
Dr. Jesse Young
Mr. Marvin Diamond, Moderator

Dr. Harris to Dr. Crenshaw: I think a number of us would be interested in knowing what your opinion about how the state of the art of sound location has changed over the years. You probably have had more experience in gun-fire location than any of us here, and you have been with the problem a long time. In particular, how has the accuracy changed as a function of time? What it is today, and what was it let's say 15 years ago or earlier? Also, what do you predict for the future.

Dr. Crenshaw: That's a big order. When I got into this type of work in 1942, shortly after the war started, I was told that sound ranging was in trouble and since I was a physicist I should try to improve the situation. The T2LB microphone had been developed by the Signal Corps at that time and has been referred to occasionally here today. However, the net corrections had not been seriously studied. At the time, there was a man at the Signal Laboratories, Mr. Lukes, who had gone through the ray tracing method. The first reference on this subject that I have run across in the literature was by E. Esclançon, published in the *Memoirs of the French Artillery*, an occasional publication so that it is difficult to obtain. This article discussed the location of projectiles, the sound waves they create, standard sound ranging techniques, the ray tracing problems, and the refractive problems when you propagate upwind as opposed to downwind because in the surface layers you normally have a gradient in the same sense as the wind direction. F. K. W. Whipple in England, who I believe is an uncle of the Whipple in America, published in the *Quarterly Journal of the Royal Meteorological Society* in the 20's, an article on the detection of the Offenback demolition of munitions from World War I. His observation consisted of reports by postcards from people who were asked to please look at the clock and report when they heard the explosions which were to go off according to a schedule announced on the radio. Knowing the gullibility and the seeking of glamour of so many people, he had announced two explosions that didn't occur and this is the way he checked the reliability of observers, since any one who heard those wasn't a reliable observer and he rejected their reports.

* E Esclançon, "L'acoustique des canons et di projectiles," Extrait du Memorial de l'artillerie française. Paris Imprimerie Nationale Gauthier Villars et cie, 1925.

From this he was able to plot the zones of silence and of audibility and demonstrated that because of low level met conditions there will be a zone of audibility around a surface explosion. Because of refraction from the upper part of the duct there will be another circle of audibility. Sometimes it isn't a circle if the duct isn't closed, depending on the wind structure. Whipple had concluded that you had to have either monsoon winds, by that he meant wind velocities of 100 miles per hour or more, or very high temperature to bring the sound back down to the surface. This is a result of this horizontal homogeneity assumption in ray tracing.

One of the early things that I thought was needed was some idea of the validity of the assumption of horizontal homogeneity. I was trapped into making an experiment to try to determine the caliber by amplitude, which I objected to strenuously, and said it wouldn't work. I thought maybe we could do it by frequency so I went ahead with the experiment with great enthusiasm. Dr. Daniels of the Signal Labs and I worked together and as we anticipated, we could not do it on amplitude at all. A five-second delay between the calibration shot of one pound TNT and the gun was enough to throw the amplitude ratios off so you could not get an indication of the caliber. We used guns in the range from 75 mm howitzer to the 155 mm gun.

Since ray tracing work had been done, I devised this rapid abbreviated calculation method that was mentioned by Dr. Swingle. His treatment has been revised to take care of the case when you do not measure the trace velocity. We had proposed to change the technique and measure it so you could do the ray tracing. Besides the inaccuracies were such that the error introduced by sound ranging was not too great for the use and employment at that time. The errors would depend on the weather, that is, the gross weather situation. They were such that you could get locations from these plots that would locate you within 150-200 yards of the source. In World War II and World War I, this was more than adequate because where a battery was, there was usually a supply dump and you didn't care whether you located the dump or the gun itself. What you wanted to do was knock the people and munitions out and they would be within 100 to 200 yards of the gun, so for the use this kind of accuracy was adequate. Today the picture is quite different, in World War II the normal range was five to ten miles while today we are going 20 to 50 miles with missiles. Since this error is linear with range, you find yourself in trouble because an error of 1% of the range becomes a little more than people like. You have to expend a lot of missiles over one target unless they are going to have area fire.

Against small arms and mortar, and things of that kind where you are using a mortar for counterbattery work, the accuracy of the sound is appreciable. At 1,000 to 2,000 yards, the accuracy of the sound even without net corrections is greater than the accuracy of the mortar, consequently, this is an excellent way of locating the enemy. The other advantages of sound are that it is passive, you don't have to put an antenna up like you do with radar, its range is of the order of somewhat longer than the range of missiles or the guns you are after. If the weather is bad and you happen to be upwind, you may not hear it, but the real advantage to the Field Army is that when it's foggy and your flash ranging doesn't do you any good, sound works wonders. So from a practical point of view it paid off a whole lot. They even insisted that we send a civilian over from our Lab to take care of the supply and straighten out some of the sound ranging equipment from World War II that were in difficulty. A sound ranging set was actually shot up in Tobruk when the Germans came through that area. Replacements were flown right over into the Field Artillery Battalion area to replace it.

Well now as to future military requirements. If you note as I said, an error of 1% of the range is due to the residual meteorological effects on locations. The exact variability of the atmosphere is of this order of magnitude. Then you have the problem of how current is your net, so to locate a missile launching site and knock it out you have an even more severe problem. If the Army adopted a shoot and scoot method, by the time you locate the launch area and get your missile back they may be gone, especially with mobile artillery. So in this case with these larger weapons now sound has been relegated from a counterfire device to an intelligence device where high precision on location is not required.

Mr. Diamond: Thank you Dr. Crenshaw. We have heard a lot in the last few days about the long distance propagation of sound and our atmospheric channel. We have also heard a number of discussions on absorption. I would like to pose a question to the panel on their opinion on the relative effects of absorption versus scattering on sound attenuation.

Dr. Harris: Well in this specific regard, I will comment only on the relatively short-range sound propagation work which I have done. Several years ago at Fort Huachuca I made some experiments on a range about two miles long, with a 45-cycle pure-tone sound source. The sound source was detected by an array of microphones at various distances up to two miles. Then the relative amplitudes and phases at the various microphones were measured. If the measurements were made before sunrise, when the wind velocity was essentially zero near the ground, the conditions were excellent for propagation. Even at propagation distances of two miles the signal-to-noise ratio was good. Then when the sun would come out, the ground would warm up, resulting in turbulence and stratification. The

attenuation resulting from these factors was much greater than that due to absorption. In fact, the attenuation was sometimes so great that we might not be able to receive signals propagated over relatively short distances. In addition to the above factors, wind conditions are, of course, very important. (Parenthetically, I might say that we spent a great deal of time in reducing the level of wind noise by sinking microphones into the ground and designing appropriate wind screens for this study.) Some of our measurements of the relative phases between microphones indicated a possible technique for obtaining an estimate of the scale of turbulence in the following way. Consider a pure-tone sound source and two microphones which are equidistant from the source. The simple source is placed along a perpendicular bisector of a line between the microphones. Assume that the source produces a circular wave front. Then the sound will arrive in phase if the atmosphere is homogeneous. This is the condition we obtained early in the morning before the sun came up. Then the signals at the two microphones were in phase and stayed in phase. However, as the turbulence developed there were resultant phase fluctuations due to the passage of the sound waves through the atmosphere. The magnitude and periodicity of these phase fluctuations is related -- in a complex manner -- to the scale of ~~atmospheric~~ turbulence. Therefore, this technique possibly could be used to get some estimate of the scale of turbulence. We actually tried some preliminary evaluations of this type and weren't too successful, but this was only a by-product to our work, we didn't have an opportunity to carry it through.

Dr. Meehan: We are interested to know, with regard to the experiments you were just talking of, Dr. Harris, whether the fluctuations you observed, were due to temperature fluctuations or air velocity fluctuations.

Dr. Harris: I really can't say for sure. We had rather poor meteorological equipment. I think that one would want to have some kind of sonic anemometer for such work, the response time of our temperature measuring equipment was too slow for such a determination.

Dr. Crenshaw: Did you try any correlation to determine the effect of sunny or cloudy conditions?

Dr. Harris: We didn't take enough data to establish a quantitative relationship, but when it was cloudy, we definitely had less phase fluctuation. Incidentally, there will be a paper in the Proceedings of the International Congress on Acoustics which took place two years ago (which hasn't been published yet) in which the results for these experiments will be given. It shows how the magnitude of the phase fluctuation changed as a function of the distance from the source, and also as a function of the distance separating the two microphones.

Dr. Crenshaw: There was some work of this type done by Dr. J. P. Maxfield at Duke University. Are you aware of this work?

Dr. Harris: Yes. Maxfield and others at Duke during the war wrote some of the earlier papers on this topic. There is also a book in Russian, which covers a great deal of this work, that came out several months ago.

Dr. Rudmose: There is a fairly extensive study that has been done recently for the Coast Guard by Bolt, Beranek, and Newman. It is interesting to note the differences in the approaches to the problem, that is, the HBN organization versus your organization. Here I get the feeling that you are predominantly meteorologists with not too much acoustics background. HBN's work was done by a group of acousticians with little meteorological background. I would like to see these two groups together. Had I known I was going to serve on this panel before I arrived, I would have tried to be a little better prepared. The data which Bolt, Beranek, and Newman took are quite extensive and they did have excellent measurements of both temperature gradients, temperature, wind speeds and wind gradients. Most of their work was done during fog conditions for this was the reason for the project. As I recall, little absorption was attributed to moisture over the distances with which they were working which was up to a couple of miles. They did show that temperature and wind gradients were more important in producing attenuation and fluctuations than the absolute magnitude of the temperature and the wind. It bothers me when I see the magnitude of the problem facing you people because you are talking about tremendous distances. In view of these large distances, I wonder where you decide to sample these gradients - near the source - near the receiver - or in between. I also wonder about the effect of fluctuations on your data. I know the magnitude of these fluctuations over distances of even a few miles. Ingard has done quite a lot of work in developing the theory of the effect of temperature gradients and velocity gradients upon sound propagation. Engineering charts have been drawn by Bolt, Beranek, and Newman, but they simply show you the rather wide range under which you can expect variations of signals. Now you are faced with obtaining data by firing a single shot. I don't know how you are going to say what's going to happen on the basis of one shot because of the tremendous variations expected. If you could fire one shot after another I have the feeling that you would find large variations in the results that you would get. This, of course, would further confound the situation.

I also have the feeling it would be nice if one had a little better knowledge of horizontal gradients, but if you could fire three or four rockets simultaneously with horizontal spacing and get horizontal gradients, then you might get a better picture of transmission from high altitude to ground. It is the horizontal gradient that will affect vertical propagation.

Mr. Diamond: Any other comments by the panel members? Incidentally, Dr. Rudmose, we are very willing to accept your proposal on firing a lot of these net rockets simultaneously at various distances. Prior to

lunch we had a rather spirited discussion on background noise at high altitude. One member of our panel has been studying infrasonic disturbances at the surface and I believe he can provide us with some information on the type of background noise that is observed at the surface.

Dr. Young: I would like to mention two types of background noise that have been observed at the surface which were reported last fall at the San Francisco Acoustical Society Meeting and which were studied primarily under the directorship of the late Peter Chrzanowski of the National Bureau of Standards. One of these sounds arrives at the surface a number of hours after the magnetic activity increases during a magnetic storm and the thing I would like to point out is that these are observed at the surface with periods predominantly from 20 seconds up so they are very low frequency and may not be of too much interest here. The other is that they do show a trace velocity along the surface in general higher than the local speed of sound which indicates that they come in at a fairly large angle. During the day they change direction. At about midnight local time they seem to arrive generally from the north. In the evening they approach from north-eastern directions and change through north about midnight and over toward the west thereafter. One would speculate that they are probably coming from regions of auroral displays, that perhaps the source is in the high atmosphere and this might account for the lack of higher frequencies. Since we know nothing about the source or its height we cannot say much about propagation conditions. These waves do not seem to be extremely coherent over distances on the surface of the order of seven kilometers or so.

The other type of background sound that I would like to mention is the sound mostly observed during the summer from tornadic storms in the Midwest. The sounds have pressure amplitudes of the order of one dyne per square centimeter at Washington, D. C., and originate about a thousand kilometers away. I might point out that what Willis Webb stated would indicate that the lower atmospheric duct could not be of much help in propagating them so I should say something about the frequency spectra. There are periods present below 20 seconds, but not very far below, down to 15 seconds and occasionally 12 seconds, and from there up to about 50 second periods and I feel that these then are perhaps guided by the higher positive temperature slope that the ARDC model atmosphere would indicate up in the vicinity of 100 kilometers. Also, I feel there is probably not much absorption because of the distance and also because of the energy you would have to ascribe to the source if there were much absorption at the very low frequencies. This would bring up the question that if you were closer to the source would you see the higher frequencies. I would be very interested to know if any effects that might be due to a source of this nature have been observed.

Dr. Meehan: The relatively small number of runs which have been made at the University of Michigan probably are not sufficient so that one could feel safe to get a time when a tornado occurred. I am quite sure

that Willis Webb's group is in better shape to talk of this. If I understand the situation, I believe it is true that on certain days abnormally high background noise occurs which might be due to bad weather. I am interested to know, could you extrapolate your measurements into the frequency range we were talking of this morning, that is, into the few cycle per second range; I wonder if you have any idea of the frequency falloff of the spectrum from low to high frequency? Is it likely that the pressure levels for these tornadic sounds at higher frequencies would be of any importance?

Dr. Young: I think this might be. When lower frequencies appear they do seem to show at larger amplitudes and in general follow the falloff with frequency that background fluctuations in pressure over long time averages show and therefore, they might be of the same order of magnitude as the turbulence fluctuations. But then, there is also the matter of extrapolating turbulence from the surface up to the higher altitudes.

Dr. Meecham: And what is the rate of falloff that you observe at the surface of the earth for turbulence effects?

Dr. Young: Well, there is an article in the Journal of Geophysical Research I think, by Gossard or Walter Munk, (Gossard-J. Geophysical Research 65, 3339, 1960) that shows a falloff rate of about 20 db per decade in frequency out at the long periods. Whether this would extrapolate on into the region around and above 1 cps, I don't know.

Dr. Meecham: I guess I misunderstood. The sort of fluctuations you are talking of then are Hydrodynamic. Is that right? If I remember Munk's work, they were working with local or non-propagation pressure fluctuations.

Dr. Young: Yes, that kind of background fluctuation.

Dr. Harris: Would you care to hazard a guess as to what sort of spectrum you would get from an aurora? If that were an important source, what might be expected from it?

Dr. Young: There have been some visual observations or some photometric measurements of the light intensity fluctuations during aurora by Wallace H. Campbell from the Boulder Laboratories of the National Bureau of Standards. These do indicate fluctuations from around 1 cps through the spectral region that I have indicated. I am not sure of the exact limits, but there are fluctuations of 1 cps to .01 cps in the visual display at around the 100 km level or just above.

Dr. Crenshaw: I might add one thing, that aurora have been heard in Scandinavia in a tremendous aurora display. Also, the Krakatora explosion was heard at 2,000 miles.

Dr. Powell: I would like to comment or perhaps ask about the background noise due to the boundary layer on the surface of the earth, because of the winds as they pass over it. The noise due to the turbulence, that is the massive activity in the air, would depend on something like the eighth power of the Mach number whereas the boundary layer noise due to roughness, trees, buildings, mountains and the like, would be more like depending on the sixth power. That means that at low speeds, low Mach numbers, such as are guaranteed there, the boundary layer noise presumably dominates over the turbulence noise. For a 60 mile an hour gale the column of turbulent air above a square mile of ground would produce something like 20 watts whereas that due to extremely rough ground might produce well over 1,000 watts. If the latter were for large areas it is obvious it would add up to a considerable amount of energy. The Empire State Building I think might produce about 1,000 watts at about 0.2 cycle per second.

Dr. Meecham: In making this calculation, at what height above the surface are you assuming a 60 mile an hour gale.

Dr. Powell: Independent.

Dr. Meecham: I see.

Dr. Powell: The higher it is the lower the frequency would be.

Dr. Meecham: One of the many confusing aspects of the problem at hand is that you have difficulty deciding just what role shear will play, not just at the surface but even at great altitude. I have generally tended to ignore the effects of the shear simply on the grounds that the average shear, is rather low (even through the jet stream) when compared with what I estimate the eddy shear to be. The real question is how the shear going across a typical eddy compares with the mean shear going through the layer.

Dr. Powell: Perhaps I didn't make myself too clear. I was including the noise made by the eddy flow around and behind an obstacle on the ground.

Dr. Meecham: It would seem to me that this should be rather dependent upon the type of surface where one was operating and whether it was a quiet day, or not, at the surface. In the experiments that were done at Ann Arbor the instruments were released over open country, then passed over a large city, then an open lake, and then over another large city. One might expect that if the sound received from the surface has a range less than something like 20 - 50 miles, then one would expect to see a change in the sound level as the instrument passes over these different areas. This is not the case. That is, the levels on a given

flight are relatively constant. Of course the level fluctuates some, but not as much as one would expect from the model you propose. It may be that on very windy days the situation changes or perhaps then the sound coming from the earth's surface becomes the most important part.

Dr. Powell: The tricky thing of course, is the lower speed the more likely it is to come from the surface. It is sixth power dependent.

Dr. Meecham: Of course the situation often is that the wind speed at considerable altitude remains even though it is quite quiet at the surface. But your point is well taken: you have a Mach number advantage, so to speak, for the surface noise as against volume-generated turbulence with no surface layer present. The only reason one might look to the volume as a source rather than to the surface is because the velocities are often higher at considerable altitudes than they are at the surface.

Dr. Powell: I am very glad that these measurements are being taken now in this day and age. It seems to be quite possible that man himself - I mean these fancy gadgets! - may well raise the background level. The situation is changing with airplanes, since in prewar time, the power was a few hundred horsepower and less than 1% of this went into noise. With the jets of today we are talking about powers from 100,000 hp where perhaps almost 1% of this goes into sound. When we get into supersonic airplanes, the wave drag is propagated straight away and this is very powerful. And not only that, the thing that is pushing it along, the jet, also has a very noticeable effect. So it looks to me that 10 large supersonic aircraft, in the air at once over the United States, might together produce about 50 megawatts power, which is a very considerable amount. I think it is very fortunate that these measurements are being taken now before this occurs and then we will be able to see if any change happens. So often it happens we make the measurements too late and the original circumstances might have disappeared.

Dr. Harris: Could we conclude that you wouldn't recommend rockets and missiles for mail delivery because of the increase in noise level?

Dr. Powell: It would depend upon the urgency of the mail!

Mr. Diamond: Any other comments from the panel on this particular subject?

Dr. Harris: Dr. Meecham, I wonder if it wouldn't be helpful if measurements were made at some lower altitudes particularly under conditions of ascent? Would it not be possible to get good analog data on a miniature tape recorder, and then bring the record down for data analysis at some later time? This must have been considered. What were the problems?

Dr. Meecham: Those are experiments which we would like to run. Of course, one of the sad facts involved in a distributed source is that the amplitude, aside from attenuation, will not change with distance from the source. We begin with that slight handicap. Suppose that one had a layer of noise-producing elements. The sound which you get, aside from attenuation, would be essentially independent of distance from the layer. However once the attenuation is included, one might certainly expect some differences to occur. I think that experiments like these could well be useful and helpful, in particular if it turns out there is noise from turbulence which is important in the background. You mentioned an analog, I'm not quite sure whether you mean a model experiment - - -

Dr. Harris: No, I meant actually recording the data in analog form. The reason I bring this point up is I recall listening to some tape records taken during a Project Michigan study in which a balloon was in flight with a man up there operating a tape recorder. As the balloon floated over a city he could hear the city noise. I wonder why this city noise does not appear in your data. Let's say the balloon is up at about 10,000 feet. At this altitude you get pretty good vertical propagation. Let's assume the signal drops off 10 or 15 db, when we get up to 60,000 feet. Why shouldn't noises produced on the ground be detected up there? Even at 5,000 to 10,000 feet the man in the balloon could actually hear a dog barking on the ground. It was a good-sized dog I suppose. But what happens to this city noise? Why doesn't it show in your records? Your records contain not only noise due to shear and turbulence, but everything -- including system noises.

Dr. Meecham: One of the confusing things about the background is that its level is so high. You see it's at very low frequency; if it were in the audible range it would be about our speaking voice level. I think that's the size of the things we are dealing with. The background we are talking about happens to be in a very low frequency range but I wonder if the dog could compete even if he were barking at one cps since his signal suffers some attenuation and the background is large. So it may be that the background in fact masks city noise (that part which remains after attenuation). City noise may be a small part of the background that is observed here.

Dr. Powell: I think it is very interesting that the local sounds showed up so well. I rather looked on the atmosphere as being a layered medium with a rigid boundary below and a sort of soft boundary above. Now most of the low-frequency noise will be reflected back before the absorption begins to really take account. So I have been looking at it as a great big flat reverberation chamber: I have been rather tending to think of a continual bouncing back and forth.

Dr. Harris: One of the records that Dr. Meecham showed apparently did indicate at least one of those bounces could be interpreted that way.

Dr. Meecham: Oh yes, yes. Of course this was not so low either. The frequencies involved are 50 to 150 cycles. In fact the size of the reflection that you get from the surface of the earth at these frequencies is rather surprising. The wave length is about 10 feet. The earth's surface is very often not regular for 10-foot wave lengths and yet the reflection shows relatively little loss. In fact, it appears that the refraction effects and directional effects often make the reflection as large or larger than the direct signal, oddly enough. This would tend to bear out that we may have some sort of a ducted propagation process.

Dr. Rudmose: Considering the record though Dr. Harris, don't you suppose that the man had a really good low frequency cutoff in his recording system so that he was differentiating against these lower frequency sounds? Ten thousand feet is only a couple of miles, and one gets pretty good transmission over this distance even over the ground.

Dr. Harris: (These records were from the University of Michigan.) I think it is probably true; certainly he was using an analog tape recorder. On the other hand, I would assume that if he had an FM tape recorder and had equipment with good response at low frequencies, when he went over a city, the power spectrum level measurements would have shown that the city was also producing a good deal of noise even at the lower frequencies. I wouldn't expect any one cps dogs, but there are other low-frequency sources over a city that you should detect.

Dr. Meecham: One would expect that the typical city has a peak spectrum which would lie above just a few cycles. Flying right over the city of Detroit, which is not quieter than others, there was, I think no marked change in the level observed at a few cycles where most of the energy, most of the background, was located.

Dr. Harris: Up to what frequency would the system respond?

Dr. Meecham: It was responding up to 50 to 100 cycles fairly faithfully. We always get traces of things like earth movers, as I mentioned. Particularly noisy devices would show up. I suppose if you looked hard you might find other traces at higher frequencies, but there didn't seem to be any sort of persistent low frequency distributed source here. Strangely, maybe, but that seemed to be the case.

Dr. Powell: I think one of the interesting things of your echo was that the sound was fairly constant over a long time average. This seems to suggest to me the possibility of atmospheric reverberations. On the other hand, the scattering or the randomness of the fluctuations are going to be very, very important in the next few years, partly from the point of view of supersonic objects. I was talking to Dr. Crenshaw earlier and he made it pretty clear that he doesn't believe much in calculating amplitudes at long distances. Nor do I, but I think that I managed to talk him into the idea that one might be able to tackle the thing on a statistical basis and draw limits. And I think this is what we are going to have to do. The commercial airlines, of course, after ten years will be flying supersonic airplanes. A small airplane at Mach 2 at the rather low altitude of 30,000 feet will give a minimum pressure rise over the ground at about one pound per square foot. This is just about the noise considered permissible with a fifth of that from 60,000 feet. The airplanes that are now being talked about would generate several times that much at the same altitude. This is getting to a potentially dangerous region. These were for straight, steady level flight. A wavy path of plus or minus 100 feet in altitude increases the pressure on the ground by a factor between 2 and 3. A 3g turn, that is when the total force on the pilot's seat is three times his weight, gives a factor of about 3 on the ground. If the airplane is accelerating 0.3g, this also gives a factor of about 3 and refraction may do the same. It's very easy to see that maneuvers which are fairly harmless might cause pressures of 20 or 30 pounds per square foot. This might bring a roof down, or crack every window in town - this is pretty bad. What we'll have to do I'm convinced is to try and work out what are permissible maneuvers at various altitudes to keep pressures down to what is tolerable. But what is going to be more and more important is how much is the atmosphere going to deviate from the standard. This is I think going to be really a crucial thing. We are going to be just as much interested in the deviations from the average for the standard as in the standard itself, because you can just imagine the havoc that would occur if by chance a really big bang came upon a city. The damage would be terrible and there's no two ways about it. I wonder how much of the actual information we are already beginning to collect might throw some light on how the refraction due to temperature and winds may affect the intensity of the bang. Would somebody like to try to settle that one?

Dr. Crenshaw: I might add a little comment. At the beginning there I think I had mentioned to somebody that I felt that ray tracing was considerably better for a shock wave than for a sound wave, since the shock wave does have a slight memory. It doesn't follow completely

the way a sound will the atmosphere velocity gradient. Also for these maneuvers which are rather slight, it's important to try to find if focal points occur above the surface. This might enable you to have the damaging place to be about 100 feet above the buildings. However if you were to do that at a constant flight altitude over ground area around El Paso it would be right on top of people in town. So we are going to have to worry about the height above the surface. The key element here is not the average met but the average gradient involved, which I think we are all well aware of today. So it isn't enough to say that you want to know what the standard met and the deviations are, but you want to know what the standard met gradients are that you are working into and the deviations in gradients from one time to another. Now the gross weather picture will make a major effect on this and this is one item I had suggested might aid in the correlation of this background noise data of balloons flown at high altitude. It is the gross weather situation; are you in a rather stable type weather or are you where a front is coming through, or are you where two fronts are fighting it out to see which one will come through. These will tend to give you somewhat different stabilities in the atmosphere, different gradients which may vary well, if these noises come from the surface, and have to go through this part of the atmosphere where the weather is occurring, give you an indication that an appreciable amount of your background in this balloon-borne thing was from the surface and then passes through this layer.

Mr. Diamond: Then Dr. Crenshaw may we quote you as saying there is a definite need for more and better meteorological data to higher and higher levels?

Dr. Crenshaw: Well, I would say there is a need; whether it can be funded or not is another thing. It depends on the relative urgency of the need as we have heard earlier, on the mail problem.

Mr. Diamond: With the permission of the panel, we might entertain a few questions from the audience if there are any people who would like to fire a question or have some problems they would like to have solved quickly.

Mr. Barnes: I'd like for Dr. Young to say something extending his comments on the very low infrasonic work that he's been doing. I think they mentioned out in San Francisco something about the earth tremors as an origin of background noise as you might call it.

Dr. Young: Yes. We have seen during very large earthquakes pressure fluctuations in the atmosphere at Washington due to the diaphragm action

of the surface of the ground as the surface wave progresses through it. But these are not large for anything but the very large earthquakes. I don't think they would form an appreciable amount of background for an appreciable amount of time. There are some lower frequency fluctuations, some fluctuations of barometric pressure you might say, down to the neighborhood of 5 to 20 minutes that do seem to show traveling wave properties over the surface of the order of 20 to 40 meters per second of fairly high amplitude. We know very little about the origin of these. This is getting down to a frequency region which I think is not of much interest here.

Dr. Powell: Can you tell me if there is any truth in the story I heard that a certain "minor earthquake" was due to a supersonic bang over a seismograph?

Dr. Crenshaw: It would pick it up all right.

Dr. Young: I don't know the case you are talking about but I think it would probably be possible that you could excite surface waves by the sound waves striking the surface at a high angle, where the trace velocity is approximately equal to the surface wave velocity in the earth.

Dr. Crenshaw: Along these lines I might point out that Frank Press about two years ago or three, wrote an article, I do not remember where, wherein he took the original work of the Royal Meteorological Society as the Society recorded a special report on the Krakatora explosion. He demonstrated that one of the waves that they had analyzed at that time as being a tidal wave arriving in England after running around Africa was in reality the coupled wave between an atmospheric pressure pulse (that had a period on the order of one-half hour), and the surface of the ocean and in driving across the Atlantic it made a big enough pressure rise in the surface to be measured in England. Another item I am reminded of is something that Dr. Swingle pointed out several years ago about when we had a major storm in Long Island Sound. In his micro-met work he indicated there was an indication of a barely discernable pressure fluctuation on the standard microbarograph which arrived at the Long Island area, at about the right time. However, the atmosphere where it propagated was relatively stable so no damage was done. However, in an unstable condition in the sound a great deal of damage was done by a sudden squall. One postulate was that it may have been initiated by this pressure fluctuation.

Mr. Jack Reed: I have one question. When would we be able to educate people to accept the order of one pound per square foot pressure where the damage doesn't really begin until four or five times that level? Will people ever get used to these things blasting all the time or do

we have to continue test explosions sites in the country, making sure that they equal below, 300 microbar like at Livermore. We got billed for stampeding a herd of turkeys at about 150 microbars.

Dr. Powell: Well, the number of one pound per square foot was what was also discovered in England in one or two flights. This was the postcard and telephone business all over again (except they didn't know anything was going to go off) and it turned out that the limit seemed to be around one pound per square foot for people to start making complaints. Whether one can become attuned to this sort of thing, I think is something different. I wouldn't like it. The danger is not so much the one pounder as this is just like a big thunder clap, but the real danger is that the atmospheric conditions or the maneuver of the airplane may turn them into blitzes. This is in an entirely different category altogether and this I feel is another question. I think people generally will tolerate quite a lot if they have some sort of interest in it. I well remember flying light aircraft on maneuvers and we flew at 3,000 feet in a little 120 horsepower airplane over one town and we got vicious complaints. The same town was producing jet airplanes with the runway close to a main street and once the chickens almost got blown around in the back yard. Nobody complained about that. Perhaps they were proud of it.

Dr. Harris: That was their noise, though!

Dr. Powell: Oh, yes, definitely.

Mr. Diamond: Any other questions? I would like to take the liberty of asking the panelists, if they feel free to do so, on the basis of what we have heard over the last day and a half, if they would like to suggest to us directions of research and study of atmospheric propagation of sounds, particular ones or maybe these meetings have presented questions which weren't apparent before these meetings.

Dr. Harris: There are a number of atmospheric acoustics problems I would like to work on, but one of the rather discouraging aspects of such activity is that although it is possible to obtain good acoustic data, there is little that can be done with these data if I do not have good met data to correlate with it. So I have been waiting for advances in meteorological instrumentation. If we are to make significant advances in the field of atmospheric acoustics, to me the most important problem is that of getting better met data.

Dr. Young: One of the things that strikes me in the talks that I have heard is the matter of background noises. I think perhaps much more work should be done in this field because we do not know enough about the sources of these background pressure fluctuations. We don't even know how much of them are due to acoustic noises or how much are due to

turbulence around our measuring system. I think a lot more work can be done here, and also perhaps in the calibration of the measuring systems themselves. One of the problems one runs into in trying to calibrate low frequency devices is that when small volume changes are introduced into a chamber, the transition from adiabatic to isothermal conditions within the chamber can give you calibration errors if care is not taken. I think better methods can be developed for calibrating the instruments in environments similar to those in which they will be used.

Dr. Meecham: I think my favorite experiment would be a flight which directly measured relative fluid flow velocity from the ground up to the altitudes we are interested in here. I am not certain of the instrumentation. The relative velocities are small, a few miles an hour is the sort of thing we're thinking of, even in the jet stream. Frankly, I'm not sure whether a hot wire measurement would work in this range or not but I'm sure there must be some relatively simple velocity measuring device that we could put on the balloon which would directly measure what the turbulent effects are as a function of altitude. This would be very valuable. Instead of continually struggling with vague estimates it would be very nice to have a direct measurement of this quantity.

Dr. Crenshaw: I might explain part of the reason for my concern in the amplitude computation. The amplitude computation as I understand the ray tracing is dependent upon the second derivative of the velocity profile with height. You have a rough time measuring the speed of sound and of the wind and its direction accurately in a thirty knot wind and if it changes 15 degrees and if you're at right angles to the direction of propagation you get a major change in your refractive index with no energy change to amount to anything during the momentum change of the medium. Things of this type, when the windstream can make a major effect. To get amplitude you must measure the second derivative of this. The first derivative gives you essentially the general ray bending. In many of these cases if we are interested in the lower frequency areas these effects appear considerably smaller than a wave length and certainly much smaller than a few wave lengths. None of the proposed treatments that I have seen work, they just say take a good mean, average value. The question is how much error have you lost in this case using a ray theory as an approximation. So that is one area where we have to get some sort of an indication. One item which will help us in this noise produced by these jets running around at random and attenuations are too small. You put a signal in that is 50 to 100 times as large as the background noise how far is it going to propagate. It won't propagate very far over the equator from this latitude because the curves we saw the first day showed appreciable latitude variations. So we just have to worry about those in the northern hemisphere I'd say.

Dr. Powell: I would second everything that's gone before. I would like to emphasize the last point from the point of view of the variability of the atmosphere as regards the second gradient because this does influence the amplitude very strongly. What we must try and do is develop some analytical techniques which could apply to models which represent the atmosphere pretty well. But we must be very practical in the way we choose these and set them up so they will be the least sensitive as possible to the inevitable variations in the models. Possibly we may have to incorporate something rather analogous to scattering theories as applied to propagation as such. Another area which will ultimately become of interest is in the ionosphere where the air is rarefied and highly ionized: this is of course magneto-hydrodynamics. I think it's only a question of time until we are interested in the properties of propagation up there and they are likely to be quite different to those low down.

Dr. Rudmose: There is a real disadvantage in being on the end - all the good ideas have already been given. I would like, however, to make just a few comments. One, is to point out that this field is really foreign to me. My field has to do primarily with the effects of noise on man. I was interested in the question about one pound per square foot. We are still worrying about how much jet noise the public can take before they begin to yell too much. We still have no simple guide as to when one starts making enough noise to annoy people or keep them from sleeping. I came here partly because of my association with the NRC committee called CHABA for we are getting the problem of the sonic boom thrown at us, and we are trying to get some idea of the reaction of these booms on the population.

I have a couple of comments to make and not being in this field I have somewhat the feeling of a man walking through a door where a child has a bucket of water over the door. I don't really know where the door is much less when the child will release the bucket. But in any event, here are my comments. It appears to me that you could do a certain number of things on the ground that might be beneficial to you. Work could be done in studying the propagation of very low frequency sounds over reasonable distances on the earth. Possibly you could learn how to correlate this propagation with the micrometeorological data which you could get right near the surface. Here such data are relatively easy to obtain. I recognize ground propagation isn't your problem, and furthermore I realize that you have been put in the position of "let's get the answer and not worry about the theory behind it," but on the other hand if one would study, with the present instrumentation that we have, the attenuation of these very low frequency sounds over moderate distances you might get a great deal of information that could be of help in studying what comes through the atmosphere. It may be that you could get some fundamental information by working with very low frequencies

in a tube. You could, if you wish, after sending out a pulse of low frequencies, block your source end and let the pulse go back and forth for awhile. The tube need not be too long. Within this tube you could put in membranes which have small attenuation for these frequencies. Then, between membranes you could introduce all degrees of turbulence along this tube and watch the pulse go back and forth. Possibly from such measurements you could get some feeling as to what happens under these controlled conditions. I recognize there is no real scattering in such a tube. But if you get clever and make the sides of this tube acoustically "leaky" then you have a little better approximation of free space. I am not sure you cannot get some good fundamental data from this approach without "leaky" sides. Such an experiment would not be too expensive when compared to the cost of firing rockets to obtain the equivalent amount of data.

Mr. Diamond: Thank you gentlemen. On behalf of those present I want to thank you for a very stimulating and informative discussion. That completes our panel discussion.

ATTENDEES

Robert C. Amme
Denver Research Institute
University of Denver
University Park
Denver 10, Colorado

Neal Anderson
Aerospace Corporation
2400 El Segundo Blvd.
El Segundo, California

Henry Baker
White Sands Missile Range
New Mexico

Harold N. Ballard
Schellenger Research Laboratories
Texas Western College
El Paso, Texas

Roswell P. Barnes
Melpar, Incorporated
Applied Science Division
Watertown, Massachusetts

Thomas G. Barnes
Schellenger Research Laboratories
Texas Western College
El Paso, Texas

James Bettie
Schellenger Research Laboratories
Texas Western College
El Paso, Texas

Norman Beyers
U. S. Army - SMSA
White Sands Missile Range
New Mexico

Mary Leticia Bradfield
Schellenger Research Laboratories
Texas Western College
El Paso, Texas

James B. Calvert
Denver Research Institute
University of Denver
University Park
Denver 10, Colorado

Charles Cantoni
Electronic Defense Laboratory
P. O. Box 205
Mountain View, California

Irving B. Chernetz
Commanding Officer
U. S. Army Signal Operation Activity
ATTN: SIGRA/OA
Fort Monmouth, New Jersey

Jack E. Chinn
University of California
Lawrence Radiation Laboratory
Livermore, California

Hugh W. Church
3113 California, NE
Albuquerque, New Mexico

John W. Coffman
White Sands Missile Range
New Mexico

George Cohen
USA SrDA
Fort Monmouth, New Jersey

George Cotten
110 Lovett Ave.
Little Silver, New Jersey

Dr. C. M. Crenshaw
Chief Signal Officer
ATTN: SIGRD-2
Department of the Army
Washington 25, D. C.

Joseph Damon
Ft. Monmouth
Belmar, New Jersey

Paul K. Dano
Schellenger Research Laboratories
Texas Western College
El Paso, Texas

E. Alan Dean
Schellenger Research Laboratories
Texas Western College
El Paso, Texas

Norma Deras
3619 Montana
El Paso, Texas

Marvin Diamond
White Sands Missile Range
New Mexico

Alton A. Duff
White Sands Missile Range
New Mexico

Philip Duran
Schellenger Reserach Laboratories
Texas Western College
El Paso, Texas

Major Thomas G. Ellis
Assistant Chief of Staff, Intelligence
Department of the Army
Washington 25, D. C.

Emmit E. Fisher
617 W. Cebada
El Paso, Texas

Jack D. Fletcher
University of California
Lawrence Radiation Laboratory
Livermore, California

Coy E. Foshee
1703 Van Court
Alamogordo, New Mexico

Robert R. Fossum
3440 Janice
Palo Alto, California

Roy I. Glass
USA SMSA
RD - MM 3
WSMR, New Mexico

Abraham Golden
Commanding Officer
U. S. Army Signal Research and
Development Laboratory
ATTN: SIGRA/SL-S
Fort Monmouth, New Jersey

Gilbert I. Good
Schellenger Research Laboratories
Texas Western College
El Paso, Texas

James B. Gose
Rt. 2 Box 725
Las Cruces, New Mexico

J. William Grady
OACSI, DA
Rm 2 B 457 Pentagon
Washington 25, D. C.

Allan B. Gray, Jr.
White Sands Missile Range
New Mexico

William Guramy
Schellenger Research Laboratories
Texas Western College
El Paso, Texas

Jack L. Halvorsen
3585 Apollo Dr.
Salt Lake City, Utah

Charles H. Handley
P. O. Box 205
Mountain View, California

Dr. Cyril M. Harris
Columbia University
632 West 125th Street
New York 27, New York

James C. Hart
Bay State Electronics Corporation
Boston, Massachusetts

A. R. Hercz
University of Michigan
Ann Arbor, Michigan

Guenther Hintze
White Sands Missile Range
New Mexico

William Hite Sr.
Schellenger Research Laboratories
Texas Western College
El Paso, Texas

Glenn B. Hoidale
White Sands Missile Range
New Mexico

Marjorie E. Hoidale
White Sands Missile Range
New Mexico

Stanley H. Hyde
Schellenger Research Laboratories
Texas Western College
El Paso, Texas

Mike Izquierdo
1007 Mundy
El Paso, Texas

William N. Jacobs
9310 Charleston
El Paso, Texas

Arthur Jurman
63 Clinton Place
Red Bank, New Jersey

George Kaschak
37 Peters Place
Red Bank, New Jersey

Major William R. King
Commanding Officer
U. S. Army Signal Operation Activity
Fort Monmouth, New Jersey

Captain Demos T. Kyrakis
Commander
U. S. Air Force Aerospace Technical
Intelligence Center
ATTN: AFCIN - 4C2b
Wright-Patterson Air Force Base, Ohio

Donald L. Lansing
National Aeronautics &
Space Administration
Research Center, Acoustic Branch
Langley Field, Virginia
Attention: Mr. D. L. Lansing

Henry H. Launspach, Jr.
Schellenger Research Laboratories
Texas Western College
El Paso, Texas

Dr. Joel S. Lawson, Jr.
Scientific Engineering Institute
Waltham 54, Massachusetts

Tom Leonard
Electronic Defense Laboratory
P. O. Box 205
Mountain View, California

G. Allison Long, Jr.
Commander
U. S. Air Force Aerospace Technical
Intelligence Center
ATTN: AFCIN/4A 3a
Wright-Patterson Air Force Base, Ohio

1/Lt. Jerry V. Marshall
1st Msl Bn (CPL) 4 th Army
Ft. Bliss, Texas

Carlos McDonald
Schellenger Research Laboratories
Texas Western College
El Paso, Texas

John A. McKinnon
Schellenger Research Laboratories
Texas Western College
El Paso, Texas

James B. Mason
Schellenger Research Laboratories
Texas Western College
El Paso, Texas

Doyle Mathews
White Sands Missile Range
New Mexico

Dr. William C. Meecham
Institute of Technology
University of Minnesota
Minneapolis 14, Minnesota

Gerald L. Mohnkern
2305 S. Espina
Las Cruces, New Mexico

Maj. Clarence E. Morrison
White Sands Missile Range
New Mexico

Annette Noland
USA SMSA
White Sands Missile Range
New Mexico

Walter S. Nordquist, Jr.
9616 Waverly Dr.
El Paso, Texas

Daniel J. Novak
2508 Stanford
Alamogordo, New Mexico

John Ohman
Bay State Electronics Corporation
Boston, Massachusetts

Robert Olsen
White Sands Missile Range
New Mexico

Clifford A. Olson
1301 Florida N. E.
Albuquerque, New Mexico

Thomas E. Owen
Department of Electronics &
Electrical Engineering
Southwest Research Institute
8500 Culebra Rd.
San Antonio 6, Texas
ATTN: Thomas E. Owen

Alyce Patterson
USA SMSA
White Sands Missile Range
New Mexico

Robert F. Plott
210 Pathfinder Lane
McLean, Virginia

Dr. Alan Powell
Department of Engineering
University of California
Los Angeles 24, California

Edmond E. Raiborn
1404 Montana
Las Cruces, New Mexico

C. M. Redman
1209 Dale Lane
Las Cruces, New Mexico

Jack Reed
Sandia Corp.
Albuquerque, New Mexico

Robert Rios
SRL, Texas Western College
El Paso, Texas

Chris H. Roach
White Sands Missile Range
New Mexico

Ralph Rotolant
SRL, Texas Western College
El Paso, Texas

Clara B. Roosa
White Sands Missile Range
New Mexico

Lee Rudlin
Commanding Officer
U. S. Naval Ordnance Laboratory
White Oaks
Silver Springs, Maryland

Wayne Rudmose
SMU
Dallas 22, Texas

Robert R. Rulifson
Radio Corp. of America
Building 13-5
Camden, New Jersey

Fred Salvatti Jr.
SRL Texas Western College
El Paso, Texas

Juana Serna
6115 Tejas Dr.
El Paso, Texas

Charles F. Shoppach
3912 McKinley Ave. B
El Paso, Texas

Donald C. Slade
White Sands Missile Range
New Mexico

Wendell C. Smith
3970 Penn. Ave.
Washington 20, D. C.

Rudy Soto
500 W. Pasiano
El Paso, Texas

R. C. Spence
3208 Burton S. E.
Albuquerque, New Mexico

Raya Stern
Fluid 6 Solid Mechanics
University of Michigan
Ann Arbor, Michigan

Leland Stewart
237 Edlee
Palo Alto, California

Charles W. Strack, Jr.
Commanding Officer
U. S. Air Force Aerospace Technical
Intelligence Center
ATTN: RADC/RCWCI
Wright-Patterson Air Force Base, Ohio

Robert N. Swanson
5928 Marlin Dr.
El Paso, Texas

Donald Swingle
Commanding Officer
U. S. Army Signal Research &
Development Laboratory
ATTN: SIGRA/SL-SA
Fort Monmouth, New Jersey

Henry Thompson
White Sands Missile Range
New Mexico

Fred M. Tingley
Melpar Incorporated
Applied Science Division
Watertown, Massachusetts

Capt. Willard Truesdell
Commander
U. S. Air Force Aerospace Technical
Intelligence Center
ATTN: AFCIN-4F3d
Wright-Patterson Air Force Base, Ohio

Salvador Villarreal
IRM
White Sands Missile Range
New Mexico

Kenneth J. Walsh
White Sands Missile Range
New Mexico

Willis L. Webb
USA SMSA
White Sands Missile Range
New Mexico

Lt. Col. G. A. Welde
USA SMSA
White Sands Missile Range
New Mexico

John Wescott
Institute of Science & Technology
University of Michigan
Ann Arbor, Michigan

Kerry Wilson
5711 Auburn
El Paso, Texas

James M. Wolf
304 Arbano Dr.
Ann Arbor, Michigan

William C. Wootton, Jr.
5508 Raymond Telles Dr.
El Paso, Texas

Luis A. Yip
SRL, Texas Western College
El Paso, Texas

Jessie M. Young
National Bureau of Standards
Washington 25, D. C.

Robert L. Schumaker
SRL, Texas Western College
El Paso, Texas